

Doctorat de Física Avançada

Bienni 2003-2005

Aspectes Clàssics i Quàntics de Forats Negres en Diverses Dimensions

Pau Figueras i Barnera

*Departament de Física Fonamental
Grup de Cosmologia i Gravitació*

Memòria presentada per optar al títol de Doctor en Física

Juny del 2007

Director de la tesi: Dr. Roberto A. Emparan García de Salazar



UNIVERSITAT DE BARCELONA



*Al pare, la mare, la Marta
i a la Laura*

Índex

Agraïments	ix
I Resum	1
1 Introducció, resultats i conclusions	3
1.1 Introducció	3
1.1.1 Context	4
1.1.2 Introducció a la tesi	6
1.2 Resum dels resultats	18
1.2.1 Anells negres no supersimètrics amb càrregues D1-D5-P	18
1.2.2 Anell negre amb rotació a la S^2	20
1.2.3 Forats negres supersimètrics en AdS_5	21
1.2.4 Saturn negre	24
1.2.5 Fases dels forats negres en cinc dimensions	26
1.2.6 Solucions supersimètriques de Teoria M amb factors AdS_3	29
1.3 Discussió i conclusions	34
1.4 Discussion and conclusions	39
II Compendi d'articles	49
2 Non-supersymmetric black rings as thermally excited supertubes	53
2.1 Introduction	53
2.2 Non-supersymmetric black rings with three charges	55
2.2.1 Generating the solution	55
2.2.2 Solution	57
2.2.3 Properties	60
2.3 Extremal and supersymmetric limits	63
2.4 Non-supersymmetric black rings in minimal 5D supergravity	66
2.5 D1-D5-P black rings	68
2.5.1 D1-D5-P/d1-d5-kkm black ring	69
2.5.2 D1-D5/kkm black rings and two-charge supertubes	70
2.5.3 D1-D5-P/d1-d5 black ring: the black double helix	74
2.5.4 Decoupling limit	75
2.6 Discussion	76
2.A Three-form fields for the 11D solution	77

2.B	The RR two-form potentials for the D1-D5-P black ring solution	78
2.C	Limit of spherical black hole	79
2.D	Infinite radius limit	79
3	A black ring with a rotating 2-sphere	85
3.1	Introduction	85
3.2	The black ring with a rotating S^2	87
3.2.1	The solution	87
3.2.2	Horizon geometry	88
3.3	Limits	89
3.3.1	Infinite radius limit	89
3.3.2	Myers-Perry black hole limit	90
3.4	Conclusions	90
4	On a class of 4D Kähler bases and AdS_5 supersymmetric Black Holes	95
4.1	Introduction	95
4.2	Supersymmetric solutions of $D = 5$ SUGRA	97
4.3	Co-homogeneity two Kähler bases	99
4.4	All known AdS_5 BH's of minimal gauged SUGRA	100
4.5	The conical structure of the Black Hole solutions	101
4.5.1	Sasakian space as a fibration over Kähler manifold	104
4.5.2	A comment on supersymmetric black rings	106
4.6	5D Near horizon solutions from Kähler cones	107
4.7	Full spacetime analysis	109
4.8	Solutions	112
4.8.1	Solutions with $U(1)^2$ spatial isometry	112
4.8.2	Solutions with angular dependence	117
4.9	Conclusions and Discussion	123
4.A	Non-toric Kähler cones	124
5	Black Saturn	131
5.1	Introduction	131
5.2	Construction of the solution	134
5.2.1	The inverse scattering method	134
5.2.2	Seed and soliton transformation for black saturn	136
5.2.3	Saturn solution	139
5.3	Analysis	141
5.3.1	Parameterization	141
5.3.2	Rod structure	142
5.3.3	Asymptotics	143
5.3.4	Regularity and balance	144
5.3.5	Horizons	144
5.3.6	ADM mass and angular momentum	146
5.3.7	Komar integrals	147
5.3.8	Closed timelike curves	149
5.3.9	Limits	150
5.4	Physics of black saturn	151

5.4.1	Parameter counting and non-uniqueness	151
5.4.2	Myers-Perry black hole and black rings	152
5.4.3	Configurations with $J_{\text{Komar}}^{\text{BH}} = 0$	153
5.4.4	Black hole with intrinsic spin	158
5.4.5	Non-uniqueness	159
5.4.6	Solutions with $\epsilon = -1$	162
5.5	Discussion	163
5.A	Limits	168
5.A.1	Myers-Perry black hole	168
5.A.2	Black ring limit	169
6	Phases of Five-Dimensional Black Holes	177
6.1	Introduction	177
6.2	Phasing in Saturn	179
6.3	Multiple rings and further parameters	182
6.4	First law of multi-black hole mechanics	183
6.5	Thermodynamical equilibrium	184
6.6	Discussion	186
7	Global geometry of the supersymmetric AdS_3/CFT_2 correspondence in . . .	191
7.1	Introduction	192
7.2	Summary of results	198
7.2.1	Cayley geometry	199
7.2.2	Kähler-4 geometry	200
7.2.3	Special Lagrangian geometry	201
7.2.4	Quaternionic Kähler geometry	203
7.2.5	Complex Lagrangian geometry	204
7.3	Spinorial realisation of the frame bundles	205
7.3.1	$Spin(7)$ and associated local AdS_3 structures	205
7.3.2	$SU(4)$ and associated local AdS_3 structures	207
7.3.3	$Sp(2)$ and associated local AdS_3 Structures	210
7.4	Truncating eleven-dimensional supergravity	213
7.4.1	$Spin(7)$, $SU(4)$ and $Sp(2)$ geometry	213
7.4.2	Cayley geometry	214
7.4.3	Kähler-4, SLAG, QK and CLAG geometry	214
7.5	The AdS_3 geometries	215
7.5.1	Coordinates for the AdS frame	216
7.5.2	AdS boundaries in Cayley geometry	217
7.5.3	AdS boundaries in Kähler-4 and SLAG geometry	220
7.5.4	AdS boundaries in QK and CLAG geometry	221
7.6	Explicit solutions	222
7.7	Conclusions	225
7.8	Acknowledgements	227

Agraïments

En un moment així, hom mira enrera i la veritat és que no sap per on començar per no deixar-se a ningú. Hi ha tanta gent que ha estat important per mi durant aquests anys que, primer de tot, voldria agrair a tothom que ha contribuït directament o indirecta a fer possible aquesta tesi.

En primer lugar querría dar las gracias a mi director, Roberto Emparan porque todo lo que sé lo he aprendido de ti y obviamente sin ti esta tesis no habría sido posible. Recuerdo cuando me introdujiste por primera vez a estos objetos (en cinco dimensiones!!!) a los que habíais llamado black rings y me paracerieron muy raros. Después de estos años me parecen extremadamente interesantes. Muchísimas gracias por enseñarme tantas cosas sobre estos objetos fascinantes y, en general, por compartir tu ciencia conmigo. También debo darte las gracias por haberme ayudado en tantísimas ocasiones y por haberme mostrado el camino que hay que seguir.

També voldria agrair a tots els professors que he tingut durant aquests anys i que també m'han ensenyat moltes coses: Enric Verdaguer, Jaume Garriga, Quim Gomis, Josep Ma. Pons, Jorge Russo, Paul Townsend, Pere Talavera, Domènec Espriu, Josep Ignasi Latorre, Joan Soto i en Joan Solà. Voldria donar les gràcies en particular a l'Enric Verdaguer per explicar-me els 'secrets' dels solitons gravitacionals i dedicar-me el seu llibre. I would also like to thank Harvey Reall for all the discussions we have had, I have learned a lot from you. I am also in debt with Jerome Gauntlett for letting me stay in your group at Imperial for a month and a half. It was a wonderful and fruitful experience. I would also like to thank Dan Waldram, Toby Wiseman, Bo Feng and Nemani V. Suryanarayana for the discussions that we had while at Imperial. I would not like to forget the Irish gang, Eoin and Oisín, thanks a lot guys.

Thank you very much to all the postdocs that I have had the pleasure to meet here in Barcelona. Thank you Aldo, Diederik, Marco, Pedro, Tassos, Samuel, Marcelo for all the discussions and friendship. It is a pity that we could not manage to organize regular football matches, but I have had a lot of fun anyway. In particular, I would like to thank Oscar Dias for being, above all, such a good friend. Also, I would like to thank you for all the discussions we have had about physics and life, and also for inviting me to so many coffees. I hope that one day we will be able to find a project in which we can collaborate.

I would also like to thank all my collaborators that I have had the pleasure and privilege to work with during these years: Henriette Elvang, Carlos Herdeiro, Filipe Paccetti, Oisín Mac Conamhna and Eoin Ó Colgáin. In particular, I would like to thank Henriette because, apart from being a wonderful collaborator, you have been a very nice friend. Thank you very much for your help in all aspects of my life.

Moltes gràcies també Joan Simón, David Mateos i Jaume Gomis pels vostres consells. Espero que algun dia pugui arribar a assemblar-me científicament a vosaltres. No voldria oblidar-me d'en Tomeu, una de les últimes incorporacions al grup. Moltes gràcies per les moltes discussions que hem tingut i, sobretot, per les moltes preguntes que sempre plantegeu i que em

fan pensar molt. He après moltes coses de tu i també espero que algun dia em pugui assemblar científicament a tu.

També voldria donar les gràcies a tots els meus companys de despatx, en Sandro, la Laia i en Guillem. També és un plaer donar les gràcies a tots els meus ‘germans’ científics: en Sandro, la Majo i en Joan. Moltes gràcies per tots aquests anys que hem compartit i per haver tingut la paciència d’ajudar-me amb la redacció d’aquesta tesi. M’ho he passat d’allò més bé parlant amb vosaltres tant de física com d’altres coses. Moltes gràcies Dani per la teva ajuda amb el Linux i el Latex. Finalment, també voldria agrair a en Diego les discussions que hem tingut i els comentaris sobre la tesi.

També voldria donar les gràcies a tota la meva ‘colla’ de companys de la carrera amb qui encara ens hem anat veient per la facultat: en Funo, en Sandro, la Marta, l’Alberto, en Dani, en Martí, en Carles, etc., i especialment a la Isabel.

No em voldria oblidar dels Flanagans, en especial d’en Xevi, l’Enric, en Miquel i en David. Moltes gràcies nois per la vostra amistat. Estic especialment en deute amb en David per tots els anys que hem passat a la facultat, per la teva amistat i per ser, en moltes ocasions, com el meu germà gran.

He d’agrair profundament l’ajuda, estimació i suport que he rebut de la meva família, i en especial de la Laura. En primer lloc, voldria tenir unes paraules de record i agraïment per al meu pare. Sempre ho havies donat tot per fer-nos feliços i que no ens faltés mai de res, i havies lluitat al màxim per un dia com avui poder llegir aquestes línies perquè la família ho era tot per a tu. Moltes gràcies per tot el que has fet per a mi, he intentat aprendre tot el que he pogut de tu. Sé que aquests anys no han estat fàcils per tu, mare, però sempre has intentat tirar endavant per tal de ser feliç i que poguéssim fer la nostra via malgrat les circumstàncies. Admiro el teu coratge i perseverància, i t’he de donar les gràcies per haver-nos ajudat incondicionalment. També vull donar les gràcies a la meva germana, la Marta. Moltes gràcies també a tots els tiets, tietes, cosins i iaies, en especial al tiet Ilde per ser, a vegades, com un pare. També estic en deute amb la iaia Maria perquè sempre m’ha tractat com la meva segona mare. Vull donar les gràcies a l’Àngel, l’Assumpta, en Francesc i a l’avi Josep perquè durant tots aquests anys, quan hem vingut a la Torra, m’hi he trobat com a casa.

Finalment, he de donar les gràcies més sinceres a la Laura perquè tots aquests anys al teu costat han estat meravellosos. Ara mateix només sóc capaç de recordar moments bons, moltes gràcies per ajudar-me tant, entendre’m millor que jo mateix i, sobretot, per fer-me tan feliç.

*“Truth is ever to be found in the simplicity,
and not in the multiplicity and confusion of things.”*

Sir Isaac Newton

*“The most incomprehensible fact about the universe,
is that it is comprehensible.”*

Albert Einstein

*“My goal is simple.
It is complete understanding of the universe,
why it is as it is and why it exists at all.”*

Stephen Hawking

Part I
Resum

Capítol 1

Introducció, resultats i conclusions

1.1 Introducció

The black holes of nature are the most perfect macroscopic objects there are in the universe: the only elements in their construction are our concepts of space and time. And since the general theory of relativity provides a single unique family of solutions for their descriptions, they are the simplest objects as well.

S. Chandrasekhar, "The Mathematical Theory of Black Holes," (1985).

En aquesta tesi hem estudiat tant aspectes clàssics (Relativitat General) com quàntics (Teoria de Cordes/Teoria M) dels forats negres en D dimensions, amb $D > 4$. Fruit d'aquests estudis, han sorgit diverses publicacions les quals conformen aquesta tesi. Hem organitzat els articles seguint l'ordre cronològic en què han aparegut, tot especificant la revista on han estat publicats. En aquest treball prenem les unitats de manera que $\hbar = c = 1$, excepte en punts molt concrets on restituïm les dimensions habituals. La signatura de la mètrica és $(-, +, \dots, +)$.

Els forats negres són objectes fascinants des de molts punts de vista. Pel que fa a la Relativitat General, la seva importància rau en el fet que són objectes intrínsecament relativistes i per tant ens aporten molta informació sobre la dinàmica de la teoria. A més, en molts casos, hom té un control analític de les solucions cosa que les fa tractables. Per altra banda, la Teoria de Cordes es postula com l'única teoria quàntica consistent que inclou la interacció gravitatòria i, com a tal, inclou la Relativitat General en un cert límit de baixes energies. Per tant, *totes les solucions de forats negres en Relativitat General són solucions de Teoria de Cordes a baixes energies*. Com a teoria fonamental que inclou la gravetat, la Teoria de Cordes ens hauria de donar les respostes als problemes que es plantegen en l'estudi de la física dels forats negres, tan a nivell clàssic com quàntic. Per tant, és gràcies a aquesta interrelació entre la Relativitat General i la Teoria de Cordes que pensem que ha de ser possible fer progressos en el nostre coneixement de la interacció gravitatòria. És més, els forats negres són precisament els objectes que hem d'estudiar. Així doncs, un dels objectius d'aquesta tesi ha estat aconseguir trobar noves solucions analítiques de forats negres en $D > 4$ ja que les solucions exactes són fonamentals per tal d'entendre la gravetat tant en Relativitat General com en Teoria de Cordes.

1.1.1 Context

La primera solució corresponent a un forat negre fou descoberta per Karl Schwarzschild [1], encara que en el seu moment no es va apreciar que es tractava d'un forat negre. La corresponent mètrica, que porta el nom del seu descobridor, és:

$$ds^2 = - \left(1 - \frac{2GM}{r} \right) dt^2 + \frac{dr^2}{1 - \frac{2GM}{r}} + r^2 (d\theta^2 + \sin^2 \theta d\phi^2) . \quad (1.1.1)$$

Gràcies a aquesta solució es va poder entendre que els forats negres apareixen de forma natural al nostre Univers com el darrer estadi de l'evolució d'una estrella prou massiva ($M \sim 10M_{\odot}$). Cal afegir que nombroses observacions indiquen la presència de forats negres supermassius, amb una massa milions de vegades més gran que la de Sol, al centre de les galàxies. Per tant, com acabem d'argumentar, els forats negres són objectes relativament comuns. Ara bé, cal tenir present que les estrelles tenen un cert moment angular i per tant el forat negre al qual puguin donar lloc també tindrà un cert moment angular. El problema que se'ns planteja quan intentem generalitzar la solució de Schwarzschild per tal d'incloure el moment angular és que les equacions d'Einstein formen un sistema d'equacions en derivades parcials no lineal i, per tant, resoldre-les suposa una tasca formidable. De fet, no va ser fins l'any 1963 en què Roy P. Kerr va aconseguir trobar un forat negre amb moment angular [2]. Com veurem tot seguit, aquesta solució representa *tots* els forats negres del nostre Univers macroscòpic que hem pogut observar fins al dia d'avui. Va ser entre els anys 60 i 70 en què es va viure l'anomenada època daurada de l'estudi dels forats negres en quatre dimensions i es van entendre aquests objectes a nivell clàssic. Durant aquests anys es van establir diversos teoremes que ens permeten descriure completament aquests objectes en quatre dimensions:

- **Teoremes d'unicitat:** Els únics forats negres que són solució de les equacions d'Einstein al buit en quatre dimensions corresponen a les solucions de Schwarzschild i Kerr, i les subseqüents generalitzacions a la teoria d'Einstein-Maxwell (Reissner-Nordström i Kerr-Newman) [3, 4, 5, 6].
- **Topologia:** La topologia de la secció espacial de l'horitzó d'un forat negre en quatre dimensions és S^2 [7].

Aquests teoremes ens diuen que els forats negres, malgrat ser objectes macroscòpics, són extremadament senzills ja que es poden descriure *exactament* mitjançant un nombre finit de paràmetres que especifiquen les càrregues conservades: la massa M , el moment angular J i la càrrega elèctrica Q . És més, els teoremes de “no-hair” afirmen que els detalls del col·lapse o l'estructura del cos que col·lapsa no són importants i que el forat negre resultant estarà descrit pels paràmetres M , J i Q . D'aquí l'afirmació de Chandrasekhar amb què obríem aquesta secció [8]. Una altra propietat remarcable que cal esmentar és que els forats negres (sense càrrega) en quatre dimensions són estables sota perturbacions lineals clàssiques. Gràcies a aquest fet podem afirmar que són objectes astronòmicament rellevants i observables.

Paral·lelament als resultats clàssics que acabem d'esmentar, s'anaren produint descobriments en què es deixaven entreveure algunes de les propietats que hauria de tenir una teoria quàntica de la gravetat. Per una banda, es va veure que els forats negres obeeixen una sèrie de lleis completament anàlogues a les lleis de la termodinàmica [9]. Segons la taula 1.1.1 podem establir les següents analogies entre diferents quantitats que apareixen en la termodinàmica clàssica i en la física dels forats negres: energia i massa $E \leftrightarrow M$, temperatura i gravetat superficial $T \leftrightarrow \alpha\kappa$, i entropia i àrea de l'horitzó $S \leftrightarrow A_{\text{H}}/(8\pi\alpha)$, on α és una certa constant

Llei	Termodinàmica	Forats Negres
Zero	la temperatura T és uniforme en un cos en equilibri tèrmic	la gravetat superficial κ de l'horitzó d'un forat negre estacionari és uniforme
Primera	$dE = TdS + \text{treball}$	$dM = \frac{\kappa}{8\pi G} dA_H + \Omega_H dJ$
Segona	$\delta S \geq 0$ en tot procés físic	$\delta A_H \geq 0$ en tot procés físic

Taula 1.1.1: Relació entre les lleis de la mecànica dels forats negres i les lleis de la termodinàmica.

de proporcionalitat. Cal tenir present però que en Relativitat General clàssica la temperatura d'un forat negre és estrictament zero ja que un forat negre no pot emetre res. Ara bé, Hawking va descobrir que quan es tenen en compte els efectes quàntics, un forat negre emet partícules amb un espectre de cos negre a una temperatura $T = \hbar\kappa/(2\pi ck_B)$ [10]. Per tant, realment $T = \hbar\kappa/(2\pi ck_B)$ és la temperatura del forat negre i $S_{\text{BH}} = A_H c^3/(4\hbar G)$ la seva entropia. Qualsevol teoria quàntica de la gravetat per tant ha de ser capaç de reproduir aquesta relació entre l'entropia, entesa com el nombre de microestats compatibles amb un mateix estat macroscòpic, i l'àrea del forat negre.¹ Fins ara, únicament la Teoria de Cordes ha estat capaç de reproduir la relació entre l'entropia i l'àrea d'un forat negre a partir del comptatge dels microestats per una classe molt concreta de forats negres (supersimètrics i a prop de supersimetria) [12]. Recentment s'han produït avenços molt destacables en el comptatge dels microestats de forats negres corresponents a solucions de gravetat pura [13].

Un aspecte que cal remarcar és que tots aquests desenvolupaments no haurien estat possibles sense les solucions exactes ja que moltes de les propietats clau dels forats negres només es posen de manifest en les solucions analítiques. Aquest fet encara s'accentua més quan hom considera espais-temps de dimensionalitat $D > 4$ on, com veurem, la dinàmica és molt més rica que en quatre dimensions. Des del punt de vista de Teoria de Cordes és natural considerar $D > 4$ ja que les teories quànticament consistents estan formulades en $D = 10$ (o $D = 11$ pel cas de Teoria M) i com hem esmentat abans, la Relativitat General emergeix en el seu límit de baixes energies. Aquesta és una de les raons per les quals ens hem plantejat l'objectiu d'obtenir noves solucions exactes en $D > 4$. Una altra raó per estudiar forats negres en dimensions més altes és que en certs escenaris de "braneworlds", les dimensions compactes són "grans" i podrien resultar observables al futur col·lisionador de partícules LHC [14]. Segons alguns d'aquests models, seria possible produir forats negres en $D > 4$ als acceleradors, que s'evaporarien ràpidament emetent radiació de Hawking.

La solució de Myers-Perry [15], la qual generalitza la solució de Kerr per $D > 4$, proporciona clares evidències de la riquesa de la dinàmica. Per exemple, es pot veure que per aquest tipus de forats negres rotants, en $D \geq 6$ el moment angular pot ser arbitràriament gran sense desenvolupar corbes temporals tancades. Altres evidències provenen del descobriment de Gregory i Laflamme de què determinades solucions de tipus "corda negra", construïdes afegint n direccions planes a forats negres en d dimensions, són inestables a nivell clàssic sota perturbacions

¹Aquesta relació entre l'entropia i l'àrea és vàlida quan el forat negre té una àrea diferent de zero a nivell clàssic (acció d'Einstein-Hilbert). En el marc de Teoria de Cordes i pels anomenats "forats negres petits", l'àrea clàssica és zero però quan hom considera correccions d'ordre superior en el tensor de curvatura, i que són proporcionals a la longitud de la corda fonamental, es pot veure que desenvolupen una àrea de l'ordre de l'àrea de Planck. En aquests casos, S_{BH} s'obté mitjançant la fórmula de Wald [11].

lineals [16]. Cal dir que (la secció espacial de) l'horitzó d'aquestes solucions en $D = d + n$ dimensions té una topologia $S^{(d-2)} \times \mathbb{R}^n$ i per tant, tot i no ser compacte, ja veiem que el teorema de Hawking sobre la topologia de l'horitzó no té una extensió senzilla a dimensions més grans que quatre. Notem que és possible compactificar les direccions planes per tal que formin un torus \mathbb{T}^n i així estabilitzar la solució, però l'espai-temps que resulta no és asimptòticament pla.

Malgrat que les evidències sobre la riquesa dinàmica que acabem d'esmentar són molt destacables per elles mateixes, creiem que el descobriment d'un forat negre asimptòticament pla en cinc dimensions de tipus "anell negre" per part d'Emparan i Reall [17] fou encara d'igual o fins i tot major importància. La mètrica es pot escriure com [17, 18]

$$ds^2 = -\frac{F(y)}{F(x)} \left(dt + C_\lambda \frac{R(1+y)}{F(y)} d\psi \right)^2 + \frac{R^2}{(x-y)^2} F(x) \left[-\frac{G(y)}{F(y)H(y)^3} d\psi^2 - \frac{dy^2}{G(y)} + \frac{dx^2}{G(x)} + \frac{G(x)}{F(x)H(x)^3} d\phi^2 \right], \quad (1.1.2)$$

on

$$F(\xi) = 1 + \lambda\xi, \quad G(\xi) = (1 - \xi^2)(1 + \nu\xi), \quad C_\lambda = \sqrt{\lambda(\lambda - \nu) \frac{1 + \lambda}{1 - \lambda}}, \quad (1.1.3)$$

amb la restricció $0 < \nu \leq \lambda < 1$, i les coordenades x i y estan definides en els intervals

$$-1 \leq x \leq 1, \quad -\infty < y \leq -1. \quad (1.1.4)$$

En primer lloc hem de dir que l'horitzó d'aquest forat negre té una topologia $S^2 \times S^1$, cosa que constitueix un exemple explícit de la diversitat de possibles horitzons dels forats negres (estacionaris) a mesura que la dimensionalitat de l'espai-temps s'incrementa.² Una altra propietat que cal esmentar és el fet que per una de les dues branques de solucions el moment angular pot ser arbitràriament gran. Ara bé, el més destacable d'aquesta solució és que presenta no unicitat (discreta): per a certs valors dels paràmetres, existeixen un forat negre i (dos) anells negres amb les mateixes càrregues conservades, M i J . Posteriorment aquestes solucions foren generalitzades i es va veure que els anells negres també podien incorporar càrregues dipolars, cosa que no és possible en forats negres esfèrics [18]. El fet més destacable és que aquestes càrregues no són conservades i, degut a la seva naturalesa dipolar, un observador a l'infinit no mesuraria cap càrrega neta. A nivell clàssic, les càrregues dipolars estan descrites per paràmetres que prenen valors continus i per tant la no unicitat esdevé infinita!

És a aquesta sèrie de troballes que esperem poder donar una resposta a nivell microscòpic des de Teoria de Cordes. A la vegada, també esperem que ens ajudin a entendre millor la teoria fonamental.

1.1.2 Introducció a la tesi

En aquesta secció presentem una breu introducció als diferents temes que hem tractat en aquesta tesi.

Anells negres no supersimètrics amb càrregues D1-D5-P

Com ja hem esmentat, totes les solucions de buit de Relativitat General són solucions de Teoria de Cordes a baixes energies. Si considerem el sector bosònic de les diferents teories de cordes, a

²Vegeu [19] per una generalització del teorema de Hawking sobre les possibles topologies de l'horitzó d'un forat negre estacionari en $D > 4$.

més del camp gravitacional G_{MN} , hi ha d'altres camps, que s'agrupen en els sectors de Neveu-Schwarz (NS-NS) i Ramond (R-R). L'espectre de partícules del sector bosònic a baixes energies (supergravetat) està resumit a la taula 1.1.2.

Teoria	sector NS-NS	sector R-R
tipus IIA	G_{MN}, B_2, Φ	C_1, C_3
tipus IIB	G_{MN}, B_2, Φ	C_0, C_2, C_4^\pm
tipus I	G_{MN}, Φ	C_2
heteròtica	G_{MN}, B_2, Φ	–

Taula 1.1.2: Espectre de partícules de les diferents teories de supergravetat en deu dimensions que emergeixen en el límit de baixes energies de les diferents teories de cordes. Els subíndex en els camps B_i i C_i indiquen el rang de les p -formes.

El punt important és que, donada una solució de buit, és possible construir analíticament una nova solució que incorpora les càrregues corresponents als camps gauge mitjançant una sèrie de transformacions (boosts i U -dualitats), que resumim tot seguit.

En primer lloc tenim la transformació de T -dualitat, que es basa en l'existència d'isometries al llarg de direccions compactes. Si z parametriza una cercle de radi R de manera que $z \sim z + 2\pi R$, després d'efectuar una T -dualitat el radi d'aquest cercle esdevé $R' = \alpha'/R$. A nivell microscòpic, aquesta operació intercanvia els modes de la corda amb moment amb modes amb “winding”. A nivell de les teories de tipus II, que és el que ens interessarà, la T -dualitat intercanvia les dues teories IIA \leftrightarrow IIB. Pel cas d'una sola direcció compacta z , l'acció de la T -dualitat en el marc de la corda³ sobre els diferents camps de baixes energies d'aquestes teories és la següent. Pels camps de NS-NS,

$$G'_{zz} = \frac{1}{G_{zz}}, \quad G'_{\mu z} = \frac{B_{\mu z}}{G_{zz}}, \quad G'_{\mu\nu} = G_{\mu\nu} - \frac{1}{G_{zz}}(G_{\mu z}G_{\nu z} - B_{\mu z}B_{\nu z}), \quad (1.1.5)$$

$$B'_{\mu z} = \frac{G_{\mu z}}{G_{zz}}, \quad B'_{\mu\nu} = B_{\mu\nu} - \frac{1}{G_{zz}}(G_{\mu z}B_{\nu z} - G_{\nu z}B_{\mu z}), \quad (1.1.6)$$

$$e^{2\Phi'} = \frac{e^{2\Phi}}{G_{zz}}, \quad (1.1.7)$$

mentre que al sector de R-R tenim,

$$C'_{n\mu\dots\nu\alpha z} = C_{n-1\mu\dots\nu\alpha} - (n-1)\frac{C_{n-1[\mu\dots\nu]z}G_{|\alpha|z}}{G_{zz}}, \quad (1.1.8)$$

$$C'_{n\mu\dots\nu\alpha\beta} = C_{n+1\mu\dots\nu\alpha\beta z} + nC_{n-1[\mu\dots\nu\alpha}B_{\beta]z} + n(n-1)\frac{C_{n-1[\mu\dots\nu]z}B_{|\alpha|z}G_{|\beta]z}}{G_{zz}}. \quad (1.1.9)$$

En aquestes expressions, ∂_z és un vector de Killing de la mètrica al llarg de la direcció del qual efectuem la T -dualitat, i els índex μ, ν, \dots , indiquen coordenades qualssevol.

En segon lloc tenim que la teoria de tipus IIB és invariant sota el que s'anomena dualitat S . Aquesta simetria, que encara no està demostrada a nivell quàntic, és no pertorbativa ja que intercanvia els règims d'acoblament fort i feble, $g'_s = 1/g_s$, on g_s és la constant d'acoblament

³Recordem que el marc de la corda i el marc d'Einstein estan relacionats per una transformació conforme que involucra el dilatò: $G_{EMN} = e^{-\Phi/2}G_{MN}$. És la mètrica G_{MN} la que realment “veu” la corda.

de la corda, la qual depèn del dilatò Φ . A nivell quàntic, el grup de simetria de la S -dualitat és $SL(2, \mathbb{Z})$. Nosaltres ens centrarem en el règim clàssic de baixes energies, i es pot comprovar que l'acció de supergravetat de tipus IIB, suposant que l'escalar de R-R C_0 és zero per simplicitat, és invariant sota les transformacions

$$\Phi' = -\Phi, \quad G'_{MN} = e^{-\Phi} G_{MN}, \quad (1.1.10)$$

$$B'_2 = C_2, \quad C'_2 = -B_2, \quad (1.1.11)$$

$$C'_4 = C_4, \quad (1.1.12)$$

mentre que la mètrica en el marc d'Einstein és invariant. Aquestes transformacions formen un subgrup de $SL(2, \mathbb{R})$, el qual deixa invariant l'acció de supergravetat de tipus IIB.

Mitjançant les transformacions (1.1.5)-(1.1.12) que acabem de descriure, que conjuntament formen el grup de U -dualitat de la Teoria de Cordes, podem generar noves solucions a partir de solucions de les equacions d'Einstein al buit de la següent manera. Partim d'una solució de buit en d dimensions i la “pugem” a deu dimensions afegint $10 - d$ dimensions planes a la solució original, que compactifiquem en un torus \mathbb{T}^{10-d} . Seguidament, mitjançant una sèrie de boosts, T -dualitats al llarg de les direccions compactes i S -dualitats, podem construir una nova solució amb càrregues de corda fonamental F1, de 5-brana solitònica NS5, de monopols de Kaluza-Klein i/o de Dp -branes. D'aquesta manera, la nova solució que haguem obtingut, sigui supersimètrica o no, admetrà una interpretació en termes dels graus de llibertat fonamentals de la teoria. Vegeu [20] per més detalls i referències.

Des de Teoria de Cordes no s'havia pogut preveure l'existència dels anells negres i per tant no quedava massa clar quin era el paper d'aquests objectes. La situació va canviar amb el descobriment dels supertubs [21]. Els supertubs consisteixen en configuracions de D2 branes cilíndriques amb cordes fonamentals i D0 branes dissoltes en el seu volum-món. Els camps elèctric i magnètic de les cordes fonamentals i de les D0 branes donen lloc a un moment angular que impedeix que la configuració col·lapsi. El més destacable d'aquestes solucions és que preserven 1/4 de les supersimetries del buit de la teoria IIA. El paper dels anells negres dins de la teoria de cordes es va dil·lucidar a [22], on es va mostrar que els anells negres amb càrregues de D1 i D5 corresponien a supertubs excitats tèrmicament. La connexió entre els anells negres i els supertubs es va veure reforçada gràcies al descobriment dels anells negres supersimètrics [23]. Quan pugem aquestes solucions a la teoria de tipus IIB, es pot veure que corresponen precisament a supertubs amb càrregues D1-D5-P.

L'anell negre supersimètric més general està descrit per 7 paràmetres independents. Ara bé, la solució no supersimètrica construïda a [22] no és prou general com per connectar contínuament amb la solució supersimètrica més general. Per tant, un primer objectiu que ens vam proposar fou el de, partint del anell negre més general de què es disposava [18], construir l'anell negre no supersimètric més general mitjançant una sèrie de boosts i U -dualitats. Pensem que disposar d'aquesta solució és interessant perquè, com acabem d'argumentar, els anells negres no supersimètrics descriuen les excitacions tèrmiques dels supertubs. D'aquesta manera i en el context de Teoria de Cordes, podríem estudiar aquestes solucions a nivell microscòpic amb supersimetria i a prop de supersimetria, on tenim un cert control sobre la teoria i, per tant, intentar respondre a qüestions com la no unicitat dels forats negres o la diversitat de topologies dels horitzons en $D > 4$. Recordem que gràcies a la supersimetria, existeixen teoremes de no-renormalització que ens permeten estudiar certes quantitats, com ara el nombre de microestats, en el règim d'acoblament feble i llavors fer extrapolacions al règim d'acoblament fort, on trobem els forats negres. Aquest treball és el que descrivim al capítol 2.

Anells negres amb rotació a la S^2

Una segona línia de recerca que hem seguit ha estat la d'intentar generalitzar les solucions de anells negres que ja es coneixien. Des del punt de vista estrictament de la Relativitat General, obtenir noves solucions exactes sempre és interessant ja que poden permetre estudiar nous aspectes de la dinàmica de l'espai-temps. Referent a aquest darrer punt, a mesura que es van descobrint noves solucions de gravetat pura en dimensions més altes, ens emportem sorpreses. Per tant, creiem que és important ampliar el ventall de solucions. En el cas concret dels anells negres, a la solució original de [17] el moment angular és al llarg de la S^1 . Per tant, una generalització natural consisteix a considerar anells negres que estiguin rotant al llarg de la S^2 . Aquesta solució ja havia estat construïda a [24] mitjançant un mètode de generació de solucions, però la forma en què havia estat presentada (coordenades de Weyl) la feien poc útil de cara a futures aplicacions. És més, algunes de les seves propietats no eren manifestes. Per tant, resultava interessant obtenir el anells negres rotant al llarg de la S^2 en unes coordenades adaptades a la geometria dels anells negres [17, 18]. Aquest treball es descriu al capítol 3.

Saturn negre

En cinc dimensions els forats negres poden presentar rotació en dos plans independents. Per tant, després de considerar l'anell negre amb rotació a la S^2 , és natural intentar trobar la solució amb rotació tant a la S^1 com a la S^2 . Aquesta solució generalitza els anells negres anteriors i el forat negre de Myers-Perry (MP) amb dos moments angulars independents, i es redueix a aquest últim en el límit en què el radi de l'anell negre tendeix a zero. Ara bé, és molt difícil resoldre les equacions d'Einstein si hom no parteix d'un bon *ansatz*. Hi ha però una classe molt especial de solucions de les equacions d'Einstein al buit, conegudes com les solucions estacionàries i axisimètriques [25], que en cinc dimensions inclouen els anells negres i els forats negres amb doble rotació. Per a aquesta classe de solucions, les equacions d'Einstein al buit se simplifiquen d'una manera extraordinària i de fet, com veurem tot seguit, existeix un mètode sistemàtic per trobar noves solucions dins d'aquesta classe.

Per definició, els espais-temps estacionaris i axisimètrics en D -dimensions són aquells que admeten $D - 2$ vectors de Killing que commuten i un dels quals és el Killing temporal [25]. Per a aquesta classe de solucions, la mètrica es pot escriure com

$$ds^2 = G_{ab} dx^a dx^b + e^{2\nu} (d\rho^2 + dz^2) , \quad (1.1.13)$$

on $a, b = 1, \dots, D - 2$, i totes les components de la mètrica són funcions solsament de ρ i z . Amb tota generalitat podem escollir les coordenades de manera que $\det G = -\rho^2$. Per a aquestes solucions, les equacions d'Einstein es divideixen en dos grups, un per a la matriu G ,

$$\partial_\rho U + \partial_z V = 0 , \quad (1.1.14)$$

on $U = \rho(\partial_\rho G)G^{-1}$ i $V = \rho(\partial_z G)G^{-1}$, i un segon grup per al factor $e^{2\nu}$,

$$\partial_\rho \nu = \frac{1}{2} \left[-\frac{1}{\rho} + \frac{1}{4\rho} \text{Tr}(U^2 - V^2) \right] , \quad \partial_z \nu = \frac{1}{4\rho} \text{Tr}(UV) . \quad (1.1.15)$$

Les equacions (1.1.15) per a ν compleixen la condició d'integrabilitat $\partial_\rho \partial_z \nu = \partial_z \partial_\rho \nu$ com a conseqüència de (1.1.14). Per tant, un cop hem trobat una solució $G_{ab}(\rho, z)$ de (1.1.14), sempre podem determinar $\nu(\rho, z)$ per mitjà d'una integral de camí i tenim garantit que la solució existeix i és única.

El sistema d'equacions format per $\det G = -\rho^2$ i (1.1.14), constitueix el que s'anomena un sistema completament integrable [26]. És a dir, existeix un parell d'equacions espectrals *lineals*, anomenat parell de Lax, tal que les seves condicions de compatibilitat es redueixen al sistema original. Gràcies a aquest fet, es poden construir un nombre infinit de solucions a partir de solucions ja conegudes mitjançant un procediment purament algebraic, que en el context de gravetat es coneix com a mètode de Belinski-Zakharov (BZ), i que descriurem tot seguit.

Pel cas que ens ocupa, les equacions espectrals són

$$D_1\Psi = \frac{\rho V - \lambda U}{\lambda^2 + \rho^2} \Psi, \quad D_2\Psi = \frac{\rho U + \lambda V}{\lambda^2 + \rho^2} \Psi, \quad (1.1.16)$$

on D_1 i D_2 són dos operadors diferencials que commuten, la forma dels quals és:

$$D_1 = \partial_z - \frac{2\lambda^2}{\lambda^2 + \rho^2} \partial_\lambda, \quad D_2 = \partial_\rho + \frac{2\lambda\rho}{\lambda^2 + \rho^2} \partial_\lambda. \quad (1.1.17)$$

El paràmetre λ que apareix a les expressions anteriors es coneix com a paràmetre espectral i, en general, és complex i independent de ρ i z . La funció $\Psi(\lambda, \rho, z)$ és l'anomenada funció generatriu i consisteix en una matriu $(D-2) \times (D-2)$ tal que $\Psi(0, \rho, z) = G(\rho, z)$, on G és solució de (1.1.14).

Gràcies al fet que (1.1.16) siguin lineals podem construir noves solucions mitjançant solucions ja conegudes amb el mètode de “vestir” les solucions. Hom parteix d'una solució “llavor” G_0 , construeix les matrius U_0 i V_0 , i determina la funció generatriu Ψ_0 que és solució de (1.1.16). Seguidament cerquem una nova solució de la forma

$$\Psi = \chi\Psi_0, \quad (1.1.18)$$

on $\chi = \chi(\lambda, \rho, z)$ és la matriu “vestit”. Introduint (1.1.18) a (1.1.16), hom obté un nou sistema d'equacions per a la matriu χ :

$$D_1\chi = \frac{\rho V - \lambda U}{\lambda^2 + \rho^2} \chi - \chi \frac{\rho V_0 - \lambda U_0}{\lambda^2 + \rho^2}, \quad D_2\chi = \frac{\rho U + \lambda V}{\lambda^2 + \rho^2} \chi - \chi \frac{\rho U_0 + \lambda V_0}{\lambda^2 + \rho^2}. \quad (1.1.19)$$

Per tal que la mètrica final $G = \Psi(0, \rho, z)$ sigui real cal que es compleixi $\bar{\chi}(\bar{\lambda}) = \chi(\lambda)$ i $\bar{\Psi}(\bar{\lambda}) = \Psi(\lambda)$, on la barra indica que prenem el complex conjugat. De la mateixa manera, per tal que G sigui simètrica, cal imposar $G = \chi(\lambda)G_0\chi^T(-\rho^2/\lambda)$. Finalment, per assegurar la compatibilitat d'aquesta última condició amb (1.1.18), hem d'imposar $\chi(\infty) = \mathbb{1}$, on $\mathbb{1}$ és la matriu identitat $(D-2) \times (D-2)$.

A nosaltres ens interessaran les anomenades solucions solitòniques. Aquest tipus de solucions es caracteritzen pel fet que la matriu vestit $\chi(\lambda, \rho, z)$ presenta pols simples al pla complex λ . Així, per una solució amb n solitons, la matriu χ tindrà n pols simples i per tant es pot escriure com

$$\chi = \mathbb{1} + \sum_{k=1}^n \frac{R_k}{\lambda - \tilde{\mu}_k}, \quad (1.1.20)$$

on les matrius R_k i les funcions $\tilde{\mu}_k$ només depenen de ρ i z . Introduint aquesta expressió de la matriu χ a les equacions (1.1.19) i tenint en compte l'estructura analítica de les equacions resultants als pols $\lambda = \tilde{\mu}_k$, hom pot determinar les funcions $\tilde{\mu}_k$ i les matrius R_k . Concretament, les posicions dels pols vénen donades per

$$\tilde{\mu}_k = \pm \sqrt{\rho^2 + (z - a_k)^2} - (z - a_k), \quad (1.1.21)$$

on els paràmetres a_k són constants complexes. Nosaltres ens restringim al cas en què les a_k són reals, ja que corresponen a solucions estacionàries. Ens referirem al pol amb signe “+” com a solitó i el denotarem per μ_k , mentre que al pol amb signe “-” l’anomenarem anti-solító i el denotarem per $\bar{\mu}_k$. Notem que $\mu_k \bar{\mu}_k = -\rho^2$.

Pel que fa a les matrius R_k , es pot veure que són degenerades i vénen donades per

$$(R_k)_{ab} = n_a^{(k)} m_b^{(k)}, \quad (1.1.22)$$

on els vectors $m^{(k)}$ es poden obtenir a partir de la solució llavor mitjançant

$$m_a^{(k)} = m_{0b}^{(k)} [\Psi_0^{-1}(\tilde{\mu}_k, \rho, z)]_{ba}. \quad (1.1.23)$$

A l’expressió anterior, els $m_0^{(k)}$ són vectors de $D - 2$ components constants, que anomenarem vectors de BZ. Ens referirem a les components d’aquests vectors com a paràmetres de BZ i, com veurem, controlaran el moment angular de la solució estacionària obtinguda a partir d’una solució estàtica. Es pot comprovar que la solució final és invariant sota una transformació d’escala del vectors de BZ, $m_0^{(k)} \rightarrow \sigma_k m_0^{(k)}$ per qualsevol constant $\sigma_k \neq 0$. Per tant, sense pèrdua de generalitat, sempre podem considerar que una de les components diferents de zero dels vectors $m_0^{(k)}$ és 1.

Definint la matriu simètrica Γ com

$$\Gamma_{kl} = \frac{m_a^{(k)} (G_0)_{ab} m_b^{(l)}}{\rho^2 + \tilde{\mu}_k \tilde{\mu}_l}, \quad (1.1.24)$$

es pot veure que els vectors $n^{(k)}$ vénen donats per

$$n_a^{(k)} = \sum_{l=1}^n \frac{(\Gamma^{-1})_{lk} m_c^{(l)} (G_0)_{ca}}{\tilde{\mu}_l}. \quad (1.1.25)$$

Finalment, utilitzant (1.1.23) i (1.1.25) a (1.1.20) i tenint en compte que $G = \Psi(0) = \chi(0)\Psi_0(0)$, obtenim un nova mètrica amb n solitons:

$$G_{ab} = (G_0)_{ab} - \sum_{k,l=1}^n \frac{(G_0)_{ac} m_c^{(k)} (\Gamma^{-1})_{kl} m_d^{(l)} (G_0)_{db}}{\tilde{\mu}_k \tilde{\mu}_l}. \quad (1.1.26)$$

La mètrica G que acabem d’obtenir no compleix la condició $\det G = -\rho^2$, sinó que hom pot comprovar que, per una transformació de n solitons,

$$\det G = (-1)^n \rho^{2n} \left(\prod_{k=1}^n \tilde{\mu}_k^{-2} \right) \det G_0. \quad (1.1.27)$$

Per tal d’obtenir una solució física $G^{(\text{fis})}$ tal que $\det G^{(\text{fis})} = -\rho^2$ podem multiplicar la mètrica G obtinguda mitjançant (1.1.26) per un cert factor que involucra potències de ρ i de les funcions $\tilde{\mu}_k$. D’aquesta manera, en quatre dimensions hom pot construir, per exemple, solucions de forats negres corresponents a (multi)Kerr-NUT a partir d’espai de Minkowski. Ara bé, aquest procediment, que anomenem renormalització uniforme, aplicat a espais-temps en $D > 4$ dóna lloc a solucions singulars.

Aquest problema aparent ha estat resolt recentment per Pomeransky [27], que ha adaptat el mètode de BZ a un nombre de dimensions D arbitrari. La idea de Pomeransky consisteix en

adonar-se que (1.1.27) és independent dels paràmetres de BZ. Així, partim d'una solució llavor diagonal $(G_0, e^{2\nu_0})$ i eliminem una sèrie de solitons amb paràmetres de BZ trivials. Seguidament, apliquem el mètode de BZ que acabem de descriure per afegir els *mateixos* solitons però ara considerem paràmetres de BZ arbitraris. La mètrica resultant satisfà, per construcció, $\det G = -\rho^2$. Finalment, podem obtenir el factor conforme $e^{2\nu}$ corresponent a la solució final a partir del factor conforme de la llavor,

$$e^{2\nu} = e^{2\nu_0} \frac{\det \Gamma_{kl}}{\det \Gamma_{kl}^{(0)}}, \quad (1.1.28)$$

on les matrius $\Gamma^{(0)}$ i Γ s'obtenen mitjançant l'equació (1.1.24) utilitzant G_0 i G respectivament.

Volem destacar que el procediment que acabem de descriure per tal d'obtenir noves solucions a partir de solucions ja conegudes és purament algebraic.

El nostre interès era en espais de cinc dimensions i mitjançant l'adaptació del mètode de BZ a dimensions $D > 4$ per part de Pomeransky [27], hem pogut intentar trobar l'anell negre amb doble rotació. Malgrat no haver estat capaços d'assolir aquesta fita,⁴ el mètode de BZ ens ha permès obtenir d'altres solucions de buit molt interessants. Concretament, hem considerat espais-temps asimptòticament plans en cinc dimensions amb més d'un forat negre i en què un dels forats negres és un anell negre.

En quatre dimensions, Kramer i Neugebauer havien construït una solució corresponent a dos forats negres de Kerr coaxials mitjançant un mètode equivalent al de BZ [29]. Per a aquesta solució però, la interacció d'espí entre els forats negres no és suficient com per compensar l'atracció gravitatòria i, per tant, la solució és singular. En aquest cas, la singularitat consisteix en una barra finita que s'estén entre els dos forats negres i que proporciona la pressió necessària per tal de mantenir el sistema en equilibri. Quan hom introdueix camps gauge i imposa la supersimetria, és possible construir solucions amb més d'un forat negre i que siguin perfectament regulars. En aquest cas però es produeix una cancel·lació entre les diferents forces que governen el sistema i gràcies a aquest fet és possible construir solucions amb un nombre arbitrari de forats negres superposant funcions harmòniques. De fet, Gutowski i Gauntlett ja havien construït una solució supersimètrica corresponent a diversos anells negres concèntrics rotants, en equilibri, que rodegen un forat negre esfèric, també amb rotació [30].

Nosaltres però ens concentrem en solucions de les equacions d'Einstein al buit i l'únic camp que considerem és el gravitatori. En cinc dimensions sabem que en els anells negres el moment angular *sí* que pot compensar l'auto-atracció gravitatòria i donar lloc a una solució perfectament regular. Per tant, hauria ser possible construir una solució que consisteixi en un anell negre amb un forat negre de MP al seu interior, en el mateix pla de l'anell. Per tal que la configuració resultant estigui en equilibri i sigui regular, caldrà que els dos objectes estiguin rotant de tal manera que el moment angular compensi l'atracció gravitatòria. Per raons de semblança amb el planeta del sistema solar, anomenem a aquesta solució *saturn negre*. La construcció d'aquesta solució i l'estudi de les seves propietats físiques es descriu al capítol 5.

Fases dels forats negres en cinc dimensions

Tal i com hem destacat, un dels aspecte més interessants dels forats negres en dimensions $D > 4$ és la no unicitat. Si ens centrem en l'exemple concret dels anells negres i els forats negres en cinc dimensions, tenim que existeixen un forat negre i dos anells negres amb les

⁴Recentment, Pomeransky i Sen'kov [28] han pogut obtenir l'anell negre amb doble rotació mitjançant el mètode de BZ.

mateixes càrregues conservades M i J [17]. Típicament es representa el diagrama de fases en la col·lectivitat microcanònica de manera que, un cop fixada l'escala del sistema (massa total), representem l'àrea del forat negre (entropia) en funció del seu moment angular. Per tant, un cop disposem d'un nou forat negre en cinc dimensions, resulta interessant determinar quina regió del diagrama de fases ocupa i fins a quin punt viola la unicitat. Així doncs, un cop obtinguda la solució del saturn negre, havíem de determinar el seu diagrama de fases amb detall.

Esperem que el diagrama de fases pel saturn negre sigui especialment ric. La raó és que els anells negres amb un moment angular prou gran tenen una àrea molt petita i a la vegada un radi arbitràriament gran, de manera que la seva influència sobre el forat negre central es pot fer negligible. Per altra banda, pel forat negre de MP en cinc dimensions, el moment angular no pot sobrepassar un cert valor màxim. Per tant, gràcies al fet que el forat negre que es troba al centre del saturn també té un moment angular intrínsec, podem pensar que ha de ser possible un cobrir rang molt gran d'àrees i moments angulars distribuïnt la massa total i el moment angular total entre els dos components. Aquest treball es presenta al capítol 6.

Forats negres supersimètrics a AdS_5

Per tal d'estudiar aspectes quàntics dels forats negres ens cal una teoria quàntica que inclogui la gravetat, que en el nostre cas és la Teoria de Cordes. Un dels avenços més importants que s'han produït recentment en Teoria de Cordes és la formulació de la correspondència AdS/CFT [31]. Segons aquesta conjectura, Supercordes de tipus IIB en $AdS_5 \times S^5$ és dual a $\mathcal{N} = 4$ $U(N)$ Super Yang Mills en $3 + 1$ dimensions. Per tant, podem estudiar gravetat quàntica mitjançant una teoria gauge en quatre dimensions sense gravetat! És més, podem tractar la teoria gauge a nivell pertorbatiu quan la constant d'acoblament de 't Hooft obeeix $g_{\text{YM}}^2 N \ll 1$. Per altra banda, la descripció de Teoria de Cordes en termes de supergravetat és acurada quan el radi de curvatura del factor AdS_5 i de la S^5 és gran comparat amb l'escala de la corda ℓ_s : $R^4/\ell_s^4 \sim g_{\text{YM}}^2 N \gg 1$. Així doncs, les dues descripcions són complementàries: podem descriure el règim no pertorbatiu de la teoria de camps mitjançant supergravetat clàssica i a la inversa. Per tant, esperem que gràcies a aquesta dualitat puguem respondre a algunes de les qüestions relacionades amb la física dels forats negres.

Una classe de forats negres que poden admetre una descripció dual en termes d'una teoria gauge són aquells que asimptòticament tendeixen a AdS_5 . En el marc de Teoria de Cordes tenim una descripció pertorbativa dels forats negres quan aquests preserven un cert nombre de supersimetries gràcies als teoremes de no-renormalització [12]. Així doncs, ens concentrem en forats negres supersimètrics que asimptòticament siguin AdS_5 .

La teoria més senzilla en què podem trobar aquest tipus de forats negres i que a la vegada està inclosa en supergravetat de tipus IIB, és supergravetat "gauged" minimal en $D = 5$:

$$I = \frac{1}{4\pi G} \int \left[\left(\frac{R_5}{4} + 3g^2 \right) \star 1 - \frac{1}{2} F_2 \wedge \star F_2 - \frac{2}{3\sqrt{3}} F_2 \wedge F_2 \wedge A_1 \right], \quad (1.1.29)$$

on R_5 és l'escalar de Ricci, $F_2 = dA_1$ és el tensor de Maxwell corresponent al camp $U(1)$, i g és l'inversa del radi AdS_5 , que és el buit de la teoria. Totes les solucions bosòniques supersimètriques d'aquesta teoria han estat classificades recentment a [32]. Aquestes solucions admeten una sèrie de tensors globalment definits que es poden construir com a bilineals de l'espino de Killing. Concretament, tenim un escalar f , un vector real V i tres 2-formes reals X^i , $i = 1, 2, 3$, però només f , V i X^1 són invariants gauge.

Mitjançant les identitats de Fierz en $D = 5$, es pot comprovar que els tensors esmentats anteriorment satisfan les següents relacions algebraiques:

$$V^\alpha V_\alpha = -f^2, \quad (1.1.30)$$

$$X^i \wedge X^j = -2\delta_{ij} f \star V, \quad (1.1.31)$$

$$i_V X^i = 0, \quad (1.1.32)$$

$$i_V \star X^i = -f X^i, \quad (1.1.33)$$

$$(X^i)_{\gamma\alpha} (X^j)_{\beta}^{\gamma} = \delta_{ij} (f^2 \eta_{\alpha\beta} + V_\alpha V_\beta) - \epsilon_{ijk} f (X^k)_{\alpha\beta}, \quad (1.1.34)$$

on $\epsilon_{123} = +1$. De la primera expressió veiem que V pot ser tipus temps ($f \neq 0$) o nul ($f = 0$).

Aplicant la derivada supercovariant als tensors anteriors podem obtenir una sèrie de relacions diferencials:

$$df = -\frac{2}{\sqrt{3}} i_V F_2, \quad (1.1.35)$$

$$D_{(\alpha} V_{\beta)} = 0, \quad (1.1.36)$$

$$dV = -\frac{4}{\sqrt{3}} f F_2 - \frac{2}{\sqrt{3}} \star (F_2 \wedge V) - 2g X^1, \quad (1.1.37)$$

$$dX^i = g\epsilon_{1ij} [2\sqrt{3} A_l \wedge X^j + 3 \star X^j]. \quad (1.1.38)$$

Mitjançant les equacions (1.1.36) i (1.1.35) es pot demostrar que $\mathcal{L}_V F_2 = 0$, on \mathcal{L} indica la derivada de Lie. Per tant, deduïm que V genera una simetria de la solució. Per altra banda, de la darrera expressió veiem que X^1 és una 2-forma tancada mentre que $X^{2,3}$ en general no ho seran.

Nosaltres estem interessats a obtenir solucions de tipus forat negre i per tant ens restringim al cas en què existeix un obert \mathcal{U} en què V és tipus temps. Per a aquesta classe de solucions, la mètrica és [32]:

$$ds^2 = -f^2(dt + w)^2 + f^{-1} ds_B^2(\mathcal{K}), \quad (1.1.39)$$

on $ds_B^2(\mathcal{K})$ és l'espai base, que és un espai de Kähler amb 2-forma de Kähler $J \equiv X^1$, w és una 1-forma definida a ds_B^2 , i tant f com w són independents de t . Sense pèrdua de generalitat podem prendre $f > 0$. La supersimetria imposa tres condicions sobre f i dw . Si definim les parts auto-dual i anti-dual de $f dw$ com

$$G^\pm = \frac{1}{2} f(dw \pm \star_4 dw), \quad (1.1.40)$$

on \star_4 denota el dual de Hodge a la base, aquestes condicions esdevénen:

$$f = -\frac{24g^2}{R}, \quad (1.1.41)$$

$$G^+ = -\frac{1}{2g} \left[\mathcal{R} + \frac{R}{4} J \right], \quad (1.1.42)$$

$$\nabla^2 f^{-1} = \frac{2}{9} G^{+mn} G_{mn}^+ - g f^{-1} G^{-mn} J_{mn} - 8g^2 f^{-2}, \quad (1.1.43)$$

on \mathcal{R} la forma de Ricci i R l'escalar de Ricci de la base. Finalment, la solució queda completament determinada especificant el camp de Maxwell:

$$F_2 = \frac{\sqrt{3}}{2} d[f(dt + w)] - \frac{G^+}{\sqrt{3}} + \sqrt{3} g f^{-1} J. \quad (1.1.44)$$

El buit de la teoria, corresponent a AdS_5 , s'obté a partir de les expressions anteriors utilitzant com a espai base la varietat de Bergmann [32]:

$$ds_{\text{Berg}}^2 = d\sigma^2 + \frac{\sinh^2(g\sigma)}{4g^2} [(\sigma_L^1)^2 + (\sigma_L^2)^2 + \cosh^2(g\sigma)(\sigma_L^3)^2] , \quad (1.1.45)$$

on les σ_L^i són les 1-formes invariants per la dreta a $SU(2)$.

Gràcies a la forma general que acabem de descriure de tota solució supersimètrica, Gutowski i Reall van ser capaços de trobar un forat negre supersimètric asimptòticament AdS_5 i perfectament regular [33]. Posteriorment aquestes solucions han estat generalitzades a [34]. De la construcció anterior deduïm que per tal d'obtenir una solució resulta clau escollir un espai base adequat. Pel forat negre de Gutowski i Reall, l'espai base és una simple deformació de la varietat de Bergmann [33]:

$$ds_B^2 = d\sigma^2 + \frac{\alpha^2 \sinh^2(g\sigma)}{g^2} [(\sigma_L^1)^2 + (\sigma_L^2)^2 + \cosh^2(g\sigma)(\sigma_L^3)^2] , \quad (1.1.46)$$

amb $\alpha > 1/2$. De la mateixa manera, per a les solucions de [34] també es pot veure que l'espai base corresponent és una altra deformació de la varietat de Bergmann. En aquest punt, la pregunta natural que ens podem fer és si és possible que existeixin anells negres supersimètrics asimptòticament AdS_5 i/o si és possible que existeixin forats negres més generals que els ja descoberts a [34]. Per tal d'intentar respondre a aquestes qüestions, és útil concentrar-se en un estudi de la geometria, en primer lloc, a prop de l'horitzó. D'aquesta manera, estudiant les propietats de l'espai base podem determinar la generalitat de les solucions ja conegudes i si és o no possible obtenir noves solucions, incloent els anells negres. Aquest treball es presenta al capítol 4.

Solucions supersimètriques de Teoria M amb factors AdS_3

Per raons fenomenològiques històricament s'havien considerat compactificacions de Teoria de Cordes a baixes energies amb factors $\mathbb{R}^{1,3}$ que preservaven un cert nombre de supersimetries. La correspondència AdS/CFT ha fet que hi hagi un gran interès per compactificacions amb factors anti-de Sitter de d dimensions, AdS_d . La raó és que aquest tipus d'espais-temps maximalment simètrics admeten espinors de Killing i apareixen típicament com la geometria de l'horitzó de solucions de supergravetat que descriuen certes configuracions de branes. Així doncs, per l'esmentada correspondència, admeten una descripció en termes d'una CFT dual. Pel cas que ens ocuparà de Teoria M, es creu que tota configuració supersimètrica amb un factor AdS_{d+2} admet una descripció dual en termes d'una teoria de camps superconforme en $(d+1)$ -dimensions. És més, gràcies a la gran simetria que presenten els espais anti-de Sitter, en molts casos hom pot construir solucions analítiques de supergravetat del tipus $AdS_{d+2} \times \mathcal{M}_n$, on \mathcal{M}_n és una certa varietat de dimensió n i així aprofundir en el coneixement de la CFT dual. Novament volem remarcar la importància de disposar de solucions exactes per tal d'entendre millor, en aquest cas, la correspondència AdS/CFT.

Paral·lelament s'ha dut a terme un programa de classificació de totes les solucions supersimètriques d'una determinada teoria que admeten, com a mínim, un espinor de Killing. La idea d'aquest programa consisteix a imposar l'existència d'un espinor de Killing, cosa que ens porta a resoldre una equació de primer ordre enlloc de les equacions del moviment, que són de segon ordre. L'avantatge rau en el fet que la condició d'integrabilitat de l'equació de l'espinor

de Killing i la identitat de Bianchi per als fluxes impliquen moltes de les components de les equacions del moviment. Per tant, construint solucions de l'equació de Killing hom pot obtenir solucions de les equacions del moviment de la teoria. A més, mitjançant l'espínor de Killing hom pot construir un cert nombre de formes diferencials com a bilineals de l'espínor. Aquestes formes en el fons descriuen propietats geomètriques de l'espai-temps i de la varietat \mathcal{M}_n . De fet, gràcies al fet que les formes diferencials s'obtenen a partir de l'espínor de Killing, és possible derivar una sèrie de condicions algebraiques i diferencials sobre aquestes formes i, per tant, sobre la geometria de la varietat. D'aquesta manera podem deduir la forma general de tota solució supersimètrica. Aquesta informació es pot codificar de forma convenient en termes de les anomenades *G-estructures* [35]. Matemàticament, una *G-estructura* en un espai-temps \mathcal{M} és un sub-fibrat principal del fibrat del marc de \mathcal{M} . Un espai-temps determinat té holonomia *G* si i només si admet una estructura *G* sense torsió. Per a solucions supersimètriques generals, la desviació del cas en què \mathcal{M} té holonomia *G* està induïda pels fluxes, i aquesta informació està codificada en la torsió intrínseca de la *G-estructura*. El punt important és que l'existència d'un espínor de Killing defineix una *G-estructura* preferida.

A nosaltres ens interessa el cas de supergravetat en onze dimensions (Teoria M a baixes energies) [36]. L'acció de la teoria és

$$I = \frac{1}{2\kappa^2} \int \left[R \star 1 - \frac{1}{2} F_4 \wedge \star F_4 - \frac{1}{6} C_3 \wedge F_4 \wedge F_4 \right]. \quad (1.1.47)$$

Per tal que una configuració dels camps bosònics preservi com a mínim una supersimetria, cal que existeixi un espínor de Killing ϵ que satisfaci l'equació

$$\nabla_\mu \epsilon + \frac{1}{288} \left[\Gamma_\mu^{\nu_1 \nu_2 \nu_3 \nu_4} - 8 \delta_\mu^{\nu_1} \Gamma^{\nu_2 \nu_3 \nu_4} \right] F_{\nu_1 \nu_2 \nu_3 \nu_4} \epsilon = 0, \quad (1.1.48)$$

on ϵ és un espínor de Majorana en onze dimensions. Vegeu [36] pels convenis. Mitjançant aquest espínor, que el prenem commutant, les formes diferencials que podem construir com a bilineals de l'espínor són:

$$\begin{aligned} K_\mu &= \bar{\epsilon} \Gamma_\mu \epsilon, \\ \Theta_{\mu_1 \mu_2} &= \bar{\epsilon} \Gamma_{\mu_1 \mu_2} \epsilon, \\ \Sigma_{\mu_1 \mu_2 \mu_3 \mu_4 \mu_5} &= \bar{\epsilon} \Gamma_{\mu_1 \mu_2 \mu_3 \mu_4 \mu_5} \epsilon, \end{aligned} \quad (1.1.49)$$

on $\bar{\epsilon} = \epsilon^T \Gamma_0$ en una representació de Majorana. Aquestes formes no són independents sinó que obeeixen una sèrie de relacions algebraiques, que es poden obtenir mitjançant les identitats de Fierz en onze dimensions. Les configuracions supersimètriques es divideixen en dos tipus segons si el vector K és tipus temps o nul. A nosaltres només ens interessa el cas en què K és nul i, en aquestes condicions, es pot veure que les formes (1.1.49) defineixen una estructura $(Spin(7) \times \mathbb{R}^8) \times \mathbb{R}$ global en onze dimensions. D'aquesta manera, tota configuració (g, F_4) supersimètrica es pot escriure com [36]:

$$ds^2 = 2e^+ \otimes e^- + ds^2(\mathcal{M}_8) + e^9 \otimes e^9, \quad (1.1.50)$$

on \mathcal{M}_8 és una varietat amb una estructura *Spin(7)* globalment definida. Les formes diferencials (1.1.49) vénen donades per:

$$K = e^+, \quad \Theta = e^+ \wedge e^9, \quad \Sigma = e^+ \wedge \phi, \quad (1.1.51)$$

on ϕ és la 4-forma de Cayley, invariant sota $Spin(7)$.

Finalment, aplicant la derivada supercovariant (1.1.48) a les formes (1.1.49), hom pot deduir les següents condicions diferencials que aquestes formes han d'obeir:

$$\begin{aligned} dK &= \frac{2}{3} \Theta \lrcorner F + \frac{1}{3} \Sigma \lrcorner \star F , \\ d\Theta &= K \lrcorner F , \\ d\Sigma &= K \lrcorner \star F - \Theta \wedge F . \end{aligned} \quad (1.1.52)$$

Les condicions (1.1.50)-(1.1.52) determinen la forma general de tota solució supersimètrica. Vegeu la segona referència de [36] pels detalls.

Malgrat que la forma general de tota solució supersimètrica de supergravetat en onze dimensions és coneguda, per a determinades aplicacions convé especialitzar-la i així obtenir resultats explícits. Concretament, si estem interessats a obtenir solucions que admetin factors AdS , resulta convenient veure l'espai AdS_{d+2} , en coordenades de Poincaré, com un cas especial d'una solució amb un factor de Minkowski $\mathbb{R}^{1,d}$ [37]. Les geometries resultants constitueixen les anomenades “wrapped brane geometries” [38], ja que els espinors de Killing que preserven són proporcionals als que preserva una M5 brana prova enrotllada en un cicle supersimètric d'una varietat amb holonomia especial. Per a aquest tipus de geometries, la forma general que ha de tenir la mètrica és:

$$ds^2 = L^{-1} ds^2(\mathbb{R}^{1,d}) + ds^2(\mathcal{M}_{10-d}) , \quad (1.1.53)$$

que és compatible amb (1.1.50), i on el factor L només depen de les coordenades de \mathcal{M}_{10-d} .

La classificació que acabem d'exposar només inclou el cas en què es preserva una supersimetria solsament. També resulta interessant poder obtenir noves solucions que preservin un cert nombre de supersimetries. Com ja hem esmentat, un espinor de Killing dóna lloc, localment, a una certa G estructura privilegiada, i quan es preserven diverses supersimetries a la vegada, les G estructures associades a cada espinor seran, en general, diferents. Així, un conjunt d'espinors de Killing definirà una G estructura preferida, el grup d'estructura de la qual serà el grup d'isotropia comú de tots els espinors de Killing. Un mètode eficient per tal obtenir la forma general de tota solució de supergravetat en onze dimensions que preserva N supersimetries és el desenvolupat a [39]. El mètode en qüestió consisteix en construir una base de l'espai d'espinors de Majorana en onze dimensions que preservi la covariància sota $Spin(7)$. Concretament, la base que s'obté és [39]:

$$\epsilon , \quad \Gamma^i \epsilon , \quad \frac{1}{8} J_{ij}^A \Gamma^{ij} \epsilon , \quad \Gamma^- \epsilon , \quad \Gamma^{-i} \epsilon , \quad \frac{1}{8} J_{ij}^A \Gamma^{-ij} \epsilon , \quad (1.1.54)$$

on les J^A , $A = 1, \dots, 7$ són un conjunt de 2-formes definides a la base $ds^2(\mathcal{M}_8) = \delta_{ij} e^i e^j$. D'aquesta manera, suposant que ϵ és Killing, qualsevol espinor de Killing adicional es pot escriure com

$$\eta = \left(f + u_i \Gamma^i + \frac{1}{8} f^A J_{ij}^A \Gamma^{ij} + g \Gamma^- + v_i \Gamma^{-i} + \frac{1}{8} g^A J_{ij}^A \Gamma^{-ij} \right) \epsilon , \quad (1.1.55)$$

on f , u_i , f^A , g , v_i i g^A són 32 funcions reals. Tenint en compte que ϵ és Killing, η serà Killing si i només si

$$\left[\mathcal{D}_\mu , f + u_i \Gamma^i + \frac{1}{8} f^A J_{ij}^A \Gamma^{ij} + g \Gamma^- + v_i \Gamma^{-i} + \frac{1}{8} g^A J_{ij}^A \Gamma^{-ij} \right] \epsilon = 0 , \quad (1.1.56)$$

on \mathcal{D}_μ és la derivada supercovariant (1.1.48). Les diferents components d'aquesta equació es poden descomposar en termes d'una suma dels espinors de la base. Per tant, el coefficient que acompanya a cada terme de la base ha de ser zero separatament. D'aquesta manera obtenim

un seguit de relacions algebraiques lineals respecte de les funcions que defineixen l'espino de Killing, les derivades primeres d'aquestes funcions, la geometria de l'espai-temps i els fluxes. El llistat complet d'aquestes equacions es troba a la quarta referència de [39].

En el nostre cas, ens hem concentrat en els aspectes *globals* dels espais-temps supersimètrics del tipus $AdS_3 \times \mathcal{M}_8$ en el marc de supergravetat en onze dimensions (1.1.47). Per tal de poder extreure les propietats globals de la geometria, imposarem que l'espai intern \mathcal{M}_8 tingui una G-estructura globalment definida amb $G = Spin(7)$, $SU(4)$ o $Sp(2)$ segons el cas. L'existència d'una estructura globalment definida a \mathcal{M}_8 és una condició més restrictiva que l'existència global d'un espino de Killing, malgrat que estan relacionades. Imposar només l'existència d'un espino de Killing en alguns casos pot donar lloc a una sèrie de complicacions que la fan poc útil des d'un punt de vista global: els espino tipus temps poden esdevenir nuls, diferents espino poden esdevenir paral·lels, etc. Una altra raó per la qual creiem que pot ser útil adoptar aquesta visió global és que són determinats aspectes globals de les solucions de supergravetat els que semblen ser rellevants en el marc la correspondència AdS/CFT.

Finalment, cal afegir que per tal d'ampliar el coneixement sobre la correspondència AdS/CFT en el marc de Teoria M, creiem que és interessant obtenir una classificació general de *totes* les solucions supersimètriques amb factors AdS . Pel cas de AdS_3 , aquest estudi no s'havia completat i per tant creiem que era necessari omplir aquest buit. Aquest treball s'exposa al capítol 7.

1.2 Resum dels resultats

1.2.1 Anells negres no supersimètrics amb càrregues D1-D5-P

En primer lloc, per tal de construir un “tub negre” amb càrregues de D1-D5-P, vam partir de l'anell amb rotació al llarg de la S^1 i tres càrregues dipolars [18]:

$$\begin{aligned}
 ds^2 &= -\frac{H(x)F(y)}{H(y)F(x)} \left(dt + C_\lambda \frac{R(1+y)}{F(y)} d\psi \right)^2 \\
 &\quad + \frac{R^2}{(x-y)^2} F(x)H(x)H(y)^2 \left[-\frac{G(y)}{F(y)H(y)^3} d\psi^2 - \frac{dy^2}{G(y)} + \frac{dx^2}{G(x)} + \frac{G(x)}{F(x)H(x)^3} d\phi^2 \right], \\
 A_1^i &= C_{-\mu_i} R \frac{1+x}{H_i(x)} d\phi,
 \end{aligned} \tag{1.2.1}$$

on

$$\begin{aligned}
 C_\lambda &= \sqrt{\lambda(\lambda-\nu)\frac{1+\lambda}{1-\lambda}}, \\
 F(\xi) &= 1 + \lambda\xi, & G(\xi) &= (1-\xi^2)(1+\nu\xi), \\
 H_i(\xi) &= 1 - \mu_i\xi, & H(\xi) &\equiv [H_1(\xi)H_2(\xi)H_3(\xi)]^{1/3}.
 \end{aligned} \tag{1.2.2}$$

Els diferents paràmetres de la solució obeeixen

$$R > 0, \quad 0 < \nu \leq \lambda < 1, \quad 0 \leq \mu_i < 1, \tag{1.2.3}$$

i les coordenades x i y prenen valors en els intervals

$$-1 \leq x \leq 1, \quad -\infty < y \leq -1, \quad \frac{1}{\min \mu_i} < y < \infty. \tag{1.2.4}$$

Quan pugem aquesta solució a la teoria IIB afegint-li cinc dimensions planes, que anomenem z i z_i , amb $i = 1, \dots, 4$ respectivament, la podem interpretar com un tub negre amb càrregues dipolars de d1, d5 i kkm:⁵

$$\begin{array}{rcl} \mu_1 & \text{kkm:} & 1 & 2 & 3 & 4 & (z) & \psi \\ \mu_2 & \text{d5:} & 1 & 2 & 3 & 4 & - & \psi \\ \mu_3 & \text{d1:} & - & - & - & - & - & \psi \end{array} , \quad (1.2.5)$$

on ψ parametriza la S^1 de l'anell. A continuació, aplicant-li la següent seqüència de boosts i dualitats,

$$S \rightarrow \text{Boost}_{\alpha_1}(z) \rightarrow T(z) \rightarrow \text{Boost}_{\alpha_2}(z) \rightarrow T(1) \rightarrow S \rightarrow T(1234) \rightarrow S \rightarrow T(z) \rightarrow T(1) \rightarrow S, \quad (1.2.6)$$

seguida d'un boost amb paràmetre α_3 al llarg de z , obtenim un tub negre amb les mateixes càrregues dipolars però, a més, amb càrregues netes de D1-D5-P. La configuració de branes resultant és

$$\begin{array}{rcl} \alpha_1 & \text{D5:} & 1 & 2 & 3 & 4 & z & - \\ \alpha_2 & \text{D1:} & - & - & - & - & z & - \\ \alpha_3 & \text{P:} & - & - & - & - & z & - \\ (\alpha_2\alpha_3), \mu_1 & \text{d1:} & - & - & - & - & - & \psi \\ (\alpha_1\alpha_3), \mu_2 & \text{d5:} & 1 & 2 & 3 & 4 & - & \psi \\ (\alpha_1\alpha_2), \mu_3 & \text{kkm:} & 1 & 2 & 3 & 4 & (z) & \psi \end{array} . \quad (1.2.7)$$

La solució que hem obtingut presenta una forma més simètrica en el marc de Teoria M, que es pot obtenir de la configuració anterior si, després de la seqüència (1.2.6), fem $\rightarrow T(34) \rightarrow T(z)$, i a continuació pugem a onze dimensions. La configuració resultant és:

$$\begin{array}{rcl} \alpha_1 & \text{M2:} & 1 & 2 & - & - & - & - \\ \alpha_2 & \text{M2:} & - & - & 3 & 4 & - & - \\ \alpha_3 & \text{M2:} & - & - & - & - & 5 & 6 \\ (\alpha_2\alpha_3), \mu_1 & \text{m5:} & - & - & 3 & 4 & 5 & 6 \\ (\alpha_1\alpha_3), \mu_2 & \text{m5:} & 1 & 2 & - & - & 5 & 6 \\ (\alpha_1\alpha_2), \mu_3 & \text{m5:} & 1 & 2 & 3 & 4 & - & - \end{array} \psi , \quad (1.2.8)$$

on hem anomenat $z_5 \equiv z$ i z_6 denota l'onzena dimensió. En aquest marc, la mètrica de la solució ve donada per:

$$\begin{aligned} ds_{11D}^2 &= ds_{5D}^2 + \left[\frac{1}{h_1} \frac{H_1(y)}{H_1(x)} \right]^{2/3} \left[h_2 h_3 \frac{H_2(x)H_3(x)}{H_2(y)H_3(y)} \right]^{1/3} (dz_1^2 + dz_2^2) \\ &+ \left[\frac{1}{h_2} \frac{H_2(y)}{H_2(x)} \right]^{2/3} \left[h_1 h_3 \frac{H_1(x)H_3(x)}{H_1(y)H_3(y)} \right]^{1/3} (dz_3^2 + dz_4^2) \\ &+ \left[\frac{1}{h_3} \frac{H_3(y)}{H_3(x)} \right]^{2/3} \left[h_1 h_2 \frac{H_1(x)H_2(x)}{H_1(y)H_2(y)} \right]^{1/3} (dz_5^2 + dz_6^2), \end{aligned} \quad (1.2.9)$$

⁵Utilitzem lletres majúscules per indicar les configuracions de D-branes que donen lloc a càrregues conservades, i amb lletres minúscules les configuracions de branes que donen lloc a càrregues dipolars (no conservades). Al costat del nom de cada càrrega indiquem els paràmetres associats a la càrrega en qüestió.

on

$$\begin{aligned}
ds_{5D}^2 &= -\frac{1}{(h_1 h_2 h_3)^{2/3}} \frac{H(x)}{H(y)} \frac{F(y)}{F(x)} \left(dt + \omega_\psi(y) d\psi + \omega_\phi(x) d\phi \right)^2 \\
&\quad + (h_1 h_2 h_3)^{1/3} F(x) H(x) H(y)^2 \\
&\quad \times \frac{R^2}{(x-y)^2} \left[-\frac{G(y)}{F(y) H(y)^3} d\psi^2 - \frac{dy^2}{G(y)} + \frac{dx^2}{G(x)} + \frac{G(x)}{F(x) H(x)^3} d\phi^2 \right],
\end{aligned} \tag{1.2.10}$$

i la 3-forma potencial és

$$\mathcal{A} = A^1 \wedge dz_1 \wedge dz_2 + A^2 \wedge dz_3 \wedge dz_4 + A^3 \wedge dz_5 \wedge dz_6. \tag{1.2.11}$$

Les expressions de les components de les 1-formes A^i ($i = 1, 2, 3$) es poden trobar a l'apèndix de [41], mentre que les funcions h_i vénen donades per

$$h_i = \cosh^2 \alpha_i - \frac{F(y) H(x)^3 H_i(y)^2}{F(x) H(y)^3 H_i(x)^2} \sinh^2 \alpha_i. \tag{1.2.12}$$

Finalment, per completitud presentem la solució corresponent a un anell negre no super-simètric amb càrregues de D1, D5 i moment P, i càrregues dipolars de d1, d5 i monopòl de Kaluza-Klein kkm. En el marc de la corda, la solució és:

$$ds_{\text{IIB}}^2 = ds_{5D}^2 + \sqrt{\frac{h_2}{h_1}} \sqrt{\frac{H_1(y) H_2(x)}{H_1(x) H_2(y)}} dz_{(4)}^2 + \frac{h_3}{\sqrt{h_1 h_2}} \frac{H_3(x)}{H_3(y)} \sqrt{\frac{H_1(y) H_2(y)}{H_1(x) H_2(x)}} \left[dz + A^3 \right]^2, \tag{1.2.13}$$

on les components de la 1-forma A^3 es troben a les equacions (A.7)-(A.9) de l'apèndix de [41], i

$$\begin{aligned}
d\tilde{s}_{5D}^2 &= -\frac{1}{h_3 \sqrt{h_1 h_2}} \frac{F(y)}{F(x)} \sqrt{\frac{H_1(x) H_2(x)}{H_1(y) H_2(y)}} \left[dt + \omega_\psi(y) d\psi + \omega_\phi(x) d\phi \right]^2 \\
&\quad + \sqrt{h_1 h_2} F(x) H_3(y) \sqrt{H_1(x) H_1(y) H_2(x) H_2(y)} \\
&\quad \times \frac{R^2}{(x-y)^2} \left[-\frac{G(y)}{F(y) H(y)^3} d\psi^2 - \frac{dy^2}{G(y)} + \frac{dx^2}{G(x)} + \frac{G(x)}{F(x) H(x)^3} d\phi^2 \right].
\end{aligned} \tag{1.2.14}$$

El dilatò és

$$e^{2\Phi} = \frac{h_2}{h_1} \frac{H_1(y) H_2(x)}{H_1(x) H_2(y)}, \tag{1.2.15}$$

mentre que les components de la 2-forma de R-R C_2 es troben a l'apèndix B de [41].

1.2.2 Anell negre amb rotació a la S^2

En segon lloc presentem la solució corresponent a un anell negre amb rotació al llarg de la S^2 . Tal i com s'exposa amb detall a [42], hem trobat la solució partint d'un ansatz prou general i analitzant els diferents límits que ha de reproduir:

límit de radi infinit \rightarrow corda negra de Kerr
 límit estàtic \rightarrow anell negre estàtic
 límit de radi zero \rightarrow forat negre de Myers-Perry

Si denotem amb ϕ la direcció azimutal de la 2-esfera, la mètrica de l'anell negre és:

$$\begin{aligned}
 ds^2 = & -\frac{H(\lambda, y, x)}{H(\lambda, x, y)} \left[dt - \frac{\lambda a y (1 - x^2)}{H(\lambda, y, x)} d\phi \right]^2 \\
 & + \frac{R^2}{(x - y)^2} H(\lambda, x, y) \left[-\frac{dy^2}{(1 - y^2)F(\lambda, y)} - \frac{(1 - y^2)F(\lambda, x)}{H(\lambda, x, y)} d\psi^2 \right. \\
 & \left. + \frac{dx^2}{(1 - x^2)F(\lambda, x)} + \frac{(1 - x^2)F(\lambda, y)}{H(\lambda, y, x)} d\phi^2 \right], \quad (1.2.16)
 \end{aligned}$$

on

$$F(\lambda, \xi) = 1 + \lambda \xi + \left(\frac{a \xi}{R} \right)^2, \quad H(\lambda, \xi_1, \xi_2) = 1 + \lambda \xi_1 + \left(\frac{a \xi_1 \xi_2}{R} \right)^2. \quad (1.2.17)$$

Les coordenades que utilitzem són les mateixes que a [18], i prenen valors en els intervals

$$1 \leq x \leq -1, \quad -\infty < y \leq -1. \quad (1.2.18)$$

En aquestes coordenades, ψ parametriza la S^1 de l'anell i $x \sim \cos \theta$, on θ és l'angle polar de la S^2 . Els paràmetres de la solució han d'obeir la relació

$$\frac{2a}{R} < \lambda < 1 + \frac{a^2}{R^2} \quad (1.2.19)$$

per tal que no hi hagi corbes temporals tancades. Finalment, notem que el paràmetre a està relacionat amb el paràmetre de rotació del forat negre de Kerr que hom retroba en el límit de radi infinit.

1.2.3 Forats negres supersimètrics en AdS_5

A continuació presentem els resultats obtinguts per a forats negres supersimètrics en AdS_5 [43].

De la construcció de [32] de totes les solucions bosòniques supersimètriques de supergravetat gauged minimal en $D = 5$ dimensions, hom podria pensar que donat un espai base qualsevol $ds_B^2(\mathcal{K})$, sempre podem trobar una solució. El primer resultat que hem obtingut consisteix a adonar-se que, com que dw és una 2-forma exacta, s'ha de complir

$$d[f^{-1}(G^+ + G^-)] = 0. \quad (1.2.20)$$

Les condicions que imposa la supersimetria impliquen que G^+ i les components de G^- al llarg de J vénen completament determinades per la geometria de la base. Per tant, la relació anterior implica que no tots els espais base \mathcal{K} que puguem escollir donaran lloc a una solució no trivial.

El segon resultat que hem obtingut consisteix a proporcionar un marc geomètric que incorpora la forma general de la geometria de prop de l'horitzó dels forats negres (esfèrics) de [34], que són els més generals que es coneixen fins al moment. En primer lloc, ens hem restringit a varietats de Kähler *tòriques* i, per tant, descrites per un potencial del tipus $\mathcal{K} = \mathcal{K}(|z_1|^2, |z_2|^2)$, on z_i , $i = 1, 2$ són coordenades complexes de la varietat. Si suposem que, en el límit $\rho \rightarrow 0$ en què ens situem a prop de l'horitzó,

(i) f^{-1} es comporta com

$$f^{-1} = \frac{c(\theta)}{\rho^2}, \quad (1.2.21)$$

(ii) $f^{-1}ds_B^2(\mathcal{K})$ té longitud pròpia finita al llarg de les direccions angulars ϕ^i , on hem definit $z_i = \exp(x^i + i\phi^i)$, amb $\phi^i \sim \phi^i + 2\pi$,

(iii) el potencial de Kähler és convex,

llavors, la forma general de la base ve donada per

$$ds_B^2 = d\rho^2 + \rho^2 \left\{ \frac{d\theta^2}{\Delta_\theta} + \left[\frac{\sin^2 \theta}{A_1^2} d\phi^1 + \frac{\cos^2 \theta}{A_2^2} d\phi^2 \right]^2 + \Delta_\theta \sin^2 \theta \cos^2 \theta \left[\frac{d\phi^1}{A_1^2} - \frac{d\phi^2}{A_2^2} \right]^2 \right\}, \quad (1.2.22)$$

on $\Delta_\theta \equiv \Delta_\theta(\theta)$ és una funció, en principi, *arbitrària*, i A_1, A_2 són constants que obeeixen $1 \geq A_1^2, A_2^2 \geq 0$. Per les solucions de [34], hom té

$$\Delta_\theta = A_1^2 \cos^2 \theta + A_2^2 \sin^2 \theta. \quad (1.2.23)$$

Mitjançant el canvi de coordenades

$$\begin{aligned} x &= \cos 2\theta, & \frac{H(x)}{1-x^2} &= \Delta_\theta, \\ \psi &= \frac{\phi^2}{A_2^2} - \frac{\phi^1}{A_1^2}, & \phi &= \frac{\phi^2}{A_2^2} - \frac{\phi^1}{A_1^2}, \end{aligned} \quad (1.2.24)$$

hem trobat que únicament tindrem una solució de les equacions del moviment supersimètrica si la funció $H(x)$ satisfà

$$(H^2 H'''''')'' = 0, \quad (1.2.25)$$

on $' = \frac{d}{dx}$. Per les solucions de [34], $H(x)$ és un polinomi cúbic en x i per tant l'equació anterior es compleix de manera trivial.

Un altre resultat que hem obtingut ha consistit a estendre aquest anàlisi a tot l'espai-temps. Concretament, per una varietat de Kähler tòrica, el "potencial" $G(x^1, x^2) = \frac{1}{2}\mathcal{K}(x^1, x^2)$ ve donat per

$$G = -\frac{1}{4g} \ln(1 - g^2 \rho^2), \quad (1.2.26)$$

on la funció $\rho = \rho(x^1, x^2)$ s'obté a partir de l'equació

$$\frac{e^{2x^1}}{(g\rho)^{2A_1^2}} + \frac{e^{2x^2}}{(g\rho)^{2A_2^2}} = 1. \quad (1.2.27)$$

En aquests casos, l'espai base es pot escriure, de forma general, de la següent manera:

$$ds_B^2(\mathcal{K}) = d\sigma^2 + \frac{\sinh^2(g\sigma)}{4g^2} \left[\frac{dx^2}{H(x)} + H(x)d\psi^2 + \cosh^2(g\sigma)(d\phi + xd\psi)^2 \right], \quad (1.2.28)$$

on $\rho^2 = \frac{\tanh^2(g\sigma)}{g^2}$, i novament $H(x)$ és una funció arbitrària. En termes de la tètrada,

$$\begin{aligned} e^\sigma &= d\sigma, & e^x &= \frac{\sinh(g\sigma)}{2g} \frac{dx}{\sqrt{H}}, \\ e^\psi &= \frac{\sinh(2g\sigma)}{2g} \sqrt{H} d\psi, & e^\phi &= \frac{\sinh(g\sigma) \cosh(g\sigma)}{2g} d(\phi + xd\psi), \end{aligned} \quad (1.2.29)$$

obtenim les formes de Kähler i de Ricci:

$$J = -(e^\sigma \wedge e^\phi + e^x \wedge e^\psi), \quad (1.2.30)$$

$$\mathcal{R} = 12g^2(1 - f^{-1})e^x \wedge e^\psi - 6g^2(e^\sigma \wedge e^\phi + e^x \wedge e^\psi). \quad (1.2.31)$$

A partir de les equacions (1.1.41) i (1.1.42) podem calcular f i G^+ en termes de la geometria de la base,

$$f^{-1} = 1 + \frac{2 + H''}{6 \sinh^2(g\sigma)}, \quad (1.2.32)$$

$$G^+ = 3g(1 - f^{-1})(e^\sigma \wedge e^\phi - e^x \wedge e^\psi). \quad (1.2.33)$$

Tenint en compte que (1.1.43) només determina les components de G^- paral·leles a J , l'expressió més general possible per a G^- , donada la nostra base (1.2.28), és:

$$\begin{aligned} G^- &= l(x, \sigma)(e^\sigma \wedge e^\phi + e^x \wedge e^\psi) + fN(\sigma, x, \phi, \psi)(e^\sigma \wedge e^\psi - e^x \wedge e^\phi) \\ &\quad + fM(\sigma, x, \phi, \psi)(e^\sigma \wedge e^x - e^\phi \wedge e^\psi). \end{aligned} \quad (1.2.34)$$

Finalment, per tal d'obtenir una solució, hem d'imposar la condició integrabilitat (1.2.20). Les condicions necessàries es poden escriure de forma convenient definint unes noves funcions

$$\begin{aligned} \tilde{M}(\sigma, x, \phi, \psi) &\equiv \cosh(g\sigma) \sinh^2(g\sigma) M(\sigma, x, \phi, \psi), \\ \tilde{N}(\sigma, x, \phi, \psi) &\equiv \cosh(g\sigma) \sinh^2(g\sigma) N(\sigma, x, \phi, \psi) - \frac{g\sqrt{H}}{6 \sinh^2(g\sigma)} \left[(H'''H)' - \frac{(2 + H'')^2}{2} \right]'. \end{aligned} \quad (1.2.35)$$

En termes d'una nova variable $u = -4\operatorname{arctanh}(e^{-2g\sigma})$, hom dedueix que \tilde{M} i \tilde{N} són funcions harmòniques al pla u - ϕ i, per tant,

$$\tilde{M} = \sum_{\alpha} c_{\alpha}^M(x, \psi) \mathcal{H}_{\alpha}(u, \phi), \quad \tilde{N} = \sum_{\alpha} c_{\alpha}^N(x, \psi) \mathcal{H}_{\alpha}(u, \phi), \quad (1.2.36)$$

on $\{\mathcal{H}_{\alpha}\}$ denota una base de funcions harmòniques. Finalment, obtenim les condicions d'integrabilitat que implica l'equació (1.2.20):

$$(H''''H^2)'' = 0, \quad (1.2.37)$$

$$\sum_{\alpha} \left[\frac{\partial_{\psi} c_{\alpha}^M - x c_{\alpha}^M \partial_{\phi}}{\sqrt{H}} - \partial_x(\sqrt{H} c_{\alpha}^N) \right] \mathcal{H}_{\alpha} = \frac{g(HH''''')'}{3}, \quad (1.2.38)$$

$$\sum_{\alpha} \left[\partial_x(\sqrt{H} c_{\alpha}^M) + \frac{\partial_{\psi} c_{\alpha}^N - x c_{\alpha}^N \partial_{\phi}}{\sqrt{H}} \right] \mathcal{H}_{\alpha} = 0, \quad (1.2.39)$$

$$\sum_{\alpha} (c_{\alpha}^M \partial_{\phi} - c_{\alpha}^N \partial_u) \mathcal{H}_{\alpha} = 0, \quad (1.2.40)$$

$$\sum_{\alpha} (c_{\alpha}^M \partial_u + c_{\alpha}^N \partial_{\phi}) \mathcal{H}_{\alpha} = 0. \quad (1.2.41)$$

Notem que la primera de les equacions anteriors coincideix amb la que ja havíem obtingut de l'anàlisi de la geometria a prop de l'horitzó (1.2.25). Per tant, per tal d'obtenir una solució supersimètrica cal que la funció $H(x)$ que parametriza la base satisfaci (1.2.25). Finalment, hem de dir que hem pogut trobar noves solucions, a més de les ja conegudes, de les equacions anteriors. Els detalls es troben a [43].

1.2.4 Saturn negre

A continuació resumim els resultats obtinguts a [44]. El nostre objectiu era construir una solució de les equacions d'Einstein al buit en cinc dimensions que consistís en un anell negre rodejant un forat negre de Myers-Perry. Hem partit de la solució llavor

$$(G_0)_{ab} dx^a dx^b = -\frac{\mu_1 \mu_3}{\mu_2 \mu_4} dt^2 + \frac{\rho^2 \mu_4}{\mu_3 \mu_5} d\phi^2 + \frac{\mu_2 \mu_5}{\mu_1} d\psi^2, \quad (1.2.42)$$

$$e^{2\nu_0} = k^2 \frac{\mu_2 \mu_5 (\rho^2 + \mu_1 \mu_2)^2 (\rho^2 + \mu_1 \mu_4) (\rho^2 + \mu_1 \mu_5) (\rho^2 + \mu_2 \mu_3) (\rho^2 + \mu_3 \mu_4)^2 (\rho^2 + \mu_4 \mu_5)}{\mu_1 (\rho^2 + \mu_3 \mu_5) (\rho^2 + \mu_1 \mu_3) (\rho^2 + \mu_2 \mu_4) (\rho^2 + \mu_2 \mu_5) \prod_{i=1}^5 (\rho^2 + \mu_i^2)}, \quad (1.2.43)$$

on $\mu_i = \sqrt{\rho^2 + (z - a_i)^2} - (z - a_i)$ i k és una constant que depèn de les condicions asimptòtiques de l'espai-temps. Els paràmetres a_i són constants que determinen la posició dels solitons i nosaltres prenem la ordenació $a_1 \leq a_5 \leq a_4 \leq a_3 \leq a_2$.

Per tal de generar la solució desitjada, apliquem una transformació de tres solitons segons el mètode de BZ [26] adaptat a un nombre de dimensions arbitràries [27]. Els passos que hem seguit són els següents:

1. Apliquem la següent transformació de tres solitons a la mètrica llavor (1.2.42):
 - Eliminem un anti-solito a $z = a_1$ amb vector de BZ trivial $(1, 0, 0)$; aquest pas és equivalent a dividir $(G_0)_{tt}$ per $-\rho^2/\bar{\mu}_1^2 = -\mu_1^2/\rho^2$.
 - Eliminem un solito a $z = a_2$ amb vector de BZ trivial $(1, 0, 0)$; aquest pas és equivalent a dividir $(G_0)_{tt}$ per $-\rho^2/\mu_2^2$.
 - Eliminem un anti-solito a $z = a_3$ amb vector de BZ trivial $(1, 0, 0)$; aquest pas és equivalent a dividir $(G_0)_{tt}$ per $-\rho^2/\bar{\mu}_3^2 = -\mu_3^2/\rho^2$.

La mètrica resultant és

$$G'_0 = \text{diag} \left\{ \frac{\rho^2 \mu_2}{\mu_1 \mu_3 \mu_4}, \frac{\rho^2 \mu_4}{\mu_3 \mu_5}, \frac{\mu_2 \mu_5}{\mu_1} \right\}, \quad (1.2.44)$$

on el primer terme correspon a la component tt , el segon a la component $\phi\phi$ i el tercer a la component $\psi\psi$.

2. Reescalem G'_0 per un factor de $\frac{\mu_1 \mu_3}{\rho^2 \mu_2}$:

$$\tilde{G}_0 = \frac{\mu_1 \mu_3}{\rho^2 \mu_2} G'_0 = \text{diag} \left\{ \frac{1}{\mu_4}, \frac{\mu_1 \mu_4}{\mu_2 \mu_5}, -\frac{\mu_3}{\bar{\mu}_5} \right\}, \quad (1.2.45)$$

on $\bar{\mu}_5 = -\rho^2/\mu_5$. Aquesta mètrica que acabem d'obtenir serà la nova llavor que utilitzarem per tal de generar la solució desitjada.

3. La matriu generatriu $\tilde{\Psi}_0$ que és solució de (1.1.16) amb \tilde{G}_0 és:

$$\tilde{\Psi}_0(\lambda, \rho, z) = \text{diag} \left\{ \frac{1}{(\mu_4 - \lambda)}, \frac{(\mu_1 - \lambda)(\mu_4 - \lambda)}{(\mu_2 - \lambda)(\mu_5 - \lambda)}, -\frac{(\mu_3 - \lambda)}{(\bar{\mu}_5 - \lambda)} \right\}. \quad (1.2.46)$$

4. Apliquem una transformació general de tres solitons utilitzant la mètrica \tilde{G}_0 com a llavor:

- Afegim un anti-solító a $z = a_1$ (pol a $\lambda = \bar{\mu}_1$) amb vector de BZ $m_0^{(1)} = (1, 0, c_1)$.
- Afegim un solító a $z = a_2$ (pol a $\lambda = \mu_2$) amb vector de BZ $m_0^{(2)} = (1, 0, c_2)$.
- Afegim un anti-solító a $z = a_3$ (pol a $\lambda = \bar{\mu}_3$) amb vector de BZ $m_0^{(3)} = (1, b_3, 0)$.

Anomenem \tilde{G} a la mètrica resultant obtinguda mitjançant (1.1.26).

5. Reescalem la mètrica \tilde{G} ,

$$G = \frac{\rho^2 \mu_2}{\mu_1 \mu_3} \tilde{G} \quad (1.2.47)$$

de manera que la nova mètrica G compleix $\det G = -\rho^2$.

6. Finalment, construïm el factor conforme $e^{2\nu}$ corresponent a la mètrica G mitjançant (1.1.28), on $\Gamma_0 = \Gamma|_{c_1=c_2=b_3=0}$. El resultat final $(G, e^{2\nu})$ constitueix la solució desitjada.

Per simplicitat, ens hem concentrat en el cas en què el saturn negre presenta rotació en un sol pla. Per aquesta raó d'ara endavant prenem $b_3 = 0$. En aquestes condicions, una transformació de dos solitons hauria estat suficient per tal d'obtenir la solució que cerquem, però hem decidit aplicar una transformació més general de tres solitons amb l'objectiu de facilitar una posterior generalització que inclogui rotació al pla perpendicular al de l'anell.

La mètrica que hem obtingut és:

$$ds^2 = -\frac{H_y}{H_x} \left[dt + \left(\frac{\omega_\psi}{H_y} + q \right) d\psi \right]^2 + H_x \left\{ k^2 P (d\rho^2 + dz^2) + \frac{G_y}{H_y} d\psi^2 + \frac{G_x}{H_x} d\phi^2 \right\}. \quad (1.2.48)$$

Les diferents funcions que apareixen a (1.2.48) vénen donades per:

$$P = (\mu_3 \mu_4 + \rho^2)^2 (\mu_1 \mu_5 + \rho^2) (\mu_4 \mu_5 + \rho^2), \quad (1.2.49)$$

$$H_x = F^{-1} \left[M_0 + c_1^2 M_1 + c_2^2 M_2 + c_1 c_2 M_3 + c_1^2 c_2^2 M_4 \right], \quad (1.2.50)$$

$$H_y = F^{-1} \frac{\mu_3}{\mu_4} \left[M_0 \frac{\mu_1}{\mu_2} - c_1^2 M_1 \frac{\rho^2}{\mu_1 \mu_2} - c_2^2 M_2 \frac{\mu_1 \mu_2}{\rho^2} + c_1 c_2 M_3 + c_1^2 c_2^2 M_4 \frac{\mu_2}{\mu_1} \right], \quad (1.2.51)$$

on

$$M_0 = \mu_2 \mu_5^2 (\mu_1 - \mu_3)^2 (\mu_2 - \mu_4)^2 (\rho^2 + \mu_1 \mu_2)^2 (\rho^2 + \mu_1 \mu_4)^2 (\rho^2 + \mu_2 \mu_3)^2, \quad (1.2.52)$$

$$M_1 = \mu_1^2 \mu_2 \mu_3 \mu_4 \mu_5 \rho^2 (\mu_1 - \mu_2)^2 (\mu_2 - \mu_4)^2 (\mu_1 - \mu_5)^2 (\rho^2 + \mu_2 \mu_3)^2, \quad (1.2.53)$$

$$M_2 = \mu_2 \mu_3 \mu_4 \mu_5 \rho^2 (\mu_1 - \mu_2)^2 (\mu_1 - \mu_3)^2 (\rho^2 + \mu_1 \mu_4)^2 (\rho^2 + \mu_2 \mu_5)^2, \quad (1.2.54)$$

$$M_3 = 2\mu_1 \mu_2 \mu_3 \mu_4 \mu_5 (\mu_1 - \mu_3) (\mu_1 - \mu_5) (\mu_2 - \mu_4) (\rho^2 + \mu_1^2) (\rho^2 + \mu_2^2) \\ \times (\rho^2 + \mu_1 \mu_4) (\rho^2 + \mu_2 \mu_3) (\rho^2 + \mu_2 \mu_5), \quad (1.2.55)$$

$$M_4 = \mu_1^2 \mu_2 \mu_3^2 \mu_4^2 (\mu_1 - \mu_5)^2 (\rho^2 + \mu_1 \mu_2)^2 (\rho^2 + \mu_2 \mu_5)^2, \quad (1.2.56)$$

$$F = \mu_1 \mu_5 (\mu_1 - \mu_3)^2 (\mu_2 - \mu_4)^2 (\rho^2 + \mu_1 \mu_3) (\rho^2 + \mu_2 \mu_3) (\rho^2 + \mu_1 \mu_4) \\ \times (\rho^2 + \mu_2 \mu_4) (\rho^2 + \mu_2 \mu_5) (\rho^2 + \mu_3 \mu_5) \prod_{i=1}^5 (\rho^2 + \mu_i^2). \quad (1.2.57)$$

Finalment,

$$G_x = \frac{\rho^2 \mu_4}{\mu_3 \mu_5}, \quad G_y = \frac{\mu_3 \mu_5}{\mu_4}, \quad (1.2.58)$$

i el terme creuat que dóna lloc a la rotació ve donat per

$$\omega_\psi = 2 \frac{c_1 R_1 \sqrt{M_0 M_1} - c_2 R_2 \sqrt{M_0 M_2} + c_1^2 c_2 R_2 \sqrt{M_1 M_4} - c_1 c_2^2 R_1 \sqrt{M_2 M_4}}{F \sqrt{G_x}}. \quad (1.2.59)$$

A l'hora d'analitzar la solució resulta convenient introduir una nova parametrització en termes de paràmetres adimensionals. Si fixem l'escala total L de manera que

$$L^2 = a_2 - a_1, \quad (1.2.60)$$

llavors les posicions dels solitons vénen determinades pels paràmetres adimensionals

$$\kappa_i = \frac{a_{i+2} - a_1}{L^2}, \quad \text{per } i = 1, 2, 3. \quad (1.2.61)$$

Els nous paràmetres κ_i han d'obeir $0 \leq \kappa_3 \leq \kappa_2 < \kappa_1 \leq 1$ per tal de respectar l'ordenació anterior. Finalment, introduint un nou paràmetre adimensional \bar{c}_2 tal que

$$\bar{c}_2 = \frac{c_2}{c_1(1 - \kappa_2)}, \quad (1.2.62)$$

la solució que hem obtingut és completament regular i no presenta singularitats còniques si

$$|c_1| = L \sqrt{\frac{2\kappa_1 \kappa_2}{\kappa_3}}, \quad (1.2.63a)$$

$$\bar{c}_2 = \frac{1}{\kappa_2} \left[\epsilon \frac{\kappa_1 - \kappa_2}{\sqrt{\kappa_1(1 - \kappa_2)(1 - \kappa_3)(\kappa_1 - \kappa_3)}} - 1 \right], \quad \text{amb } \begin{cases} \epsilon = +1 & \text{per } \bar{c}_2 > -\kappa_2^{-1} \\ \epsilon = -1 & \text{per } \bar{c}_2 < -\kappa_2^{-1} \end{cases}. \quad (1.2.63b)$$

La solució corresponent a $\bar{c}_2 = -\kappa_2^{-1}$ dóna lloc a una singularitat despullada i per tant la descartem. Així doncs, segons el signe de ϵ tenim dues branques disconnexes de solucions. L'anàlisi complet d'aquestes solucions i les seves propietats físiques es troba a [44].

1.2.5 Fases dels forats negres en cinc dimensions

En aquesta secció resumim els resultats obtinguts a [45] relacionats amb el diagrama de fases dels forats negres en cinc dimensions.

Per tal de determinar la regió de l'espai de fases que cobreixen els saturns negres partim de dues observacions:

1. Entre totes les configuracions en què tenim un únic forat negre amb una certa massa M fixada, l'objecte amb una major entropia és el forat negre estàtic ($J = 0$).
2. El moment angular d'un anell negre amb una certa massa fixada pot ser arbitràriament gran si el radi de la seva S^1 és prou gran i, per tant, el radi de la S^2 prou petit.

Per tant, arribem a la conclusió que podem construir un saturn negre amb una entropia màxima si “posem” tota la massa en el forat negre estàtic central, i distribuïm el moment angular en un anell negre arbitràriament gran i prim. De fet, podem argumentar que per un moment angular total fixat, existeixen saturns negres en tot el rang d'àrees

$$0 < \mathcal{A} < \mathcal{A}_{\max} = \frac{32}{3} \sqrt{\frac{2\pi}{3}} (GM)^{3/2}, \quad (1.2.64)$$

on \mathcal{A}_{\max} és l'àrea del forat negre estàtic.

Per tal de simplificar les expressions, treballem amb moments angulars i àrees reescalats:

$$\tilde{J} \equiv \sqrt{\frac{27\pi}{32G}} J, \quad \tilde{\mathcal{A}} \equiv \sqrt{\frac{27}{256\pi G^3}} \mathcal{A}. \quad (1.2.65)$$

D'aquesta manera, el forat negre de MP amb massa M_h i moment angular J_h està caracteritzat per l'àrea

$$\tilde{\mathcal{A}}_h = 2\sqrt{2\left(M_h^3 - \tilde{J}_h^2\right)}, \quad (1.2.66)$$

mentre que l'anell negre amb massa M_r ve determinat, de forma paramètrica, per

$$\tilde{\mathcal{A}}_r = 2\sqrt{M_r^3\nu(1-\nu)}, \quad \tilde{J}_r^2 = M_r^3 \frac{(1+\nu)^3}{8\nu}. \quad (1.2.67)$$

Podem caracteritzar la mida dels dos objectes introduint el radi de la circumferència del forat negre de MP al pla de rotació

$$R_h = 2\sqrt{\frac{G}{3\pi}} \sqrt{\frac{2M_h}{1 - \tilde{J}_h^2/M_h^3}}, \quad (1.2.68)$$

i el radi interior de la S^1 de l'anell,

$$R_1 = 2\sqrt{\frac{G}{3\pi}} \sqrt{M_r \frac{1-\nu}{\nu}}. \quad (1.2.69)$$

En general, si fixem la massa total i introduïm moment angular, l'àrea del forat negre disminueix. Per tant, l'entropia màxima és la del forat negre estàtic

$$\tilde{\mathcal{A}}_{\max} = (2M)^{3/2}. \quad (1.2.70)$$

En Relativitat General clàssica tenim la llibertat de fixar una escala i nosaltres escollim la massa total. Per tant, si fixem $M = 1$, volem determinar quines solucions existeixen amb un moment angular J donat i quina és la seva entropia.

A continuació argumentem que la regió del pla $(\tilde{J}, \tilde{\mathcal{A}})$ que cobreixen els saturns negres és:

$$\begin{aligned} 0 < \tilde{\mathcal{A}} < \tilde{\mathcal{A}}_{\max} = 2\sqrt{2}, \\ 0 \leq \tilde{J} < \infty, \end{aligned} \quad (1.2.71)$$

a més del punt $(\tilde{J}, \tilde{\mathcal{A}}) = (0, 2\sqrt{2})$, que correspon al forat negre estàtic.

- Obtenim configuracions arbitràriament properes al límit superior de la banda ($\tilde{J} > 0, \tilde{\mathcal{A}} = 2\sqrt{2}$) mitjançant anells infinitament llargs i prim.

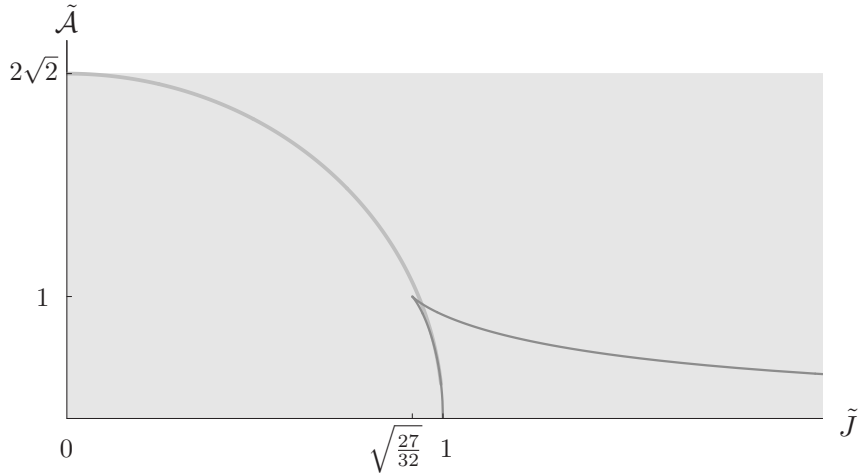


Figura 1.1: Fases dels forats negres en cinc dimensions incloent-hi els saturns negres. Fixem la massa total $M = 1$ i representem l'àrea vs. moment angular. Les corbes corresponen a un únic forat negre de MP i a un únic anell negre respectivament. La regió ombrejada $0 \leq \tilde{J} < \infty$, $0 < \tilde{\mathcal{A}} < 2\sqrt{2}$, està coberta per saturns negres. De fet, cada punt d'aquesta regió correspon a una família uniparamètrica de saturns negres.

- El límit inferior ($\tilde{J} \geq 0, \tilde{\mathcal{A}} = 0$) correspon a singularitats despulades. Per tal d'assolir aquestes configuracions cal que el forat negre tendeixi a la solució extremal $\tilde{J}_h^2 \rightarrow M_h^3$ i el moment angular a $\tilde{J} - M_h^{3/2}$, mentre que al mateix temps hem de prendre el límit $M_r \rightarrow 0$ i $\nu \rightarrow 0$.
- Les solucions amb ($\tilde{J} = 0, 0 < \tilde{\mathcal{A}} \leq 2\sqrt{2}$) corresponen a saturns negres en què el forat negre i l'anell negre estan rotant en sentits oposats. Es pot veure que aquestes solucions cobreixen tot el rang $0 < \tilde{\mathcal{A}} \leq 2\sqrt{2}$: podem considerar un forat negre central rotant amb l'àrea necessària i un anell negre llarg i prim rotant en sentit contrari de tal manera que el moment angular total s'anul·li.
- Finalment, notem que és possible obtenir com a mínim un saturn negre a qualsevol punt dins d'aquests límits. La raó és que, novament, podem tenir un forat negre amb rotació que doni compte de l'àrea $\tilde{\mathcal{A}}$, i un anell negre arbitràriament llarg i prim amb el moment angular necessari per tal d'obtenir el valor de \tilde{J} desitjat.

El diagrama de fases que resulta d'incloure els saturns negres es mostra a la figura 1.1.

Un altre resultat que hem obtingut ha estat la generalització de la primera llei de la mecànica dels forats negres pel cas en què tenim més d'un forat negre. El resultat és:

$$\delta M = \sum_i \left(\frac{\kappa_i}{8\pi G} \delta \mathcal{A}_i + \Omega_i \delta J_i \right), \quad (1.2.72)$$

on J_i és el moment angular de Komar de cada forat negre,

$$J_i = \frac{1}{16\pi G} \int_{H_i} \epsilon_{abcde} \nabla^d \zeta^e, \quad (1.2.73)$$

i ζ és el vector de Killing que genera les rotacions a infinit.

Un últim resultat que presentem correspon al diagrama de les fases en equilibri termodinàmic. En general, el forat negre i l'anell negre que conformen el saturn negre tenen temperatures i

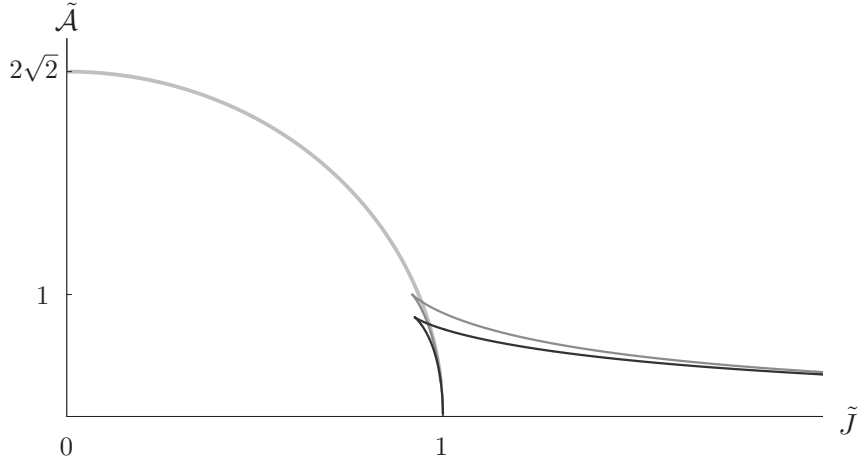


Figura 1.2: Fases en equilibri termodinàmic. Juntament amb les corbes en gris corresponents al forat negre de MP i a l’anell negre, hem representat en negre el saturn negre en què el forat negre central i l’anell negre tenen la mateixa temperatura i velocitat angular. Hi ha un únic saturn negre (i no una família contínua) per cada punt d’aquesta corba.

velocitats angulars diferents i per tant no estan en equilibri termodinàmic. Imposant que la temperatura i la velocitat angular del forat negre i l’anell negre coincideixin elimina dos paràmetres de la solució i, per tant, la no unicitat contínua dels saturns negres generals es veu reduïda a una no unicitat discreta. Així doncs, els saturns negres en equilibri termodinàmic formen una corba al pla (\tilde{J}, \tilde{A}) , que hem obtingut de la solució exacta de [44]. El resultat es presenta a la figura 1.2

1.2.6 Solucions supersimètriques de Teoria M amb factors AdS_3

Finalment exposem els resultats obtinguts a [46]. Per tal de trobar les solucions que en un determinat límit admetin factors AdS_3 , proseguim com a [38] i requerim l’existència d’un factor $\mathbb{R}^{1,1}$ “warped”, de manera que la mètrica vingui donada per (1.1.50) amb $e^+ = L^{-1}dx^+$, $e^- = dx^-$, $L < \infty$ i $e^9 \neq 0$ globalment. A la vegada, imposem que la solució preservi les isometries del factor de Minkowski de manera que tant L com la mètrica de \mathcal{M}_8 i e^9 no depenguin de les coordenades x^\pm , i el flux vingui donat per

$$F = e^{+-} \wedge H + G, \quad (1.2.74)$$

amb H i G també independents de x^\pm . La darrera hipòtesi que fem consisteix a suposar que \mathcal{M}_8 admet una G -estructura globalment definida. Concretament, a [46] ens hem centrat en els casos en què $G = Spin(7)$, $SU(4)$ i $Sp(2)$. Suposar l’existència a \mathcal{M}_8 d’una estructura de $Spin(7)$ globalment definida és equivalent a suposar l’existència d’una 4-forma de Cayley ϕ invariant sota $Spin(7)$ globalment no nul·la. Pel cas de $SU(4)$, les formes globalment no nul·les són l’estructura quasi-complexa J i la $(4,0)$ -forma Ω . Finalment, per $Sp(2)$, imposar l’existència d’una estructura global és equivalent a imposar l’existència d’un triplet d’estructures quasi-complexes J^A , $A = 1, 2, 3$, globalment no nul·les.

Per obtenir les geometries amb factors AdS_3 observem que, en coordenades de Poincaré, tot espai AdS_3 admet la següent foliació:

$$\frac{1}{m^2} ds^2(AdS_3) = e^{-2mr} ds^2(\mathbb{R}^{1,1}) + dr^2. \quad (1.2.75)$$

on m és el radi de curvatura d'anti-de Sitter. Comparant amb (1.1.50), identifiquem $L = e^{2mr} \lambda$, on λ és una certa funció independent de les coordenades d' AdS . Per tal d'obtenir la mètrica AdS hem de seleccionar la direcció radial $\hat{r} = \lambda^{-1/2} dr$ de l'espai transvers al factor $\mathbb{R}^{1,1}$. En general, \hat{r} serà una combinació lineal de e^9 i una 1-forma definida a \mathcal{M}_8 , que sempre podem escollir que sigui e^8 . D'aquesta manera, localment sempre podem escriure

$$\begin{aligned}\hat{r} &= \sin \theta e^8 + \cos \theta e^9, \\ \hat{\rho} &= \cos \theta e^8 - \sin \theta e^9,\end{aligned}\tag{1.2.76}$$

amb $0 < \theta \leq \pi/2$ i $\hat{\rho} = \frac{\lambda}{2m \sin \theta} d\rho$. Finalment, hem d'imposar que tant $\hat{\rho}$ com la resta de 1-formes de la base transverses al factor AdS siguin independents de les coordenades d' AdS . D'aquesta manera, localment, obtenim la mètrica amb el factor AdS_3 :

$$ds^2 = \frac{1}{\lambda m^2} ds^2(AdS_3) + \hat{\rho} \otimes \hat{\rho} + ds^2(\mathcal{N}_7).\tag{1.2.77}$$

Pel cas en què les geometries tenen un factor $\mathbb{R}^{1,1}$, la component elèctrica del flux ve donada per $F_{\text{elec}} = d(e^{+-9})$. En prendre el límit AdS hom pot veure que, independentment de la G -estructura de \mathcal{M}_8 , la component elèctrica del flux ve donada per:

$$F_{\text{elec}} = \frac{1}{m^2} \text{Vol}_{AdS_3} \wedge d(\rho - \lambda^{-3/2} \cos \theta).\tag{1.2.78}$$

Com que en prendre el límit d' AdS hem seleccionat una direcció preferida a \mathcal{M}_8 , el grup d'estructura que actua sobre \mathcal{N}_7 es veurà reduït. Pel cas de $Spin(7)$, el grup d'estructura de \mathcal{N}_7 es veu reduït a G_2 , per $SU(4)$ la reducció és a $SU(3)$ i finalment per $Sp(2)$ trobem una reducció a $SU(2)$.

A continuació exposem de forma resumida els resultats obtinguts segons el nombre de supersimetries que es preserven:

Geometria de Cayley

Ens referim al cas en què \mathcal{M}_8 admet una estructura de $Spin(7)$ globalment definida com a geometria de Cayley. Aquest cas es pot realitzar amb un únic espinor de Killing η globalment nul que satisfà

$$\Gamma^{+-} \frac{1}{14} \phi \cdot \eta = -\eta.\tag{1.2.79}$$

Restringint les condicions generals de supergravetat en onze dimensions (1.1.52) al cas que ens ocupa i tenint en compte les nostres hipòtesis, hem obtingut les següents condicions sobre la geometria:

$$e^9 \wedge \left[-L^3 e^9 \lrcorner d(L^{-3} e^9) + \frac{1}{2} \phi \lrcorner \phi \right] = 0,\tag{1.2.80}$$

$$(e^9 \wedge + \star_9) [e^9 \lrcorner d(L^{-1} \phi)] = 0,\tag{1.2.81}$$

mentre que el flux ve donat per:

$$F = d(e^{+-9}) - \star d(e^{+-} \wedge \phi) - \frac{L^{10/7}}{2} e^9 \lrcorner d(L^{-10/7} \phi) + \frac{1}{4} \phi \diamond [e^9 \lrcorner (e^9 \wedge de^9)] + F^{27}.\tag{1.2.82}$$

En prendre el límit AdS , la mètrica esdevé

$$ds^2 = \frac{1}{\lambda m^2} \left[ds^2(AdS_3) + \frac{\lambda^3}{4 \sin^2 \theta} d\rho \otimes d\rho \right] + ds^2(\mathcal{N}_7), \quad (1.2.83)$$

on \mathcal{N}_7 admet una estructura G_2 , amb una 3-forma associativa Φ i una 4-forma co-associativa Υ . Les condicions que ha de satisfer la geometria són:

$$\hat{\rho} \wedge d(\lambda^{-1} \Upsilon) = 0, \quad (1.2.84)$$

$$\lambda^{5/2} d(\lambda^{-5/2} \sin \theta \text{Vol}_7) = -4m\lambda^{1/2} \cos \theta \hat{\rho} \wedge \text{Vol}_7, \quad (1.2.85)$$

$$d\Phi \wedge \Phi = \frac{4m\lambda^{1/2}}{\sin \theta} (4 - \sin^2 \theta) \text{Vol}_7 - 2 \cos \theta \star_8 d \log \left(\frac{\lambda^{3/2} \cos \theta}{\sin^2 \theta} \right), \quad (1.2.86)$$

mentre que les components magnètiques del flux vénen donades per:

$$F_{\text{mag}} = \frac{\lambda^{3/2}}{\sin^2 \theta} (\cos \theta + \star_8) \left[d(\lambda^{-3/2} \sin \theta \Phi) - 4m\lambda^{-1} \Upsilon \right] + 2m\lambda^{1/2} \Phi \wedge \hat{\rho}. \quad (1.2.87)$$

Geometria de Kähler-4

En aquest cas \mathcal{M}_8 admet una estructura $SU(4)$ globalment definida, que es pot realitzar amb dos espinors de Killing globalment nuls, que són les solucions de

$$\frac{1}{12} \Gamma^{+-} (J \wedge J) \cdot \eta = -\eta. \quad (1.2.88)$$

Els dos espinors de Killing que s'obtenen de l'equació anterior donen lloc a dues estructures $Spin(7)$:

$$\phi_{\pm} = - \left(\frac{1}{2} J \wedge J \pm \text{Re} \Omega \right). \quad (1.2.89)$$

Imposant que les dues estructures anteriors satisfacin (1.2.80)-(1.2.82) simultàniament, obtenim les condicions que ha d'obeeir la geometria:

$$\begin{aligned} J \lrcorner de^9 &= 0, \\ d(L^{-1} \text{Re} \Omega) &= 0, \\ e^9 \wedge [J \lrcorner dJ - L e^9 \lrcorner d(L^{-1} e^9)] &= 0, \end{aligned} \quad (1.2.90)$$

mentre que el flux ve donat per

$$F = d(e^{+-9}) + \frac{1}{2} \star d(e^{+-} \wedge J \wedge J) + \frac{1}{4} L^2 e^9 \lrcorner d(L^{-2} J \wedge J) - \frac{1}{4} (J \wedge J) \diamond [e^9 \lrcorner (e^9 \wedge de^9)] + F^{\mathbf{20}}. \quad (1.2.91)$$

En aquesta expressió, $F^{\mathbf{20}}$ és una 4-forma definida a \mathcal{M}_8 en la representació $\mathbf{20}$ de $SU(4)$, i no està fixada per les condicions que imposa la supersimetria. La resta de casos que presentem tot seguit s'obtenen de la mateixa manera.

En el límit d' AdS trobem que la mètrica, localment, es pot escriure com

$$ds^2 = \frac{1}{\lambda m^2} \left[ds^2(AdS_3) + \frac{\lambda^3}{4 \sin^2 \theta} d\rho \otimes d\rho \right] + e^7 \otimes e^7 + ds^2(\mathcal{N}_6), \quad (1.2.92)$$

on ara \mathcal{N}_6 admet una estructura $SU(3)$ definida per J i Ω . Les condicions que ha d'obeir la nova geometria són:

$$\hat{\rho} \wedge d(\lambda^{-1} J \wedge J) = 0, \quad (1.2.93)$$

$$d(\lambda^{-3/2} \sin \theta \operatorname{Im} \Omega) = 2m\lambda^{-1}(e^7 \wedge \operatorname{Re} \Omega - \cos \theta \hat{\rho} \wedge \operatorname{Im} \Omega), \quad (1.2.94)$$

$$J \lrcorner de^7 = \frac{2m\lambda^{1/2}}{\sin \theta} (2 - \sin^2 \theta) - \cos \theta \hat{\rho} \lrcorner d \log \left(\frac{\lambda^{3/2} \cos \theta}{\sin^2 \theta} \right), \quad (1.2.95)$$

i les components magnètiques del flux vénen donades per:

$$F_{\text{mag}} = \frac{\lambda^{3/2}}{\sin^2 \theta} (\cos \theta + \star_8) \left[d(\lambda^{-3/2} \sin \theta J \wedge e^7) - 2m\lambda^{-1} J \wedge J \right] + 2m\lambda^{1/2} J \wedge e^7 \wedge \hat{\rho}. \quad (1.2.96)$$

Geometria SLAG-4

En aquest cas \mathcal{M}_8 també admet una estructura $SU(4)$ globalment definida, que es pot realitzar amb els dos espinors de Killing globalment nuls que són solució de:

$$\begin{aligned} \Gamma^{+-} \eta &= \pm \eta, \\ \frac{1}{8} \Gamma^{+-} \operatorname{Re} \Omega \cdot \eta &= -\eta. \end{aligned} \quad (1.2.97)$$

L'estructura $SU(4)$ global ha de satisfer les següents relacions:

$$\begin{aligned} d(L^{-1/2} J) &= 0, \\ \operatorname{Im} \Omega \wedge d \operatorname{Re} \Omega &= 0, \\ e^9 \wedge [\operatorname{Re} \Omega \lrcorner d \operatorname{Re} \Omega - 2L^{3/2} e^9 \lrcorner d(L^{-3/2} e^9)] &= 0, \end{aligned} \quad (1.2.98)$$

i el flux ve donat per

$$F = d(e^{+-9}) + \star d(e^{+-} \wedge \operatorname{Re} \Omega) + \frac{1}{2} L^{7/4} e^9 \lrcorner d(L^{-7/4} \operatorname{Re} \Omega) - \frac{1}{2} \operatorname{Re} \Omega \diamond [e^9 \lrcorner (e^9 \wedge de^9)] + F^{20}. \quad (1.2.99)$$

En prendre el límit d' AdS , localment, la mètrica té la mateixa forma que el cas anterior (1.2.92), i novament \mathcal{N}_6 admet una estructura $SU(3)$. Les condicions que han d'obeir les formes J i Ω que defineixen l'estructura $SU(3)$ són:

$$e^7 \wedge \hat{\rho} \wedge d \left(\frac{\operatorname{Re} \Omega}{\sin \theta} \right) = 0, \quad (1.2.100)$$

$$d(\lambda^{-1} \sin \theta e^7) = m\lambda^{-1/2} (J + \cos \theta e^7 \wedge \hat{\rho}), \quad (1.2.101)$$

$$\operatorname{Im} \Omega \wedge d \operatorname{Im} \Omega = \frac{m\lambda^{1/2}}{\sin \theta} (6 + 4 \cos^2 \theta) \operatorname{Vol}_6 \wedge e^7 - 2 \cos \theta \star_8 d \log \left(\frac{\lambda^{3/2} \cos \theta}{\sin^2 \theta} \right), \quad (1.2.102)$$

i les components magnètiques del flux vénen donades per:

$$F_{\text{mag}} = -\frac{\lambda^{3/2}}{\sin^2 \theta} (\cos \theta + \star_8) \left[d(\lambda^{-3/2} \sin \theta \operatorname{Im} \Omega) + 4m\lambda^{-1} \operatorname{Re} \Omega \wedge e^7 \right] - 2m\lambda^{1/2} \operatorname{Im} \Omega \wedge \hat{\rho}. \quad (1.2.103)$$

Geometria de Kähler quaterniònica

En aquest cas \mathcal{M}_8 admet una estructura $Sp(2)$ globalment definida. Si definim la forma Ξ_1 en termes de les tres estructures quasi-complexes

$$\Xi_1 = \frac{1}{2} J^A \wedge J^A, \quad (1.2.104)$$

llavors l'estructura $Sp(2)$ global es pot realitzar en termes dels tres espinors de Killing globalment nuls que són solució de

$$\frac{1}{10} \Gamma^{+-} \Xi_1 \cdot \eta = -\eta. \quad (1.2.105)$$

Les condicions que ha de complir l'estructura són:

$$\begin{aligned} J^A \lrcorner de^9 &= 0, \\ d(L^{-1} \text{Re} \Omega^A) &= 0, \\ e^9 \wedge [J^A \lrcorner dJ^A - L e^9 \lrcorner d(L^{-1} e^9)] &= 0, \end{aligned} \quad (1.2.106)$$

on a la darrera equació no sumem sobre l'índex A . A la segona equació, les Ω^A són les (4,0)-formes associades a cada J^A , i les seves expressions es poden trobar a [46]. El flux magnètic és:

$$F = d(e^{+-9}) + \frac{1}{3} \star d(e^{+-} \wedge \Xi_1) + \frac{1}{6} L^{14/5} e^9 \lrcorner d(L^{-14/5} \Xi_1) - \frac{1}{4} \Xi_1 \diamond [e^9 \lrcorner (e^9 \wedge de^9)] + F^{14}, \quad (1.2.107)$$

on ara F^{14} és una 4-forma en la representació **14** de $Sp(2)$.

En el límit AdS , localment la mètrica es pot escriure com

$$ds^2 = \frac{1}{\lambda m^2} ds^2(AdS_3) + e^A \otimes e^A + \hat{\rho} \otimes \hat{\rho} + ds^2(\mathcal{N}_4), \quad (1.2.108)$$

on \mathcal{N}_4 és una varietat que admet una estructura $SU(2)$ determinada per un triplet K^A de formes auto-duals. Les condicions que ha de satisfer la geometria són:

$$\hat{\rho} \wedge d \left[\lambda^{-1} \left(\text{Vol}_4 + \frac{1}{6} \epsilon^{ABC} K^A \wedge e^{BC} \right) \right] = 0, \quad (1.2.109)$$

$$\frac{1}{3} \left(K^A + \frac{1}{2} \epsilon^{ABC} e^{BC} \right) \lrcorner de^A = \frac{2m\lambda^{1/2}}{\sin \theta} (2 - \sin^2 \theta) - \cos \theta \hat{\rho} \lrcorner d \log \left(\frac{\lambda^{3/2} \cos \theta}{\sin^2 \theta} \right), \quad (1.2.110)$$

$$\begin{aligned} d[\lambda^{-3/2} \sin \theta (K^2 \wedge e^2 - K^1 \wedge e^1)] &= 2m\lambda^{-1} [K^2 \wedge e^{31} - K^1 \wedge e^{23}] \\ &+ 2m\lambda^{-1} \cos \theta [K^2 \wedge e^2 - K^1 \wedge e^1] \wedge \hat{\rho}, \end{aligned} \quad (1.2.111)$$

i les permutacions òbvies de l'última equació. Les components magnètiques del flux vénen donades per:

$$\begin{aligned} F_{\text{mag}} &= -\frac{\lambda^{3/2}}{\sin^2 \theta} (\cos \theta + \star_8) \left\{ d \left[\lambda^{-3/2} \sin \theta \left(\frac{1}{3} K^A \wedge e^A + e^{123} \right) \right] \right. \\ &\quad \left. - 4m\lambda^{-1} \left(\text{Vol}_4 + \frac{1}{6} \epsilon^{ABC} K^A \wedge e^{BC} \right) \right\} - 2m\lambda^{1/2} \left[\frac{1}{3} K^A \wedge e^A + e^{123} \right] \wedge \hat{\rho}. \end{aligned} \quad (1.2.112)$$

Geometria CLAG

En aquest cas \mathcal{M}_8 també admet una estructura $Sp(2)$ global. Si definim

$$\Xi_2 = \frac{1}{2}(J^1 \wedge J^1 - \text{Re}\Omega^2 + \text{Re}\Omega^3), \quad (1.2.113)$$

podem trobar una realització d'aquesta estructura en termes de tres espinors de Killing globalment nuls que són les solucions del sistema

$$\Gamma^{+-}\eta = \pm\eta, \quad (1.2.114)$$

$$\frac{1}{10}\Gamma^{+-}\Xi_2 \cdot \eta = -\eta. \quad (1.2.115)$$

Obtenir les relacions que s'han de satisfer per a aquesta geometria, tenint en compte els nostres requeriments, a partir de les condicions generals que ha d'obeeir tota solució supersimètrica nul·la de supergravetat en onze dimensions (1.2.80)-(1.2.81), és tècnicament més complicat que en els casos anteriors. Per tal de derivar les condicions corresponents hem hagut de fer la hipòtesi addicional de que $e^9 \wedge de^9 = 0$. D'aquesta manera, hem obtingut

$$\begin{aligned} d(L^{-1/2}J^2) = d(L^{-1/2}J^3) &= 0, \\ e^9 \wedge [J^1 \lrcorner dJ^1 - Le^9 \lrcorner d(L^{-1}e^9)] &= 0, \end{aligned} \quad (1.2.116)$$

mentre que el flux ve donat per:

$$F = d(e^{+-9}) + \frac{1}{2} \star d(e^{+-} \wedge \Xi_2) + \frac{1}{4} L^{11/5} e^9 \lrcorner d(L^{-11/5} \Xi_2) + F^{14}, \quad (1.2.117)$$

on novament F^{14} és una 4-forma en la representació **14** de $Sp(2)$.

En el límit AdS , localment, la mètrica pren la mateixa forma que en el cas anterior (1.2.108). Per tal de derivar les condicions que ha d'obeeir la geometria en el límit AdS , en comptes de partir de (1.2.116), hem descomposat les condicions que s'han de complir pels casos de SLAG i Kähler-4. Per tant, les condicions que exposem a continuació no depenen de la hipòtesi de que $e^9 \wedge de^9 = 0$. Les condicions que s'han de complir són:

$$\hat{\rho} \wedge d[\lambda^{-1}(\text{Vol}_4 + K^3 \wedge e^{12})] = 0, \quad (1.2.118)$$

$$(K^3 + e^{12}) \lrcorner de^3 = \frac{2m\lambda^{1/2}}{\sin\theta}(2 - \sin^2\theta) - \cos\theta \hat{\rho} \lrcorner d \log \left(\frac{\lambda^{3/2} \cos\theta}{\sin^2\theta} \right), \quad (1.2.119)$$

$$d(\lambda^{-1} \sin\theta e^1) = m\lambda^{-1/2}(K^1 + e^{23} + \cos\theta e^1 \wedge \hat{\rho}), \quad (1.2.120)$$

$$d(\lambda^{-1} \sin\theta e^2) = m\lambda^{-1/2}(K^2 + e^{31} + \cos\theta e^2 \wedge \hat{\rho}), \quad (1.2.121)$$

mentre que les components magnètiques del flux vénen donades per:

$$\begin{aligned} F_{\text{mag}} &= \frac{\lambda^{3/2}}{\sin^2\theta} (\cos\theta + \star_8) \left\{ d[\lambda^{-3/2} \sin\theta (K^3 \wedge e^3 + e^{123})] - 4m\lambda^{-1} (\text{Vol}_4 + K^3 \wedge e^{12}) \right\} \\ &\quad + 2m\lambda^{1/2} [K^3 \wedge e^3 + e^{123}] \wedge \hat{\rho}. \end{aligned} \quad (1.2.122)$$

1.3 Discussió i conclusions

En aquesta secció presentem la discussió i les conclusions dels resultats que hem resumit a la secció anterior i indiquem possibles línies per a continuar la recerca.

Anells negres no supersimètrics amb càrregues de D1-D5-P

Hem mostrat com construir un anell negre no supersimètric amb càrregues de D1-D5-P a partir de boosts i dualitats, resolent els problemes que s'havien trobat a [22] gràcies a la inclusió dels dipòls a la solució llavor. El punt clau consisteix a imposar que la 1-forma w associada a la rotació estigui ben definida, cosa que equival a imposar l'absència de cordes de Dirac-Misner.

Dels resultats d'aquest estudi, esperem que existeixin anells negres no supersimètrics descrits per nou paràmetres $(M, J_\psi, J_\phi, Q_{1,2,3}, q_{1,2,3})$ de manera que puguem recuperar les solucions de [23] en el límit supersimètric. La no unicitat (contínua) d'aquesta família de solucions estaria parametritzada per les tres càrregues dipolars $q_{1,2,3}$. Creiem que un dels paràmetres d'aquesta solució no hauria de descriure excitacions a prop de supersimetria del supertub, sinó que s'haurien d'interpretar com cordes o branes dipolars superposades al supertub, de manera que trenquin totes les supersimetries.

Amb els paràmetres extra que manquen a la nostra solució esperem que es pugui variar J_ϕ i les tres càrregues dipolars de forma independent. Per tant, haurien d'existir anells negres amb dues càrregues i dos moments angulars J_ϕ i J_ψ , mentre que a les nostres solucions el moment angular total J_ϕ ha de ser zero. Notem però que en el límit supersimètric J_ϕ tendeix a zero, cosa que està d'acord amb el fet que microscòpicament J_ϕ es pugui explicar com degut excitacions fermiòniques coherents de cordes obertes amb polaritzacions de dretes i d'esquerres. Per tant, les nostres solucions només poden descriure excitacions tèrmiques amb $J_\phi = 0$. Tot i aquesta limitació, les nostres solucions ens haurien de permetre adreçar qüestions com la no unicitat dels forats negres i el comptatge de l'entropia en anells negres a prop de supersimetria seguint la proposta de [22].

De la mateixa manera, les solucions que hem presentat amb tres càrregues i dos dipòls descriuen certes excitacions no supersimètriques de la superhèlix D1-D5-P/d1-d5. Concretament, només podem descriure excitacions en què $J_\psi - J_\phi$ pren la meitat del valor màxim permès. Novament, esperem que amb una família de solucions més general puguem descriure totes les excitacions tèrmiques.

Finalment, cal remarcar que hem trobat evidències de què cal considerar com a físiques aquelles solucions de supergravetat amb singularitats despullades però que admeten deformacions tèrmiques; és a dir, que apareixen en el límit de temperatura zero de forats negres amb horitzons regulars.

Anells negres amb rotació a la S^2

En aquest treball hem presentat una nova solució de les equacions d'Einstein al buit en cinc dimensions, asimptòticament plana, i que consisteix en un anell negre en què el moment angular es troba al llarg de l'equador de la 2-esfera. L'horitzó d'aquesta solució té una topologia $S^1 \times S^2$ però presenta una singularitat cònica a l'interior de l'anell, que impedeix que col·lapsi. Malgrat que en el seu moment vam considerar que aquesta solució era un pas intermedi cap a l'obtenció de l'anell negre amb dos moments angulars, hom hauria de poder comprovar que es recupera la nostra solució en un determinat límit de l'anell negre amb doble rotació anunciat a [28]. Concretament, hauríem de partir del cas en què encara no s'ha equilibrat la configuració.

Podem utilitzar la nostra solució com a llavor i aplicar-li un seguit de boosts i dualitats [22, 41], i així obtenir un anell negre amb rotació a la S^2 i càrregues de F1-P. Aquesta nova solució també presenta una singularitat cònica, excepte en el límit supersimètric. En aquest límit, en què desapareix el moment angular, obtenim una configuració que es pot interpretar com una distribució de cordes F1-P al llarg d'un cercle. Degut a les raons que s'exposen a

[22], esperem que no sigui possible afegir més de dues càrregues a aquesta solució sense generar cordes de Dirac-Misner. Finalment, pensem que podria ser interessant generalitzar l'anell negre que hem presentat i incloure-hi càrregues dipolars. Malgrat la inclusió de noves càrregues i per tant de nous paràmetres, creiem que la singularitat cònica persistiria degut a què les càrregues dipolars tendeixen a incrementar la tensió de la corda [18] i per tant caldria una força externa per tal d'equilibrar la configuració.

Forats negres supersimètrics en AdS_5

En aquest treball hem estudiat els forats negres supersimètrics asimptòticament AdS_5 més generals que es coneixen. Partint d'una sèrie d'hipòtesis sobre la geometria de la base de Kähler i que són compatibles amb els forats negres coneguts, hem construït una família d'espais base que depèn únicament d'una funció. Des d'un bon principi però les nostres hipòtesis exclouen els anells negres en AdS_5 .

Per tal d'obtenir una solució supersimètrica, hem vist que la funció que caracteritza l'espai base ha d'obeir una equació diferencial de sisè ordre. Per a tots els forats negres coneguts, aquesta funció és un polinomi cúbic. La resta de solucions de l'esmentada equació donen lloc a horitzons no compactes o bé singulars. Per tant, els nostres resultats semblen indicar que els forats negres ja coneguts són de fet els més generals que existeixen amb topologia esfèrica i dues isometries $U(1)$. Ara bé, el nostre anàlisi no exclou la possibilitat que existeixin forats negres amb menys isometries.

Un altre resultat que hem obtingut ha estat la construcció d'un conjunt infinit de deformacions supersimètriques de AdS_5 i dels forats negres ja coneguts. Aquestes deformacions tendeixen a zero a l'horitzó però canvien l'estructura asimptòtica de l'espai-temps. El més interessant és que aquestes deformacions, en coordenades estàtiques, depenen del temps. Malgrat això, i tal i com requereix la supersimetria, encara existeix un vector de Killing tipus temps a la regió externa a l'horitzó. Seria interessant entendre aquestes deformacions des del punt de vista de la CFT dual.

Una possible línia per a futures investigacions seria generalitzar les nostres hipòtesis per tal incloure els anells negres. Cal tenir present, però, que els resultats de [47] demostren que els anells negres supersimètrics en AdS_5 i amb dues isometries $U(1)$ sempre presenten singularitats còniques. Finalment, seria interessant estudiar la possibilitat de què existeixin espais-temps amb més d'un forat negre en AdS_5 . En aquest cas, hom hauria de trobar una base de Kähler que esdevingués una varietat de Kähler cònica en un conjunt de punts corresponents a l'horitzó de cada forat negre.

Saturn negre

En aquest treball hem presentat i analitzat una solució de les equacions d'Einstein al buit en cinc dimensions corresponent a un saturn negre: un forat negre de MP envoltat per un anell negre. Gràcies a la rotació al llarg del pla de l'anell, la solució està equilibrada i no presenta singularitats còniques. També hem comprovat numèricament que la solució no té corbes temporals tancades.

Aquesta solució presenta una sèrie de propietats físiques interessants:

- No unicitat: la massa total M i el moment angular J mesurats a l'infinit es poden distribuir de manera contínua entre els dos objectes. Aquesta no unicitat depèn de dos paràmetres continus.

- No unicitat de la solució de Schwarzschild en cinc dimensions: l'anell negre i el forat negre poden rotar en sentits oposats i encara mantenir el sistema en equilibri. És possible assolir una configuració tal que el moment angular total J mesurat a l'infinit sigui zero.
- “Frame dragging” degut a la rotació: la interacció gravitatòria entre el forat negre i l'anell negre es manifesta en termes de frame dragging rotacional. Quan considerem el cas d'un forat negre sense moment angular intrínsec, la presència de l'anell amb rotació fa que el forat negre adquireixi una velocitat angular Ω^{BH} diferent de zero, ja que l'anell negre arrossega l'espai-temps del seu voltant. També és possible trobar una configuració en què els dos objectes estan rotant en sentits oposats de tal manera que $\Omega^{\text{BH}} = 0$.

És molt probable que el saturn negre sigui clàssicament inestable ja que els anells negres ho són. Per tant, esperem que el saturn negre experimenti les mateixes inestabilitats que els anells [17, 48]. Ara bé, és possible que el saturn negre exhibeixi noves inestabilitats, com per exemple les derivades de les pertorbacions del centre de masses del forat negre.

Seria interessant disposar de la solució en coordenades (x, y) adaptades als anells negres, cosa que facilitaria l'estudi, entre altres coses, de les ergo-regions i les corbes temporals tancades de forma analítica.

Possibles generalitzacions del saturn negre inclouen anells múltiples de saturn, que es poden construir afegint nous anells negres concèntrics a la nostra solució. També es poden construir saturns negres amb doble rotació, ja sigui donant rotació intrínseca al forat negre al pla ortogonal al de l'anell o bé generalitzant la solució de [28]. Els anells negres també poden portar càrregues dipolars i, per tant, incloent les càrregues dipolars a l'anell negre podríem construir un saturn negre dipolar.⁶ Finalment, pujant la solució a deu dimensions seguit d'una sèrie de boosts i dualitats podríem construir un saturn negre amb càrregues de D1-D5. Per tal de construir la general solució amb tres càrregues, hauríem de partir del saturn negre més general possible que inclogués tres càrregues dipolars.

Fases dels forats negres en cinc dimensions

En aquest treball hem vist que en cinc dimensions existeixen configuracions estacionàries de forats negres, i concretament de saturns negres, tals que recobreixen *tot* l'espai de fases. És més, els saturns negres maximitzen l'entropia. Aquestes configuracions amb entropia màxima, consisteixen en un forat negre central estàtic que conté pràcticament tota la massa del sistema rodejat per un anell negre llarg i prim que és el portador del moment angular.

El fet que els saturns negres maximitzin l'entropia sembla indicar que tant els forats negres de MP com els anells negres podrien incrementar la seva entropia fragmentant-se en saturns negres. Així doncs, podríem pensar que *tots* els forats negres en cinc dimensions amb $J \neq 0$ són clàssicament inestables. Ara bé, sembla difícil que un forat negre de MP pugui evolucionar dinàmicament cap a un saturn negre amb entropia màxima ja que aquest últim té una extensió en el pla de rotació molt més gran que el forat negre inicial. En canvi, resulta més plausible pensar que el forat negre pugui evolucionar cap a un saturn negre de les mateixes dimensions si l'àrea total s'incrementa.

Recentment s'han construït saturns negres amb càrregues dipolars [40] de manera que les úniques càrregues conservades són M i J . Pels anells negres amb càrregues dipolars i extremals la inestabilitat de Gregory i Laflamme hauria de desaparèixer. A la vegada s'ha argumentat

⁶Aquesta solució ha estat construïda recentment a [40].

que els anells negres dipolars primis són clàssicament estables sota pertorbacions radials [48]. Per tant, és possible que es puguin trobar saturns negres amb càrregues dipolars clàssicament estables. Els saturns negres supersimètrics de la referència [30], que són clàssicament estables, en alguns casos poden tenir una entropia més gran que un forat negre amb les mateixes càrregues conservades. Per tant, és possible que els saturns negres no supersimètrics i extremals tinguin propietats similars.

Finalment, s'ha argumentat que els anells negres existeixen en dimensions $D \geq 5$. Per tant, els saturns negres també haurien d'existir i les configuracions amb entropia màxima haurien de tenir propietats semblants a les que hem descrit en aquest treball. Concretament, un nombre infinit de famílies de solucions haurien de recobrir una banda semi-infinita del pla $(\tilde{J}, \tilde{\mathcal{A}})$, però només algunes d'elles estarien en equilibri termodinàmic.

Solucions supersimètriques de Teoria M amb factors AdS_3

En el context de la dualitat AdS_3/CFT_2 en Teoria M, en aquest treball hem formalitzat una proposta sobre aspectes globals universals de la geometria de tota solució de supergravetat. Concretament, afirmem que tota solució de supergravetat que admet una descripció en termes d'una CFT dual, és a dir, amb una regió de l'espai-temps que conté un factor AdS , ha d'admetre un factor $\mathbb{R}^{1,1}$ globalment definit i una reducció global del fibrat a un altre fibrat amb grup d'estructura contingut a $Spin(7)$. Partint d'aquest fet, veiem com diversos aspectes de la correspondència AdS/CFT emergeixen de forma natural en aquest context. Per exemple, les projeccions de kappa-simetria de les branes prova apareixen de la definició global de la realització espinorial del fibrat. Solucions en què els fluxes tendeixen a zero asimptòticament automàticament tendeixen a varietats amb holonomia especial. Finalment, l'existència d'un fibrat globalment definit ens permet particularitzar les equacions del moviment de supergravetat en onze dimensions de forma global. Així, podem obtenir les condicions necessàries i suficients per l'existència d'una solució de Teoria M amb un factor AdS_3 i que preservi com a mínim una supersimetria: en particularitzar la solució general de supergravetat a un fibrat de Cayley hem d'imposar condicions de contorn AdS_3 .

Els nostres resultats, juntament amb els de la primera referència de [38], constitueixen la classificació de totes les solucions supersimètriques de Teoria M amb factors AdS_3 i menys de setze supersimetries. Les solucions que preserven la meitat de les supersimetries no estan classificades.

Una futura línia de recerca consisteix a utilitzar les condicions que han d'obeeir les geometries per tal d'obtenir noves solucions explícites. Igualment interessant és l'estudi de les condicions de contorn amb tota generalitat. Un tipus de condicions de contorn interessants són aquelles en què tenim holonomia especial a l'infinit i AdS a l'horitzó. Les úniques solucions que coneixem que obeeixen aquestes condicions de contorn són les branes elementals, i aquestes solucions interpolants estan associades a la resolució de les singularitats de les varietats amb holonomia especial que trobem a l'infinit.

Conclusions finals

En aquesta tesi hem obtingut noves solucions de forat negre en dimensions $D > 4$. Com hem vist, disposar de solucions de les equacions d'Einstein al buit és molt importat. Des d'un punt de vista de la Relativitat General ens permet entendre millor la dinàmica de la teoria i, a la vegada, mitjançant una sèrie de boosts i dualitats podem generar noves solucions de Teoria de

Cordes a baixes energies. Tot just hem començat a explorar la dinàmica de gravetat en $D > 4$ i queda clar que hi ha molt camí per recórrer. Sembla ser però que per tal de trobar noves solucions amb menys simetries faran falta noves tècniques.

La correspondència AdS/CFT ens proporciona una definició de la gravetat quàntica en espais amb factors AdS_d . Per tant, és molt interessant explorar els forats negres amb aquesta assintòtica ja que ens ha de permetre respondre a les qüestions més fonamentals que involucra la física dels forats negres en una situació en què tenim la teoria microscòpica sota control. A la vegada, esperem que gravetat ens permeti entendre aspectes no pertorbatius de les teories gauge que governen el nostre món de baixes energies.

1.4 Discussion and conclusions

In this section we discuss the main results, we present the conclusions and provide some ideas for future research.

Non-supersymmetric black rings with D1-D5-P charges

We have shown how to construct non-supersymmetric black rings carrying D1-D5-P charges by means of boosts and dualities, overcoming the problems previously encountered in [22]. We have achieved this by having more parameters associated to the dipole charges in the seed solution. The main issue is the requirement that the 1-form ω associated to the rotation be well defined, which is equivalent to imposing the absence of Dirac-Misner strings.

From our results, we expect that a larger family of non-supersymmetric black rings with nine-parameters $(M, J_\psi, J_\phi, Q_{1,2,3}, q_{1,2,3})$ exists, and that the general solutions of [23] are recovered in the non-supersymmetric limit. The nine-parameters would yield three-fold (continuous) non-uniqueness, furnished by the non-conserved dipole charges $q_{1,2,3}$. Presumably, one of the additional parameters in the conjectured larger family of solutions will not describe proper near-supersymmetric excitations of the supertube. Instead they should be interpreted as the presence of dipole strings or branes in the configuration that are not bound to the supertube but rather superimposed on it and hence they break all the supersymmetries.

The extra parameters that are still missing from our current solutions should provide the freedom to vary the angular momentum J_ϕ and all the three dipoles independently of other parameters. In particular, we expect that black rings with two charges should exist that carry both angular momenta J_ψ and J_ϕ . Note, though, that in the supersymmetric limit J_ϕ disappears, which is consistent with the fact that J_ϕ is expected to be carried by the coherent polarization of (R-charged) left- and right-moving fermionic open string excitations. In our solutions the total macroscopic J_ϕ must vanish. So the two-charge solutions in this paper can describe the non-BPS excitations that carry total $J_\phi = 0$. This should be already enough to address in detail the issues of black hole non-uniqueness and near-supersymmetric black ring entropy from a microscopic viewpoint, along the lines proposed in ref. [22].

The solutions with three charges and two dipoles in this paper are similarly expected to describe the non-BPS excitations that do not add to the J_ϕ of a D1-D5-P/d1-d5 super-helix. However, in this case we seem to be restricted to considering only excitations above the supersymmetric state with half the maximum value of $J_\psi - J_\phi$. Once again, we expect that with a larger family of solutions, we should be able to describe all thermal excitations.

Finally, we have found evidence in favor of considering as physically sensible those naked singularities in supergravity that admit thermal deformations. That is, solutions that arise as

the zero-temperature limit of black holes with a regular horizon.

A black ring with a rotating 2-sphere

We have presented a new asymptotically flat solution of Einstein's vacuum equations in five dimensions corresponding to a black ring with rotation on the plane orthogonal to the ring. Although our solution has a horizon with topology $S^1 \times S^2$, there is a conical singularity inside the ring that prevents it from collapsing. At the moment of writing the paper we thought of this solution as an intermediate step towards a more general black ring with two independent angular momenta. However, it should be possible to recover our solution as a particular limit of the general doubly spinning ring announced in [28]. In particular, one should start from the unbalanced solution.

One can use our solution as a seed and construct the black ring with a rotating S^2 and carrying F1-P charges by means of boosts and dualities. In this charged black ring the conical singularity persists except in the extremal supersymmetric limit. In this limit, in which the angular momentum disappears, we find a configuration which can be interpreted as a continuous distribution of straight F1-P strings on a circle. We do not expect to be able to add more than two charges to the solution without generating Dirac-Misner strings for the reasons discussed in [22]. Furthermore, it would be interesting to construct the ϕ -spinning ring carrying dipole charges. Even then, we do not expect to be able to remove the conical singularity since the dipole charges typically increase the tension of the string [18] and hence an external force is required in order to balance the configuration.

Supersymmetric black holes in AdS_5

In this work we have studied the most general supersymmetric black holes that are asymptotically AdS_5 . Starting from some assumptions regarding the geometry of the Kähler base, which are compatible with the known solutions, we have constructed a family of Kähler bases which depend only on a single function. However, from the very beginning, our hypothesis excluded supersymmetric AdS_5 black rings from our study.

The function that characterises the family of bases obeys a remarkably simple 6th order differential equation. A family of solutions, albeit not the most general one, is a cubic polynomial, which turns out to describe all known AdS_5 supersymmetric black holes. The remaining solutions of the sixth order equation that we found are spaces with non-compact horizons or spaces with singular horizons. This suggests that indeed, the family of solutions found so far describes the most general black holes with spherical topology and two $U(1)$ isometries in AdS_5 . Our analysis does not seem to exclude more general black holes, with fewer isometries.

Secondly, we found an infinite set of supersymmetric deformations of both AdS_5 space and the black holes living on it. These deformations vanish at the horizon and they change the asymptotic structure of the spacetime. Interestingly, these deformations, are time dependent, when one writes AdS_5 in static coordinates, but there is still an everywhere timelike Killing vector field. Also, they provide an example of supersymmetric AdS_5 solutions, where the five dimensional spacetime has less spatial isometries than the base space. Of course it would be interesting to understand better these solutions and if they have some CFT correspondence.

There are several directions in which one could extend the work herein. One of the outstanding questions in this field, is the possible existence of AdS_5 black rings. However, the recent results of [47] show that supersymmetric black rings in AdS_5 with two $U(1)$ isometries

always have conical singularities. Finally, let us mention that the issue of the existence of multi-black hole solutions in AdS_5 remains open. Clearly, a strategy to look for such solutions is to consider a Kähler base that reduces to a conical Kähler manifold at a set of points, which would correspond to each of the horizons.

Black saturn

In this work we have constructed and analysed a new solution of Einstein's vacuum equations in five dimensions corresponding to a black saturn: a MP black hole surrounded by a black ring. Thanks to the rotation along the plane of the ring, the solution is balanced and hence free from conical singularities. Moreover, we have checked numerically that our solution does not have closed timelike curves either.

This solution exhibits some interesting physical properties, which we summarise below:

- Non-uniqueness: The total mass M and angular momentum J measured at infinity can be distributed continuously between the two black objects in the balanced saturn configuration. This non-uniqueness depends on two continuous parameters.
- Non-uniqueness of the five-dimensional Schwarzschild black hole: Strikingly, the black ring and S^3 black hole can be counter-rotating to give zero total angular momentum J at infinity.
- Rotational frame-dragging: The gravitational interaction between the black ring and the S^3 black hole manifests itself in form of rotational frame-dragging. This is most cleanly illustrated when the intrinsic angular momentum of the S^3 black hole is set to zero. The angular velocity Ω^{BH} , however, is not zero but follows the behavior of the angular velocity Ω^{BR} of the black ring. We interpret this as frame-dragging: the rotating black ring drags the spacetime around with it, and in effect the black hole rotates too, despite having no intrinsic spin. Counter-rotation makes it possible to reach a configuration for which the angular velocity of the black hole vanishes: $\Omega^{\text{BH}} = 0$.

The saturn system may well be classically unstable. The black ring of black saturn likely suffers from the same instabilities as the single black ring [17, 48]. While some stability properties of black saturn can be expected to be inherited from the individual components, the Myers-Perry black hole and the single black ring, there can also be new instabilities for the black saturn system, for instance, perturbation of the center-of-mass of the S^3 black hole away from the center of the ring.

It would be interesting to write the black saturn metric in the (x, y) coordinates adapted to black rings, since it would make it easier to study analytically both the ergoregions and the existence of closed timelike curves.

Possible generalizations include multiple rings of saturn, which can be constructed adding more concentric black rings to our present configuration. It should also be possible to construct doubly spinning black saturns giving intrinsic rotation to the black hole on plane orthogonal to that of the ring or generalizing the solution of [28]. Black rings can also carry dipole charges so adding dipole charges to the black ring should give the dipole black saturn solution.⁷ Finally, uplifting the solution to ten dimensions followed by a suitable series of boosts and dualities should result in the D1-D5 black saturn. However, in order to construct the three charge solution, we should start from the most general black saturn with three dipole charges.

⁷This solution has been constructed recently in [40].

Phases of five-dimensional black holes

In this work we have shown that there exist black hole configurations in five dimensions, and more specifically black saturns, such that they cover the *whole* phase space. What is more remarkable is that black saturns maximize the entropy. In these configurations with maximal entropy, a central almost static black hole carries most of the mass and a very large and thin black ring is responsible for the required angular momentum.

The fact that the black saturns maximize the entropy seems to indicate that both a MP black hole or a black ring could increase their entropy by fragmentation into black saturns. This could signal a classical instability of all five-dimensional black holes with $J \neq 0$. However, it seems difficult for a MP black hole or a black ring to dynamically evolve into a black saturn of near-maximal area since the latter is much larger in extend on the rotation plane than the initial black hole. But it could possibly evolve towards a black saturn of roughly the same size as the initial black hole if the final area were larger.

Recently black saturns carrying dipole charges have been constructed [40], and therefore the only conserved charges such systems are M and J . For black rings with dipole charges that saturate the extremal bound, the Gregory-Laflamme instability is expected to disappear. Thin dipole black rings have also been argued to be radially stable [48]. So dipole black saturns can presumably be made classically stable. The supersymmetric multi-ring black saturns constructed in [30], also expected stable, in some cases can have larger entropy than a single black hole with the same charges. Therefore, it is likely that the extremal non-supersymmetric black saturns have similar properties.

Finally, it has been recently argued that black rings should exist in $D \geq 5$. Hence, higher dimensional black saturns should also exist, and in particular the configurations that maximize the entropy should have the same qualitative properties that we have described. A semi-infinite strip in the $(\tilde{J}, \tilde{\mathcal{A}})$ plane will then be covered by an infinite number of families of solutions, but only a few of them are expected to be in thermal equilibrium.

Supersymmetric solutions of M-theory with AdS_3 factors

In this work, we have formalised a proposal for a universal feature of the global geometry of supergravity solutions of relevance to the supersymmetric AdS_3/CFT_2 correspondence in M-theory. A supergravity solution associated to a CFT – a region of spacetime containing a local AdS region – should admit a globally-defined $\mathbb{R}^{1,1}$ frame, and a global reduction of its frame bundle, to one with structure group contained in $Spin(7)$. From this starting assumption, we have seen how many individual features of AdS/CFT geometry may be assembled into a coherent overall picture. Probe brane kappa-symmetry projections arise from the global definition of the spinorial realisation of the frame bundle. Solutions with asymptotically vanishing flux automatically asymptote to special holonomy manifolds. The existence of a globally-defined frame bundle allows for the global truncation of the field equations of eleven-dimensional supergravity. The general necessary and sufficient conditions for minimally supersymmetric AdS_3 geometry in M-theory may be derived by imposing an AdS_3 boundary condition on the truncation of supergravity to a Cayley frame bundle.

Our results, together with those in the first reference of [38], constitute a classification of all supersymmetric solutions of M-theory with AdS_3 factors and less than sixteen supersymmetries. The classification of the solutions that preserve half of the supersymmetries remains an open problem.

One possible future line of research is to use the geometrical insight provided by the *AdS* torsion conditions to construct new explicit *AdS* solutions. A more important question is the development of a theory of boundary conditions for solutions of the truncated supergravity equations. A class of boundary conditions which is particularly interesting mathematically is special holonomy spacelike asymptotics with vanishing fluxes, and spacelike *AdS* asymptotics associated to event horizons. To our knowledge, the only known solutions of this form are the elementary brane solutions. These interpolating solutions are intimately associated to the resolution of singularities of the asymptotic special holonomy manifolds.

Final conclusions

In this thesis we have found new black hole type of solutions in $D > 4$. We have stressed the importance of having explicit analytic solutions to the Einstein's vacuum equations in higher dimensions. From the General Relativity point of view, these solutions allow us to gain more insight into the dynamics of the theory. Moreover, we have seen that by means of boosts and dualities we can obtain new solutions of String Theory at low energies. We have just started to explore the dynamics of gravity in $D > 4$, but it is clear that we are just seeing the tip of the iceberg. However, it seems that in order to find new solutions with less symmetries, new techniques will be required.

The AdS/CFT correspondence provides a definition of quantum gravity in spacetimes which contain AdS_d factors. Therefore, it is very interesting to study black hole solutions with this asymptopia since it may help us to answer some of the most fundamental questions that the physics of black holes poses in a situation where the underlying microscopic theory is under control. At the same time, we hope that gravity may provide some clues to non-perturbative aspects of the usual gauge theories that govern our low energy world.

Bibliography

- [1] K. Schwarzschild, “On The Gravitational Field Of A Mass Point According To Einstein’s Theory,” *Sitzungsber. Preuss. Akad. Wiss. Berlin (Math. Phys.)* **1916** (1916) 189 [arXiv:physics/9905030].
- [2] R. P. Kerr, “Gravitational field of a spinning mass as an example of algebraically special metrics,” *Phys. Rev. Lett.* **11** (1963) 237.
- [3] B. Carter, “Axisymmetric Black Hole Has Only Two Degrees of Freedom,” *Phys. Rev. Lett.* **26** (1971) 331.
- [4] D. C. Robinson, “Uniqueness of the Kerr black hole,” *Phys. Rev. Lett.* **34** (1975) 905.
- [5] P. O. Mazur, “Proof Of Uniqueness Of The Kerr-Newman Black Hole Solution,” *J. Phys. A* **15** (1982) 3173.
- [6] G. L. Bunting, “Proof of the Uniqueness Conjecture for Black Holes,” PHD thesis, Univ. of New England, Armidale N.S.W. 1983.
- [7] S. W. Hawking, “Black holes in general relativity,” *Commun. Math. Phys.* **25** (1972) 152.
S. W. Hawking and G. F. R. Ellis, “The Large scale structure of space-time,” *Cambridge University Press, Cambridge, 1973*.
- [8] S. Chandrasekhar, “The Mathematical Theory of Black Holes,” *Oxford, UK: Clarendon (1992) 646 p.*
- [9] J. M. Bardeen, B. Carter and S. W. Hawking, “The Four laws of black hole mechanics,” *Commun. Math. Phys.* **31** (1973) 161.
- [10] S. W. Hawking, “Particle Creation By Black Holes,” *Commun. Math. Phys.* **43** (1975) 199 [Erratum-*ibid.* **46** (1976) 206].
- [11] R. M. Wald, “Black hole entropy in the Noether charge,” *Phys. Rev. D* **48** (1993) 3427 [arXiv:gr-qc/9307038].
V. Iyer and R. M. Wald, “Some properties of Noether charge and a proposal for dynamical black hole entropy,” *Phys. Rev. D* **50** (1994) 846 [arXiv:gr-qc/9403028].
- [12] A. Strominger and C. Vafa, “Microscopic Origin of the Bekenstein-Hawking Entropy,” *Phys. Lett. B* **379** (1996) 99 [arXiv:hep-th/9601029].

- [13] R. Emparan and G. T. Horowitz, “Microstates of a neutral black hole in M theory,” *Phys. Rev. Lett.* **97** (2006) 141601 [arXiv:hep-th/0607023].
R. Emparan and A. Maccarrone, “Statistical description of rotating Kaluza-Klein black holes,” *Phys. Rev. D* **75** (2007) 084006 [arXiv:hep-th/0701150].
- [14] N. Arkani-Hamed, S. Dimopoulos and G. R. Dvali, “Phenomenology, astrophysics and cosmology of theories with sub-millimeter dimensions and TeV scale quantum gravity,” *Phys. Rev. D* **59** (1999) 086004 [arXiv:hep-ph/9807344].
Per a una discussió més recent, vegeu: R. Maartens, “Brane-world gravity,” *Living Rev. Rel.* **7** (2004) 7 [arXiv:gr-qc/0312059].
- [15] R. C. Myers and M. J. Perry, “Black Holes In Higher Dimensional Space-Times,” *Annals Phys.* **172** (1986) 304.
- [16] R. Gregory and R. Laflamme, “Black strings and p-branes are unstable,” *Phys. Rev. Lett.* **70** (1993) 2837 [arXiv:hep-th/9301052].
- [17] R. Emparan and H. S. Reall, “A rotating black ring in five dimensions,” *Phys. Rev. Lett.* **88** (2002) 101101 [arXiv:hep-th/0110260].
- [18] R. Emparan, “Rotating circular strings, and infinite non-uniqueness of black rings,” *JHEP* **0403** (2004) 064 [arXiv:hep-th/0402149].
- [19] G. J. Galloway and R. Schoen, “A generalization of Hawking’s black hole topology theorem to higher dimensions,” *Commun. Math. Phys.* **266** (2006) 571 [arXiv:gr-qc/0509107].
- [20] A. W. Peet, “TASI lectures on black holes in string theory,” [arXiv:hep-th/0008241].
- [21] D. Mateos and P. K. Townsend, “Supertubes,” *Phys. Rev. Lett.* **87** (2001) 011602 [arXiv:hep-th/0103030].
R. Emparan, D. Mateos and P. K. Townsend, “Supergravity supertubes,” *JHEP* **0107** (2001) 011 [arXiv:hep-th/0106012].
- [22] H. Elvang and R. Emparan, “Black rings, supertubes, and a stringy resolution of black hole JHEP **0311** (2003) 035 [arXiv:hep-th/0310008].
- [23] H. Elvang, R. Emparan, D. Mateos and H. S. Reall, “A supersymmetric black ring,” *Phys. Rev. Lett.* **93** (2004) 211302 [arXiv:hep-th/0407065].
H. Elvang, R. Emparan, D. Mateos and H. S. Reall, “Supersymmetric black rings and three-charge supertubes,” *Phys. Rev. D* **71** (2005) 024033 [arXiv:hep-th/0408120].
- [24] T. Mishima and H. Iguchi, “New axisymmetric stationary solutions of five-dimensional vacuum Einstein equations with asymptotic flatness,” *Phys. Rev. D* **73** (2006) 044030 [arXiv:hep-th/0504018].
- [25] R. Emparan and H. S. Reall, “Generalized Weyl solutions,” *Phys. Rev. D* **65** (2002) 084025 [arXiv:hep-th/0110258].
T. Harmark, “Stationary and axisymmetric solutions of higher-dimensional general relativity,” *Phys. Rev. D* **70** (2004) 124002 [arXiv:hep-th/0408141].

- [26] V. A. Belinsky and V. E. Zakharov, “Integration Of The Einstein Equations By The Inverse Scattering Problem Technique And The Calculation Of The Exact Soliton Solutions,” *Sov. Phys. JETP* **48** (1978) 985 [*Zh. Eksp. Teor. Fiz.* **75** (1978) 1953].
V. A. Belinsky and V. E. Zakharov, “Stationary Gravitational Solitons With Axial Symmetry,” *Sov. Phys. JETP* **50** (1979) 1 [*Zh. Eksp. Teor. Fiz.* **77** (1979) 3].
Vegeu també: V. Belinski and E. Verdaguer, “Gravitational solitons,” *Cambridge, UK: Univ. Pr. (2001) 258 p.*
- [27] A. A. Pomeransky, “Complete integrability of higher-dimensional Einstein equations with additional symmetry, and rotating black holes,” *Phys. Rev. D* **73** (2006) 044004 [arXiv:hep-th/0507250].
- [28] A. A. Pomeransky and R. A. Sen’kov, “Black ring with two angular momenta,” [arXiv:hep-th/0612005].
- [29] D. Kramer and G. Neugebauer, “The superposition of two Kerr solutions,” *Phys. Lett. A.* **75** 4 (1980) 259-261
- [30] J. P. Gauntlett and J. B. Gutowski, “Concentric black rings,” *Phys. Rev. D* **71**, 025013 (2005) [arXiv:hep-th/0408010].
J. P. Gauntlett and J. B. Gutowski, “General concentric black rings,” *Phys. Rev. D* **71**, 045002 (2005) [arXiv:hep-th/0408122].
- [31] J. M. Maldacena, “The large N limit of superconformal field theories and supergravity,” *Adv. Theor. Math. Phys.* **2** (1998) 231 [*Int. J. Theor. Phys.* **38** (1999) 1113] [arXiv:hep-th/9711200].
- [32] J. P. Gauntlett and J. B. Gutowski, “All supersymmetric solutions of minimal gauged supergravity in five dimensions,” *Phys. Rev. D* **68** (2003) 105009 [Erratum-ibid. *D* **70** (2004) 089901] [arXiv:hep-th/0304064].
- [33] J. B. Gutowski and H. S. Reall, “Supersymmetric AdS(5) black holes,” *JHEP* **0402** (2004) 006 [arXiv:hep-th/0401042].
J. B. Gutowski and H. S. Reall, “General supersymmetric AdS(5) black holes,” *JHEP* **0404** (2004) 048 [arXiv:hep-th/0401129].
- [34] Z. W. Chong, M. Cvetič, H. Lu and C. N. Pope, “Five-dimensional gauged supergravity black holes with independent rotation parameters,” *Phys. Rev. D* **72** (2005) 041901 [arXiv:hep-th/0505112].
Z. W. Chong, M. Cvetič, H. Lu and C. N. Pope, “General non-extremal rotating black holes in minimal five-dimensional gauged supergravity,” *Phys. Rev. Lett.* **95**, 161301 (2005) [arXiv:hep-th/0506029].
H. K. Kunduri, J. Lucietti and H. S. Reall, “Supersymmetric multi-charge AdS(5) black holes,” *JHEP* **0604** (2006) 036 [arXiv:hep-th/0601156].
- [35] J. P. Gauntlett, D. Martelli, S. Pakis and D. Waldram, “G-structures and wrapped NS5-branes,” *Commun. Math. Phys.* **247** (2004) 421 [arXiv:hep-th/0205050].
J. P. Gauntlett, D. Martelli and D. Waldram, “Superstrings with intrinsic torsion,” *Phys. Rev. D* **69** (2004) 086002 [arXiv:hep-th/0302158].

- [36] J. P. Gauntlett and S. Pakis, “The geometry of $D = 11$ Killing spinors. ((T),” JHEP **0304** (2003) 039 [arXiv:hep-th/0212008].
J. P. Gauntlett, J. B. Gutowski and S. Pakis, “The geometry of $D = 11$ null Killing spinors,” JHEP **0312** (2003) 049 [arXiv:hep-th/0311112].
- [37] J. P. Gauntlett, D. Martelli, J. Sparks and D. Waldram, “Supersymmetric AdS(5) solutions of M-theory,” Class. Quant. Grav. **21** (2004) 4335 [arXiv:hep-th/0402153].
- [38] J. P. Gauntlett, O. A. P. Mac Conamhna, T. Mateos and D. Waldram, “AdS spacetimes from wrapped M5 branes,” JHEP **0611** (2006) 053 [arXiv:hep-th/0605146].
O. A. P. Mac Conamhna and E. O Colgain, “Supersymmetric wrapped membranes, AdS(2) spaces, and bubbling geometries,” JHEP **0703** (2007) 115 [arXiv:hep-th/0612196].
- [39] O. A. P. Mac Conamhna, “Refining G-structure classifications,” Phys. Rev. D **70** (2004) 105024 [arXiv:hep-th/0408203].
M. Cariglia and O. A. P. Mac Conamhna, “Null structure groups in eleven dimensions,” Phys. Rev. D **73** (2006) 045011 [arXiv:hep-th/0411079].
O. A. P. Mac Conamhna, “Eight-manifolds with G-structure in eleven dimensional supergravity,” Phys. Rev. D **72** (2005) 086007 [arXiv:hep-th/0504028].
O. A. P. Mac Conamhna, “The geometry of extended null supersymmetry in M-theory,” Phys. Rev. D **73** (2006) 045012 [arXiv:hep-th/0505230].
- [40] S. Yazadjiev, “Black Saturn with dipole ring,” arXiv:0705.1840 [hep-th].
- [41] H. Elvang, R. Emparan and P. Figueras, “Non-supersymmetric black rings as thermally excited supertubes,” JHEP **0502** (2005) 031 [arXiv:hep-th/0412130].
- [42] P. Figueras, “A black ring with a rotating 2-sphere,” JHEP **0507** (2005) 039 [arXiv:hep-th/0505244].
- [43] P. Figueras, C. A. R. Herdeiro, F. P. Correia, “On a class of 4D Kähler bases and AdS₅ supersymmetric Black Holes,” JHEP **0611** (2006) 036 [arXiv:hep-th/0608201].
- [44] H. Elvang and P. Figueras, “Black Saturn,” arXiv:hep-th/0701035.
- [45] H. Elvang, R. Emparan and P. Figueras, “Phases of Five-Dimensional Black Holes,” arXiv:hep-th/0702111.
- [46] P. Figueras, O. A. P. Mac Conamhna and E. O Colgain, “Global geometry of the supersymmetric AdS(3)/CFT(2) correspondence in M-theory,” arXiv:hep-th/0703275.
- [47] H. K. Kunduri, J. Lucietti and H. S. Reall, “Do supersymmetric anti-de Sitter black rings exist?,” JHEP **0702** (2007) 026 [arXiv:hep-th/0611351].
- [48] H. Elvang, R. Emparan and A. Virmani, “Dynamics and stability of black rings,” JHEP **0612** (2006) 074 [arXiv:hep-th/0608076].

Part II
Compendi d'articles

Aquesta tesi és un compendi de les següents publicacions:

1. H. Elvang, R. Emparan and P. Figueras, “Non-supersymmetric black rings as thermally excited supertubes,” JHEP **0502** (2005) 031 [arXiv:hep-th/0412130].
2. P. Figueras, “A black ring with a rotating 2-sphere,” JHEP **0507** (2005) 039 [arXiv:hep-th/0505244].
3. P. Figueras, C. A. R. Herdeiro and F. P. Correia, “On a class of 4D Kähler bases and AdS₅ supersymmetric Black Holes,” JHEP **0611** (2006) 036 [arXiv:hep-th/0608201].
4. H. Elvang and P. Figueras, “Black Saturn,” JHEP **0705** (2007) 050 [arXiv:hep-th/0701035].
5. H. Elvang, R. Emparan and P. Figueras, “Phases of Five-Dimensional Black Holes,” JHEP **0705** (2007) 056 [arXiv:hep-th/0702111].
6. P. Figueras, O. A. P. Mac Conamhna and E. O Colgain, “Global geometry of the supersymmetric AdS(3)/CFT(2) correspondence in M-theory,” Phys. Rev. D **76** (2007) 046007 [arXiv:hep-th/0703275].

Chapter 2

Non-supersymmetric black rings as thermally excited supertubes

Henriette Elvang,^a Roberto Emparan,^{b,c} Pau Figueras^c

^a *Department of Physics, University of California, Santa Barbara, CA 93106-9530, USA*

^b *Institució Catalana de Recerca i Estudis Avançats (ICREA)*

^c *Departament de Física Fonamental, and
C.E.R. en Astrofísica, Física de Partícules i Cosmologia,
Universitat de Barcelona, Diagonal 647, E-08028 Barcelona, Spain*

elvang@physics.ucsb.edu, emparan@ub.edu,
pfigueras@ffn.ub.es

ABSTRACT

We construct a seven-parameter family of supergravity solutions that describe non-supersymmetric black rings and black tubes with three charges, three dipoles and two angular momenta. The black rings have regular horizons and non-zero temperature. They are naturally interpreted as the supergravity descriptions of thermally excited configurations of supertubes, specifically of supertubes with two charges and one dipole, and of supertubes with three charges and two dipoles. In order to fully describe thermal excitations near supersymmetry of the black supertubes with three charges and three dipoles a more general family of black ring solutions is required.

2.1 Introduction

Black rings are a fascinating outcome of recent studies of higher-dimensional gravity. They show that several classic results of black hole theory cannot be generalized to five dimensions: black rings have non-spherical horizon topology $S^1 \times S^2$, and their mass and spin are insufficient to fully distinguish between them and between other black holes of spherical topology [1, 2].

The remarkable progress in the string theory description of black holes had not hinted at the existence of black rings. So, initially, black rings appeared to be uncalled-for objects, and their role in string theory was unclear. A step to improve the understanding of black rings

in string theory was taken in ref. [3] (following [4]), where a connection was found between black rings with two charges and another class of objects of recent interest in string theory, the so-called supertubes [5, 6]. More recently this connection has been significantly strengthened and extended with the discovery in [7] of a supersymmetric black ring of five-dimensional supergravity, with a regular horizon of finite area. This has prompted the further study of supersymmetric rings, including the generalization to three-charge solutions [8, 9, 10] and other extensions and applications [11, 12, 13, 14, 15]. The authors of [15] have actually succeeded in providing a statistical counting of their Bekenstein-Hawking entropy. It is naturally interesting to try to extend these results to include near-supersymmetric black rings.

In this paper, we present a seven-parameter family of non-supersymmetric black ring solutions which generalize the ones studied in ref. [3]. The new solutions describe black rings with three conserved charges, three dipole charges, two unequal angular momenta, and finite energy above the BPS bound. We are motivated by the wish to understand the microscopic nature of the thermal excitations of two- and three-charge supertubes. We argue that the near-supersymmetric limits of the black rings in this paper can be interpreted as thermally excited supertubes with two charges and one dipole, or thermally excited supertubes with three charges and two dipoles. As a further motivation, note that — contrary to spherical black holes — the black rings carry non-conserved charges (the dipole charges). As such the non-supersymmetric black ring solutions provide an exciting laboratory for examining new features of black holes, for instance the appearance of the non-conserved charges in the first law of black hole thermodynamics [2, 16].

We find the non-supersymmetric black rings by solution-generating techniques (boosts and U-dualities). This was also the approach in [3, 4], where the neutral five-dimensional black ring was first uplifted to six dimensions, to become a black tube.¹ Then a sequence of solution-generating transformations yielded new two-charge black tube solutions with the same charges as a supertube [5, 6]. In the supersymmetric limit the area of these black tubes vanishes and one recovers the supergravity description of a two-charge supertube [6]. Thus these charged black rings can be regarded as the result of thermally exciting a supertube. A limitation of the charged black rings built in [3] is that their supersymmetric limit could only yield supertubes with half the maximum value of the angular momentum, instead of the whole range of angular momenta that supertubes can have. This shortcoming is automatically resolved in this paper. The additional parameters in our new solutions allow us to construct thermal deformations for supertubes with angular momenta covering precisely the entire physically permitted range.

The extra parameters in our solutions come from choosing a more general seed solution to which the generating transformations are applied. While in [3] the seed solution was the neutral black tube, we here use the dipole black tubes of [2] as seed solutions.

The additional degrees of freedom in the dipole solutions in fact allow us to construct non-supersymmetric black rings with three charges and three dipoles. Spherical five-dimensional black holes with three charges are the most thoroughly studied black holes in string theory [17], so having three-charge black rings should be instrumental to develop the proposal in ref. [3] for a microscopic understanding of non-uniqueness and non-spherical topologies. A different motivation to further study D1-D5-P configurations is Mathur's programme to identify string microstates as non-singular horizonless solutions [18]. In fact this led the authors of [19, 20] to independently conjecture the existence of supersymmetric black rings.

The supersymmetric limit of our solutions can only reproduce a supersymmetric ring with

¹Throughout this paper we refer to the same object as a ring (in the five-dimensional description) or as a tube, when lifted to six or more dimensions.

three charges and at most two dipoles. The complete three-charge/three-dipole black rings presented in [8, 9, 10], and the minimal supersymmetric ring of [7], are not limits of the solutions in this paper. Indeed, this becomes obvious by simply counting parameters. The supersymmetric rings of [8, 9, 10] have seven independent parameters. This is the same number as in the solutions in this paper, but in the latter, one of the parameters measures the deviation away from supersymmetry. It appears that in order to find the appropriately larger family of non-supersymmetric black ring solutions one should start with a more general seed, presumably a dipole black ring with two independent angular momenta. Nevertheless, the solutions we present here seem to be adequate to describe thermal excitations near supersymmetry of supertubes with two charges and one dipole, and of some supertubes with three charges and two dipoles.

The rest of the paper is organized as follows: in the next section we discuss the general problem of how to construct the solutions, and then present them and compute their main physical properties. In section 2.3 we analyze the extremal and supersymmetric limits of these black rings. Section 2.4 analyzes the particular case of solutions to minimal five-dimensional supergravity. In section 2.5 we study black rings as thermally excited D1-D5-P supertubes, and consider in particular the cases of tubes with two charges and one dipole, and three charges and two dipoles. We also study the decoupling limit. We conclude in section 2.6 with a discussion of the consequences of our results. In appendices 2.A and 2.B we provide the details for the form fields in the solutions, and in appendices 2.C and 2.D we study the limits where the solutions reproduce spherical rotating black holes (at zero radius), and black strings (at infinite radius).

2.2 Non-supersymmetric black rings with three charges

In this section we first describe the sequence of boosts and dualities that we exploit to generate the charged black ring solutions. The idea is to follow the same path that yielded the three-charge rotating black hole [21, 22, 23, 24], but this procedure becomes quite more complex and subtle when applied to black rings. We then present the solution in its most symmetric form, as an eleven dimensional supergravity supertube with three M2 charges and three M5 dipole charges, and analyze its structure and physical properties.

2.2.1 Generating the solution

We begin by reviewing the process followed in [3] to obtain two-charge black rings, and why a problem arises when trying to add a third charge. Starting from a five-dimensional neutral black ring that rotates along the direction ψ , add to it a flat direction z to build a six-dimensional black tube. This is then embedded into IIB supergravity by further adding four toroidal directions z_1, z_2, z_3, z_4 (which will play little more than a spectator role in the following). Now submit the solution to the following sequence of transformations: IIB S-duality; boost along z with rapidity parameter α_1 ; T-duality along z ; boost along z with parameter α_2 ; T-duality along z_1 ; S-duality; T-duality along z_1, z_2, z_3, z_4 ; S-duality; T-duality along z ; T-duality along z_1 ; S-duality. Schematically,²

$$S \rightarrow \text{Boost}_{\alpha_1}(z) \rightarrow T(z) \rightarrow \text{Boost}_{\alpha_2}(z) \rightarrow T(1) \rightarrow S \rightarrow T(1234) \rightarrow S \rightarrow T(z) \rightarrow T(1) \rightarrow S. \quad (2.2.1)$$

²The first and last S-dualities, and the two T(1) dualities, are introduced simply to have both the initial and final solutions later in this subsection as configurations of a D1-D5 system.

As a result we obtain a non-supersymmetric solution of IIB supergravity. The system has two net charges corresponding to D1 and D5-branes, and there is a dipole charge from a Kaluza-Klein monopole (kkm). The branes are arranged as

$$\begin{array}{rcl}
\alpha_1 & \text{D5:} & 1 \ 2 \ 3 \ 4 \ z \ - \\
\alpha_2 & \text{D1:} & - \ - \ - \ - \ z \ - \\
(\alpha_1\alpha_2) & \text{kkm:} & 1 \ 2 \ 3 \ 4 \ (z) \ \psi \ .
\end{array} \tag{2.2.2}$$

Following ref. [8], we use uppercase letters to denote brane components with net conserved charges (D1, D5), and lowercase for dipole brane charges (kkm). If the parameters on the left are set to zero then the corresponding brane constituent disappears, *e.g.*, when either of the α_i is zero the corresponding D-brane is absent, and the kkm dipole, which is fibered in the z direction, vanishes. Note that the dipole is induced as a result of charging up the tube, and would not be present if instead one charged up a spherical black hole. Ref. [3] argued that these black rings describe thermally excited supertubes: configurations where D1 and D5 branes are ‘dissolved’ in the worldvolume of a tubular KK monopole.

It is natural in this context to try to have a third charge on the ring, coming from momentum P propagating along the tube direction z . In order to endow the system with this charge, one might try to perform a third boost on the solution. However, as discussed in [3], the kkm fibration along the direction z is incompatible with such a boost. A naive application of a boost transformation to the solution results into a globally ill-defined geometry with Dirac-Misner string singularities (a geometric analogue of Dirac strings, to be discussed in detail later in this section).

To overcome this problem, in this paper we choose to start from a different seed solution which already contains three dipole charges, with parameters μ_i , but no net conserved charges [2]. Beginning now from a black tube with dipole charges d1, d5 and kkm given as

$$\begin{array}{rcl}
\mu_1 & \text{kkm:} & 1 \ 2 \ 3 \ 4 \ (z) \ \psi \\
\mu_2 & \text{d5:} & 1 \ 2 \ 3 \ 4 \ - \ \psi \\
\mu_3 & \text{d1:} & - \ - \ - \ - \ - \ \psi \ ,
\end{array} \tag{2.2.3}$$

and acting with the sequence (2.2.1) followed by a boost α_3 along z , we obtain a black tube with the same dipole charges but now also D1-D5-P net charges. The branes are arranged as

$$\begin{array}{rcl}
\alpha_1 & \text{D5:} & 1 \ 2 \ 3 \ 4 \ z \ - \\
\alpha_2 & \text{D1:} & - \ - \ - \ - \ z \ - \\
\alpha_3 & \text{P:} & - \ - \ - \ - \ z \ - \\
(\alpha_2\alpha_3), \mu_1 & \text{d1:} & - \ - \ - \ - \ - \ \psi \\
(\alpha_1\alpha_3), \mu_2 & \text{d5:} & 1 \ 2 \ 3 \ 4 \ - \ \psi \\
(\alpha_1\alpha_2), \mu_3 & \text{kkm:} & 1 \ 2 \ 3 \ 4 \ (z) \ \psi \ .
\end{array} \tag{2.2.4}$$

We will show that by appropriately choosing the parameters of the solution we can manage to eliminate the global pathologies produced by having boosted the Kaluza-Klein monopoles along their fiber directions. Roughly speaking, the pathology from boosting the kkm dipole induced by charging up the solution is cancelled against the pathologies from boosting the dipoles of the initial configuration (2.2.3). To this effect, a single dipole in the seed solution would be sufficient, but using the complete solution (2.2.3) we will obtain a larger family of charged black rings.

There is a more symmetrical M-theory version of the solutions, obtained by performing $\rightarrow T(34) \rightarrow T(z)$ and then uplifting to eleven dimensions. This configuration is

$$\begin{array}{rcl}
\alpha_1 & \text{M2:} & 1 \ 2 \ - \ - \ - \ - \ - \\
\alpha_2 & \text{M2:} & - \ - \ 3 \ 4 \ - \ - \ - \\
\alpha_3 & \text{M2:} & - \ - \ - \ - \ 5 \ 6 \ - \\
(\alpha_2\alpha_3), \mu_1 & \text{m5:} & - \ - \ 3 \ 4 \ 5 \ 6 \ \psi \\
(\alpha_1\alpha_3), \mu_2 & \text{m5:} & 1 \ 2 \ - \ - \ 5 \ 6 \ \psi \\
(\alpha_1\alpha_2), \mu_3 & \text{m5:} & 1 \ 2 \ 3 \ 4 \ - \ - \ \psi \ ,
\end{array} \tag{2.2.5}$$

where we have set $z_5 \equiv z$, and the eleventh dimensional direction is z_6 . It is this form of the solution that we present next.

2.2.2 Solution

The metric for the eleven-dimensional solution is

$$\begin{aligned}
ds_{11\text{D}}^2 &= ds_{5\text{D}}^2 + \left[\frac{1}{h_1} \frac{H_1(y)}{H_1(x)} \right]^{2/3} \left[h_2 h_3 \frac{H_2(x)H_3(x)}{H_2(y)H_3(y)} \right]^{1/3} (dz_1^2 + dz_2^2) \\
&+ \left[\frac{1}{h_2} \frac{H_2(y)}{H_2(x)} \right]^{2/3} \left[h_1 h_3 \frac{H_1(x)H_3(x)}{H_1(y)H_3(y)} \right]^{1/3} (dz_3^2 + dz_4^2) \\
&+ \left[\frac{1}{h_3} \frac{H_3(y)}{H_3(x)} \right]^{2/3} \left[h_1 h_2 \frac{H_1(x)H_2(x)}{H_1(y)H_2(y)} \right]^{1/3} (dz_5^2 + dz_6^2),
\end{aligned} \tag{2.2.6}$$

where

$$\begin{aligned}
ds_{5\text{D}}^2 &= -\frac{1}{(h_1 h_2 h_3)^{2/3}} \frac{H(x)}{H(y)} \frac{F(y)}{F(x)} \left(dt + \omega_\psi(y) d\psi + \omega_\phi(x) d\phi \right)^2 \\
&+ (h_1 h_2 h_3)^{1/3} F(x) H(x) H(y)^2 \\
&\times \frac{R^2}{(x-y)^2} \left[-\frac{G(y)}{F(y)H(y)^3} d\psi^2 - \frac{dy^2}{G(y)} + \frac{dx^2}{G(x)} + \frac{G(x)}{F(x)H(x)^3} d\phi^2 \right],
\end{aligned} \tag{2.2.7}$$

and the three-form potential is

$$\mathcal{A} = A^1 \wedge dz_1 \wedge dz_2 + A^2 \wedge dz_3 \wedge dz_4 + A^3 \wedge dz_5 \wedge dz_6. \tag{2.2.8}$$

The explicit expressions for the components of the one-forms A^i ($i = 1, 2, 3$) are given in appendix 2.A.

We have defined the following functions

$$\begin{aligned}
F(\xi) &= 1 + \lambda\xi, & G(\xi) &= (1 - \xi^2)(1 + \nu\xi), \\
H_i(\xi) &= 1 - \mu_i\xi, & H(\xi) &\equiv [H_1(\xi)H_2(\xi)H_3(\xi)]^{1/3},
\end{aligned} \tag{2.2.9}$$

and

$$h_i = c_i^2 - U_i s_i^2, \tag{2.2.10}$$

where the functions U_i are defined in (2.A.10) and, in order to reduce notational clutter, we have introduced

$$c_i \equiv \cosh \alpha_i, \quad s_i \equiv \sinh \alpha_i. \quad (2.2.11)$$

It is useful to give explicit expressions for the h_i :

$$h_1 = 1 + \frac{H_1(y)s_1^2}{H_1(x)F(x)H(y)^3} \left[(\lambda - \mu_1 + \mu_2 + \mu_3)(x - y) - (\mu_2\mu_3 + \lambda\mu_1)(x^2 - y^2) \right. \\ \left. + (\mu_1\mu_2\mu_3 + \lambda\mu_1\mu_2 + \lambda\mu_1\mu_3 - \lambda\mu_2\mu_3)xy(x - y) \right], \quad (2.2.12)$$

and h_2, h_3 obtained by exchanging $1 \leftrightarrow 2$ and $1 \leftrightarrow 3$, respectively.

The components of the one-form $\omega = \omega_\psi d\psi + \omega_\phi d\phi$ are

$$\omega_\psi(y) = R(1 + y) \left[\frac{C_\lambda}{F(y)} c_1 c_2 c_3 - \frac{C_1}{H_1(y)} c_1 s_2 s_3 - \frac{C_2}{H_2(y)} s_1 c_2 s_3 - \frac{C_3}{H_3(y)} s_1 s_2 c_3 \right], \quad (2.2.13)$$

$$\omega_\phi(x) = -R(1 + x) \left[\frac{C_\lambda}{F(x)} s_1 s_2 s_3 - \frac{C_1}{H_1(x)} s_1 c_2 c_3 - \frac{C_2}{H_2(x)} c_1 s_2 c_3 - \frac{C_3}{H_3(x)} c_1 c_2 s_3 \right],$$

where

$$C_\lambda = \epsilon_\lambda \sqrt{\lambda(\lambda - \nu) \frac{1 + \lambda}{1 - \lambda}}, \quad C_i = \epsilon_i \sqrt{\mu_i(\mu_i + \nu) \frac{1 - \mu_i}{1 + \mu_i}} \quad (2.2.14)$$

for $i = 1, 2, 3$. A choice of sign $\epsilon_i, \epsilon_\lambda = \pm 1$ has been included explicitly.

We assume that the coordinates $z_i, i = 1, \dots, 6$ are periodically identified. The coordinates x and y take values in the ranges

$$-1 \leq x \leq 1, \quad -\infty < y \leq -1, \quad \frac{1}{\min \mu_i} < y < \infty. \quad (2.2.15)$$

The solution has three Killing vectors, $\partial_t, \partial_\psi$, and ∂_ϕ , and is characterized by eight dimensionless parameters $\lambda, \nu, \mu_i, \alpha_i$, plus the scale parameter R , which has dimension of length.

Without loss of generality we can take $R > 0$. The parameters λ, ν, μ_i are restricted as

$$0 < \nu \leq \lambda < 1, \quad 0 \leq \mu_i < 1, \quad (2.2.16)$$

while the α_i can initially take any real value. These ranges of values are typically sufficient to avoid the appearance of naked curvature singularities. Below we will discuss how the elimination of other pathologies will reduce the total number of free parameters from nine to seven.

Each α_i is associated with an M2-brane charge; taking $\alpha_i = 0$ sets the corresponding M2-brane charge to zero. In particular, taking all $\alpha_i = 0$, we recover the dipole black rings of [2]. The solutions contain contributions to the M5-brane dipole charges that originate both from the parameters μ_i as well as from the boosts, see (2.2.5). The precise relation between the parameters and the charges will be given below.

Asymptotic infinity is at $x, y \rightarrow -1$. Since $x = -1$ and $y = -1$ are fixed point sets of respectively ∂_ϕ and ∂_ψ , the periodicities of ψ and ϕ must be chosen so as to avoid conical defects that would extend to infinity. The required periodicities are

$$\Delta\psi = \Delta\phi = 2\pi \frac{\sqrt{1 - \lambda}}{1 - \nu} \prod_{i=1}^3 \sqrt{1 + \mu_i}. \quad (2.2.17)$$

Defining canonical angular variables

$$\tilde{\psi} = \frac{2\pi}{\Delta\psi} \psi, \quad \tilde{\phi} = \frac{2\pi}{\Delta\phi} \phi, \quad (2.2.18)$$

and performing the coordinate transformation

$$\zeta_1 = \tilde{R} \frac{\sqrt{-1-y}}{x-y}, \quad \zeta_2 = \tilde{R} \frac{\sqrt{1+x}}{x-y}, \quad \tilde{R}^2 = 2R^2 \frac{1-\lambda}{1-\nu} \prod_{i=1}^3 (1+\mu_i), \quad (2.2.19)$$

the five-dimensional asymptotic metric takes the manifestly flat form

$$ds_{5D}^2 = -dt^2 + d\zeta_1^2 + \zeta_1^2 d\tilde{\psi}^2 + d\zeta_2^2 + \zeta_2^2 d\tilde{\phi}^2. \quad (2.2.20)$$

Thus the metric is asymptotically five-dimensional Minkowski space times a six-torus.

Removing Dirac-Misner strings

We are interested in ring-like solutions with horizon topology $S^1 \times S^2$. In order that (x, ϕ) parameterize a two-sphere, ∂_ϕ must have fixed-points at $x = \pm 1$, corresponding to the poles of the S^2 . However, note that when the three α_i are non-zero, the orbit of ∂_ϕ does not close off at $x = 1$, since $\omega_\phi(x = 1) \neq 0$. This can be interpreted as the presence of Dirac-Misner strings — a geometric analogue of Dirac strings discussed by Misner in the Taub-NUT solution [25]. Their appearance in this solution can be traced to the fact that, to obtain it, we have boosted along the fiber of a Kaluza-Klein monopole [3]. By analogy with the Dirac monopoles, one might try to eliminate the strings by covering the geometry with two patches, each one regular at each pole. However, the coordinate transformation in the region where the two patches overlap would require t to be periodically identified with period $\Delta t = \omega_\phi(x = 1)\Delta\phi$ (or an integer fraction of this). Closed timelike curves would then be present everywhere outside the horizon.

To remove the pathology we must therefore require that the form ω be globally well-defined, *i.e.*, that $\omega_\phi(x = \pm 1) = 0$. This places a constraint on the parameters of the solution of the form

$$\frac{C_\lambda}{1+\lambda} s_1 s_2 s_3 = \frac{C_1}{1-\mu_1} s_1 c_2 c_3 + \frac{C_2}{1-\mu_2} c_1 s_2 c_3 + \frac{C_3}{1-\mu_3} c_1 c_2 s_3. \quad (2.2.21)$$

Imposing this condition, ω_ϕ can be written as

$$\omega_\phi(x) = -\frac{R(1-x^2)}{F(x)} \left[\frac{\lambda + \mu_1}{1 - \mu_1} \frac{C_1}{H_1(x)} s_1 c_2 c_3 + \frac{\lambda + \mu_2}{1 - \mu_2} \frac{C_2}{H_2(x)} c_1 s_2 c_3 + \frac{\lambda + \mu_3}{1 - \mu_3} \frac{C_3}{H_3(x)} c_1 c_2 s_3 \right], \quad (2.2.22)$$

which is manifestly regular.

Balancing the ring

The choice (2.2.17) for the period of ϕ makes the orbits of ∂_ϕ close off smoothly at $x = -1$. We have also required that the orbits of ∂_ϕ close off at the other pole, $x = +1$, by imposing the condition (2.2.21), but there still remains the possibility that conical defects are present at

this pole. Smoothness at $x = 1$ requires another, specific value for $\Delta\phi$, and it is easy to see that this is compatible with (2.2.17) only if the parameters satisfy the equation

$$\left(\frac{1-\nu}{1+\nu}\right)^2 = \frac{1-\lambda}{1+\lambda} \prod_{i=1}^3 \frac{1+\mu_i}{1-\mu_i}. \quad (2.2.23)$$

Violating this condition results in a disk-like conical singularity inside the ring at $x = 1$. Depending on whether there is an excess or deficit angle, the disk provides a push or pull to keep the ring in equilibrium. Thus (2.2.23) is a balancing condition. We assume the ring is balanced, *i.e.*, that (2.2.23) holds. This condition is independent of α_i and hence the same condition was found for the dipole black rings in [2].

With the balancing condition (2.2.23) and the Dirac-Misner condition (2.2.21), the solution contains seven independent parameters: the scale R , plus six dimensionless parameters. These may be taken to be μ_i and α_i , if λ and ν are eliminated through (2.2.21) and (2.2.23).

2.2.3 Properties

We give here expressions for the conserved charges (mass, angular momentum and net charge) as well as for the dipole charges. We then analyze the horizon geometry and compute the horizon area, temperature and angular velocity of the black rings.

Asymptotic charges

If we assume that the z_i directions are all compact with period $2\pi\ell$ then the five-dimensional Newton's constant is related to the 11D coupling constant κ through $\kappa^2 = 8\pi G_5(2\pi\ell)^6$. Also, note that the six-torus parametrized by the z_i has constant volume. This constraint implies that the five-dimensional metric ds_{5D}^2 is the same as the Einstein-frame metric arising from the reduction of the eleven-dimensional metric (2.2.6) on the T^6 . The mass and angular momenta in five dimensions can then be obtained from the asymptotic form of the metric.

The mass is most simply expressed as

$$M = \frac{\pi}{4G_5} \left(Q_1 \coth 2\alpha_1 + Q_2 \coth 2\alpha_2 + Q_3 \coth 2\alpha_3 \right), \quad (2.2.24)$$

in terms of the M2-brane charges carried by the solution,

$$\begin{aligned} Q_1 &= \frac{R^2 \sinh 2\alpha_1}{1-\nu} \left[\lambda - \mu_1 + \mu_2 + \mu_3 + 2(\mu_2\mu_3 + \lambda\mu_1) + \lambda(\mu_1\mu_2 + \mu_1\mu_3 - \mu_2\mu_3) + \mu_1\mu_2\mu_3 \right], \\ Q_2 &= \frac{R^2 \sinh 2\alpha_2}{1-\nu} \left[\lambda + \mu_1 - \mu_2 + \mu_3 + 2(\mu_1\mu_3 + \lambda\mu_2) + \lambda(\mu_1\mu_2 - \mu_1\mu_3 + \mu_2\mu_3) + \mu_1\mu_2\mu_3 \right], \\ Q_3 &= \frac{R^2 \sinh 2\alpha_3}{1-\nu} \left[\lambda + \mu_1 + \mu_2 - \mu_3 + 2(\mu_1\mu_2 + \lambda\mu_3) + \lambda(-\mu_1\mu_2 + \mu_1\mu_3 + \mu_2\mu_3) + \mu_1\mu_2\mu_3 \right], \end{aligned} \quad (2.2.25)$$

and satisfies the BPS bound

$$M \geq \frac{\pi}{4G_5} \left(|Q_1| + |Q_2| + |Q_3| \right). \quad (2.2.26)$$

The two angular momenta are

$$J_\psi = \frac{\pi R^3 (1-\lambda)^{3/2}}{2G_5 (1-\nu)^2} \left[\prod_{i=1}^3 (1+\mu_i)^{3/2} \right] \times \left[\frac{C_\lambda}{1-\lambda} c_1 c_2 c_3 - \frac{C_1}{1+\mu_1} c_1 s_2 s_3 - \frac{C_2}{1+\mu_2} s_1 c_2 s_3 - \frac{C_3}{1+\mu_3} s_1 s_2 c_3 \right], \quad (2.2.27)$$

$$J_\phi = -\frac{\pi R^3 (1-\lambda)^{3/2}}{2G_5 (1-\nu)^2} \left[\prod_{i=1}^3 (1+\mu_i)^{3/2} \right] \times \left[\frac{C_\lambda}{1-\lambda} s_1 s_2 s_3 - \frac{C_1}{1+\mu_1} s_1 c_2 c_3 - \frac{C_2}{1+\mu_2} c_1 s_2 c_3 - \frac{C_3}{1+\mu_3} c_1 c_2 s_3 \right]. \quad (2.2.28)$$

Eq. (2.2.21) can be used to write the latter as

$$J_\phi = -\frac{\pi R^3 \sqrt{1-\lambda}}{G_5 (1-\nu)^2} \left[\prod_{i=1}^3 (1+\mu_i)^{3/2} \right] \times \left[\frac{\lambda+\mu_1}{1-\mu_1^2} C_1 s_1 c_2 c_3 + \frac{\lambda+\mu_2}{1-\mu_2^2} C_2 c_1 s_2 c_3 + \frac{\lambda+\mu_3}{1-\mu_3^2} C_3 c_1 c_2 s_3 \right], \quad (2.2.29)$$

although it does not lead to any simpler expressions for J_ψ or Q_i .

Dipole charges

The dipole charges are given by

$$q_i = \frac{1}{2\pi(2\pi\ell)^2} \int_{S^2 \times T^2} d\mathcal{A} = \frac{1}{2\pi} \int_{S^2} dA^i = \frac{\Delta\phi}{2\pi} [A_\phi^i(x=1) - A_\phi^i(x=-1)], \quad (2.2.30)$$

where the two-sphere parameterized by (x, ϕ) surrounds a constant- ψ slice of the black ring and for $i = 1, 2, 3$ the two-torus is parameterized by z_1 - z_2 , z_3 - z_4 or z_5 - z_6 , respectively. For generic values of the parameters the dipole charges are not well-defined since the expressions (2.2.30) are y -dependent. The condition for the corresponding gauge fields to be well-defined is the same as imposing the absence of Dirac-Misner strings (2.2.21). With this, the y -dependence drops out and we find

$$q_1 = -\frac{2R \sqrt{1-\lambda}}{s_1 (1-\nu)} \left[\prod_{i=1}^3 \sqrt{1+\mu_i} \right] \left[\frac{C_2}{1-\mu_2} s_2 c_3 + \frac{C_3}{1-\mu_3} c_2 s_3 \right], \quad (2.2.31)$$

$$q_2 = -\frac{2R \sqrt{1-\lambda}}{s_2 (1-\nu)} \left[\prod_{i=1}^3 \sqrt{1+\mu_i} \right] \left[\frac{C_1}{1-\mu_1} s_1 c_3 + \frac{C_3}{1-\mu_3} c_1 s_3 \right], \quad (2.2.32)$$

$$q_3 = -\frac{2R \sqrt{1-\lambda}}{s_3 (1-\nu)} \left[\prod_{i=1}^3 \sqrt{1+\mu_i} \right] \left[\frac{C_2}{1-\mu_2} s_2 c_1 + \frac{C_1}{1-\mu_1} c_2 s_1 \right]. \quad (2.2.33)$$

One can easily verify that

$$J_\phi = \frac{\pi}{8G_5} (q_1 Q_1 + q_2 Q_2 + q_3 Q_3). \quad (2.2.34)$$

This identity reflects the fact that the second angular momentum J_ϕ appears as a result of charging up the dipole rings.

Non-uniqueness

There are seven parameters in the solution, but only six conserved charges at infinity, (M , J_ψ , J_ϕ , $Q_{1,2,3}$). So fixing these parameters we can expect to find a one-parameter continuous non-uniqueness.

Horizon

As for the dipole black rings of [2], we expect the event horizon to be located at $y = y_h \equiv -1/\nu$. At $y = y_h$, g_{yy} blows up, but this is just a coordinate singularity which can be removed by the coordinate transformation $(t, \psi) \rightarrow (v, \psi')$ given as

$$dt = dv + \omega_\psi(y) \frac{\sqrt{-F(y)H(y)^3}}{G(y)} dy, \quad d\psi = d\psi' - \frac{\sqrt{-F(y)H(y)^3}}{G(y)} dy. \quad (2.2.35)$$

Then the five-dimensional part of the metric is

$$\begin{aligned} ds_{5D}^2 = & -\frac{1}{(h_1 h_2 h_3)^{2/3}} \frac{H(x) F(y)}{H(y) F(x)} \left(dv + \omega_\psi(y) d\psi' + \omega_\phi(x) d\phi \right)^2 \\ & + (h_1 h_2 h_3)^{1/3} H(x) H(y)^2 F(x) \\ & \times \frac{R^2}{(x-y)^2} \left[-\frac{G(y)}{F(y)H(y)^3} d\psi'^2 - \frac{2 d\psi' dy}{\sqrt{-F(y)H(y)^3}} + \frac{dx^2}{G(x)} + \frac{G(x)}{F(x)H(x)^3} d\phi^2 \right], \end{aligned} \quad (2.2.36)$$

and thus the full metric is manifestly regular at $y = y_h$.

The metric on (a spatial section of) the horizon is

$$\begin{aligned} ds_H^2 = & \frac{1}{(h_1 h_2 h_3)^{2/3}} \frac{H(x) |F(y_h)|}{F(x) H(y_h)} \left(\omega_\psi(y_h) d\psi' + \omega_\phi(x) d\phi \right)^2 \\ & + (h_1 h_2 h_3)^{1/3} H(x) H(y_h)^2 F(x) \frac{R^2}{(x-y_h)^2} \left[\frac{dx^2}{G(x)} + \frac{G(x)}{F(x)H(x)^3} d\phi^2 \right], \end{aligned} \quad (2.2.37)$$

where the h_i are evaluated at y_h , but recall that they also depend on x .

In order to better understand the geometry of this horizon, let us consider first the following simpler metric,

$$\begin{aligned} ds^2 = & R_1^2 (d\psi' + k(1-x^2)d\phi)^2 + R_2^2 \left(\frac{dx^2}{1-x^2} + (1-x^2)d\phi^2 \right) \\ = & R_1^2 (d\psi' + k \sin^2 \theta d\phi)^2 + R_2^2 (d\theta^2 + \sin^2 \theta d\phi^2), \end{aligned} \quad (2.2.38)$$

where the second expression is obtained by making $x = \cos \theta$, and R_1 , R_2 , k , are constants. This is topologically $S^1 \times S^2$. Due to the cross-term $g_{\psi'\phi}$ the product is twisted³, but, since $g_{\psi'\phi}$ vanishes at $\theta = 0, \pi$, *i.e.*, at $x = \pm 1$, the fibration of the S^1 over the S^2 is topologically trivial and globally well-defined.

³Note that at constant $\theta \neq 0, \pi$ one recognizes a twisted 2-torus.

The horizon metric (2.2.37) describes a geometry topologically equivalent to (2.2.38) (recall that $G(x), \omega_\phi(x) \propto (1-x^2)$), but now R_1, R_2, k are functions of the polar coordinate $x \in [-1, 1]$, everywhere regular and non-vanishing. So the horizon of these black rings is topologically $S^1 \times S^2$, but the radii of the S^1 and S^2 , and the twisting, are not constant but change with the latitude of the S^2 .

The horizon area is

$$\begin{aligned} \mathcal{A}_H = & 8\pi^2 R^3 \frac{(1-\lambda)(\lambda-\nu)^{1/2}}{(1-\nu)^2(1+\nu)} \left[\prod_{i=1}^3 (1+\mu_i)(\nu+\mu_i)^{1/2} \right] \\ & \times \left| \frac{C_\lambda}{\lambda-\nu} c_1 c_2 c_3 + \frac{C_1}{\nu+\mu_1} c_1 s_2 s_3 + \frac{C_2}{\nu+\mu_2} s_1 c_2 s_3 + \frac{C_3}{\nu+\mu_3} s_1 s_2 c_3 \right|. \end{aligned} \quad (2.2.39)$$

When all μ_i are nonzero, there is also an inner horizon at $y = -\infty$. At $y = 1/\min \mu_i$ there is a curvature singularity hidden behind the horizons. The Killing vector ∂_t becomes spacelike at $y = -1/\lambda$, so $-1/\nu < y < -1/\lambda$ is the ergoregion. The ergosurface at $y = -1/\lambda$ has topology $S^1 \times S^2$.

The horizon is generated by the orbits of the Killing vector $\xi = \partial/\partial t - \Omega_\psi \partial/\partial \tilde{\psi}$ (where $\tilde{\psi}$ is the angle in (2.2.18)), with the angular velocity of the horizon given by

$$\begin{aligned} \Omega_\psi^{-1} &= \frac{\Delta^\psi}{2\pi} \omega_\psi(y_h) \\ &= R\sqrt{1-\lambda} \left[\prod_i \sqrt{1+\mu_i} \right] \left| \frac{C_\lambda}{\lambda-\nu} c_1 c_2 c_3 + \frac{C_1}{\nu+\mu_1} c_1 s_2 s_3 + \frac{C_2}{\nu+\mu_2} s_1 c_2 s_3 + \frac{C_3}{\nu+\mu_3} s_1 s_2 c_3 \right|. \end{aligned} \quad (2.2.40)$$

Note that the angular velocity in the ϕ direction vanishes even if $J_\phi \neq 0$, which is rather unusual for a non-supersymmetric solution.

The temperature, obtained from the surface gravity at the horizon, is

$$T_H^{-1} = 4\pi R \frac{\sqrt{\lambda-\nu} \prod_i \sqrt{\mu_i+\nu}}{\nu(1+\nu)} \left| \frac{C_\lambda}{\lambda-\nu} c_1 c_2 c_3 + \frac{C_1}{\nu+\mu_1} c_1 s_2 s_3 + \frac{C_2}{\nu+\mu_2} s_1 c_2 s_3 + \frac{C_3}{\nu+\mu_3} s_1 s_2 c_3 \right|. \quad (2.2.41)$$

The entropy of the black ring is $S = \mathcal{A}_H/4$. We note that $T_H S$ is quite simple, but $\Omega_\psi J_\psi$ is not. It will be interesting to understand the thermodynamics of these non-supersymmetric black rings. The first law for black rings with dipole charges is currently being investigated [16].

2.3 Extremal and supersymmetric limits

In order to avoid possible confusion, it may be worth recalling that the extremal limit and the supersymmetric limit of a black hole solution, even if they often coincide, in general need not be the same. The extremal limit is defined as the limit where the inner and outer horizons of a black hole coincide. Then, if the horizon remains regular, its surface gravity, and hence its temperature, vanish. The supersymmetric limit, instead, is one where the limiting solution preserves a fraction of supersymmetry and saturates a BPS bound. If the horizon remains regular in the supersymmetric limit, it must be degenerate, hence extremal. But the converse is not true in general. The extremal limit of a black hole need not be supersymmetric. A familiar

example of this is the Kerr-Newman solution, whose extremal limit at maximal rotation is not supersymmetric, and whose supersymmetric limit, with $M = |Q|$, cannot have a regular horizon at finite rotation.

Let us first discuss the extremal limit, since it is simpler. If $\nu = 0$, and all the μ_i are non-zero, the inner and outer horizon coincide and the ring has a degenerate horizon with zero temperature. So the extremal limit is $\nu \rightarrow 0$. One finds a regular horizon of *finite area* as long as all μ_i are non-vanishing. Such extremal solutions have proven useful in order to understand the microphysics of black rings [2]. However, for finite values of the parameters other than ν , these extremal solutions are not supersymmetric. This is clear from the fact that they do not saturate the BPS bound (2.2.26).

In order to saturate this bound, we see from (2.2.24) that we must take $|\alpha_i| \rightarrow \infty$. But before analyzing this limit, it is important to realize that the solutions in this paper cannot reproduce the most general supersymmetric rings with three charges and three dipoles in ref. [8]. A simple way to see this is by noting that the latter have

$$J_\phi = \frac{\pi}{8G_5} (q_1 Q_1 + q_2 Q_2 + q_3 Q_3 - q_1 q_2 q_3) \quad (\text{BPS ring}), \quad (2.3.1)$$

instead of (2.2.34). The parameter count mentioned in the introduction also leads to this conclusion. Furthermore, for the supersymmetric solutions with all three charges and three dipoles, each of the functions ω_ψ and ω_ϕ depend on *both* x and y , whereas here we have $\omega_\psi(y)$ and $\omega_\phi(x)$.

It follows that at most we can recover a supersymmetric ring with three charges and *two* dipoles. This ring does not have a regular horizon. We believe, however, that this limitation of the non-supersymmetric solutions is not fundamental, but instead is just a shortcoming of our construction starting from the seed in [2] (so far the most general seed solution available). We expect that a more general non-supersymmetric black ring solution which retains the three charges and the three dipoles in the supersymmetric limit exists.

In order to take the supersymmetric limit in such a way that three charges and two dipoles survive, take $\alpha_1, \alpha_2, \alpha_3 \rightarrow \infty$ and $\lambda, \nu, \mu_i \rightarrow 0$ such that $e^{2\alpha_1} \sim e^{2\alpha_2} \sim e^{\alpha_3}$ and $\lambda \sim \mu_3 \sim e^{-\alpha_3}$, while $\mu_1 \sim \mu_2 \sim \nu \sim (\lambda - \mu_3) \sim e^{-2\alpha_3}$. Note the latter implies that $\lambda = \mu_3 + O(e^{-2\alpha_3})$, which we shall use in the following.

These scalings are conveniently encoded by saying that in the limit we keep fixed the following quantities:

$$\lambda e^{2\alpha_1} = \frac{Q_1}{R^2}, \quad \lambda e^{2\alpha_2} = \frac{Q_2}{R^2}, \quad \frac{1}{2}(\lambda + \mu_1 + \mu_2 - \mu_3 + 2\lambda\mu_3)e^{2\alpha_3} = \frac{Q_3}{R^2}, \quad (2.3.2)$$

$$-\epsilon_3 \lambda e^{\alpha_3 + \alpha_2 - \alpha_1} = \frac{q_1}{R}, \quad -\epsilon_3 \lambda e^{\alpha_3 - \alpha_2 + \alpha_1} = \frac{q_2}{R}, \quad (2.3.3)$$

$$(\mu_1 + \mu_2 + \nu)e^{2\alpha_3} = \frac{a^2}{R^2}, \quad (2.3.4)$$

$$\frac{1}{2} \left[\mu_1 + \mu_2 + \nu + \epsilon_\lambda \left(\epsilon_1 \sqrt{\mu_1(\nu + \mu_1)} + \epsilon_2 \sqrt{\mu_2(\nu + \mu_2)} \right) \right] e^{2\alpha_3} = \frac{b^2}{R^2}. \quad (2.3.5)$$

The Q_i and q_i are actually the limits of the charges and dipoles in (2.2.25) and (2.2.30). Note that now the limiting $q_{1,2}$ and $Q_{1,2}$ are not independent, but satisfy

$$q_1 Q_1 = q_2 Q_2. \quad (2.3.6)$$

Recall that the $\epsilon_\lambda, \epsilon_i$ are choices of signs, $\epsilon_\lambda, \epsilon_i = \pm 1$. We have arbitrarily chosen the boosts α_i to be positive. This then requires the sign choice $\epsilon_\lambda = \epsilon_3$ in order that the cancellation of

Dirac-Misner strings (2.2.21) be possible. The parameters a^2 and b^2 are non-negative numbers, $a^2 \geq b^2 \geq 0$ (for any choice of the signs $\epsilon_\lambda, \epsilon_i$), and we shall presently see that after imposing the balancing condition and the Dirac-Misner condition, they drop out from the solution.

We demand that the supersymmetric limit is approached through a sequence of black rings which are regular (on and outside the horizon), and therefore require that they satisfy the balancing condition (2.2.23). In the limit, this becomes

$$2\nu = \lambda - \mu_1 - \mu_2 - \mu_3, \quad (2.3.7)$$

which can be written

$$Q_3 - q_1 q_2 = a^2. \quad (2.3.8)$$

The Dirac-Misner condition (2.2.21) gives

$$R^2 q_1 q_2 (Q_1 + Q_2) = Q_1 Q_2 (Q_3 - q_1 q_2 - b^2). \quad (2.3.9)$$

Now turning to the solution, we find in the supersymmetric limit that

$$h_1 = 1 + \frac{Q_1}{2R^2}(x-y), \quad h_2 = 1 + \frac{Q_2}{2R^2}(x-y), \quad h_3 = 1 + \frac{Q_3 - q_1 q_2}{2R^2}(x-y) - \frac{q_1 q_2}{4R^2}(x^2 - y^2). \quad (2.3.10)$$

Also, using the balancing condition (2.3.7), the Dirac-Misner condition (2.3.9), and (2.3.6) to rewrite the expressions, we get

$$\begin{aligned} \omega_\psi(y) &= \epsilon_\lambda \left[\frac{1}{2}(q_1 + q_2)(1+y) - \frac{1}{8R^2}(y^2 - 1)(q_1 Q_1 + q_2 Q_2) \right], \\ \omega_\phi(x) &= -\epsilon_\lambda \frac{1}{8R^2}(1-x^2)(q_1 Q_1 + q_2 Q_2). \end{aligned}$$

The supersymmetric-limit metric is

$$\begin{aligned} ds_{11}^2 &= -\frac{1}{(h_1 h_2 h_3)^{2/3}} [dt + \omega_\psi(y)d\psi + \omega_\phi(x)d\phi]^2 \\ &\quad + (h_1 h_2 h_3)^{1/3} \left\{ \frac{R^2}{(x-y)^2} \left[(y^2 - 1) d\psi^2 + \frac{dy^2}{y^2 - 1} + \frac{dx^2}{1 - x^2} + (1 - x^2) d\phi^2 \right] \right. \\ &\quad \left. + \frac{1}{h_1}(dz_1^2 + dz_2^2) + \frac{1}{h_2}(dz_3^2 + dz_4^2) + \frac{1}{h_3}(dz_5^2 + dz_6^2) \right\}. \quad (2.3.11) \end{aligned}$$

For the three-form potentials (given in appendix 2.A), we find after imposing the balancing condition (2.3.7) and the Dirac-Misner condition (2.3.17)

$$A_t^i = h_i^{-1} - 1, \quad i = 1, 2, 3, \quad (2.3.12)$$

while

$$A_\psi^i = \frac{1}{h_i} \omega_\psi - \frac{q_i}{2}(1+y), \quad A_\phi^i = \frac{1}{h_i} \omega_\phi - \frac{q_i}{2}(1+x), \quad i = 1, 2, \quad (2.3.13)$$

and

$$A_\psi^3 = \frac{1}{h_3} \omega_\psi, \quad A_\phi^3 = \frac{1}{h_3} \omega_\phi. \quad (2.3.14)$$

Choosing $\epsilon_\lambda = +1$, this matches exactly the full eleven-dimensional supersymmetric solution of [8] with $q_3 = 0$.

So, as advertised, a and b disappear from the limiting solution. However, a remnant of their presence survives in the form of two constraints on the values of the parameters. Note that since $a^2 \geq 0$, the balancing condition (2.3.8) gives rise to the bound

$$Q_3 \geq q_1 q_2, \quad (2.3.15)$$

which was also found in [8]. Further, using that $0 \leq b^2 \leq a^2$, the Dirac-Misner condition (2.3.9) gives

$$R^2 \leq \frac{Q_1 Q_2 (Q_3 - q_1 q_2)}{q_1 q_2 (Q_1 + Q_2)}, \quad (2.3.16)$$

which is more meaningfully rewritten, using (2.3.6), as a bound on a combination of the angular momenta,

$$\frac{4G_5}{\pi} (J_\psi - J_\phi) \leq \sqrt{\frac{Q_1 Q_2}{q_1 q_2}} (Q_3 - q_1 q_2). \quad (2.3.17)$$

The bound (2.3.16) and the constraint (2.3.6) are precisely the conditions found in [8] in order to avoid closed causal curves for the BPS solution. It is curious that the condition for eliminating Dirac-Misner strings in the non-supersymmetric geometry becomes precisely the same as the condition of avoiding causal pathologies in the supersymmetric solution.

The supersymmetric limit of a black ring with two charges Q_1, Q_2 and one dipole q_3 does not arise as a special case of the above limit. It must be taken in a different manner, which we present in sec. 2.5.2.

2.4 Non-supersymmetric black rings in minimal 5D supergravity

A particular case of interest of our solutions is obtained when the three charges and the three dipoles are set equal,

$$\alpha_1 = \alpha_2 = \alpha_3 \equiv \alpha, \quad \mu_1 = \mu_2 = \mu_3 \equiv \mu. \quad (2.4.1)$$

Then the three gauge fields in (2.2.8) associated to each of the brane components are equal, $A^1 = A^2 = A^3$, and the moduli associated to the size of the dimensions z_i are constant. The solution then becomes a non-supersymmetric black ring of the minimal supergravity theory in five dimensions. The action for the bosonic sector of this theory is

$$I = -\frac{1}{16\pi G_5} \int \sqrt{-g} \left(R - \frac{1}{4} F^2 - \frac{1}{6\sqrt{3}} \epsilon^{\mu\alpha\beta\gamma\delta} A_\mu F_{\alpha\beta} F_{\gamma\delta} \right), \quad (2.4.2)$$

where $F = dA \equiv \sqrt{3} dA^i$. The form of the solution is obtained in a straightforward manner from the one in Sec. 2.2.2, but since it becomes quite simpler it is worth giving explicit expressions.

The metric is

$$\begin{aligned}
ds_{5D}^2 = & -\frac{1}{h_\alpha^2(x,y)} \frac{H(x)}{H(y)} \frac{F(y)}{F(x)} \left(dt + \omega_\psi(y) d\psi + \omega_\phi(x) d\phi \right)^2 \\
& + h_\alpha(x,y) F(x) H(x) H(y)^2 \\
& \times \frac{R^2}{(x-y)^2} \left[-\frac{G(y)}{F(y)H(y)^3} d\psi^2 - \frac{dy^2}{G(y)} + \frac{dx^2}{G(x)} + \frac{G(x)}{F(x)H(x)^3} d\phi^2 \right],
\end{aligned} \tag{2.4.3}$$

with $H(\xi) = 1 - \mu\xi$, and F and G as in (2.2.9). The functions h_i now simplify to

$$h_\alpha(x,y) = 1 + \frac{(\lambda + \mu)(x-y)}{F(x)H(y)} \sinh^2 \alpha. \tag{2.4.4}$$

The one-form ω has components

$$\omega_\psi(y) = R(1+y) \cosh \alpha \left[\frac{C_\lambda}{F(y)} \cosh^2 \alpha - \frac{3C_\mu}{H(y)} \sinh^2 \alpha \right] \tag{2.4.5}$$

and

$$\omega_\phi(x) = -R \frac{1-x^2}{F(x)H(x)} \frac{\lambda + \mu}{1 + \lambda} C_\lambda \sinh^3 \alpha, \tag{2.4.6}$$

where C_λ and $C_\mu \equiv C_i$ are given in (2.2.14). To obtain (2.4.6) we have used the condition

$$\frac{C_\lambda}{1 + \lambda} \sinh^2 \alpha = \frac{3C_\mu}{1 - \mu} \cosh^2 \alpha \tag{2.4.7}$$

necessary to guarantee the absence of Dirac-Misner strings.

The physical parameters of the solution are

$$M = \frac{3\pi R^2 (\lambda + \mu)(1 + \mu)^2}{4G_5 (1 - \nu)} \cosh 2\alpha, \tag{2.4.8}$$

$$J_\psi = \frac{\pi R^3 (1 - \lambda)^{3/2} (1 + \mu)^{9/2}}{2G_5 (1 - \nu)^2} \cosh \alpha \left[\frac{C_\lambda}{1 - \lambda} \cosh^2 \alpha - \frac{3C_\mu}{1 + \mu} \sinh^2 \alpha \right], \tag{2.4.9}$$

$$J_\phi = -\frac{3\pi R^3 \sqrt{1 - \lambda} (1 + \mu)^{7/2} (\lambda + \mu)}{G_5 (1 - \nu)^2 (1 - \mu)} C_\mu \cosh^2 \alpha \sinh \alpha, \tag{2.4.10}$$

$$\mathcal{A}_H = 8\pi^2 R^3 \frac{(1 - \lambda)(\lambda - \nu)^{1/2} (1 + \mu)^3 (\nu + \mu)^{3/2}}{(1 - \nu)^2 (1 + \nu)} \left| \frac{C_\lambda}{\lambda - \nu} \cosh^2 \alpha + \frac{3C_\mu}{\nu + \mu} \sinh^2 \alpha \right| \cosh \alpha. \tag{2.4.11}$$

$$T_H^{-1} = 4\pi R \frac{\sqrt{\lambda - \nu} (\mu + \nu)^{3/2}}{\nu(1 + \nu)} \cosh \alpha \left| \frac{C_\lambda}{\lambda - \nu} \cosh^2 \alpha + \frac{3C_\mu}{\nu + \mu} \sinh^2 \alpha \right|. \tag{2.4.12}$$

$$\Omega_\psi^{-1} = R \sqrt{1 - \lambda} (1 + \mu)^{3/2} \cosh \alpha \left| \frac{C_\lambda}{\lambda - \nu} \cosh^2 \alpha + \frac{3C_\mu}{\nu + \mu} \sinh^2 \alpha \right|. \tag{2.4.13}$$

We have used the Dirac-Misner condition (2.2.21) to simplify only the expression for J_ϕ . The charge is obtained from the relation

$$Q = \frac{4G_5}{3\pi} M \tanh 2\alpha, \quad (2.4.14)$$

and the dipole charge is

$$\begin{aligned} q &= -4R \frac{\sqrt{1-\lambda}(1+\mu)^{3/2}}{(1-\nu)(1-\mu)} C_\mu \cosh \alpha \\ &= \frac{8G_5}{3\pi} \frac{J_\phi}{Q}. \end{aligned} \quad (2.4.15)$$

The solution contains five parameters, $(\lambda, \nu, \mu, \alpha, R)$, but the two constraints from absence of Dirac-Misner strings and of conical defects leave only three independent parameters. This implies that, out of the four conserved charges of the solution, (M, Q, J_ψ, J_ϕ) , at most only three of them, (M, Q, J_ψ) , are independent. Eq. (2.4.15) shows that the dipole charge q is not an independent parameter and therefore there cannot be any continuous violation of uniqueness. This is in contrast with the situation when the net charge Q is zero, in which the dipole q is an independent parameter and so uniqueness is violated by a continuous parameter [2]. In the solutions in this paper, the addition of a charge, however small, implies that the net charge and the dipole charge must be related so as to avoid Dirac-Misner strings.

One can also argue that the solutions in this section do not exhibit discrete non-uniqueness, *i.e.*, that there are no two (or more) ring solutions which have the same four conserved charges⁴. To see this, fix the scale in the solutions by fixing the mass. Then define, like in [8], dimensionless quantities $j_{\psi,\phi} \propto J_{\psi,\phi}/\sqrt{G_5 M^3}$, which characterize the spins for fixed mass, and the (relative) energy above supersymmetry $m = [M - (3\pi/4G_5)Q]/M$. Note that m depends on α only. For fixed m , impose the balancing condition and the Dirac-Misner condition. Then there is only one free parameter, say μ , so one can use this to plot a curve in the (j_ψ, j_ϕ) -plane showing which values of j_ψ and j_ϕ are allowed. If this curve manages somehow to self-intersect then we would have two solutions with the same (m, j_ψ, j_ϕ) , *i.e.*, discrete non-uniqueness. We have checked this for a large representative set of values of m , and found that the curve does not self-intersect, so uniqueness appears to hold among the rings in this section. Note, though, that we can expect charged spherical black holes of minimal supergravity to exist with the same conserved charges as some of these rings.

The solutions in this section do not admit any non-trivial supersymmetric limit to BPS rings. A natural conjecture is the existence of a five-parameter non-BPS ring solution, characterized by $(M, Q, J_\psi, J_\phi, q)$. This family would allow to describe thermal excitations above the BPS solution of [7], and presumably would exhibit continuous non-uniqueness, as in [2], through the parameter q . One would also expect discrete two-fold non-uniqueness for fixed parameters $(M, Q, J_\psi, J_\phi, q)$, at least for small enough values of Q and J_ϕ , by continuity to the solutions with $Q = 0 = J_\phi$, which are known to present this feature [2].

2.5 D1-D5-P black rings

Solutions where the three charges are interpreted as D1-D5-P charges are of particular relevance since, near supersymmetry, they will admit a dual description in terms of a rather

⁴There can be two solutions with the same values of the independent parameters, say (M, Q, J_ψ) , but then they will be distinguished by the value of J_ϕ .

well-understood 1+1 supersymmetric conformal field theory. Here we analyze the most general such solution obtainable with our methods and also two other important particular cases obtained by setting some dipoles or charges to zero. We denote by Q/q a solution with net charges Q and dipole charges q.

2.5.1 D1-D5-P/d1-d5-kkm black ring

The non-supersymmetric black ring with three charges, D1, D5 and momentum P, and dipole charges d1, d5, and Kaluza-Klein monopole kkm has metric in the string frame

$$ds_{\text{IIB}}^2 = d\tilde{s}_{\text{5D}}^2 + \sqrt{\frac{h_2}{h_1}} \sqrt{\frac{H_1(y)H_2(x)}{H_1(x)H_2(y)}} dz_{(4)}^2 + \frac{h_3}{\sqrt{h_1 h_2}} \frac{H_3(x)}{H_3(y)} \sqrt{\frac{H_1(y)H_2(y)}{H_1(x)H_2(x)}} \left[dz + A^3 \right]^2, \quad (2.5.1)$$

where the non-vanishing components of the one-form A^3 are given in (2.A.7)-(2.A.9), and

$$\begin{aligned} d\tilde{s}_{\text{5D}}^2 = & -\frac{1}{h_3 \sqrt{h_1 h_2}} \frac{F(y)}{F(x)} \sqrt{\frac{H_1(x)H_2(x)}{H_1(y)H_2(y)}} \left[dt + \omega_\psi(y) d\psi + \omega_\phi(x) d\phi \right]^2 \\ & + \sqrt{h_1 h_2} F(x) H_3(y) \sqrt{H_1(x)H_1(y)H_2(x)H_2(y)} \\ & \times \frac{R^2}{(x-y)^2} \left[-\frac{G(y)}{F(y)H(y)^3} d\psi^2 - \frac{dy^2}{G(y)} + \frac{dx^2}{G(x)} + \frac{G(x)}{F(x)H(x)^3} d\phi^2 \right]. \end{aligned} \quad (2.5.2)$$

The dilaton is

$$e^{2\Phi} = \frac{h_2}{h_1} \frac{H_1(y)H_2(x)}{H_1(x)H_2(y)}, \quad (2.5.3)$$

and the components of the RR 2-form potential $C^{(2)}$ are given in appendix 2.B.

6D structure

KK dipole quantization

The solution (2.5.1) has a non-trivial structure along the sixth direction z due to the presence of the term $dz + A^3$. The quantization of the KK dipole can then be obtained easily by requiring regularity of the fibration. In order to eliminate the Dirac string singularity of A^3 at $x = +1$ we have to perform a coordinate (gauge) transformation $z \rightarrow \hat{z} - A_\phi^3(x = +1)$. The y -dependence here cancels if we impose the condition (2.2.21), and then the transformation is,

$$z \rightarrow \hat{z} = z - \frac{2R}{s_3} \left[\frac{C_2}{1 - \mu_2} s_2 c_1 + \frac{C_1}{1 - \mu_1} c_2 s_1 \right] \phi. \quad (2.5.4)$$

With this, the geometry is free of Dirac singularities at $x = +1$. However, since z parametrizes a compact Kaluza-Klein direction, $z \sim z + 2\pi R_z$ the coordinate transformation (2.5.4) is globally well-defined only if

$$2\pi R_z = \pm \frac{2R}{n_{\text{KK}} s_3} \left[\frac{C_2}{1 - \mu_2} s_2 c_1 + \frac{C_1}{1 - \mu_1} c_2 s_1 \right] \Delta\phi \quad (2.5.5)$$

for some (positive) integer n_{KK} . This condition gives rise to the KK monopole charge quantization:

$$q_{\text{KK}} = \mp n_{\text{KK}} R_z = -\frac{2R}{s_3} \left[\frac{C_2}{1-\mu_2} s_2 c_1 + \frac{C_1}{1-\mu_1} c_2 s_1 \right] \frac{\Delta\phi}{2\pi}, \quad (2.5.6)$$

and then $q_{\text{KK}} = q_3$ as given in (2.2.33).

Horizon geometry

Making use of the change of coordinates given by (2.2.35), it is clear that the five-dimensional part of the metric of the type IIB solution is regular at $y_h = -1/\nu$. Note that the conformal factors multiplying the different terms in (2.5.1) remain finite and non-zero at y_h . In order to make the term $dz + A^3$ also regular at this point, we perform a change of coordinates

$$dz = dz' + R(1+y) \left[\frac{C_\lambda}{F(y)} c_1 c_2 s_3 - \frac{C_1}{H_1(y)} c_1 s_2 c_3 - \frac{C_2}{H_2(y)} s_1 c_2 c_3 - \frac{C_3}{H_3(y)} s_1 s_2 s_3 \right] \frac{\sqrt{|F(y)|H(y)^3}}{G(y)} dy. \quad (2.5.7)$$

In the (v, ψ') coordinates this term becomes manifestly analytic at y_h ,

$$dz + A^3 = dz' + A_t^3 dv + A_\psi^3 d\psi' + A_\phi^3 d\phi, \quad (2.5.8)$$

and imposing the charge quantization condition (2.5.6), it is perfectly regular on the horizon.

The horizon in six dimensions is a $U(1)$ fibration over the $S^1 \times S^2$ geometry of the five-dimensional horizon (2.2.37). In the supersymmetric case [8], it was found that for certain values of the parameters the $U(1)$ would Hopf-fiber over the S^2 to yield an S^3 . In the present case, to find the same result we would have to perform the coordinate transformation

$$dz'' = dz' + A_\psi^3(x, y_h) \left(d\psi' + \frac{\omega_\phi(x)}{\omega_\psi(y_h)} d\phi \right) \quad (2.5.9)$$

to eliminate the leg along the S^1 in the fiber in (2.5.8), but given the x -dependence this change is not compatible with the global periodicities of z and ϕ . Hence, the six-dimensional horizon of these rings is never globally of the form $S^1 \times S^3$. It may still be, though, that the more general non-supersymmetric solutions that we have conjectured to exist can actually have such a horizon geometry.

2.5.2 D1-D5/kkm black rings and two-charge supertubes

This is the simplest case of a two-charge black ring, with one dipole charge, that can be connected to a well-understood supersymmetric configuration in string theory. We will show that the supersymmetric limit of these black rings results into a two-charge supertube.

A particular case of these solutions (with all $\mu_i = 0$) was constructed in [3], but the supersymmetric limit of those rings could only yield supertubes with half the maximum angular momentum (for given charges and dipole)⁵. Below we show how the inclusion of dipole parameters μ_i allows us to recover supertubes within the full range of allowed angular momenta. Hence we expect that the present solutions are sufficient to consistently describe the thermal excitations that keep $J_\phi = 0$ of supertubes with two charges, Q_1 and Q_2 , and angular momentum J_ψ .

⁵When comparing to the solutions in [3], the reader should be aware that a slightly different form of the seed is used, so the functions F , G and parameters λ, ν used below are not the same as those in [3].

Solution

In the general solution set $\alpha_3 = 0$ and $\mu_1 = \mu_2 = 0$. The string-frame metric for the D1-D5/kkm black ring is

$$ds^2 = ds_{5D}^2 + \sqrt{\frac{h_2}{h_1}} \left(dz_1^2 + dz_2^2 + dz_3^2 + dz_4^2 \right) + \frac{1}{\sqrt{h_1 h_2}} \frac{H_3(x)}{H_3(y)} \left[dz - R(1+x) \left(\frac{C_\lambda}{F(x)} s_1 s_2 - \frac{C_3}{H_3(x)} c_1 c_2 \right) d\phi \right]^2, \quad (2.5.10)$$

where

$$ds_{5D}^2 = -\frac{1}{\sqrt{h_1 h_2}} \frac{F(y)}{F(x)} \left[dt + R(1+y) \left(\frac{C_\lambda}{F(y)} c_1 c_2 - \frac{C_3}{H_3(y)} s_1 s_2 \right) d\psi \right]^2 + \sqrt{h_1 h_2} F(x) H_3(y) \frac{R^2}{(x-y)^2} \left[-\frac{G(y)}{F(y) H_3(y)} d\psi^2 - \frac{dy^2}{G(y)} + \frac{dx^2}{G(x)} + \frac{G(x)}{F(x) H_3(x)} d\phi^2 \right]. \quad (2.5.11)$$

Note that now

$$h_i = 1 + \frac{(\lambda + \mu_3)(x-y)}{F(x) H_3(y)} s_i^2 \quad (2.5.12)$$

for $i = 1, 2$. The dilaton is

$$e^{2\Phi} = \frac{h_2}{h_1}, \quad (2.5.13)$$

and the non-vanishing components of the RR two-form potential are

$$C_{tz}^{(2)} = -\frac{(x-y)}{F(x) H_3(y) h_2} (\lambda + \mu_3) c_2 s_2, \quad (2.5.14)$$

$$C_{\psi z}^{(2)} = \frac{R(1+y)}{h_2} \frac{H_3(x)}{H_3(y)} \left[\frac{C_\lambda}{F(x)} c_1 s_2 - \frac{C_3}{H_3(x)} s_1 c_2 \right], \quad (2.5.15)$$

$$C_{t\phi}^{(2)} = -\frac{R(1+x)}{h_2} \frac{F(y)}{F(x)} \left[\frac{C_\lambda}{F(y)} s_1 c_2 - \frac{C_3}{H_3(y)} c_1 s_2 \right], \quad (2.5.16)$$

$$C_{\psi\phi}^{(2)} = -\frac{R^2}{2} \sinh 2\alpha_1 \left\{ \frac{G(x)}{(x-y)} \frac{\lambda + \mu_3}{F(x) H_3(x)} + (1+x) \left(\frac{C_\lambda^2}{\lambda F(x)} + \frac{C_3^2}{\mu_3 H_3(x)} \right) + \frac{1}{h_2} (1+x)(1+y) \frac{H_3(x)}{H_3(y)} \left[\frac{C_\lambda^2}{F(x)^2} s_2^2 + \frac{C_3^2}{H_3(x)^2} c_2^2 \right] \right\} + \frac{(1+x)(1+y)}{h_2} \frac{R^2}{2} \cosh 2\alpha_1 \sinh 2\alpha_2 \frac{C_\lambda C_3}{F(x) H_3(y)}. \quad (2.5.17)$$

Since $\omega_\phi = 0$ there are no dangerous Dirac-Misner strings in this solution.

Properties

The ADM mass of the black ring is

$$M = \frac{\pi R^2}{4G_5} \frac{1}{1-\nu} \left\{ \lambda - \mu_3 + 2\lambda\mu_3 + (\lambda + \mu_3)(\cosh 2\alpha_1 + \cosh 2\alpha_2) \right\}, \quad (2.5.18)$$

and the angular momentum is

$$J_\psi = \frac{\pi R^3}{2G_5} \frac{\sqrt{(1-\lambda)(1+\mu_3)}}{(1-\nu)^2} \left[(1+\mu_3)C_\lambda c_1 c_2 - (1-\lambda)C_3 s_1 s_2 \right]. \quad (2.5.19)$$

The D1- and D5 charges are

$$Q_{D1} = \frac{R^2(\lambda + \mu_3) \sinh 2\alpha_2}{1-\nu}, \quad Q_{D5} = \frac{R^2(\lambda + \mu_3) \sinh 2\alpha_1}{1-\nu}, \quad (2.5.20)$$

and the dipole charge from the tubular Kaluza-Klein-monopole is⁶

$$q_{KK} = 2R \left[\frac{C_\lambda}{1+\lambda} s_1 s_2 - \frac{C_3}{1-\mu_3} c_1 c_2 \right] \frac{\Delta\phi}{2\pi}. \quad (2.5.21)$$

The horizon area is

$$\begin{aligned} \mathcal{A}_H = 8\pi^2 R^3 \frac{1}{(1-\nu)^2(1+\nu)} & \left| \epsilon_\lambda \sqrt{\lambda(1-\lambda^2)(\mu_3+\nu)}(1+\mu_3)c_1 c_2 \right. \\ & \left. + \epsilon_3 \sqrt{\mu_3(1-\mu_3^2)(\lambda-\nu)}(1-\lambda)s_1 s_2 \right|. \end{aligned} \quad (2.5.22)$$

Supersymmetric limit: Two-charge supertubes

Now take the supersymmetric limit $\alpha_1 \sim \alpha_2 \rightarrow \infty$ and $\mu_3 \sim \nu \sim \lambda \rightarrow 0$ keeping fixed

$$(\lambda + \mu_3)e^{2\alpha_1} = \frac{2Q_{D5}}{R^2}, \quad (\lambda + \mu_3)e^{2\alpha_2} = \frac{2Q_{D1}}{R^2}. \quad (2.5.23)$$

Note that the dipole charge remains finite in the limit,

$$q_{KK} = \frac{R}{2} \left(\epsilon_\lambda \sqrt{\lambda(\lambda-\nu)} - \epsilon_3 \sqrt{\mu_3(\mu_3+\nu)} \right) e^{\alpha_1+\alpha_2}. \quad (2.5.24)$$

Taking the supersymmetric limit gives the string-frame metric

$$ds^2 = -\frac{1}{\sqrt{h_1 h_2}} \left(dt + \frac{q_{KK}}{2}(1+y)d\psi \right)^2 + \sqrt{h_1 h_2} dx_4^2 + \frac{1}{\sqrt{h_1 h_2}} \left(dz - \frac{q_{KK}}{2}(1+x)d\phi \right)^2 + \frac{h_2}{h_1} dz_4^2 \quad (2.5.25)$$

with

$$h_1 = 1 + \frac{Q_{D5}}{2R^2}(x-y), \quad h_2 = 1 + \frac{Q_{D1}}{2R^2}(x-y). \quad (2.5.26)$$

The rest of the fields in the solution are also easily obtained.

⁶This is the same result as for q_3 in (2.2.33) but with the sign reversed so as to agree with the sign choices in [3, 8].

This is exactly the 2-charge/1-dipole BPS solution of [8], which is the same as the two-charge supergravity supertube of [26, 6]. However, it is important to realize that if we approach the supersymmetric limit through a sequence of regular non-supersymmetric black rings, then the condition that they are balanced imposes restrictions on the parameters. Specifically, balancing the ring requires, in the limit, $2\nu = \lambda - \mu_3$. It is now convenient to define

$$k = \frac{2\mu_3}{\lambda + \mu_3}. \quad (2.5.27)$$

Since we must have $0 \leq \mu_3 \leq \lambda < 1$, k takes values between 0 and 1. Defining the function

$$f(k) = \frac{1}{2} \left(\epsilon_\lambda \sqrt{2-k} - \epsilon_3 \sqrt{k} \right), \quad (2.5.28)$$

we can then write

$$q_{\text{KK}} = \frac{\sqrt{Q_{\text{D1}} Q_{\text{D5}}}}{R} f(k). \quad (2.5.29)$$

This can be used to eliminate R (which is not a proper invariant quantity of the supergravity solutions) from the angular momentum

$$J_\psi = \frac{\pi}{4G_5} R^2 q_{\text{KK}}, \quad (2.5.30)$$

and then express it in terms of the number of branes and Kaluza-Klein monopoles as⁷

$$J_\psi = \frac{N_{\text{D1}} N_{\text{D5}}}{n_{\text{KK}}} \text{sgn}[f(k)] f(k)^2. \quad (2.5.31)$$

Using the four combinations of $\epsilon_\lambda, \epsilon_3 = \pm 1$, the values of the function $f(k)$ cover precisely the interval $[-1, 1]$ when k is varied between 0 and 1. Thus the supergravity solution yields exactly the range of angular momentum

$$|J_\psi| \leq \frac{N_{\text{D1}} N_{\text{D5}}}{n_{\text{KK}}} \quad (2.5.32)$$

expected from the worldvolume supertube analysis [5, 6, 27, 28]. The solutions constructed earlier in [3] correspond instead to having $\mu_3 = 0$, hence $k = 0$ and $f^2(0) = 1/2$. Since we can now vary μ_3 and recover the whole range of expected values of the parameters, it seems that the solution above should be the most general non-supersymmetric black ring with two charges and one angular momentum.

The supersymmetric supertube solutions with angular momentum strictly below the bound (2.5.32) have naked singularities, while if the bound is saturated the solution is regular [29]. The saturation of the bound as a limit of our solutions is slightly subtle, since one must take $k = 1$ *i.e.*, $\mu_3 = \lambda$. For finite values of the parameters this would require $\nu = 0$, which corresponds to an extremal singular solution. So it would seem that in order to thermally deform the non-singular, maximally rotating supertube, one has to consider μ_3 strictly different from λ . This suggests that the energy gap of non-BPS excitations above the non-singular, maximally rotating supertube is larger than for under-rotating supertubes. Indeed this is expected, since in the former all the effective D1-D5 strings are singly wound (it is a ground state of the non-twisted

⁷See *e.g.*, [3, 8] for the expressions for the quantized brane numbers in terms of supergravity charges. Note that we take n_{KK} to be positive.

sector of the dual CFT) and therefore the left- and right-moving open strings are energetically more expensive to excite.

Finally, on the issue of non-uniqueness, the solutions contain five parameters (*i.e.*, $(\alpha_{1,2}, \mu_3, \nu, \lambda, R)$, minus one constraint) but only four conserved charges $(M, Q_{1,2}, J_\psi)$, so we have a continuous one-parameter non-uniqueness. This is of course controlled by the dipole charge q_{KK} . It is possible to see this explicitly by drawing plots of the area of the rings vs. J_ψ at different values of q_{KK} , for fixed values of the mass and the charges. These curves look very similar to the ones for the dipole black ring with $N = 1$ in [2], so we shall not reproduce them here.

2.5.3 D1-D5-P/d1-d5 black ring: the black double helix

The supersymmetric configuration in the previous subsection is U-dual to a D1-P/d1 supergravity supertube. This is the supergravity description of a D1-helix: a D1-brane with a gyrating momentum wave, such that it coils around the ψ direction (hence the dipole d1) while carrying momentum along z . The supergravity solution is smeared along the direction of the tube [26]. T-dualizing along the internal T^4 directions one obtains a D5-P/d5 configuration, *i.e.*, a D5-helix.

The D1 and D5 can bind to form a supersymmetric double D1-D5 helix. To obtain a non-supersymmetric black D1-D5 helix (without a kkm tube), we must first demand

$$q_3 = 0 \quad \text{and} \quad q_1, q_2 \neq 0. \quad (2.5.33)$$

However, if we want the configuration to actually describe the excitations of a bound state of the D1-D5 helix, we must also require

$$q_1 Q_1 = q_2 Q_2 \quad (2.5.34)$$

even away from the supersymmetric state. Since Q_1 and q_2 (Q_2 and q_1) are associated to the number of windings of D5-branes (D1-branes) along z and along ψ , respectively, this equation is the condition that the pitches of the D1 and D5 helices are equal (see also [8]). The two helices can then bind and these black tubes are naturally interpreted as thermal excitations of a D1-D5 superhelix.

It is straightforward to see that the two conditions (2.5.33) and (2.5.34) imply

$$\mu_1 = \mu_2 = 0, \quad (2.5.35)$$

while all other parameters take non-zero values.

The supersymmetric limit of these solutions, as shown in section 2.3, correctly yields the BPS solutions with three charges and two dipoles of [8]. However, (2.5.35) implies that the two ‘‘constraint parameters’’ a and b in (2.3.4), (2.3.5), are not independent but satisfy $a^2 = 2b^2$. From (2.3.8) and (2.3.9) we obtain again the inequality (2.3.15), but now, instead of the bound (2.3.16), we find that

$$\frac{4G_5}{\pi} (J_\psi - J_\phi) = \frac{1}{2} \sqrt{\frac{Q_1 Q_2}{q_1 q_2}} (Q_3 - q_1 q_2), \quad (2.5.36)$$

i.e., we can only obtain half the maximum value for $J_\psi - J_\phi$. This restriction is reminiscent of the former situation for D1-D5/kkm supertubes in [3], and suggests that we need a still larger family of non-BPS solutions in order to describe the thermal deformations of supertubes with three charges and two dipoles and generic values of $J_\psi - J_\phi$.

2.5.4 Decoupling limit

The decoupling limit, relevant to AdS₃/CFT₂ duality of the D1-D5 system, is obtained by taking the string length to zero, $\alpha' = \ell_s^2 \rightarrow 0$, and then scaling the parameters in the solution in such a way that

$$\lambda, \quad \nu, \quad \mu_i, \quad \alpha_3, \quad \alpha' e^{2\alpha_{1,2}}, \quad R/\alpha', \quad (2.5.37)$$

remain fixed. The (dimensionless) coordinates x, y also remain finite. Note in particular that the boosts associated to D5- and D1-brane charges become $\alpha_{1,2} \rightarrow \infty$, and that the energy of the excitations near the core of the solution is kept finite by scaling the parameter $R \sim \alpha'$. To keep the ten-dimensional string metric finite, we rescale it by an overall factor of α' .

The metric in the decoupling limit is of the same form as (2.5.1), with the functions F, G, H_i and h_3 unmodified, but $h_{1,2}, \omega$ and A^3 do change. One can see in general that the metric asymptotes to AdS₃ \times S^3 \times T^4 , but we shall provide details only for the two cases of interest of the previous subsections, with $\mu_1 = \mu_2 = 0$ (and in general $\alpha_3 \neq 0$), where the expressions get somewhat simplified. In this case one gets

$$h_{1,2} = \frac{Q_{1,2}}{2R^2} (1 - \nu) \frac{x - y}{F(x)H_3(y)}, \quad (2.5.38)$$

and

$$\begin{aligned} \omega_\psi &= \frac{G_5 J_\psi}{\pi R^2} \frac{2(1+y)}{F(y)H_3(y)} \frac{C_\lambda H_3(y) - C_3 F(y)}{C_\lambda(1+\mu_3) - C_3(1-\lambda)} \frac{(1-\nu)^2}{\sqrt{(1-\lambda)(1+\mu_3)}}, \\ \omega_\phi &= \frac{G_5 J_\phi}{\pi R^2} \frac{1-x^2}{F(x)H_3(x)} \frac{(1-\nu)^2}{\sqrt{(1-\lambda)(1+\mu_3)}}, \end{aligned} \quad (2.5.39)$$

while the expression for A^3 is not comparatively simpler. The asymptotic region is again at $x \rightarrow y \rightarrow -1$. If we perform the change of coordinates

$$r^2 = R^2 \frac{1-x}{x-y} \frac{(1-\lambda)(1+\mu_3)}{1-\nu}, \quad \cos^2 \theta = \frac{1+x}{x-y}, \quad (2.5.40)$$

introduce canonical angular variables (2.2.18), and gauge-transform so that A_t^3 vanishes at infinity, then the asymptotic metric at $r \rightarrow \infty$ is

$$ds_{\text{IIB}}^2 \rightarrow \frac{r^2}{\sqrt{Q_1 Q_2}} (-dt^2 + dz^2) + \sqrt{Q_1 Q_2} \frac{dr^2}{r^2} + \sqrt{Q_1 Q_2} (d\theta^2 + \sin^2 \theta d\tilde{\psi}^2 + \cos^2 \theta d\tilde{\phi}^2) + \sqrt{\frac{Q_2}{Q_1}} dz_{(4)}^2, \quad (2.5.41)$$

i.e., the correct asymptotic geometry of AdS₃ \times S^3 \times T^4 .

Away from the asymptotic boundary the geometry does not factorize into a product space AdS₃ \times S^3 \times T^4 , not even locally. In general, the geometry does not appear to become simple even near the horizon. This is in contrast to what was found in the supersymmetric case with three charges and three dipoles, where near the horizon a second, different factorization into (locally) AdS₃ \times S^3 \times T^4 happens [8, 12]. With three charges and only two dipoles, this factorization does not happen even near the core of the supersymmetric solutions. But perhaps the yet to be found non-BPS solution that can retain all three dipoles in the supersymmetric limit will show this property.

2.6 Discussion

We have shown how to construct non-supersymmetric three-charge black rings via boosts and dualities, overcoming the problems previously encountered in ref. [3]. Technically, the main issue is the requirement that the one-form ω associated to the rotation of the ring be well-defined (absence of Dirac-Misner strings). This was also an important ingredient when constructing the supersymmetric rings by solving the supersymmetry-preservation equations of [30]. In the present case, we have achieved it by having more parameters, associated to dipole charges, in our seed solution.

We expect that a larger family of non-supersymmetric black rings with nine-parameters $(M, J_\psi, J_\phi, Q_{1,2,3}, q_{1,2,3})$ exists, and that the general solutions of [7, 8, 9, 10] are recovered in the supersymmetric limit. The nine parameters would yield three-fold continuous non-uniqueness, furnished by the non-conserved dipole charges $q_{1,2,3}$. This is like in the dipole ring solutions in [2] but larger than the two-fold continuous non-uniqueness of the supersymmetric rings of [8]. Presumably, one of the additional parameters in the conjectured larger family of solutions will not describe proper near-supersymmetric excitations of the supertube. Instead they should be interpreted as the presence of dipole strings or branes in the configuration that are not bound to the supertube but rather superimposed on it. Since these dipole branes break all supersymmetries, they must disappear in the BPS limit.

The extra parameters that are still missing from our current solutions should provide the freedom to vary the angular momentum J_ϕ and all the three dipoles independently of other parameters. In particular, we expect that black rings with two charges should exist that carry both angular momenta J_ψ and J_ϕ . Note, though, that in the supersymmetric limit J_ϕ disappears, which is consistent with the fact that J_ϕ is expected to be carried by the coherent polarization of (R-charged) left- and right-moving fermionic open string excitations. In our solutions the total macroscopic J_ϕ must vanish. So the two-charge solutions in this paper can describe the non-BPS excitations that carry total $J_\phi = 0$.⁸ This should be already enough to address in detail the issues of black hole non-uniqueness and near-supersymmetric black ring entropy from a microscopic viewpoint, along the lines proposed in ref. [3]. We hope to tackle these problems in the future.

The solutions with three charges and two dipoles in this paper are similarly expected to describe the non-BPS excitations that do not add to the J_ϕ of a D1-D5-P/d1-d5 super-helix. However, in this case we seem to be restricted to considering only excitations above the supersymmetric state with half the maximum value of $J_\psi - J_\phi$. This is analogous to the former situation in [3], and once again points to the need to find a larger family of solutions. Note, however, that by including more general excitations our solutions do describe thermally deformed D1-D5-P/d1-d5 supertubes with any value of $J_\psi - J_\phi$ in the permitted range (2.3.17). As we have seen, these solutions are free of pathologies and are regular on and outside the horizons.

One can speculate about generalizations of the non-supersymmetric black rings. Refs. [9, 14] constructed supersymmetric ring solutions with arbitrary cross-sections. However, it was argued in [31] that unless the cross-section is circular these rings are not truly black holes, since they do not have smooth horizons. Adding energy to a ring with a non-circular cross-section is unlikely to yield a stationary black ring, since the lumpiness of the rotating ring will presumably cause the system to radiate when it is not supersymmetric.

⁸We could have two-charge supertubes with $J_\phi \neq 0$ if $\mu_1, \mu_2 \neq 0$. But then $q_1, q_2 \neq 0$, so these excitations take the system further away from the supersymmetric state.

Finally, a particularly interesting spin-off of our study is the evidence we have found in favor of the proposal in ref. [32] for one criterion to admit naked singularities in supergravity solutions. The supersymmetric limits of our black rings do indeed typically result in solutions with naked singularities. Ref. [32] proposed that solutions which admit thermal deformations, *i.e.*, arise as the zero-temperature limit of black holes with a regular horizon, should be regarded as physically sensible. This is precisely what we have found, and in a very non-trivial manner. Taking the supersymmetric limit of our rings results in supertubes with parameters precisely within the ranges that were earlier determined using entirely different criteria — worldvolume theory constraints (including unitarity), and absence of localized causal violations in BPS solutions. Solutions with sick worldvolume theories, or spacetime causal pathologies, such as over-rotating supertubes, do not admit thermal deformations. This is a remarkable consistency check of the low energy supergravity description of string theory configurations.

Acknowledgments

We thank Gary Horowitz, David Mateos, Harvey Reall and Toby Wiseman for useful discussions. We would also like to thank the organizers and the participants at the Berkeley mini-conference on black rings for lively discussions. HE was supported by NSF grant PHY-0244764 and the Danish Research Agency. RE and PF were supported in part by CICYT grant FPA2001-3598, by DURSI 2001-SGR-00188 and by the European Commission RTN program under contract MRTN-CT-2004-005104. RE was additionally supported in part by UPV00172.310-14497, and PF by a FI scholarship from Generalitat de Catalunya.

Appendices

2.A Three-form fields for the 11D solution

We here give explicitly the non-zero components of the three-form potential for the eleven-dimensional solution in section 2.2:

$$A_t^1 = \frac{U_1 - 1}{h_1} c_1 s_1, \quad (2.A.1)$$

$$A_\psi^1 = \frac{R(1+y)}{h_1} \left[U_1 \frac{C_\lambda}{F(y)} s_1 c_2 c_3 - U_1 \frac{C_1}{H_1(y)} s_1 s_2 s_3 - \frac{C_2}{H_2(y)} c_1 c_2 s_3 - \frac{C_3}{H_3(y)} c_1 s_2 c_3 \right], \quad (2.A.2)$$

$$A_\phi^1 = -\frac{R(1+x)}{h_1} \left[\frac{C_\lambda}{F(x)} c_1 s_2 s_3 - \frac{C_1}{H_1(x)} c_1 c_2 c_3 - U_1 \frac{C_2}{H_2(x)} s_1 s_2 c_3 - U_1 \frac{C_3}{H_3(x)} s_1 c_2 s_3 \right], \quad (2.A.3)$$

$$A_t^2 = \frac{U_2 - 1}{h_2} c_2 s_2, \quad (2.A.4)$$

$$A_\psi^2 = \frac{R(1+y)}{h_2} \left[U_2 \frac{C_\lambda}{F(y)} c_1 s_2 c_3 - \frac{C_1}{H_1(y)} c_1 c_2 s_3 - U_2 \frac{C_2}{H_2(y)} s_1 s_2 s_3 - \frac{C_3}{H_3(y)} s_1 c_2 c_3 \right], \quad (2.A.5)$$

$$A_\phi^2 = -\frac{R(1+x)}{h_2} \left[\frac{C_\lambda}{F(x)} s_1 c_2 s_3 - U_2 \frac{C_1}{H_1(x)} s_1 s_2 c_3 - \frac{C_2}{H_2(x)} c_1 c_2 c_3 - U_2 \frac{C_3}{H_3(x)} c_1 s_2 s_3 \right], \quad (2.A.6)$$

$$A_t^3 = \frac{U_3 - 1}{h_3} c_3 s_3, \quad (2.A.7)$$

$$A_\psi^3 = \frac{R(1+y)}{h_3} \left[U_3 \frac{C_\lambda}{F(y)} c_1 c_2 s_3 - \frac{C_1}{H_1(y)} c_1 s_2 c_3 - \frac{C_2}{H_2(y)} s_1 c_2 c_3 - U_3 \frac{C_3}{H_3(y)} s_1 s_2 s_3 \right], \quad (2.A.8)$$

$$A_\phi^3 = -\frac{R(1+x)}{h_3} \left[\frac{C_\lambda}{F(x)} s_1 s_2 c_3 - U_3 \frac{C_1}{H_1(x)} s_1 c_2 s_3 - U_3 \frac{C_2}{H_2(x)} c_1 s_2 s_3 - \frac{C_3}{H_3(x)} c_1 c_2 c_3 \right]. \quad (2.A.9)$$

where the functions U_i are defined as

$$U_i = \frac{F(y)H(x)^3 H_i(y)^2}{F(x)H(y)^3 H_i(x)^2}. \quad (2.A.10)$$

2.B The RR two-form potentials for the D1-D5-P black ring solution

We here give the expressions for the non-zero components of the Ramond-Ramond two-form potential of the D1-D5-P non-supersymmetric black ring solution of type IIB supergravity given in section 2.5:

$$C_{tz}^{(2)} = \frac{U_2 - 1}{h_2} c_2 s_2, \quad (2.B.1)$$

$$C_{\psi z}^{(2)} = \frac{R(1+y)}{h_2} \left[U_2 \frac{C_\lambda}{F(y)} c_1 s_2 c_3 - \frac{C_1}{H_1(y)} c_1 c_2 s_3 - U_2 \frac{C_2}{H_2(y)} s_1 s_2 s_3 - \frac{C_3}{H_3(y)} s_1 c_2 c_3 \right], \quad (2.B.2)$$

$$C_{\phi z}^{(2)} = -\frac{R(1+x)}{h_2} \left[\frac{C_\lambda}{F(x)} s_1 c_2 s_3 - U_2 \frac{C_1}{H_1(x)} s_1 s_2 c_3 - \frac{C_2}{H_2(x)} c_1 c_2 c_3 - U_2 \frac{C_3}{H_3(x)} c_1 s_2 s_3 \right], \quad (2.B.3)$$

$$C_{t\psi}^{(2)} = \frac{R(1+y)}{h_2} \left[U_2 \frac{C_\lambda}{F(y)} c_1 s_2 s_3 - \frac{C_1}{H_1(y)} c_1 c_2 c_3 - U_2 \frac{C_2}{H_2(y)} s_1 s_2 c_3 - \frac{C_3}{H_3(y)} s_1 c_2 s_3 \right], \quad (2.B.4)$$

$$C_{t\phi}^{(2)} = -\frac{R(1+x)}{h_2} \left[\frac{C_\lambda}{F(x)} s_1 c_2 c_3 - U_2 \frac{C_1}{H_1(x)} s_1 s_2 s_3 - \frac{C_2}{H_2(x)} c_1 c_2 s_3 - U_2 \frac{C_3}{H_3(x)} c_1 s_2 c_3 \right], \quad (2.B.5)$$

$$\begin{aligned} C_{\psi\phi}^{(2)} = & -R^2 c_1 s_1 \left\{ \frac{G(x)}{(x-y)} \left(\frac{\lambda + \mu_3}{F(x)H_3(x)} + \frac{\mu_2 - \mu_1}{H_1(x)H_2(x)} \right) \right. \\ & + \frac{1}{h_2} (1+x)(1+y) \left[U_2 \frac{C_\lambda^2}{F(x)F(y)} s_2^2 - \frac{C_1^2}{H_1(x)H_1(y)} c_2^2 \right. \\ & \quad \left. \left. - U_2 \frac{C_2^2}{H_2(x)H_2(y)} s_2^2 + \frac{C_3^2}{H_3(x)H_3(y)} c_2^2 \right] \right. \\ & \left. + (1+x) \left(\frac{C_\lambda^2}{\lambda F(x)} - \frac{C_1^2}{\mu_1 H_1(x)} + \frac{C_2^2}{\mu_2 H_2(x)} + \frac{C_3^2}{\mu_3 H_3(x)} \right) \right\} \\ & + \frac{(1+x)(1+y)}{h_2} R^2 c_2 s_2 \left\{ \frac{C_\lambda C_3}{F(x)H_3(y)} s_1^2 + U_2 \frac{C_\lambda C_3}{F(y)H_3(x)} c_1^2 \right. \\ & \quad \left. + U_2 \frac{C_1 C_2}{H_1(x)H_2(y)} s_1^2 + \frac{C_1 C_2}{H_1(y)H_2(x)} c_1^2 \right\}, \quad (2.B.6) \end{aligned}$$

where U_i were defined in (2.A.10).

2.C Limit of spherical black hole

We can take a limit of our solutions to recover non-supersymmetric spherical black holes with three charges. This limit is actually the same as described in [2], and involves taking $\lambda, \nu \rightarrow 1$ and $R \rightarrow 0$ while keeping finite the parameters a, m , defined as

$$m = \frac{2R^2}{1-\nu}, \quad a^2 = 2R^2 \frac{\lambda-\nu}{(1-\nu)^2}. \quad (2.C.1)$$

The coordinates x, y degenerate in this limit, so we introduce new ones, r, θ , through

$$\begin{aligned} x &= -1 + 2 \left(1 - \frac{a^2}{m}\right) \frac{R^2 \cos^2 \theta}{r^2 - (m - a^2) \cos^2 \theta}, \\ y &= -1 - 2 \left(1 - \frac{a^2}{m}\right) \frac{R^2 \sin^2 \theta}{r^2 - (m - a^2) \cos^2 \theta}, \end{aligned} \quad (2.C.2)$$

and rescale ψ and ϕ

$$(\psi, \phi) \rightarrow \sqrt{\frac{m-a^2}{2R^2}} (\psi, \phi) \quad (2.C.3)$$

so they have canonical periodicity 2π . Then we recover the metric

$$\begin{aligned} ds_{5D}^2 &= -(h_1 h_2 h_3)^{-2/3} \left(1 - \frac{m}{\Sigma}\right) \left(dt - \frac{ma \sin^2 \theta}{\Sigma - m} c_1 c_2 c_3 d\psi - \frac{ma \cos^2 \theta}{\Sigma} s_1 s_2 s_3 d\phi\right)^2 \\ &+ (h_1 h_2 h_3)^{1/3} \left[\Sigma \left(\frac{dr^2}{\Delta} + d\theta^2\right) + \frac{\Delta \sin^2 \theta}{1 - m/\Sigma} d\psi^2 + r^2 \cos^2 \theta d\phi^2\right], \end{aligned} \quad (2.C.4)$$

$$\Delta \equiv r^2 - m + a^2, \quad \Sigma \equiv r^2 + a^2 \cos^2 \theta, \quad h_i = 1 + \frac{ms_i^2}{\Sigma}. \quad (2.C.5)$$

This is the particular case of the rotating black hole with three charges in [22] that is obtained by setting one of the two rotation parameters of the initial seed black hole to zero.

Note that we have not prescribed any limiting value for the parameters μ_i . As was the case for the dipole rings in [2], in the limit all the functions $H_i(\xi) \rightarrow 1 + \mu_i$ become constants that can be absorbed in rescalings of the coordinates. Then the limiting spherical black hole solution is actually independent of these parameters and therefore they cannot provide it with any kind of ‘hair’.

2.D Infinite radius limit

In the limit where the radius of the S^1 of the ring becomes infinite the ring becomes a black string carrying momentum along its length. The dipole charges become conserved charges, so in this limit we obtain a five-dimensional black string with six charges and momentum. Reduction to four dimensions along the length of the string results in a non-supersymmetric four-dimensional black hole with seven charges. Their extremal limit in this case is also a supersymmetric limit.

We take $R \rightarrow \infty$ while keeping fixed

$$r = -\frac{R}{y}, \quad \cos \theta = x, \quad \eta = R\psi. \quad (2.D.1)$$

In order to get a finite limit, we also take $\lambda, \nu, \mu_i \rightarrow 0$ keeping fixed

$$r_0 = \nu R, \quad r_0 \cosh^2 \sigma = \lambda R, \quad r_0 \sinh^2 \gamma_i = \mu_i R. \quad (2.D.2)$$

Note first that the balancing condition gives

$$\sinh^2 \sigma = 1 + \sum_{i=1}^3 \sinh^2 \gamma_i \quad (2.D.3)$$

and the Dirac-Misner condition (2.2.21) becomes

$$0 = \omega_\phi = \epsilon_\lambda \sinh 2\sigma s_1 s_2 s_3 - \epsilon_1 \sinh 2\gamma_1 s_1 c_2 c_3 - \epsilon_2 \sinh 2\gamma_2 c_1 s_2 c_3 - \epsilon_3 \sinh 2\gamma_3 c_1 c_2 s_3. \quad (2.D.4)$$

The metric becomes

$$\begin{aligned} ds_{11D}^2 = & -\frac{1}{(h_1 h_2 h_3)^{2/3}} \frac{\hat{f}}{(\hat{h}_1 \hat{h}_2 \hat{h}_3)^{1/3}} \left[dt + \omega_\eta d\eta \right]^2 \\ & + (h_1 h_2 h_3)^{1/3} \left\{ \frac{f}{\hat{f}(\hat{h}_1 \hat{h}_2 \hat{h}_3)^{1/3}} d\eta^2 + (\hat{h}_1 \hat{h}_2 \hat{h}_3)^{2/3} \left(\frac{dr^2}{f} + r^2 d\Omega_2^2 \right) \right. \\ & \left. + \frac{1}{(\hat{h}_1 \hat{h}_2 \hat{h}_3)^{1/3}} \left[\frac{\hat{h}_1}{h_1} (dz_1^2 + dz_2^2) + \frac{\hat{h}_2}{h_2} (dz_3^2 + dz_4^2) + \frac{\hat{h}_3}{h_3} (dz_5^2 + dz_6^2) \right] \right\}, \end{aligned} \quad (2.D.5)$$

where

$$f = 1 - \frac{r_0}{r}, \quad \hat{f} = 1 - \frac{r_0 \cosh^2 \sigma}{r}, \quad \hat{h}_i = 1 + \frac{r_0 \sinh^2 \gamma_i}{r}, \quad (2.D.6)$$

and

$$\begin{aligned} \omega_\eta = & -\frac{r_0}{2r} \left[\hat{f}^{-1} \epsilon_\lambda \sinh 2\sigma c_1 c_2 c_3 - \hat{h}_1^{-1} \epsilon_1 \sinh 2\gamma_1 c_1 s_2 s_3 \right. \\ & \left. - \hat{h}_2^{-1} \epsilon_2 \sinh 2\gamma_2 s_1 c_2 s_3 - \hat{h}_3^{-1} \epsilon_3 \sinh 2\gamma_3 s_1 s_2 c_3 \right]. \end{aligned} \quad (2.D.7)$$

Further, using the balancing condition we have

$$h_i = 1 + \frac{2r_0 \hat{h}_i s_i^2}{r \hat{h}_1 \hat{h}_2 \hat{h}_3} \left[\sinh^2 \sigma - \sinh^2 \gamma_i + \frac{r_0}{2r} \left(\cosh^2 \sigma \sinh^2 \gamma_i + \frac{\prod_{j=1}^3 \sinh^2 \gamma_j}{\sinh^2 \gamma_i} \right) \right]. \quad (2.D.8)$$

Bibliography

- [1] R. Emparan and H. S. Reall, “A rotating black ring in five dimensions,” *Phys. Rev. Lett.* **88**, 101101 (2002) [arXiv:hep-th/0110260].
- [2] R. Emparan, “Rotating circular strings, and infinite non-uniqueness of black rings,” *JHEP* **0403**, 064 (2004) [arXiv:hep-th/0402149].
- [3] H. Elvang and R. Emparan, “Black rings, supertubes, and a stringy resolution of black hole non-uniqueness,” *JHEP* **0311**, 035 (2003) [arXiv:hep-th/0310008].
- [4] H. Elvang, “A charged rotating black ring,” *Phys. Rev. D* **68** (2003) 124016 [arXiv:hep-th/0305247].
- [5] D. Mateos and P. K. Townsend, “Supertubes,” *Phys. Rev. Lett.* **87**, 011602 (2001) [arXiv:hep-th/0103030].
- [6] R. Emparan, D. Mateos and P. K. Townsend, “Supergravity supertubes,” *JHEP* **0107** (2001) 011 [arXiv:hep-th/0106012].
- [7] H. Elvang, R. Emparan, D. Mateos and H. S. Reall, “A supersymmetric black ring,” *Phys. Rev. Lett.* **93**, 211302 (2004) [arXiv:hep-th/0407065].
- [8] H. Elvang, R. Emparan, D. Mateos and H. S. Reall, *Phys. Rev. D* **71** (2005) 024033 [arXiv:hep-th/0408120].
- [9] I. Bena and N. P. Warner, “One ring to rule them all ... and in the darkness bind them?,” arXiv:hep-th/0408106.
- [10] J. P. Gauntlett and J. B. Gutowski, “General concentric black rings,” arXiv:hep-th/0408122.
- [11] J. P. Gauntlett and J. B. Gutowski, “Concentric black rings,” arXiv:hep-th/0408010.
- [12] I. Bena and P. Kraus, “Microscopic description of black rings in AdS/CFT,” arXiv:hep-th/0408186.
- [13] T. Ortín, “A note on supersymmetric Goedel black holes, strings and rings of minimal $d=5$ supergravity,” arXiv:hep-th/0410252.
- [14] I. Bena, C. W. Wang and N. P. Warner, “Black rings with varying charge density,” arXiv:hep-th/0411072.
- [15] M. Cyrier, M. Guica, D. Mateos and A. Strominger, “Microscopic Entropy of the Black Ring,” arXiv:hep-th/0411187.

- [16] K. Copsey and G. T. Horowitz, work in progress.
- [17] A. W. Peet, “TASI lectures on black holes in string theory,” arXiv:hep-th/0008241.
J. R. David, G. Mandal and S. R. Wadia, “Microscopic formulation of black holes in string theory,” Phys. Rept. **369** (2002) 549 [arXiv:hep-th/0203048].
- [18] S. D. Mathur, A. Saxena and Y. K. Srivastava, “Constructing ‘hair’ for the three charge hole,” Nucl. Phys. B **680** (2004) 415 [arXiv:hep-th/0311092].
O. Lunin and S. D. Mathur, “Statistical interpretation of Bekenstein entropy for systems with a stretched horizon,” Phys. Rev. Lett. **88**, 211303 (2002) [arXiv:hep-th/0202072].
- [19] I. Bena and P. Kraus, “Three charge supertubes and black hole hair,” Phys. Rev. D **70** (2004) 046003 [arXiv:hep-th/0402144].
- [20] I. Bena, “Splitting hairs of the three charge black hole,” arXiv:hep-th/0404073.
- [21] J. C. Breckenridge, R. C. Myers, A. W. Peet and C. Vafa, “D-branes and spinning black holes,” Phys. Lett. B **391**, 93 (1997) [arXiv:hep-th/9602065].
- [22] J. C. Breckenridge, D. A. Lowe, R. C. Myers, A. W. Peet, A. Strominger and C. Vafa, “Macroscopic and Microscopic Entropy of Near-Extremal Spinning Black Holes,” Phys. Lett. B **381**, 423 (1996) [arXiv:hep-th/9603078].
- [23] M. Cvetič and D. Youm, “General Rotating Five Dimensional Black Holes of Toroidally Compactified Heterotic String,” Nucl. Phys. B **476**, 118 (1996) [arXiv:hep-th/9603100].
- [24] A. A. Tseytlin, “Extreme dyonic black holes in string theory,” Mod. Phys. Lett. A **11**, 689 (1996) [arXiv:hep-th/9601177].
- [25] C. W. Misner, “The flatter regions of Newman, Unti and Tamburino’s generalized Schwarzschild space,” J. Math. Phys. **4**, 924 (1963).
- [26] O. Lunin and S. D. Mathur, “Metric of the multiply wound rotating string,” Nucl. Phys. B **610** (2001) 49 [arXiv:hep-th/0105136].
- [27] D. Mateos, S. Ng and P. K. Townsend, “Tachyons, supertubes and brane/anti-brane systems,” JHEP **0203** (2002) 016 [arXiv:hep-th/0112054].
- [28] Y. Hyakutake and N. Ohta, “Supertubes and Supercurves from M-Ribbons,” Phys. Lett. B **539** (2002) 153 [arXiv: hep-th/0204161].
- [29] V. Balasubramanian, J. de Boer, E. Keski-Vakkuri and S. F. Ross, “Supersymmetric conical defects: Towards a string theoretic description of black hole formation,” Phys. Rev. D **64**, 064011 (2001) [arXiv:hep-th/0011217].
J. M. Maldacena and L. Maoz, “De-singularization by rotation,” JHEP **0212**, 055 (2002) [arXiv:hep-th/0012025].
- [30] J. P. Gauntlett, J. B. Gutowski, C. M. Hull, S. Pakis and H. S. Reall, “All supersymmetric solutions of minimal supergravity in five dimensions,” Class. Quant. Grav. **20** (2003) 4587 [arXiv:hep-th/0209114].

-
- [31] G. T. Horowitz and H. S. Reall, “How hairy can a black ring be?,” arXiv:hep-th/0411268.
- [32] S. S. Gubser, “Curvature singularities: The good, the bad, and the naked,” *Adv. Theor. Math. Phys.* **4** (2002) 679 [arXiv:hep-th/0002160].

Chapter 3

A black ring with a rotating 2-sphere

Pau Figueras

*Departament de Física Fonamental, and
C.E.R. en Astrofísica, Física de Partícules i Cosmologia,
Universitat de Barcelona, Diagonal 647, E-08028 Barcelona, Spain*

pfigueras@ffn.ub.es

ABSTRACT

We present a solution of the vacuum Einstein's equations in five dimensions corresponding to a black ring with horizon topology $S^1 \times S^2$ and rotation in the azimuthal direction of the S^2 . This solution has a regular horizon up to a conical singularity, which can be placed either inside the ring or at infinity. This singularity arises due to the fact that this black ring is not balanced. In the infinite radius limit we correctly reproduce the Kerr black string, and taking another limit we recover the Myers-Perry black hole with a single angular momentum.

3.1 Introduction

The discovery of the black ring by [1] showed that the four-dimensional black hole theorems [2] do not have a simple extension to higher dimensions. Black rings have a horizon with topology $S^1 \times S^2$ while the Myers-Perry (MP) black hole [3] in five dimensions has a horizon with the topology of an S^3 . On the other hand, in four dimensions, the black hole theorems state that the only allowed horizon topology is that of an S^2 . Moreover, it was shown in [1] that both the black hole and the black ring can carry the same conserved charges, namely the mass and a single angular momentum, and hence there is no uniqueness theorem in five dimensions. Further studies on black rings showed that they can also carry nonconserved charges [4], which is a completely novel feature with respect to spherical black holes. The fact that black rings can have *dipole* charges gives rise to infinite continuous nonuniqueness at the classical level since the parameters describing these charges can be varied continuously without altering the conserved charges.

If string theory is the correct theory of quantum gravity, it should account for the microscopic states of both spherical black holes and black rings. Therefore, black rings constitute an interesting test ground for string theory. A step towards the understanding of black rings in

string theory was taken in [5], following [6], where it was found that black rings were related to supertubes [7, 8], which are well-known objects within the string theory framework. The recent discovery of supersymmetric black rings [9] (see also [10, 11, 12]) and the generalization to non-BPS black rings with three charges and three dipoles [13], has provided further evidence of this relationship. Both the BPS and the non-BPS black rings with three charges and three dipoles have two angular momenta J_ψ and J_ϕ . In fact, [1] already conjectured the existence a neutral black ring with two independent angular momenta. Moreover, in [13] a further conjecture was made about the existence of a family of non-supersymmetric black rings with nine parameters $(M, J_\psi, J_\phi, Q_{1,2,3}, q_{1,2,3})$. Recently [14] conjectured the existence of an even larger family of black rings, which would depend on twenty-one parameters, up to duality transformations. Motivated by these conjectures, in this paper we present a neutral black ring with rotation in the azimuthal direction of the S^2 , which from now on we call ϕ . Recall that the black ring of [1] has rotation on the plane of the ring along the direction of the S^1 , which we call ψ . Our solution should be the $J_\psi \rightarrow 0$ limit of the more general yet to be found doubly spinning black ring. The solution we present in this paper provides new evidence in favour of the existence of this neutral black ring with two independent angular momenta.

Ref. [15] has independently constructed a black ring with rotation in the S^2 . It is claimed that their solution reproduces, in appropriate limits, the Kerr black string and the MP black hole with a single angular momentum, as does ours and hence both solutions may be equivalent. However, this is not evident since the coordinates used in [15] are rather involved. Instead, we present the solution in essentially the same coordinates as in [4] so that the connections with the previously known black ring solutions are immediately apparent. Using these coordinates we study all its properties, including the different limits that this solution meets. Specifically, we find that our solution has a regular horizon except for the conical excess singularity inside the ring which prevents it from collapsing. We could also choose to place the conical defect at infinity, which would equally stabilize the configuration, but the resulting spacetime would not be asymptotically flat. The presence of this singularity can be understood intuitively; a black ring can be constructed by taking a black string, identifying its ends so as to form an S^1 and adding angular momentum in the direction of the S^1 in order to compensate the self-attraction and the tension of the string. In our case, since the angular momentum is on the plane orthogonal to the ring, it does not balance the configuration and a conical singularity inside the ring is required. Our solution has three independent parameters, namely R , which is roughly the radius of the ring, λ , which plays a similar role as the ν parameter in the static ring [16]¹ and is related to the conical singularity, and a new parameter a with dimensions of length, which is associated to the angular momentum. Taking the limit $a \rightarrow 0$ of our solution, one obtains the static ring [16] in the form given in [4].

The rest of the paper is organized as follows. In section 3.2 we present the solution and compute the main physical properties. Also, we study the horizon geometry and derive the Smarr relation. In section 3.3 we study the different limits of our solution. Specifically, taking infinite radius limit we obtain the Kerr black string. Moreover, we also study the limit which connects our solution with the MP black hole with a single angular momentum. The conclusions are presented in section 3.4.

¹Note that the C-metric coordinates used in [16, 1] are different from the ones used in [5, 17], which in turn are different from those in [4]. Throughout this paper we use the same coordinates as ref. [4].

3.2 The black ring with a rotating S^2

In this section we present the black ring with rotation on the S^2 . The solution has been obtained by educated guesswork, from limits it would be expected to reproduce. It looks rather similar to the other neutral black ring solutions, which involve simple polynomial functions of x and y . Here we study the physical properties of the solution and the horizon geometry.

3.2.1 The solution

The metric for the ϕ -spinning ring is

$$\begin{aligned}
 ds^2 = & -\frac{H(\lambda, y, x)}{H(\lambda, x, y)} \left[dt - \frac{\lambda a y (1 - x^2)}{H(\lambda, y, x)} d\phi \right]^2 \\
 & + \frac{R^2}{(x - y)^2} H(\lambda, x, y) \left[-\frac{dy^2}{(1 - y^2)F(\lambda, y)} - \frac{(1 - y^2)F(\lambda, x)}{H(\lambda, x, y)} d\psi^2 \right. \\
 & \left. + \frac{dx^2}{(1 - x^2)F(\lambda, x)} + \frac{(1 - x^2)F(\lambda, y)}{H(\lambda, y, x)} d\phi^2 \right], \quad (3.2.1)
 \end{aligned}$$

where

$$F(\lambda, \xi) = 1 + \lambda \xi + \left(\frac{a \xi}{R} \right)^2, \quad H(\lambda, \xi_1, \xi_2) = 1 + \lambda \xi_1 + \left(\frac{a \xi_1 \xi_2}{R} \right)^2. \quad (3.2.2)$$

The coordinates are the same as those used in [4], and their ranges are

$$1 < x < -1, \quad -\infty < y < -1. \quad (3.2.3)$$

Recall that in this set of coordinates, ψ parametrizes an S^1 and (x, ϕ) an S^2 , with $x \sim \cos \theta$, where θ is the polar angle, and ϕ the azimuthal angle. From (3.2.1) one sees that the black ring is rotating along the azimuthal direction of the S^2 , while the previously known neutral black ring [1] rotates along the ψ direction of the S^1 .

Throughout this paper we assume that

$$\frac{2a}{R} < \lambda < 1 + \frac{a^2}{R^2} \quad (3.2.4)$$

where the upper bound guarantees that both g_{xx} and $g_{\phi\phi}$ are positive and hence there are no closed time-like curves [9, 10]. As we will show later on, the lower bound is required for there to be a horizon. Setting $a = 0$ in (3.2.1) gives the static ring first found in [16].

As in other black ring solutions, R corresponds roughly to the radius of the black ring, whereas a is a new parameter with dimensions of length which is related to the angular momentum, as will be seen from the expressions of the conserved charges. In fact, in section 3.3 it will become manifest that a is roughly equivalent to the rotation parameter of the four dimensional Kerr black hole.

In order to avoid a conical singularity at $x = -1$ and $y = -1$, we have to identify the periods of the angular coordinates ψ and ϕ according to

$$\Delta\phi = \Delta\psi = \frac{2\pi}{\sqrt{1 - \lambda + a^2/R^2}}. \quad (3.2.5)$$

Also, in order for the orbits of ∂_ϕ to close off smoothly at $x = 1$ we must require

$$\Delta\phi = \frac{2\pi}{\sqrt{1 + \lambda + a^2/R^2}}, \quad (3.2.6)$$

which cannot be satisfied at the same time as (3.2.5) for nonzero λ . For the asymptotically flat ring, eq. (3.2.5) holds and there is a conically singular disk at $x = 1$ supporting the ring. From now on we will stick to this case.

Asymptotic infinity is at $x, y \rightarrow -1$. Now, defining canonical angular variables,

$$\tilde{\psi} = \frac{2\pi}{\Delta\psi} \psi, \quad \tilde{\phi} = \frac{2\pi}{\Delta\phi} \phi, \quad (3.2.7)$$

with $\Delta\psi$ and $\Delta\phi$ given in (3.2.5), and performing the coordinate transformation

$$\zeta = R \frac{\sqrt{2(-1-y)}}{x-y}, \quad \eta = R \frac{\sqrt{2(1+x)}}{x-y}, \quad (3.2.8)$$

the metric (3.2.1) takes the manifestly flat form

$$ds^2 \sim -dt^2 + \zeta^2 d\tilde{\psi}^2 + d\zeta^2 + \eta^2 d\tilde{\phi}^2 + d\eta^2. \quad (3.2.9)$$

The ADM mass and angular momentum are given by

$$\begin{aligned} M &= \frac{3\pi R^2}{4G} \frac{\lambda}{1 - \lambda + a^2/R^2}, \\ J_\phi &= -\frac{\pi R^2}{G} \frac{\lambda a}{(1 - \lambda + a^2/R^2)^{3/2}}. \end{aligned} \quad (3.2.10)$$

Again, for $a = 0$ the angular momentum vanishes and the mass coincides with that of the static ring given in [4].

The Killing vector field ∂_t becomes spacelike at the least negative zero of $H(\lambda, y, x)$, y_e ; this point defines the ergosurface. Similarly, the zeros of $F(\lambda, y)$

$$y_i = \frac{-\lambda - \sqrt{\lambda^2 - 4a^2/R^2}}{2a^2/R^2}, \quad y_h = \frac{-\lambda + \sqrt{\lambda^2 - 4a^2/R^2}}{2a^2/R^2}, \quad (3.2.11)$$

determine the locations of the inner and outer horizons, respectively. In the limit $a \rightarrow 0$, we have $y_h \rightarrow -1/\lambda$, which is the location of the horizon for the static black ring, and $y_i \rightarrow -\infty$, for which the static ring has a curvature singularity. Both the ergosurface and the horizon have topology $S^1 \times S^2$, but we will come back to this point in the next subsection. Moreover, it can be checked that the Killing vector field ∂_ϕ remains spacelike throughout the ergoregion, which is the region $y_h < y < y_e$. As in the four-dimensional Kerr black hole, in the ϕ -spinning ring the ergoregion coincides with the horizon at the poles of the S^2 ($x = \pm 1$). Finally, from (3.2.11) it is clear that we must impose $\lambda > 2a/R$ so as to have a horizon.

3.2.2 Horizon geometry

The Kretschmann invariant is finite at $y = y_i, y_h$, but blows up when $H(\lambda, x, y) = 0$. To find coordinates that are good on the horizon we proceed as in [9, 10] and define $\bar{y} = y - y_h$. Consider the following change of coordinates

$$dt = dv + \frac{A}{\bar{y}} d\bar{y}, \quad d\phi = d\chi + \frac{B}{\bar{y}} d\bar{y}, \quad (3.2.12)$$

where A and B are determined by requiring that the solution in the coordinates $(v, x, \bar{y}, \psi, \chi)$ is analytic at $\bar{y} = 0$. When we expand near $\bar{y} = 0$, we find that $g_{v\bar{y}}$ and $g_{\chi\bar{y}}$ diverge as $1/\bar{y}$. Both divergences can be removed by imposing $A = -B \lambda R^2 / (a y_h)$. This choice also removes the $1/\bar{y}^2$ -divergence in $g_{\bar{y}\bar{y}}$. Then $g_{\bar{y}\bar{y}}$ diverges as $1/\bar{y}$ unless we impose

$$B^2 = \frac{y_h^2 a^2 / R^2}{(y_h^2 - 1)(\lambda^2 - 4a^2/R^2)}. \quad (3.2.13)$$

The metric is now analytic at $\bar{y} = 0$, and its form on a spatial cross-section of the horizon is rather simple:

$$ds_{\text{H}}^2 = \frac{R^2}{(x - y_h)^2} \left[(y_h^2 - 1)F(\lambda, x) d\psi^2 + \frac{H(\lambda, x, y_h)}{(1 - x^2)F(\lambda, x)} dx^2 \right] + (1 - x^2) \frac{\lambda^2 R^2}{H(\lambda, x, y_h)} d\chi^2. \quad (3.2.14)$$

This expression shows that the horizon is regular, up to the conical singularity, and that its topology is indeed $S^1 \times S^2$, where the S^1 is parametrized by the angle ψ and the S^2 by (x, ϕ) . Using (3.2.14) we can compute the horizon area

$$\mathcal{A}_{\text{H}} = \frac{8\pi^2 R^3 \lambda}{(1 - \lambda + a^2/R^2)\sqrt{y_h^2 - 1}}. \quad (3.2.15)$$

For $a = 0$ this agrees with the $\nu = \lambda$ limit of the ψ -rotating black ring.

The Killing vector field

$$\partial_v - \frac{a y_h}{\lambda R^2} \partial_\chi \quad (3.2.16)$$

becomes null at $y = y_h$, and hence we can identify it as the null generator of the horizon. The angular velocity of the horizon and the temperature are given by

$$\Omega_\phi = -\frac{\sqrt{1 - \lambda + a^2/R^2} [\lambda - \sqrt{\lambda^2 - 4a^2/R^2}]}{2\lambda a}, \quad (3.2.17)$$

$$T_{\text{BH}} = \frac{\sqrt{(\lambda^2 - 4a^2/R^2)(y_h^2 - 1)}}{4\pi R \lambda}. \quad (3.2.18)$$

Using these results, a straightforward calculation shows that the ϕ -spinning ring also satisfies a Smarr relation,

$$M = \frac{3}{2} \left[\frac{1}{4G} \mathcal{A}_{\text{H}} T_{\text{BH}} + \Omega_\phi J_\phi \right]. \quad (3.2.19)$$

This relationship holds in the case in which the solution is asymptotically flat, that is, the conical defect is inside the ring.

3.3 Limits

3.3.1 Infinite radius limit

In order to obtain the infinite radius limit we have to send $R \rightarrow \infty$ while keeping fixed

$$r = -\frac{R}{y}, \quad \cos \theta = x, \quad 2M = \lambda R, \quad \eta = R\psi. \quad (3.3.1)$$

We then have

$$F(\lambda, x) \rightarrow 1, \quad F(\lambda, y) \rightarrow \Delta/r^2, \quad H(\lambda, x, y) \rightarrow \Sigma/r^2, \quad H(\lambda, y, x) \rightarrow (\Sigma - 2Mr)/r^2, \quad (3.3.2)$$

with $\Delta = r^2 - 2Mr + a^2$ and $\Sigma = r^2 + a^2 \cos^2 \theta$. In this limit the metric (3.2.1) becomes the Kerr black string,

$$ds^2 = - \left(1 - \frac{2Mr}{\Sigma}\right) \left[dt + \frac{2Mr}{\Sigma - 2Mr} a \sin^2 \theta d\phi\right]^2 + \Sigma \left(\frac{dr^2}{\Delta} + d\theta^2\right) + \frac{\Delta \sin^2 \theta}{1 - \frac{2Mr}{\Sigma}} d\phi^2 + d\eta^2. \quad (3.3.3)$$

In this limit, the singularity encountered at $H(\lambda, x, y) = 0$ becomes the ring-like singularity of the Kerr spacetime.

3.3.2 Myers-Perry black hole limit

In order to recover the five-dimensional MP black hole with rotation in the ϕ direction from (3.2.1), we have to take a limit similar to the one described in [4]. We define new parameters

$$m = \frac{2(R^2 + a^2)}{1 + a^2/R^2 - \lambda}, \quad \alpha^2 = \frac{4a^2}{1 + a^2/R^2 - \lambda}, \quad (3.3.4)$$

such that they remain finite as $\lambda \rightarrow 1 + a^2/R^2$, $R \rightarrow 0$ and $a \rightarrow 0$. Furthermore, we perform a change of coordinates $(x, y) \rightarrow (r, \theta)$

$$x = -1 + \frac{2R^2 \cos^2 \theta}{r^2 - (m - \alpha^2) \cos^2 \theta}, \quad (3.3.5)$$

$$y = -1 - \frac{2R^2 \sin^2 \theta}{r^2 - (m - \alpha^2) \cos^2 \theta}, \quad (3.3.6)$$

and rescale ψ and ϕ so that in this limit they have the canonical periodicity 2π ,

$$(\tilde{\phi}, \tilde{\psi}) = \sqrt{\frac{2(R^2 + a^2)}{m}} (\phi, \psi). \quad (3.3.7)$$

Then, we obtain the MP black hole with rotation in ϕ

$$ds^2 = - \left(1 - \frac{m}{\Sigma}\right) \left(dt - \frac{m\alpha \cos^2 \theta}{\Sigma - m} d\tilde{\phi}\right)^2 + \Sigma \left(\frac{dr^2}{\Delta} + d\theta^2\right) + \frac{\Delta \cos^2 \theta}{1 - \frac{m}{\Sigma}} d\tilde{\phi}^2 + r^2 \sin^2 \theta d\tilde{\psi}^2, \quad (3.3.8)$$

where

$$\Delta = r^2 - m + \alpha^2, \quad \Sigma = r^2 + \alpha^2 \sin^2 \theta. \quad (3.3.9)$$

3.4 Conclusions

In this paper we have presented a black ring solution with rotation on the plane orthogonal to the ring. Although our solution has a horizon with topology $S^1 \times S^2$, there is a conical singularity inside the ring that prevents it from collapsing. This solution should be an intermediate step towards a more general black ring with two independent angular momenta.

Using (3.2.1) as a seed solution and following the procedure outlined in [5, 13], one can construct the black ring with a rotating S^2 and carrying F1-P charges. In this charged black ring, which we do not present here, the conical singularity persists except in the extremal supersymmetric limit. In this limit, in which the angular momentum disappears, we find a configuration which can be interpreted as a continuous distribution of straight F1-P strings on a circle. We do not expect to be able to add more than two charges to the solution (3.2.1) without generating Dirac-Misner strings for the reasons discussed in [5]. Furthermore, it would be very interesting to construct the ϕ -spinning ring carrying dipole charges. Even then, we do not expect to be able to remove the conical singularity since the dipole charges typically increase the tension of the string [4]. Adding three charges to this more general solution should result in a charged ϕ -ring with dipole charges. We hope our results are of help towards a classification of the possible black holes of five-dimensional vacuum gravity. This is also a step in the construction of the seed solution that would generate the 9-parameter non-supersymmetric black rings conjectured in [13] (and, further, the larger family conjectured in [14]), that should describe thermal excitations of three-charge supertubes. We hope to tackle these problems in the future.

Acknowledgments

We thank Henriette Elvang and Roberto Emparan for their invaluable help in this work. We also thank Harvey Reall for useful comments and discussions. This work was supported by a FI scholarship from Generalitat de Catalunya, CICYT FPA2004-04582-C02-02 and European Comission RTN program under contract MRTN-CT-2004-005104.

Bibliography

- [1] R. Emparan and H. S. Reall, “A rotating black ring in five dimensions,” *Phys. Rev. Lett.* **88**, 101101 (2002) [arXiv:hep-th/0110260].
- [2] W. Israel, “Event Horizons In Static Vacuum Space-Times,” *Phys. Rev.* **164**, 1776 (1967).
B. Carter, *Phys. Rev. Lett.* **26** 331 (1971).
D. C. Robinson, *Phys. Rev. Lett.* **34** 905 (1975).
S. W. Hawking, “Black Holes In General Relativity,” *Commun. Math. Phys.* **25**, 152 (1972).
- [3] R. C. Myers and M. J. Perry, “Black Holes In Higher Dimensional Space-Times,” *Annals Phys.* **172** (1986) 304.
- [4] R. Emparan, “Rotating circular strings, and infinite non-uniqueness of black rings,” *JHEP* **0403**, 064 (2004) [arXiv:hep-th/0402149].
- [5] H. Elvang and R. Emparan, “Black rings, supertubes, and a stringy resolution of black hole non-uniqueness,” *JHEP* **0311**, 035 (2003) [arXiv:hep-th/0310008].
- [6] H. Elvang, “A charged rotating black ring,” *Phys. Rev. D* **68**, 124016 (2003) [arXiv:hep-th/0305247].
- [7] D. Mateos and P. K. Townsend, “Supertubes,” *Phys. Rev. Lett.* **87**, 011602 (2001) [arXiv:hep-th/0103030].
- [8] R. Emparan, D. Mateos and P. K. Townsend, “Supergravity supertubes,” *JHEP* **0107** (2001) 011 [arXiv:hep-th/0106012].
- [9] H. Elvang, R. Emparan, D. Mateos and H. S. Reall, “A supersymmetric black ring,” *Phys. Rev. Lett.* **93**, 211302 (2004) [arXiv:hep-th/0407065].
- [10] H. Elvang, R. Emparan, D. Mateos and H. S. Reall, “Supersymmetric black rings and three-charge supertubes,” [arXiv:hep-th/0408120].
- [11] I. Bena and N. P. Warner, “One ring to rule them all ... and in the darkness bind them?,” [arXiv:hep-th/0408106].
- [12] J. P. Gauntlett and J. B. Gutowski, “General concentric black rings,” *Phys. Rev. D* **71** (2005) 045002 [arXiv:hep-th/0408122].
- [13] H. Elvang, R. Emparan and P. Figueras, “Non-supersymmetric black rings as thermally excited supertubes,” *JHEP* **0502** (2005) 031 [arXiv:hep-th/0412130].

- [14] F. Larsen, “Entropy of Thermally Excited Black Rings,” [arXiv:hep-th/0505152].
- [15] T. Mishima and H. Iguchi, “New axisymmetric stationary solutions of five-dimensional vacuum Einstein equations with asymptotic flatness,” [arXiv:hep-th/0504018].
- [16] R. Emparan and H. S. Reall, “Generalized Weyl solutions,” Phys. Rev. D **65** (2002) 084025 [arXiv:hep-th/0110258].
- [17] K. Hong and E. Teo, “A new form of the C-metric,” Class. Quant. Grav. **20** (2003) 3269 [arXiv:gr-qc/0305089].

Chapter 4

On a class of 4D Kähler bases and AdS_5 supersymmetric Black Holes

Pau Figueras,^a Carlos A R Herdeiro,^b Filipe Paccetti Correia^b

^a *Departament de Física Fonamental, and
C.E.R. en Astrofísica, Física de Partícules i Cosmologia,
Universitat de Barcelona, Diagonal 647, E-08028 Barcelona, Spain*

^b *Centro de Física do Porto,
Faculdade de Ciências da Universidade do Porto,
Rua do Campo Alegre, 687, 4169-007 Porto, Portugal*

pfigueras@ffn.ub.es, crherdei@fc.up.pt,
paccetti@fc.up.pt

ABSTRACT

We construct a class of toric Kähler manifolds, \mathcal{M}_4 , of real dimension four, a subset of which corresponds to the Kähler bases of all known 5D asymptotically AdS_5 supersymmetric black-holes. In a certain limit, these Kähler spaces take the form of cones over Sasaki spaces, which, in turn, are fibrations over toric manifolds of real dimension two. The metric on \mathcal{M}_4 is completely determined by a single function $H(x)$, which is the conformal factor of the two dimensional space. We study the solutions of minimal five dimensional gauged supergravity having this class of Kähler spaces as base and show that in order to generate a five dimensional solution $H(x)$ must obey a simple sixth order differential equation. We discuss the solutions in detail, which include all known asymptotically AdS_5 black holes as well as other spacetimes with non-compact horizons. Moreover we find an infinite number of supersymmetric deformations of these spacetimes with less spatial isometries than the base space. These deformations vanish at the horizon, but become relevant asymptotically.

4.1 Introduction

The study of supersymmetric, asymptotically AdS_5 , black hole type solutions has been a topic of interest over the last few years. The reason is, at least, two-folded.

On the one hand, the *AdS/CFT* correspondence [1, 2, 3] is best understood in the case of *AdS₅/CFT₄*, the latter corresponding to $\mathcal{N} = 4$, $D = 4$, Super Yang Mills Theory. Thus, the discovery of explicit black hole solutions on the gravity side, especially supersymmetric ones [4, 5, 6, 7, 8, 9], opened the possibility of a microscopic description of their entropy using the correspondence. This programme, which has been pursued by several authors [10, 11, 12, 13], has not been fully successful yet. One of the puzzling points is that there is a discrepancy in the counting of parameters of the most general supersymmetric black hole solution known and the number of parameters expected from the CFT side. The most general supersymmetric black holes known are characterised by 5 parameters, two angular momenta and three charges, which are not all independent. In particular this leads to an ambiguity in writing an entropy formula, since one can take different choices for the 4 independent parameters (see [13] for a promising proposal for such formula). From the CFT viewpoint one would, in principle, expect these 5 parameters to be independent. Thus it would be interesting to further explore more general black hole solutions, which were also conjectured to exist in [11].

On the other hand, five dimensional gravity has provided the first examples of black hole non-uniqueness. The most striking example is the existence of black holes with different horizon topologies and with the same conserved charges [14]. This discrete non-uniqueness was first found for non-supersymmetric, asymptotically flat configurations, and was generalised to supersymmetric solutions of non-minimal five dimensional supergravity in [15, 16, 17]. In the minimal supergravity case, however, these solutions reduce to a three parameter family, where uniqueness holds. The physical parameters are charge, and the two independent angular momenta of $SO(4)$, J_1 and J_2 . Interestingly, there is no region of physical parameters where black rings and black holes with a (topologically) spherical horizon may coexist [18], which legitimates the string theory counting of black hole micro-states for the BMPV black hole performed in [19]. In fact, a topologically spherical horizon requires $J_1 = J_2$, whereas supersymmetric black rings require $J_1 \neq J_2$. By contrast, in the asymptotically *AdS* case, there are already supersymmetric black holes with a (topologically) spherical horizon and two independent angular momenta; moreover, no supersymmetric black ring is yet known. The spectrum of supersymmetric black holes is, therefore, quite different in the *AdS* case, and some black objects, like black rings, are yet to be found. Again we conclude it would be interesting to further explore the spectrum of asymptotically *AdS₅* black objects.

Another suggestion of a richer structure for asymptotically *AdS* black holes is the inability to derive the general form for the geometry and topology of the horizon [5] using the approach originally taken in [20] for the asymptotically flat space case. For the *AdS* case this method used the construction of [21] for general supersymmetric solutions of five dimensional gauged supergravity, together with the assumption of the existence of physical horizon, which must be a Killing horizon. Whereas in the asymptotically flat case, the resulting equations could be integrated to obtain two theorems concerning the geometry of the solution near the horizon and the horizon itself [20], in the asymptotically *AdS₅* case, no general answer could be obtained and only some special solutions were found [5].

In this paper, therefore, we will pursue a different programme. Our starting point will be the general equations for the timelike supersymmetric solutions of $D = 5$ minimal gauged SUGRA found by Gauntlett and Gutowski [21]. Their construction starts off with a choice of a four dimensional Kähler manifold - the *base* space -; once chosen the base, the full solution follows from a series of constraint equations that involve the base. We will make some assumptions for the base in order for the full solution to be compatible with having a finite size horizon. These assumptions lead to the conclusion that the base should behave, near the putative horizon, as

a Kähler cone. In the most general framework, this Kähler cone admits a single $U(1)$ action. However we will focus on a special case in which the base admits a $U(1)^2$ action, which is more tractable. Any Kähler cone is a cone over a three dimensional Sasaki space which is always a fibration over a two dimensional space. For the case under study herein, the four dimensional base is described by a single function which is the conformal factor of the two dimensional space. The full base (i.e. not only close to the putative horizon) is obtained by a plausible ansatz for the Kähler potential, and it turns out to be a simple generalisation of the Kähler base studied earlier in [8].

Our assumptions are not fully general, and, in particular, we expect a possible asymptotically AdS_5 black ring not to obey them, as explained in section 4.5.2. Still, our assumptions are sufficiently general to give i) all known black hole solutions in a simple way and somewhat suggestive that these are all the possible asymptotically AdS_5 solutions with a (topologically) spherical horizon and a $U(1)^2$ spatial isometry group; ii) some other previously known and unknown solutions with non-compact or singular horizons; iii) an infinite set of new solutions which correspond to deformations of the known black hole solutions (or even AdS_5). Such deformations vanish at the horizon but become relevant asymptotically. These latter solutions have some hitherto unexplored features: the five dimensional spacetime has less spatial isometries than the base and, if one writes AdS_5 in coordinates that reduce to static coordinates in the absence of deformations, these solutions are time dependent.

It was argued in [21] that any Kähler base should originate a five dimensional solution of $D = 5$ minimal gauged SUGRA. However, one other result of our analysis is that some Kähler bases do not originate any five dimensional solution. Also, we give explicit examples of Kähler bases with a finite number of parameters (that could be even zero) which originate an infinite parameter family of five dimensional solutions, a fact already anticipated, albeit not explored, in [21].

This paper is organised as follows. In section 4.2 we review the formalism in [21] for supersymmetric solutions of minimal gauged supergravity in $D = 5$. In section 4.3 we make some remarks about co-homogeneity two Kähler manifolds, which will be at the heart of the present paper. In section 4.4, we note that all known supersymmetric AdS_5 black holes are defined by a simple two variable function and use this fact to recover the base space used in their construction. In section 4.5 we introduce our assumptions for the Kähler base, and derive that it behaves as a Kähler cone near the putative horizon. We also make a few remarks about the geometrical structure of toric Kähler cones and suggest why black rings should violate our assumptions. In section 4.6 we study the five dimensional solutions in the near horizon limit, and in section 4.7 we extend the base space away from the horizon and obtain the equations for the most general five dimensional solutions possessing this base space. The solutions are analysed in section 4.8. We draw our conclusions in section 4.9. The appendix makes some comments on non-toric Kähler cones, which might be of relevance for finding black holes solutions with less isometries.

4.2 Supersymmetric solutions of $D = 5$ SUGRA

The bosonic part of the minimal gauged supergravity theory in five spacetime dimensions is described by the action

$$\mathcal{S} = \frac{1}{16\pi G_5} \int d^5x \sqrt{-\det g_{\mu\nu}} \left(R + 12g^2 - F^2 - \frac{2}{3\sqrt{3}} \tilde{\epsilon}^{\alpha\beta\gamma\mu\nu} F_{\alpha\beta} F_{\gamma\mu} A_\nu \right), \quad (4.2.1)$$

where $F = dA$, $\tilde{\epsilon}$ is the Levi-Civita tensor, related to the Levi-Civita tensor density by $\tilde{\epsilon}^{\alpha\beta\gamma\delta\mu} = \epsilon^{\alpha\beta\gamma\delta\mu} / \sqrt{-\det g_{\mu\nu}}$, g is the inverse of the AdS radius and we use a ‘mostly plus’ signature. The equations of motion are

$$R_{\mu\nu} + (4g^2)g_{\mu\nu} = 2 \left(F_{\mu\alpha}F_{\nu}^{\alpha} - \frac{1}{6}g_{\mu\nu}F^2 \right), \quad D_{\mu}F^{\mu\nu} = \frac{1}{2\sqrt{3}}\tilde{\epsilon}^{\alpha\beta\gamma\mu\nu}F_{\alpha\beta}F_{\gamma\mu}. \quad (4.2.2)$$

In [21], it was shown that all supersymmetric solutions of this theory, with a timelike Killing vector field, can be casted in the form

$$ds^2 = -f^2(dt + w)^2 + f^{-1}ds_B^2(\mathcal{K}), \quad (4.2.3)$$

where the 4d base $ds_B^2(\mathcal{K})$ is Kähler and f, w do not depend on t . Moreover, supersymmetry imposes three additional constraints. Defining the self-dual and anti-self-dual parts of fdw by

$$G^{\pm} = \frac{1}{2}f(dw \pm \star_4 dw), \quad (4.2.4)$$

where \star_4 is the Hodge dual on the Kähler base, these constraints read

$$f = -\frac{24g^2}{R}, \quad (4.2.5)$$

$$G^+ = -\frac{1}{2g} \left[\mathcal{R} + \frac{R}{4}J \right], \quad (4.2.6)$$

and

$$\nabla^2 f^{-1} = \frac{2}{9}G^{+mn}G_{mn}^+ - gf^{-1}G^{-mn}J_{mn} - 8g^2f^{-2}. \quad (4.2.7)$$

Given a certain Kähler base, we can determine its Kähler form J (which is anti-self-dual, i.e. $\star_4 J = -J$, according to the conventions of [21]), Ricci form \mathcal{R} and Ricci scalar R . From these quantities one computes f^{-1} , which is proportional to the latter, and G^+ . Then, from (4.2.7) we determine G^- . In general, G^- may be determined only up to some arbitrary functions from this equation. Combining the most general form allowed for G^- with the form for G^+ determined from (4.2.6), we require, from (4.2.4), that

$$d(f^{-1}(G^+ + G^-)) = 0. \quad (4.2.8)$$

The resulting constraints mean that *not all Kähler bases may give rise to a non-trivial five dimensional solution*. For the family of Kähler bases we study in this paper, this is shown explicitly in section 4.7. If G^- can be chosen such that the last equation has a solution, then we can choose an ω that satisfies (4.2.4) and find a non-trivial five dimensional solution. The solution is completed by the Maxwell field strength which is given by

$$F = \frac{\sqrt{3}}{2}d[f(dt + w)] - \frac{G^+}{\sqrt{3}} + \sqrt{3}gf^{-1}J. \quad (4.2.9)$$

These solutions preserve at least 1/4 of the supersymmetry of the full theory, i.e two real supercharges.

4.3 Co-homogeneity two Kähler bases

Let us consider four (real) dimensions Kähler manifolds defined by a Kähler potential of the type

$$\mathcal{K} = \mathcal{K} (|z_1|^2, |z_2|^2) , \quad (4.3.1)$$

that is, \mathcal{K} depends on the complex coordinates z_i only through their squared moduli. The resulting Kähler base is *toric* and has co-homogeneity two or lower. There are at least two Killing vector fields on the base space, which are not necessarily Killing vector fields of the five dimensional spacetime too, as we will illustrate in section 4.8. Note, however, that it can be shown that requiring the five dimensional spacetime to admit two $U(1)$ actions implies that the base space should also admit such actions.¹ Thus, the above Kähler potential is the most generic one that can lead to axisymmetric black holes (or black rings) with two azimuthal Killing vector fields. As a particular case of a Kähler base that can be written in this way let us recall Bergmann space, with the Kähler potential

$$\mathcal{K}_{Berg} = -\frac{1}{2g^2} \ln (1 - |z_1|^2 - |z_2|^2) . \quad (4.3.2)$$

Bergmann space is the base space of empty AdS₅ [21].

Let us set our notations and conventions. The metric is obtained from the second derivatives of \mathcal{K} ($\mathcal{K}_{i\bar{j}} = \partial^2 \mathcal{K} / \partial z^i \partial \bar{z}^{\bar{j}}$), ($i, j = 1, 2$),

$$ds^2 = \mathcal{K}_{i\bar{j}} dz^i \otimes d\bar{z}^{\bar{j}} + \mathcal{K}_{\bar{i}j} d\bar{z}^{\bar{i}} \otimes dz^j , \quad (4.3.3)$$

while the Kähler 2-form is

$$J = -i \mathcal{K}_{i\bar{j}} dz^i \wedge d\bar{z}^{\bar{j}} , \quad (4.3.4)$$

and the Ricci-form reads

$$\mathcal{R} = -i (\partial_i \partial_{\bar{j}} \ln \det(\mathcal{K})) dz^i \wedge d\bar{z}^{\bar{j}} . \quad (4.3.5)$$

An useful choice of *real* coordinates is (see, e.g. [22])

$$z^i = \exp(x^i + i\phi^i) , \quad (4.3.6)$$

which leads to a suggestive form of the metric (we denote $G_{ij} \equiv \partial_{x^i} \partial_{x^j} G$, $G_i \equiv \partial_{x^i} G$)

$$ds^2 = G_{ij}(x) (dx^i dx^j + d\phi^i d\phi^j) . \quad (4.3.7)$$

Here, the *two*-dimensional metric G_{ij} is the Hessian of $G(x^1, x^2) = \frac{1}{2} \mathcal{K}(x^1, x^2)$. Due to this relation, we will often refer to $G(x^1, x^2)$ as the “potential”; $G(x^1, x^2)$ also determines the Kähler form

$$J = -d (G_i(x) d\phi^i) , \quad (4.3.8)$$

and the Ricci-form

$$\mathcal{R} = -\frac{1}{2} d [(\partial_i \ln \det(G)) d\phi^i] . \quad (4.3.9)$$

Finally, one can also show that the curvature scalar reads

$$R = -G^{ij} \partial_i \partial_j \ln \det(G) . \quad (4.3.10)$$

¹One assumes that these two isometries commute with the supersymmetry Killing vector field. We thank Harvey Reall for this comment.

4.4 All known AdS_5 BH's of minimal gauged SUGRA

We will now observe that all co-homogeneity two (or less) Kähler bases, can be described by a family of two-dimensional *curved surfaces* parameterised by $(\exp(x^1), \exp(x^2))$. This includes, of course, the bases of all presently known supersymmetric asymptotically anti-de Sitter black holes of five-dimensional minimal gauged supergravity. The most general family was first presented in [7], but the base space was first computed in [8]. We believe that these curved surfaces might help building some intuition to search for more general solutions, including black rings.

To be concrete, let us introduce $\rho(x^1, x^2)$, related to the ‘‘potential’’ G as

$$G = -\frac{1}{4g^2} \ln(1 - g^2 \rho^2) . \quad (4.4.1)$$

We claim that, to obtain the solutions of [8], $\rho(x^1, x^2)$ must be determined by

$$\frac{e^{2x^1}}{(g\rho)^{2A_1^2}} + \frac{e^{2x^2}}{(g\rho)^{2A_2^2}} = 1 , \quad (4.4.2)$$

where $1 \geq A_1^2, A_2^2 > 0$. For $A_1^2 = A_2^2 = 1$ we recover Bergmann space, for $A_1^2 = A_2^2 \neq 1$ we retrieve the co-homogeneity one base metric of the Gutowski-Reall black hole [4], otherwise we have the base space of the AdS_5 black holes with two independent angular momenta, first found in [7] - see the figures: The function $\rho^2(|z_1|^2, |z_2|^2)$ is plotted for the Bergmann manifold, Gutowski-Reall and Chong et al. black holes. ρ varies from 0 to 1. For the first two cases $\rho = const$ surfaces are circles, but for the third case they are ellipses, which, however become a circle as $\rho \rightarrow 1$. This is a manifestation of the asymptotic AdS_5 structure of the most general black holes.

To prove the above claim, we make a coordinate transformation $(x^1, x^2) \rightarrow (\sigma, \theta)$ to the coordinates used in [8]:

$$e^{2x^1} = (\tanh g\sigma)^{2A_1^2} \frac{A_2^2 \sin^2 \theta}{A_1^2 \cos^2 \theta + A_2^2 \sin^2 \theta} , \quad (4.4.3)$$

$$e^{2x^2} = (\tanh g\sigma)^{2A_2^2} \frac{A_1^2 \cos^2 \theta}{A_1^2 \cos^2 \theta + A_2^2 \sin^2 \theta} . \quad (4.4.4)$$

From (4.4.2) we then see that our function ρ is related to the coordinate σ used in [8] by $g\rho = \tanh g\sigma$ and, from (4.4.1), we find that the function G is, in terms of (σ, θ) coordinates,

$$G = \frac{1}{4g^2} \ln \cosh^2 g\sigma . \quad (4.4.5)$$

It can be now explicitly checked, using (4.3.7), that this potential generates the base space used in [8], which is

$$ds_B^2 = d\sigma^2 + \frac{\sinh^2 g\sigma}{g^2} \left(\frac{d\theta^2}{\Delta_\theta} + \Delta_\theta \sin^2 \theta \cos^2 \theta \left[\frac{d\phi^1}{A_1^2} - \frac{d\phi^2}{A_2^2} \right]^2 \right) + \frac{\sinh^2 g\sigma \cosh^2 g\sigma}{g^2} \left[\frac{\sin^2 \theta}{A_1^2} d\phi^1 + \frac{\cos^2 \theta}{A_2^2} d\phi^2 \right]^2 , \quad (4.4.6)$$

with

$$\Delta_\theta = A_1^2 \cos^2 \theta + A_2^2 \sin^2 \theta . \quad (4.4.7)$$

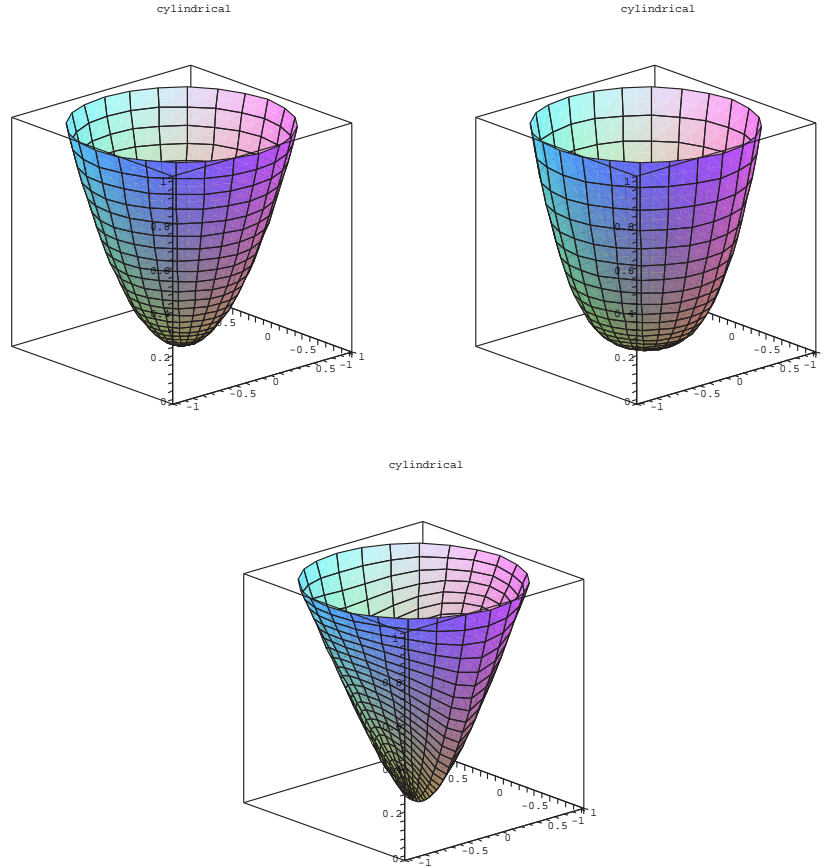


Figure 4.1: Function $\rho^2(|z_1|^2, |z_2|^2)$ for the Bergmann manifold, Gutowski-Reall and Chong et al. black holes, respectively. ρ varies from 0 to 1. For the first two cases $\rho = \text{const}$ surfaces are circles, but for the third case they are ellipses, which, however become a circle as $\rho \rightarrow 1$. This is a manifestation of the asymptotic AdS_5 structure of the most general black holes.

4.5 The conical structure of the Black Hole solutions

In the following we make some remarks on the structure of the Kähler base \mathcal{K} near a possible horizon. We will present some arguments for \mathcal{K} being a Kähler cone in the near horizon limit, for a certain class of solutions which includes all known black holes. We will state our assumptions as we exhibit the argument.

- 1) Near the horizon we assume that f^{-1} should behave as

$$f^{-1} = \frac{c(\theta)}{\rho^2}, \quad (4.5.1)$$

where the coordinate ρ vanishes at the horizon. We allow the numerator to depend on some *other* coordinate, θ . Note that the coordinates (ρ, θ) are functions of (x^1, x^2) . From (4.2.5), we conclude that the base space will therefore have a curvature singularity at $\rho = 0$. Note that ρ in equation (4.5.1), is going to be the same as the ρ in (4.4.1) up to the transformation explained after equation (4.5.6).

- 2) In view of the singularity of the base, we impose that $f^{-1}ds_B^2(\mathcal{K})$ has a finite proper size along the angular directions ϕ^i , in the $\rho = 0$ limit. Writing the metric in the form (4.3.7)

and using (ρ, θ) coordinates instead of (x^1, x^2) , this means that the metric coefficients for the ϕ coordinates should scale as ρ^2 :

$$ds_B^2(\mathcal{K}) \simeq ds_2^2(\rho, \theta) + \rho^2 f_{ij}(\theta) d\phi^i d\phi^j. \quad (4.5.2)$$

The idea underlying this assumption is to allow a finite size horizon. However, one could conceive achieving a finite size horizon not by requiring $f^{-1}ds_B^2(\mathcal{K})$ to have a finite proper size along the angular directions, but rather by requiring the *full metric* (4.2.3) to have a finite size along such directions. We will comment in subsection 4.5.2 that, in principle, this is exactly what happens for a possible asymptotically AdS_5 black ring, which will, therefore, be excluded from our analysis.

Our assumptions and the equations (4.5.1) and (4.5.2) that followed, allow us to infer some more properties of the near-horizon geometry, from the way different objects transform under the following scaling:

$$\rho \rightarrow \lambda\rho, \quad \theta \rightarrow \theta.$$

From (4.5.2) and (4.3.7) we see that

$$G_{ij} \rightarrow \lambda^2 G_{ij}, \quad (4.5.3)$$

while from (4.5.1) and (4.2.5), we see that

$$R \rightarrow R/\lambda^2,$$

which are the behaviours to be expected from the proper size of angular coordinates and curvatures, respectively. It follows that $G^{ij} \rightarrow G^{ij}/\lambda^2$ and consequently, using (4.3.10),

$$x^i \rightarrow x^i + f^{(i)}(\lambda), \quad (4.5.4)$$

where $f^{(i)}(\lambda)$, $i = 1, 2$, are arbitrary functions. Note that this is exactly what happens for the known black holes, as can be seen from (4.4.3)-(4.4.4). Together with (4.5.3) this last equation implies that the ‘‘potential’’ transforms as

$$G(x) \rightarrow \lambda^2 G(x) + f^{(3)}(\lambda). \quad (4.5.5)$$

From this equation, we conclude that in terms of the (ρ, θ) coordinates, the ‘‘potential’’ G must be proportional to ρ^2 , up to an additive constant which is pure Kähler gauge. Thus,

$$G(\rho, \theta) = \chi(\theta)\rho^2. \quad (4.5.6)$$

We will redefine ρ in such a way as to have $\chi(\theta) = 1/4$. This amounts to a redefinition of the function $c(\theta)$ in eq.(4.5.1). We thus have

$$G = \frac{\rho^2}{4}. \quad (4.5.7)$$

Note that this coincides with the definition of ρ given by equation (4.4.1) in the limit of small ρ^2 . Therefore, we might suspect that all Kähler bases obeying our requirements are described by a two dimensional surface similar to (4.4.2). To see this is indeed the case note that under two consecutive re-scalings, (4.5.4) implies that

$$f^{(i)}(\lambda_1\lambda_2) = f^{(i)}(\lambda_1) + f^{(i)}(\lambda_2). \quad (4.5.8)$$

Therefore

$$f^{(i)}(\lambda) = A_i^2 \ln \lambda , \quad (4.5.9)$$

$i = 1, 2$, and we take $A_i^2 \geq 0$, which can always be achieved by a holomorphic coordinate change, $z^i \rightarrow 1/z^i$. Thus, the combination

$$t^i \equiv \frac{2x^i}{A_i^2} - 2 \ln \rho ,$$

is inert under scalings and therefore in (ρ, θ) coordinates $t^i = t^i(\theta)$ is a function of θ only. The function ρ (and hence G) can thus be defined as a $2d$ surface in \mathbb{R}^3 ,

$$F(t^1, t^2) = 0 , \quad (4.5.10)$$

which is scaling independent. The case of all known black holes (4.4.2) is given by the curve $F = e^{A_1^2 t^1} + e^{A_2^2 t^2} - 1$, even away from the horizon.

We shall now determine the family of Kähler bases which obey our requirements together with one last technical assumption:

3) We impose the convexity of the “potential” G . Since at $x^i = -\infty$, $G_{ij} = G_k = 0$, it follows that (at least near the horizon) we have

$$\frac{\partial G}{\partial x^i} \geq 0 . \quad (4.5.11)$$

A small computation, using (4.5.10), then shows that

$$\frac{\partial G}{\partial x^i} = \frac{\rho^2 \gamma_i(\theta)}{2} , \quad \text{where} \quad \gamma_i = \frac{1}{A_i^2} \frac{\partial F}{\partial t^i} \frac{1}{\sum_i \frac{\partial F}{\partial t^i}} . \quad (4.5.12)$$

This expression makes clear that $\gamma_i \geq 0$ and that $\sum A_i^2 \gamma_i = 1$. It is thus sensible to define the θ coordinate through

$$\gamma_1 = \frac{\sin^2 \theta}{A_1^2} , \quad \gamma_2 = \frac{\cos^2 \theta}{A_2^2} . \quad (4.5.13)$$

We now have all the information required to compute the generic form of the Kähler bases consistent with our assumptions, which we shall do in $(\rho, \theta, \phi^1, \phi^2)$ coordinates. The $g_{\rho\rho}$, $g_{\theta\rho}$ and $g_{\theta\theta}$ components are

$$g_{\rho\rho} = \frac{\partial x^i}{\partial \rho} \frac{\partial x^j}{\partial \rho} G_{ij} = \frac{\partial^2 G}{\partial \rho^2} - \frac{\partial^2 x^i}{\partial \rho^2} G_i = 1 , \quad (4.5.14)$$

$$g_{\theta\rho} = \frac{\partial^2 G}{\partial \rho \partial \theta} - \frac{\partial^2 x^i}{\partial \rho \partial \theta} G_i = 0 . \quad (4.5.15)$$

$$g_{\theta\theta} = -\frac{\partial^2 x^i}{\partial \theta^2} G_i \equiv \frac{\rho^2}{\Delta_\theta} , \quad (4.5.16)$$

which defines an arbitrary function of θ , Δ_θ . This arbitrary function can also be re-expressed as

$$\Delta_\theta = \frac{2A_1^2}{\sin 2\theta} \frac{\partial \theta}{\partial x^1} . \quad (4.5.17)$$

We can now conclude that our Kähler base is a cone:

$$ds_B^2 = d\rho^2 + \rho^2 ds_3^2, \quad (4.5.18)$$

where the metric of the $d = 3$ Sasakian space is, using also (4.5.2)

$$ds_3^2 = \frac{d\theta^2}{\Delta_\theta} + f_{ij}(\theta) d\phi^i d\phi^j. \quad (4.5.19)$$

The 2-dimensional metric $f_{ij}(\theta)$ is now determined by

$$f_{ij}(\theta) = \frac{G_{ij}}{\rho^2} = \gamma_i(\theta)\gamma_j(\theta) + \frac{1}{2} \frac{\partial\gamma_i}{\partial\theta} \frac{\partial\theta}{\partial x^j}. \quad (4.5.20)$$

Noting that the symmetry between i and j determines that $\sum_i A_i^2 \partial_i \theta = 0$, we find that

$$f_{ij}(\theta) d\phi^i d\phi^j = \left[\frac{\sin^2 \theta}{A_1^2} d\phi^1 + \frac{\cos^2 \theta}{A_2^2} d\phi^2 \right]^2 + \sin \theta \cos \theta \frac{\partial\theta}{\partial x^1} A_1^2 \left[\frac{d\phi^1}{A_1^2} - \frac{d\phi^2}{A_2^2} \right]^2. \quad (4.5.21)$$

Thus, we can finally write our Kähler base as

$$ds_B^2 = d\rho^2 + \rho^2 \left\{ \frac{d\theta^2}{\Delta_\theta} + \left[\frac{\sin^2 \theta}{A_1^2} d\phi^1 + \frac{\cos^2 \theta}{A_2^2} d\phi^2 \right]^2 + \Delta_\theta \sin^2 \theta \cos^2 \theta \left[\frac{d\phi^1}{A_1^2} - \frac{d\phi^2}{A_2^2} \right]^2 \right\}. \quad (4.5.22)$$

Our family of Kähler bases is fully determined up to just *one arbitrary function* of θ , Δ_θ . In the known black hole solutions this function is

$$\Delta_\theta = A_1^2 \cos^2 \theta + A_2^2 \sin^2 \theta. \quad (4.5.23)$$

4.5.1 Sasakian space as a fibration over Kähler manifold

Taking the result from the previous section that the near horizon geometry of the base is a Kähler cone, we can obtain the metric (4.5.22) in a different way, which naturally introduces a very useful new coordinate.

It is a general result (see e.g. [23]) that a $(2n+1)$ -dimensional Sasakian space can be written as a fibration over a $2n$ -dimensional Kähler space. In the case at hand $n = 1$ and the base is two dimensional. To see this we note that the Kähler potential of a four dimensional Kähler cone can be written as

$$\mathcal{K} = |z|^2 e^{2\hat{\mathcal{K}}(w, \bar{w})} \equiv \frac{1}{2} \rho^2. \quad (4.5.24)$$

A tedious calculation then shows that

$$ds_3^2 = \eta \otimes \eta + 2\hat{\mathcal{K}}_{w\bar{w}} dw d\bar{w}, \quad (4.5.25)$$

where the 1-form η is

$$\eta = d\phi - i(\hat{\mathcal{K}}_w dw - \hat{\mathcal{K}}_{\bar{w}} d\bar{w}), \quad (4.5.26)$$

and ϕ is defined through $z = \rho e^{-\hat{\mathcal{K}}} e^{i\phi} / \sqrt{2}$. This also shows that the Kähler form J_2 of the two dimensional base is related to η as

$$J_2 = -\frac{1}{2} d\eta. \quad (4.5.27)$$

Furthermore, for the Kähler cone one finds that

$$J = -\frac{1}{2}d[\rho^2\eta] . \quad (4.5.28)$$

Two additional suggestive relations between the geometry of the four dimensional Kähler cone and the two dimensional base are

$$\mathcal{R} = 4J_2 + \mathcal{R}_2 , \quad (4.5.29)$$

and

$$R = \frac{R_2 - 8}{\rho^2} , \quad (4.5.30)$$

where \mathcal{R}_2 and R_2 are the Ricci form and the Ricci scalar of the 2d base.

From the present perspective, the cones we presented above are obtained by requiring the 2d base space to be toric. We comment on non-toric cones in appendix 4.A. Being toric means (see section 4.3) that the metric of the base can be written as

$$ds_2^2 = G_2''(y)[dy^2 + d\bar{\psi}^2] , \quad (4.5.31)$$

where $2G_2(y)$ is the Kähler potential written in suitable coordinates, while J_2 is

$$J_2 = -d(G_2'd\bar{\psi}) . \quad (4.5.32)$$

We can change to symplectic coordinates (x, ψ) defined through

$$x = 2G_2'(y), \quad \psi = 2\bar{\psi} . \quad (4.5.33)$$

With $H(x) \equiv G_2''(y(x))$, we rewrite the metric as

$$ds_2^2 = \frac{dx^2}{4H(x)} + \frac{1}{4}H(x)d\psi^2 , \quad (4.5.34)$$

and the Kähler form as

$$J_2 = -\frac{1}{4}d(xd\psi) . \quad (4.5.35)$$

This then shows that $2\eta = d\phi + xd\psi$ and the 3d Sasakian space is

$$ds_3^2 = \frac{dx^2}{4H(x)} + \frac{1}{4}H(x)d\psi^2 + \frac{1}{4}(d\phi + xd\psi)^2 . \quad (4.5.36)$$

Setting

$$x = \cos 2\theta , \quad \frac{H(x)}{1-x^2} = \Delta_\theta , \quad (4.5.37)$$

$$\psi = \frac{\phi^2}{A_2^2} - \frac{\phi^1}{A_1^2} , \quad \phi = \frac{\phi^2}{A_2^2} + \frac{\phi^1}{A_1^2} ,$$

and using (4.5.18) we retrieve the cone (4.5.22). Note that $H(x)$ can be faced as the conformal factor of the two dimensional space (4.5.34).

4.5.2 A comment on supersymmetric black rings

Consider the asymptotically flat supersymmetric black ring found in [18]. The metric still has the form (4.2.3), but where the base space is now a hyper-Kähler manifold, in fact flat space \mathbb{R}^4 conveniently written in ring type coordinates:

$$ds_B^2(\mathbb{R}^4) = \frac{R^2}{(x-y)^2} \left[\frac{dy^2}{y^2-1} + (y^2-1)d\psi^2 + \frac{dx^2}{1-x^2} + (1-x^2)d\phi^2 \right]. \quad (4.5.38)$$

The remaining metric functions are

$$f^{-1} = 1 + \frac{Q-q^2}{2R^2}(x-y) - \frac{q^2}{4R^2}(x^2-y^2), \quad (4.5.39)$$

and $\omega = \omega_\psi(x,y)d\psi + \omega_\phi(x,y)d\phi$, where

$$\begin{aligned} \omega_\phi &= -\frac{q}{8R^2}(1-x^2) [3Q - q^2(3+x+y)], \\ \omega_\psi &= \frac{3}{2}q(1+y) + \frac{q}{8R^2}(1-y^2) [3Q - q^2(3+x+y)]. \end{aligned} \quad (4.5.40)$$

The solution has three independent parameters: R , Q and q which are all positive constants; the latter two are proportional to the net charge and to the local dipole charge of the ring, respectively. The coordinate ranges are $-1 \leq x \leq 1$, $-\infty \leq y \leq -1$, $0 \leq \phi, \psi \leq 2\pi$, and the near horizon limit of this solution is obtained by taking $y \rightarrow -\infty$. Taking this limit and introducing simultaneously the coordinates ρ, θ as $\rho = -R/y$ and $\theta = \arccos x$, we have

$$f^{-1} = \frac{q^2}{4\rho^2} + \mathcal{O}\left(\frac{1}{\rho}\right), \quad (4.5.41)$$

and

$$ds_B^2(\mathbb{R}^4) \simeq d\rho^2 + \rho^2 d\theta^2 + R^2 d\psi^2 + \rho^2 \sin^2 \theta d\phi^2. \quad (4.5.42)$$

It is simple to see that this ring solution violates the assumptions we have made above to derive (4.5.22). Indeed, although assumption 1) is obeyed, as can be checked by comparing (4.5.41) with (4.5.1), assumption 2) is clearly violated, since ψ and ϕ are the ϕ^i coordinates of the previous section and the base space (4.5.42) does not fall in the form (4.5.2), due to the scaling of the metric coefficient for ψ , $g_{\psi\psi}^B$. This coefficient is constant and therefore $f^{-1}g_{\psi\psi}^B$ diverges on the horizon. So, $\rho = 0$ represents, in the base space, a circle of radius R , which becomes a singular surface for the metric $f^{-1}ds_B^2$, but becomes again a regular surface, in fact a ring shaped horizon, in the full metric. This is made possible by a cancellation of the divergent terms coming from both $f^{-1}ds_B^2$ and $f^2\omega_\psi^2$. Explicitly, expanding the metric functions to second order

$$f^{-1} = \frac{q^2}{4\rho^2} \left(1 + \frac{2(Q-q^2)}{q^2 R} \rho + \mathcal{O}(\rho^2) \right), \quad \omega_\psi = -\frac{q^3 R}{8\rho^3} - \frac{q}{8\rho^2} [3Q - (3 + \sin \theta)q^2] + \mathcal{O}\left(\frac{1}{\rho}\right), \quad (4.5.43)$$

as well as the metric coefficient $g_{\psi\psi}^B$ of the base space

$$g_{\psi\psi}^B = R^2 - 2 \sin \theta R \rho + \mathcal{O}(\rho^2), \quad (4.5.44)$$

we find that

$$g_{\psi\psi} = -f^2 \omega_\psi^2 + f^{-1} g_{\psi\psi}^B = \mathcal{O}(\rho^0). \quad (4.5.45)$$

Indeed, the divergent terms ($\mathcal{O}(1/\rho)$ and $\mathcal{O}(1/\rho^2)$) all cancel leaving only finite contributions to the proper size of the ψ direction.

We expect therefore, that the base space of a possible AdS₅ black ring will not approach a Kähler cone near the horizon.

4.6 5D Near horizon solutions from Kähler cones

Our goal is now to determine what are the constraints on Δ_θ such that, given the base (4.5.22), a non-trivial five dimensional solution exists. Even though it has been claimed [21, 4] that a five dimensional solution always exists for any four dimensional Kähler base, we will show that this is not the case. In this section we obtain a constraint equation on Δ_θ , choosing a special ansatz for the 2-form G^- and hence the five dimensional solution. In the next section we will show that this constraint still holds even if we take the most generic form for the five dimensional solution.

The Ricci scalar for (4.5.22) is

$$R = -\frac{1}{\rho^2} \left[8(1 - \Delta_\theta) + \frac{1}{\sin^3 2\theta} \frac{d}{d\theta} \left(\sin^3 2\theta \frac{d\Delta_\theta}{d\theta} \right) \right] \equiv -\frac{24g^2}{\rho^2} c(\theta) , \quad (4.6.1)$$

which defines the function $c(\theta)$ and determines the metric function f , via (4.2.5), to be

$$f^{-1} = \frac{c(\theta)}{\rho^2} . \quad (4.6.2)$$

The Ricci form (4.3.9) can be found to be

$$\mathcal{R}_{ij} = \frac{R}{2} \left(G_{ij} - \frac{4}{\rho^2} G_i G_j \right) = \frac{R}{2} \rho^2 \Delta_\theta \sin^2 \theta \cos^2 \theta \frac{(-1)^{i+j}}{A_i^2 A_j^2} . \quad (4.6.3)$$

This can then be used to determine G^+ ,

$$G_{ij}^+ = -\frac{R}{4g} \left(\frac{1}{2} G_{ij} - \frac{4}{\rho^2} G_i G_j \right) , \quad (4.6.4)$$

and $(G^+)^2$,

$$G^{+ij} G_{ij}^+ = \frac{R^2}{16g^2} . \quad (4.6.5)$$

Plugging this back in (4.2.7) we find that

$$\nabla^2 f^{-1} = -g f^{-1} G^{-mn} J_{mn} . \quad (4.6.6)$$

Recall that according to our assumptions, this equation is valid only at the horizon; moreover, it only determines the components of G^- ‘parallel’ to the Kähler form; thus we will have some undetermined functions in the general form allowed by this equation for G^- . To write such an ansatz for G^- , it is useful to introduce the following set of 1-forms

$$\mathbf{e}^\rho = d\rho , \quad \mathbf{e}^\theta = \rho \frac{d\theta}{\sqrt{\Delta_\theta}} ,$$

$$\mathbf{e}^1 = \rho \left[\frac{\sin^2 \theta}{A_1^2} d\phi^1 + \frac{\cos^2 \theta}{A_2^2} d\phi^2 \right], \quad \mathbf{e}^2 = \rho \sqrt{\Delta_\theta} \sin \theta \cos \theta \left[\frac{d\phi^1}{A_1^2} - \frac{d\phi^2}{A_2^2} \right]. \quad (4.6.7)$$

In this basis, the Kähler form and G^+ read

$$J = -(\mathbf{e}^\rho \wedge \mathbf{e}^1 + \mathbf{e}^\theta \wedge \mathbf{e}^2), \quad (4.6.8)$$

$$G^+ = -3gf^{-1}(\mathbf{e}^\rho \wedge \mathbf{e}^1 - \mathbf{e}^\theta \wedge \mathbf{e}^2). \quad (4.6.9)$$

Furthermore, the 4d Hodge star product is chosen to act as $\star(\mathbf{e}^\rho \wedge \mathbf{e}^1) = -\mathbf{e}^\theta \wedge \mathbf{e}^2$ and $\star(\mathbf{e}^\rho \wedge \mathbf{e}^2) = \mathbf{e}^\theta \wedge \mathbf{e}^1$. The most general form for G^- (in leading order in ρ) that allows the symmetries of the base space to be present in the five dimensional spacetime is

$$G^- = \frac{l(\theta)}{\rho^2}(\mathbf{e}^\rho \wedge \mathbf{e}^1 + \mathbf{e}^\theta \wedge \mathbf{e}^2) + \frac{n(\theta)}{\rho^2}(\mathbf{e}^\rho \wedge \mathbf{e}^2 - \mathbf{e}^\theta \wedge \mathbf{e}^1) + \frac{m(\theta)}{\rho^b}(\mathbf{e}^1 \wedge \mathbf{e}^2 - \mathbf{e}^\theta \wedge \mathbf{e}^\rho); \quad (4.6.10)$$

we will come back to this point in section 4.7. It follows that

$$G^{-nm} J_{nm} = 2 \star (\star G^- \wedge J) = -\frac{4l(\theta)}{\rho^2}. \quad (4.6.11)$$

From (4.6.6) and (4.6.2) we can determine $l(\theta)$ in terms of the derivatives of $c(\theta)$,

$$l(\theta) = \frac{1}{4g c(\theta) \sin \theta \cos \theta} \frac{d}{d\theta} \left(\Delta_\theta \sin \theta \cos \theta \frac{dc(\theta)}{d\theta} \right), \quad (4.6.12)$$

where $c(\theta)$ was defined in (4.6.1) to be

$$c(\theta) = \frac{1}{24g^2} \left[8(1 - \Delta_\theta) + \frac{1}{\sin^3 2\theta} \frac{d}{d\theta} \left(\sin^3 2\theta \frac{d\Delta_\theta}{d\theta} \right) \right]. \quad (4.6.13)$$

Combining the expressions for f , G^+ and G^- given by (4.6.2), (4.6.9) and (4.6.10) we compute dw via

$$dw = f^{-1}(G^+ + G^-); \quad (4.6.14)$$

the requirement that this form is closed (4.2.8) determines $b = 0$ and the following three conditions:

$$m(\theta) = \frac{\text{constant}}{\sin \theta \cos \theta \sqrt{\Delta_\theta} c(\theta)}, \quad (4.6.15)$$

$$n(\theta) = \frac{\sqrt{\Delta_\theta}}{2c(\theta)} \frac{d}{d\theta} [c(\theta) (l(\theta) - 3g c(\theta))], \quad (4.6.16)$$

so that both $m(\theta)$ and $n(\theta)$ are completely determined in terms of $c(\theta)$; finally

$$\frac{d}{d\theta} \left(\Delta_\theta \sin \theta \cos \theta \frac{d}{d\theta} \left[c(\theta) \left(l(\theta) - 3g c(\theta) + \frac{2}{g} \right) \right] \right) = 0. \quad (4.6.17)$$

This is a 6th order ODE on Δ_θ which is considerably involved. But it can be reduced to a much simpler form in the following way. Introduce new independent and dependent variables x and $H(x)$, as in (4.5.37). Then we have

$$c(x) = \frac{2 + H''}{6g^2}, \quad l(x) = \frac{1}{g(2 + H'')} (HH''')', \quad (4.6.18)$$

where 'primes' denote x derivatives. After some manipulations (4.6.17) becomes the remarkably simpler equation

$$(H^2 H'''')'' = 0 . \quad (4.6.19)$$

This equation can be now reduced to a fourth order equation:

$$H^2 H'''' = \alpha x + \beta . \quad (4.6.20)$$

For $\alpha = \beta = 0$, the general solution is a cubic polynomial in x :

$$H(x) = a_0 + a_1 x + a_2 x^2 + a_3 x^3 . \quad (4.6.21)$$

All known black holes fall in this class of solutions. We will analyse the solutions of (4.6.19) in section 4.8, after showing, in section 4.7, that this equation, which was obtained from a near horizon analysis, still arises in a full spacetime analysis. Moreover, we will show in section 4.7 that, even taking the most general form for G^- , the constraint (4.6.19) still holds. Thus, as claimed above, not all Kähler bases will provide a non-trivial five dimensional solution.

4.7 Full spacetime analysis

As we are searching for asymptotically AdS₅ BH solutions, it is sensible to find Kähler bases which for $\rho \rightarrow 0$ reduce to the above discussed cones while for $\rho \rightarrow 1$ approach Bergmann space. It is not difficult to find that

$$G = -\frac{1}{4g^2} \ln(1 - g^2 \rho^2) , \quad (4.7.1)$$

where ρ is defined exactly as in (4.5.10), fulfils these criteria, as we will now see. Note that one could discuss forms of $G = G(\rho^2)$ other than (4.7.1) but we will not pursue such analysis in this paper.²

We easily find that

$$G_i = \frac{1}{2} \frac{\rho^2}{1 - g^2 \rho^2} \gamma_i(\theta) , \quad (4.7.2)$$

and

$$G_{ij} = \frac{\rho^2}{1 - g^2 \rho^2} \left[\frac{\gamma_i(\theta) \gamma_j(\theta)}{1 - g^2 \rho^2} + \frac{1}{2} \frac{\partial \gamma_i}{\partial \theta} \frac{\partial \theta}{\partial x^j} \right] . \quad (4.7.3)$$

With $\rho^2 = \tanh^2 g\sigma/g^2$, we can now write the metric of the full Kähler base as

$$ds_B^2 = d\sigma^2 + \frac{\sinh^2 g\sigma}{g^2} \left(\frac{d\theta^2}{\Delta_\theta} + \Delta_\theta \sin^2 \theta \cos^2 \theta \left[\frac{d\phi^1}{A_1^2} - \frac{d\phi^2}{A_2^2} \right]^2 \right) + \frac{\sinh^2 g\sigma \cosh^2 g\sigma}{g^2} \left[\frac{\sin^2 \theta}{A_1^2} d\phi^1 + \frac{\cos^2 \theta}{A_2^2} d\phi^2 \right]^2 , \quad (4.7.4)$$

while the Kähler 2-form reads

$$J = -d \left[\frac{\sinh^2 g\sigma}{2g^2} \left(\frac{\sin^2 \theta d\phi^1}{A_1^2} + \frac{\cos^2 \theta d\phi^2}{A_2^2} \right) \right] . \quad (4.7.5)$$

²A class of Kähler-Einstein spaces that differ from Bergmann space in the form of the function $G(\rho)$ was studied in [24].

Notice that these spaces include the Kähler bases discussed in [8] (which correspond to take Δ_θ given by (4.4.7)). Remarkably, we obtained them from making some mild assumptions on the behaviour of the metric near a singularity. Finally, we record the Ricci form for later convenience:

$$\mathcal{R} = -\frac{3}{2}d \left\{ \sinh^2 g\sigma(d\phi + x d\psi) + \frac{x}{3} \left[2 - A_1^2 - A_2^2 - \frac{3}{2}(A_1^2 - A_2^2)x \right] d\psi \right\} \quad (4.7.6)$$

For $g\sigma \rightarrow 0$ the bases reduce to the above discussed Kähler cones as they should. To see that in the $g\sigma \rightarrow \infty$ limit these spaces have negative constant scalar curvature note that

$$R = -24g^2 \left[1 + \frac{g^2 c(\theta)}{\sinh^2 g\sigma} \right], \quad (4.7.7)$$

where $c(\theta)$ was defined in (4.6.1).

We now show that a full spacetime analysis of the supersymmetry constraints leads to the same equation (4.6.19) as the near horizon analysis. It is simpler to do the analysis in x coordinates, in terms of which the Kähler base (4.7.4) can be written

$$ds_B^2 = d\sigma^2 + \frac{\sinh^2 g\sigma}{4g^2} \left(\frac{dx^2}{H(x)} + H(x)d\psi^2 + \cosh^2 g\sigma(d\phi + x d\psi)^2 \right). \quad (4.7.8)$$

This is a remarkably simple form for the base space. In particular notice that the known black holes simply correspond to taking $H(x)$ to be a cubic polynomial. In terms of the obvious tetrad

$$\begin{aligned} \mathbf{e}^\sigma &= d\sigma, & \mathbf{e}^x &= \frac{\sinh g\sigma}{2g} \frac{dx}{\sqrt{H}}, \\ \mathbf{e}^\psi &= \frac{\sinh g\sigma}{2g} \sqrt{H} d\psi, & \mathbf{e}^\phi &= \frac{\sinh g\sigma \cosh g\sigma}{2g} (d\phi + x d\psi), \end{aligned} \quad (4.7.9)$$

the Kähler form and Ricci form are

$$J = -(\mathbf{e}^\sigma \wedge \mathbf{e}^\phi + \mathbf{e}^x \wedge \mathbf{e}^\psi), \quad (4.7.10)$$

$$\mathcal{R} = 12g^2(1 - f^{-1})\mathbf{e}^x \wedge \mathbf{e}^\psi - 6g^2(\mathbf{e}^\sigma \wedge \mathbf{e}^\phi + \mathbf{e}^x \wedge \mathbf{e}^\psi), \quad (4.7.11)$$

whereas the function f , computed from the Ricci scalar is

$$f^{-1} = 1 + \frac{2 + H''}{6 \sinh^2 g\sigma}. \quad (4.7.12)$$

It is curious to notice that the Kähler form does not depend on $H(x)$ and hence, it is the same for the whole family of bases. The Ricci form, of course, depends on $H(x)$. From (4.2.6) it follows that

$$G^+ = 3g(1 - f^{-1})(\mathbf{e}^\sigma \wedge \mathbf{e}^\phi - \mathbf{e}^x \wedge \mathbf{e}^\psi). \quad (4.7.13)$$

From (4.2.7) we determine the part of G^- parallel to J . Thus, the most general expression for G^- is

$$G^- = l(x, \sigma)(\mathbf{e}^\sigma \wedge \mathbf{e}^\phi + \mathbf{e}^x \wedge \mathbf{e}^\psi) + fN(\sigma, x, \phi, \psi)(\mathbf{e}^\sigma \wedge \mathbf{e}^\psi - \mathbf{e}^x \wedge \mathbf{e}^\phi) + fM(\sigma, x, \phi, \psi)(\mathbf{e}^\sigma \wedge \mathbf{e}^x - \mathbf{e}^\phi \wedge \mathbf{e}^\psi), \quad (4.7.14)$$

where

$$l(x, \sigma) = gf \left(2 + \frac{2 + H''}{2 \sinh^2 g\sigma} + \frac{(H'''H)'}{6 \sinh^4 g\sigma} \right), \quad (4.7.15)$$

and N, M are arbitrary functions of their arguments. Since we are taking the most generic form of G^- , the restriction given by the integrability conditions on $H(x)$, if any, indeed restrict the Kähler bases that can generate five dimensional solutions. These integrability conditions can be computed from (4.2.8) and yield the following four equations:

$$\partial_\phi M = \frac{\partial_\sigma(N \cosh g\sigma \sinh^2 g\sigma)}{2g \sinh g\sigma} + \frac{g\sqrt{H} \cosh g\sigma}{6 \sinh^4 g\sigma} \left[(H'''H)' - \frac{(2 + H'')^2}{2} \right]'; \quad (4.7.16)$$

$$\frac{(\partial_\psi - x\partial_\phi)M}{\sqrt{H}} = \partial_x(N\sqrt{H}) + \frac{g \cosh g\sigma}{3 \sinh^4 g\sigma} (H'''H)'; \quad (4.7.17)$$

$$\partial_\phi N = -\frac{\partial_\sigma(M \cosh g\sigma \sinh^2 g\sigma)}{2g \sinh g\sigma}; \quad (4.7.18)$$

$$\frac{(\partial_\psi - x\partial_\phi)N}{\sqrt{H}} = -\partial_x(M\sqrt{H}). \quad (4.7.19)$$

Define the new dependent variables

$$\tilde{M}(\sigma, x, \phi, \psi) \equiv \cosh g\sigma \sinh^2 g\sigma M(\sigma, x, \phi, \psi), \quad (4.7.20)$$

$$\tilde{N}(\sigma, x, \phi, \psi) \equiv \cosh g\sigma \sinh^2 g\sigma N(\sigma, x, \phi, \psi) - \frac{g\sqrt{H}}{6 \sinh^2 g\sigma} \left[(H'''H)' - \frac{(2 + H'')^2}{2} \right]', \quad (4.7.21)$$

and the new independent variable

$$u \equiv 4g \int \frac{d\sigma}{\sinh 2g\sigma} = -4\text{arcth}(e^{-2g\sigma}), \quad (4.7.22)$$

where u varies from $u = -\infty$ at a possible horizon and $u = 0$ at spatial infinity; one finds, from (4.7.16) and (4.7.18), that the function \tilde{M} and \tilde{N} are harmonic in the u, ϕ plane:

$$(\partial_\phi^2 + \partial_u^2) \tilde{M} = 0, \quad (\partial_\phi^2 + \partial_u^2) \tilde{N} = 0. \quad (4.7.23)$$

The fact that we find harmonic equations is reminiscent of other “linearisations” that arise in supersymmetric solutions, namely the ones that allow multi black hole spacetimes and indicate “no-force” configurations. In this case, this linearisation indicates, as we shall see below, the ability of superimposing in any background defined by a base with some $H(x)$, an infinite set of angular and radial deformations. It follows that

$$\tilde{M} = \sum_\alpha c_\alpha^M(x, \psi) \mathcal{H}_\alpha(u, \phi), \quad \tilde{N} = \sum_\alpha c_\alpha^N(x, \psi) \mathcal{H}_\alpha(u, \phi), \quad (4.7.24)$$

where $\{\mathcal{H}_\alpha\}$ is a basis of harmonic functions. Substituting (4.7.20) and (4.7.21) with (4.7.24) this expressions in (4.7.17), we find the integrability condition

$$(H''''H^2)'' = 6 \sinh^2 g\sigma \left\{ -\frac{(HH''''')'}{3} + \frac{1}{g} \sum_\alpha \left[\frac{\partial_\psi c_\alpha^M - x c_\alpha^M \partial_\phi}{\sqrt{H}} - \partial_x(\sqrt{H} c_\alpha^N) \right] \mathcal{H}_\alpha \right\}. \quad (4.7.25)$$

The left hand side does not depend on either σ or ϕ ; it depends only on x . Since \mathcal{H}_α is either a function of both σ and ϕ or it is linear in one of them, the right hand side is never a function solely of x . Thus both sides must vanish. We therefore recover condition (4.6.19), but we have the additional constraint:

$$\sum_{\alpha} \left[\frac{\partial_{\psi} c_{\alpha}^M - x c_{\alpha}^M \partial_{\phi}}{\sqrt{H}} - \partial_x (\sqrt{H} c_{\alpha}^N) \right] \mathcal{H}_{\alpha} = \frac{g(HH''''')}{3}. \quad (4.7.26)$$

The remaining integrability conditions give the following constraints for the coefficients c_{α}^N and c_{α}^M :

$$\sum_{\alpha} \left[\partial_x (\sqrt{H} c_{\alpha}^M) + \frac{\partial_{\psi} c_{\alpha}^N - x c_{\alpha}^N \partial_{\phi}}{\sqrt{H}} \right] \mathcal{H}_{\alpha} = 0, \quad (4.7.27)$$

$$\sum_{\alpha} (c_{\alpha}^M \partial_{\phi} - c_{\alpha}^N \partial_u) \mathcal{H}_{\alpha} = 0, \quad (4.7.28)$$

$$\sum_{\alpha} (c_{\alpha}^M \partial_u + c_{\alpha}^N \partial_{\phi}) \mathcal{H}_{\alpha} = 0. \quad (4.7.29)$$

Constraints (4.7.26)-(4.7.29), together with (4.6.19) define the most general solution for our family of Kähler bases. To get it explicitly, we have to integrate the equation for w (4.6.14), where G^+ and G^- are given in (4.7.13) and (4.7.14) respectively. As is well known, the field equations of the theory are all satisfied once we impose the equations of motion for the Maxwell field [4, 8]. Writing the field strength as

$$F = \frac{\sqrt{3}}{2} d[f(dt + w)] + \frac{1}{2g\sqrt{3}} \mathcal{R}, \quad (4.7.30)$$

and using (4.7.6), it is clear that once we have obtained a solution for w , we can easily find potentials such that $F = dA$ and hence the Bianchi identities are trivially satisfied. It can be similarly checked that the dynamical Maxwell equations are satisfied and hence all supergravity equations.

4.8 Solutions

As we mentioned before, the spatial isometries of the base need not be present in the full five dimensional solutions. We will split the analysis of the solutions into two cases: when the five dimensional solution has $U(1)^2$ spatial isometry and when it does not.

4.8.1 Solutions with $U(1)^2$ spatial isometry

The simplest way to obey constraints (4.7.26)-(4.7.29) is to take

$$c_0^N = -\frac{g\sqrt{H}H''''}{3} - \frac{C_1}{\sqrt{H}}, \quad (4.8.1)$$

and all remaining c_{α}^N and c_{α}^M zero, where $\mathcal{H}_0 = 1$ is the constant harmonic form. This ensures that w does not depend on ϕ or ψ . It follows that we can determine w explicitly even without

solving the remaining integrability condition (4.6.19). Start by noting that

$$\begin{aligned} \left[(H'''H)' - \frac{(2+H'')^2}{2} \right]' &= \frac{1}{H} \frac{d}{dx} (H^2 H''''') - 2H''' , \\ &= \frac{C_H}{H} - 2H''' , \end{aligned} \quad (4.8.2)$$

where, from (4.6.19), we have defined $(H^2 H''''')' = C_H$. C_H is a constant and vanishes for all known *AdS* black holes, since they will be described by cubic polynomials. It follows that $\tilde{M} = M = 0$ and, from (4.7.21),

$$N = -\frac{1}{\cosh(g\sigma) \sinh^2(g\sigma)} \left[\frac{g \cosh^2(g\sigma) \sqrt{H} H''''}{3 \sinh^2(g\sigma)} + \frac{1}{\sqrt{H}} \left(C_1 - \frac{g C_H}{6 \sinh^2(g\sigma)} \right) \right] . \quad (4.8.3)$$

Then, using (4.6.14) we find

$$w = w_\phi(x, \sigma) \mathbf{e}^\phi + w_\psi(x, \sigma) \mathbf{e}^\psi , \quad (4.8.4)$$

with

$$\begin{aligned} w_\phi &= \frac{1}{\sinh(2g\sigma)} \left\{ 2 \sinh^2(g\sigma) - \frac{1}{6 \sinh^2(g\sigma)} \left[(H'''H)' - \frac{(2+H'')^2}{2} \right] + \frac{1}{3} H'' \right. \\ &\quad \left. + \frac{C_1}{g} \int \frac{dx}{H} + C_\phi \right\} , \\ w_\psi &= \frac{1}{\sinh(g\sigma)} \left\{ \frac{\sqrt{H} H''''}{6 \sinh^2(g\sigma)} - \frac{1}{\sqrt{H}} \left[\frac{C_1}{g} \ln \tanh(g\sigma) + \frac{C_H}{6} \left(\frac{1}{2 \sinh^2(g\sigma)} + \ln \tanh(g\sigma) \right) \right] \right. \\ &\quad \left. + \frac{1}{2\sqrt{H}} \left[(2 - C_\phi)x + \frac{2}{3} H' - \frac{C_1}{g} \int dx \int \frac{dx}{H} + C_\psi \right] \right\} . \end{aligned} \quad (4.8.5)$$

Let us now specialise these expressions for concrete forms of $H(x)$.

$H(x)$ polynomial

Set $C_1 = 0$ in (4.8.1) and take $H(x)$ to be a cubic polynomial in x

$$H(x) = a_0 + a_1 x + a_2 x^2 + a_3 x^3 .$$

The integrability condition (4.6.19) is trivially satisfied since $H'''' = 0$. In this case, it is easy to see that

$$\left[(H'''H)' - \frac{(2+H'')^2}{2} \right]' = -2H''' , \quad (4.8.6)$$

and, from (4.7.21) and (4.8.1), we get

$$N(\sigma, x) = -\frac{g \cosh(g\sigma) \sqrt{H} H''''}{3 \sinh^4(g\sigma)} . \quad (4.8.7)$$

This family of solutions includes all known black holes of minimal gauged SUGRA (which form a two parameter family - plus cosmological constant) as well as solutions with non compact horizons, whose spatial sections are homogeneous *Nil* or $SL(2, \mathbb{R})$ manifolds. We can summarise the situation in the following way:

Cubic polynomial, $a_3 \neq 0$; Generically the spatial sections of the horizon are non-homogeneous spaces; with appropriate choice of roots it reduces to the supersymmetric AdS_5 black hole with two rotation parameters found in [7];

Quadratic polynomial $a_3 = 0$ and $a_2 \neq 0$; The compactness, and even existence, of an horizon depends crucially on the roots. For $a_2 < 0$, $a_0 > 0$ the spatial sections of the horizon are the homogeneous $SU(2)$ group manifold and the five dimensional spacetime is the Gutowski-Reall black hole [4], which reduces to empty AdS_5 when $a_2 = -1$, $a_0 = 1$. For $a_2 > 0$ the spatial sections of the horizon are the homogeneous $SL(2, \mathbb{R})$ group manifold.

Linear polynomial $a_3 = a_2 = 0$; For all linear polynomials (including constant ones) the spatial sections of the horizon are the Nil or Bianchi II group manifold.

All the solutions with quadratic polynomials were originally found in [4], but the ones with non-compact horizons were only studied in the near horizon limit. In our setup we can easily extend them to the whole spacetime.

To justify the statements above note that, for $H'''' = 0$,

$$\begin{aligned} w_\phi &= \frac{1}{\sinh(2g\sigma)} \left\{ 2 \sinh^2(g\sigma) - \frac{1}{6 \sinh^2(g\sigma)} \left[(H''''H)' - \frac{(2 + H'')^2}{2} \right] + \frac{1}{3} H'' + C_\phi \right\} , \\ w_\psi &= \frac{1}{\sqrt{H} \sinh(g\sigma)} \left\{ \frac{HH''''}{6 \sinh^2(g\sigma)} + \frac{1}{2} \left[(2 - C_\phi)x + \frac{2}{3} H' + C_\psi \right] \right\} , \end{aligned} \quad (4.8.8)$$

where C_ϕ and C_ψ are integration constants. In the near horizon limit ($\sigma \rightarrow 0$), therefore,

$$w = -\frac{1}{24g^3\sigma^2} \left[(H''''H)' - \frac{(2 + H'')^2}{2} \right] (d\phi + x d\psi) + \frac{HH''''}{12g^3\sigma^2} d\psi . \quad (4.8.9)$$

The metric on the spatial sections of the horizon is

$$ds^2 = -f^2 w^2 + f^{-1} ds_B^2|_{\sigma=0} .$$

For a generic **cubic** polynomial, the Ricci scalar of this metric depends on x ; thus it is a non-homogeneous space. Take the cubic polynomial to be

$$H(x) = \frac{1}{2}(1 - x^2) [A_1^2 + A_2^2 + (A_1^2 - A_2^2)x] , \quad (4.8.10)$$

where $-1 \leq x \leq 1$, and $1 > A_1^2, A_2^2 > 0$, which are the two parameters that characterise the solution. From (4.5.36), one can see that these are the required ranges so that the 3d Sasakian space consists of an S^1 fibration over a base S^2 . Hence, locally, the topology of the horizon is S^3 . In fact, we get the the near horizon geometry of the general supersymmetric AdS black holes of [7].

The full geometry is obtained as follows. For the 1-form w to be well-defined, the w_ψ component has to vanish on the two poles of the base S^2 , which implies that w_ψ should be of the form $w_\psi \sim (1 - x^2)$. Upon inserting (4.8.10) into (4.8.8) and imposing this condition, we can fix C_ϕ and C_ψ in terms of the parameters of the Kähler base,

$$C_\phi = 2 - \frac{2}{3}(A_1^2 + A_2^2) , \quad C_\psi = \frac{2}{3}(A_1^2 - A_2^2) . \quad (4.8.11)$$

Using these values of C_ϕ and C_ψ in (4.8.8), we obtain the final expression for w_ϕ and w_ψ :

$$w_\phi = \frac{1}{\sinh(2g\sigma)} \left\{ 2 \sinh^2(g\sigma) + 2 - (A_1^2 + A_2^2) - (A_1^2 - A_2^2)x \right. \\ \left. + \frac{1}{3 \sinh^2(g\sigma)} \left[1 - A_1^2 - A_2^2 + A_1^4 + A_2^4 - A_1^2 A_2^2 - 3(A_1^2 - A_2^2)x \right] \right\}, \quad (4.8.12)$$

$$w_\psi = \frac{(1-x^2)(A_1^2 - A_2^2)}{2\sqrt{H} \sinh(g\sigma)} \left\{ 1 - \frac{1}{2 \sinh^2(g\sigma)} \left[A_1^2 + A_2^2 + (A_1^2 - A_2^2)x \right] \right\}.$$

Using the relations given in (4.5.37) and setting

$$A_1^2 = \frac{\Xi_a}{g^2 \alpha^2}, \quad A_2^2 = \frac{\Xi_b}{g^2 \alpha^2}, \quad (4.8.13)$$

with $\Xi_a = 1 - a^2 g^2$, $\Xi_b = 1 - b^2 g^2$ and $\alpha^2 = g^{-2}(1 + ag + bg)^2$, one can readily check that our solution reproduces the general *AdS* supersymmetric black hole of [7], in the form presented in [8].³

A generic **quadratic** polynomial (i.e. $a_3 = 0$, $a_2 \neq 0$) can be taken in the form $H(x) = a_0 + a_2 x^2$. The horizon geometry is always homogeneous and can be written

$$ds_H^2 = \frac{1 + a_2}{12g^2} \left[\frac{dx^2}{a_0 + a_2 x^2} + (a_0 + a_2 x^2) d\psi^2 + \frac{1 - 3a_2}{4} (d\phi + x d\psi)^2 \right]. \quad (4.8.14)$$

- If $a_2 < 0$ (in which case the metric is positive definite for some x domain iff $a_0 > 0$), define new coordinates $\theta, \tilde{\phi}, \tilde{\psi}$ by

$$x = \sqrt{\frac{a_0}{|a_2|}} \cos \theta, \quad \psi = \frac{\tilde{\psi}}{\sqrt{a_0 |a_2|}}, \quad \phi = \frac{\tilde{\phi}}{|a_2|},$$

the metric on the spatial section of the horizon can be written as

$$ds_H^2 = \frac{|a_2|^{-1} - 1}{12g^2} \left(d\theta^2 + \sin^2 \theta d\tilde{\psi}^2 + \frac{|a_2|^{-1} + 3}{4} (d\tilde{\phi} + \cos \theta d\tilde{\psi})^2 \right).$$

This is a standard metric on $SU(2)$ corresponding to a squashed S^3 . It is the near horizon geometry of the Gutowski-Reall black hole [4] which has only one independent rotation, and is obtained from the generic black hole studied above taking $A_1^2 = A_2^2 = \frac{1}{4\alpha^2}$ in (4.8.12) and $(\phi, \psi) \rightarrow 4\alpha^2(\phi, \psi)$ (to make contact with the form given in [4]). Note that in the limit $a_2 \rightarrow 1$, corresponding to taking in the generic black hole $A_1^2 = A_2^2 = 1$, there is no horizon and we find empty *AdS*₅ (make $g = \frac{\chi}{2\sqrt{3}}$ to find the form given in [21]).

- If $a_2 > 0$, define new coordinates $y, \tilde{\phi}, \tilde{\psi}$ by

$$\text{For } \begin{cases} a_0 > 0 \\ a_0 = 0 \\ a_0 < 0 \end{cases}, \begin{cases} x = \sqrt{a_0/a_2} \sinh y \\ x = e^y \\ x = \sqrt{|a_0|/a_2} \cosh y \end{cases}, \begin{cases} \psi = \tilde{\psi}/\sqrt{a_0 a_2} \\ \psi = \tilde{\psi}/a_2 \\ \psi = \tilde{\psi}/\sqrt{|a_0| a_2} \end{cases}, \quad \phi = \frac{\tilde{\phi}}{a_2},$$

³To see that our solution matches that of [8] one has to set $\beta_2 = 4r_m^4/3$ in their paper, which is the correct value for the minimal theory. Also note that our solution is rotating in the opposite sense.

the metric on the spatial section of the horizon can be written as

$$ds_H^2 = \frac{a_2^{-1} + 1}{12g^2} \left(dy^2 + F_1(y)d\tilde{\psi}^2 + \frac{a_2^{-1} - 3}{4}(d\tilde{\phi} + F_2(y)d\tilde{\psi})^2 \right),$$

where

$$\text{For } \begin{cases} a_0 > 0 \\ a_0 = 0 \\ a_0 < 0 \end{cases}, \quad \begin{cases} F_1(y) = \cosh^2 y, & F_2(y) = \sinh y \\ F_1(y) = \exp 2y, & F_2(y) = \exp y \\ F_1(y) = \sinh^2 y, & F_2(y) = \cosh y \end{cases}.$$

These are all metrics on $SL(2, \mathbb{R})$. For instance, if one neglects the conformal factor and uses the triad

$$\mathbf{e}^1 = dy, \quad \mathbf{e}^2 = \sqrt{F_1(y)}d\tilde{\psi}, \quad \mathbf{e}^3 = \sqrt{\frac{a_2^{-1} - 3}{4}}(d\tilde{\phi} + F_2(y)d\tilde{\psi}),$$

one checks that for all cases the curvature in an orthonormal frame is

$$R_{(1)(2)(1)(2)} = -1 - \frac{3(a_2^{-1} - 3)}{16}, \quad R_{(1)(3)(1)(3)} = \frac{1}{4}, \quad R_{(2)(3)(2)(3)} = \frac{1}{4}.$$

A generic **linear** polynomial (i.e. $a_3 = a_2 = 0, a_1 \neq 0$) can be taken in the form $H(x) = a_1 x$. The horizon geometry is again homogeneous and can be written

$$ds_H^2 = \frac{1}{12g^2} \left[\frac{dx^2}{a_1 x} + a_1 x d\psi^2 + \frac{7}{4}(d\phi + x d\psi)^2 \right]. \quad (4.8.15)$$

Defining new coordinates

$$x = \frac{A^2 + B^2}{4}, \quad \psi = \frac{2 \arctan B/A}{\sqrt{a_1}}, \quad \phi = \frac{\tilde{\phi}}{2\sqrt{a_1}},$$

the horizon metric is rewritten

$$ds_H^2 = \frac{1}{12g^2} \left[dA^2 + dB^2 + \frac{7}{16a_1}(d\tilde{\phi} + AdB - BdA)^2 \right]. \quad (4.8.16)$$

the standard homogeneous metric on Nil, or the Heisenberg group. A similarly simple analysis shows that an equivalent metric is still obtained if $H(x) = a_0$. It is now very simple to get the metrics on the whole spacetime for the $SL(2, \mathbb{R})$ case and the Nil using (4.8.8).

$H(x)$ non-polynomial

Equation (4.6.19) has solutions which do not take a polynomial form when $\alpha \neq 0$ or $\beta \neq 0$ in (4.6.20). We were not able to find the general solution in this case. Nevertheless we can find some particular solutions, which have, generically, singular horizons.

For $\alpha = 0, \beta \neq 0$, a solution takes the form

$$H(x) = kx^{4/3}, \quad k \equiv \left(\frac{3^4 \beta}{40} \right)^{1/3}.$$

The one-form w can be written, in the near horizon limit, for this case

$$w = \frac{1}{12g^3\sigma^2} \left[\left(1 + \frac{2k}{9x^{2/3}} \right) (d\phi + xd\psi) - \frac{8k^2}{27x^{1/3}} d\psi \right].$$

It is now very simple to compute the metric on the spatial sections of the horizon. Its form is not particularly enlightening; but one verifies that the Ricci scalar depends on x and actually diverges for some positive value of $x = x_0$; for $x > x_0$, the metric is positive definite; the Ricci scalar decreases monotonically from $+\infty$ to a negative value beyond which it increases monotonically approaching zero at $x = +\infty$. The horizon has, therefore, a localised singularity, which makes the solution uninteresting.

For $\alpha \neq 0$, a solution takes the form

$$H(x) = k(\alpha x + \beta)^{5/3}, \quad k \equiv \left(\frac{3^4}{40\alpha^4} \right)^{1/3}.$$

The one-form w can be written, in the near horizon limit, for this case

$$w = \frac{1}{12g^3\sigma^2} \left[\left(1 + \frac{10k\alpha^2}{9(\alpha x + \beta)^{1/3}} + \frac{10k^2\alpha^4}{3^3(\alpha x + \beta)^{2/3}} \right) (d\phi + xd\psi) - \frac{10k^2\alpha^3}{3^3} (\alpha x + \beta)^{1/3} d\psi \right].$$

Again, it is simple to compute the metric on the spatial sections of the horizon and one finds a similar behaviour to the previous situation. The Ricci scalar depends on x and diverges for some positive value of $x = x_0$; for $x > x_0$, the metric is positive definite; the Ricci scalar decreases monotonically from $+\infty$ to a negative value beyond which it increases monotonically approaching a negative value at $x = +\infty$. Again, the horizon is singular.

4.8.2 Solutions with angular dependence

We now turn to solutions of equations (4.7.23) which exhibit ϕ dependence. We consider explicitly solutions for \tilde{M} only since solutions for \tilde{N} will follow in the same way.

Since ϕ parametrises an angular direction, we assume \tilde{M} to be a periodic function of ϕ and hence it should be of the general form

$$\tilde{M} = \sum_{n \in \mathbb{Z}} \left[a_n^M \cos L_n \phi + c_n^M \sin L_n \phi \right], \quad L_n \equiv \frac{2\pi n}{\Delta\phi}, \quad (4.8.17)$$

where a_n^M and c_n^M may depend on u, x, ψ and $\phi \sim \phi + \Delta\phi$. Plugging this expression into (4.7.23) we get the general solution

$$\begin{aligned} \tilde{M} = \sum_{n \in \mathbb{Z}} \left\{ [A_n^M \cosh L_n u + B_n^M \sinh L_n u] \cos L_n \phi \right. \\ \left. + [C_n^M \cosh L_n u + D_n^M \sinh L_n u] \sin L_n \phi \right\}, \end{aligned} \quad (4.8.18)$$

and similarly for \tilde{N} . Here, $A_n^{M,N}$, $B_n^{M,N}$, $C_n^{M,N}$ and $D_n^{M,N}$ are functions of x and ψ .

The integrability conditions (4.7.28)-(4.7.29) imply

$$A_n^M = -D_n^N, \quad B_n^M = -C_n^N, \quad C_n^M = B_n^N, \quad D_n^M = A_n^N, \quad (4.8.19)$$

and hence

$$\begin{aligned} \tilde{N} = \sum_{n \in \mathbb{Z}} \left\{ [D_n^M \cosh L_n u + C_n^M \sinh L_n u] \cos L_n \phi \right. \\ \left. - [B_n^M \cosh L_n u + A_n^M \sinh L_n u] \sin L_n \phi \right\}. \end{aligned} \quad (4.8.20)$$

From now on we drop the superscript M to avoid cluttering since it should cause no confusion.

The remaining constraints (4.7.26)-(4.7.27) yield

$$\partial_x(\sqrt{H}A_n^\pm) \pm \frac{1}{\sqrt{H}} [L_n x A_n^\pm + \partial_\psi C^\pm] = 0, \quad (4.8.21a)$$

$$\partial_x(\sqrt{H}C_n^\pm) \pm \frac{1}{\sqrt{H}} [L_n x C_n^\pm - \partial_\psi A^\pm] = 0, \quad (4.8.21b)$$

for $n \neq 0$, together with

$$\frac{\partial_\psi A_0}{\sqrt{H}} - \partial_x(\sqrt{H}D_0) = \frac{g(HH''')'}{3}, \quad (4.8.22a)$$

$$\frac{\partial_\psi D_0}{\sqrt{H}} + \partial_x(\sqrt{H}A_0) = 0, \quad (4.8.22b)$$

where we have defined $A_n^\pm \equiv A_n \pm B_n$ and $C_n^\pm \equiv C_n \pm D_n$. These equations are general, but we will focus on ψ independent solutions. We take the functions A_n^\pm, C_n^\pm to have *no* ψ dependence; equations (4.8.21a)-(4.8.21b) decouple and have solution

$$A_n^\pm = \frac{a_n^\pm}{\sqrt{H}} \exp \left[\mp L_n \int^x dx' \frac{x'}{H(x')} \right], \quad C_n^\pm = \frac{c_n^\pm}{\sqrt{H}} \exp \left[\mp L_n \int^x dx' \frac{x'}{H(x')} \right], \quad (4.8.23)$$

where a_n^\pm and c_n^\pm are constants. Equations (4.8.22a)-(4.8.22b) are solved by

$$D_0(x) = -\frac{g\sqrt{H}H'''}{3} - \frac{C_1}{\sqrt{H}}, \quad A_0(x) = 0, \quad (4.8.24)$$

so that we recover the known solutions setting $n = 0$ in the expressions above. Rescaling a_n^\pm and c_n^\pm , we can write down the general solution with ϕ -dependence:

$$\tilde{M} = \sum_{n \in \mathbb{Z}/\{0\}} \left[(A_n^+ e^{L_n u} + A_n^- e^{-L_n u}) \cos L_n \phi + (C_n^+ e^{L_n u} + C_n^- e^{-L_n u}) \sin L_n \phi \right], \quad (4.8.25)$$

$$\begin{aligned} \tilde{N} = -\frac{g\sqrt{H}H'''}{3} - \frac{C_1}{\sqrt{H}} + \sum_{n \in \mathbb{Z}/\{0\}} \left[(C_n^+ e^{L_n u} - C_n^- e^{-L_n u}) \cos L_n \phi \right. \\ \left. - (A_n^+ e^{L_n u} - A_n^- e^{-L_n u}) \sin L_n \phi \right]. \end{aligned} \quad (4.8.26)$$

The next step is to compute the one-form w . Due to our assumption of ψ independence it suffices to consider the following form for w

$$w = w_x \mathbf{e}^x + w_\phi \mathbf{e}^\phi + w_\psi \mathbf{e}^\psi, \quad (4.8.27)$$

where the w_i may depend on σ , x and ϕ . From (4.6.14) we get,

$$w_x = \frac{\sqrt{e^{-u}-1}}{2g} \left\{ \sum_{n \in \mathbb{Z}/\{0\}} \frac{1}{L_n} \left[(A_n^+ e^{L_n u} - A_n^- e^{-L_n u}) \cos L_n \phi \right. \right. \\ \left. \left. + (C_n^+ e^{L_n u} - C_n^- e^{-L_n u}) \sin L_n \phi \right] + k_x(x, \phi) \right\}, \quad (4.8.28)$$

$$w_\phi = w_\phi^0 + \sinh(-u/2) \frac{k_\phi(x, \phi)}{g}, \\ w_\psi = w_\psi^0 + \frac{\sqrt{e^{-u}-1}}{2g} \left\{ \sum_{n \in \mathbb{Z}/\{0\}} \frac{1}{L_n} \left[(C_n^+ e^{L_n u} + C_n^- e^{-L_n u}) \cos L_n \phi \right. \right. \\ \left. \left. - (A_n^+ e^{L_n u} + A_n^- e^{-L_n u}) \sin L_n \phi \right] + k_\psi(x, \phi) \right\}, \quad (4.8.29)$$

where w_ϕ^0 and w_ψ^0 are given in (4.8.5). The functions k_x , k_ϕ and k_ψ obey

$$\partial_\phi k_x = \sqrt{H} \partial_x k_\phi, \quad (4.8.30a)$$

$$\partial_x (\sqrt{H} k_\psi + x k_\phi) = 0, \quad (4.8.30b)$$

$$\partial_\phi (\sqrt{H} k_\psi + x k_\phi) = 0. \quad (4.8.30c)$$

The last two equations require

$$k_\psi = -\frac{x}{\sqrt{H}} k_\phi + k, \quad (4.8.31)$$

where k is constant. Therefore, the full solution is given by eqs.(4.8.28)-(4.8.29), where k_x and k_ϕ should obey (4.8.30a).

ϕ dependent deformations of AdS₅

As a first case study of ϕ dependent solutions we take

$$H(x) = 1 - x^2,$$

together with $C_H = C_1 = C_\psi = 0$ and $C_\phi = 2/3$ in (4.8.5). Then $f = 1$. We further take $k_\phi = k_x = k = 0$ as to consider the simplest possible case. Introducing coordinate $x = \cos \theta$ for the base, we get, from (4.8.23),

$$A_n^\pm = a_n^\pm (\sin \theta)^{\pm \frac{n}{2}-1}, \quad C_n^\pm = c_n^\pm (\sin \theta)^{\pm \frac{n}{2}-1}.$$

Thus, putting together (4.8.5) and (4.8.28)-(4.8.29), we find

$$w = \frac{\sinh^2 g\sigma}{2g} (d\phi + \cos \theta \psi) + \frac{\sin \theta \Sigma^\psi}{4g^2} d\psi - \frac{\Sigma^x}{4g^2} d\theta, \quad (4.8.32)$$

where, noting that the periodicity of ϕ is $\Delta\phi = 4\pi$

$$\Sigma^\psi = \sum_{n \in \mathbb{Z}/\{0\}} \frac{2}{n \sin \theta} \left[(c_n^+ \sin^{\frac{n}{2}} \theta \tanh^n g\sigma + c_n^- \sin^{-\frac{n}{2}} \theta \tanh^{-n} g\sigma) \cos \frac{n\phi}{2} \right. \\ \left. - (a_n^+ \sin^{\frac{n}{2}} \theta \tanh^n g\sigma + a_n^- \sin^{-\frac{n}{2}} \theta \tanh^{-n} g\sigma) \sin \frac{n\phi}{2} \right], \quad (4.8.33)$$

$$\Sigma^x = \sum_{n \in \mathbb{Z}/\{0\}} \frac{2}{n \sin \theta} \left[(a_n^+ \sin^{\frac{n}{2}} \theta \tanh^n g\sigma - a_n^- \sin^{-\frac{n}{2}} \theta \tanh^{-n} g\sigma) \cos \frac{n\phi}{2} + (c_n^+ \sin^{\frac{n}{2}} \theta \tanh^n g\sigma - c_n^- \sin^{-\frac{n}{2}} \theta \tanh^{-n} g\sigma) \sin \frac{n\phi}{2} \right]. \quad (4.8.34)$$

Thus, we find a family of solutions of minimal five dimensional gauged SUGRA of the form

$$ds^2 = -[dt + w]^2 + ds_B^2, \quad A = \frac{\sqrt{3}}{8g^2} (\sin \theta \Sigma^\psi d\psi - \Sigma^x d\theta), \quad (4.8.35)$$

where w is given by (4.8.32), and ds_B^2 by (4.7.8) with (4.8.32). As a simple example take

$$c_m^+ = \frac{c}{2},$$

for a given positive m , and all remaining $c_n^\pm = 0 = a_n^\pm$. Then, the full spacetime metric is, explicitly

$$ds^2 = - \left[dt + \frac{\sinh^2 g\sigma}{2g} (d\phi + \cos \theta d\psi) + \frac{c \tanh^m g\sigma \sin^{\frac{m}{2}-1} \theta}{4g^2} \left(\sin \theta \cos \frac{m\phi}{2} d\psi - \sin \frac{m\phi}{2} d\theta \right) \right]^2 + d\sigma^2 + \frac{\sinh^2 g\sigma}{4g^2} (d\theta^2 + \sin^2 \theta d\psi^2 + \cosh^2 g\sigma (d\phi + \cos \theta d\psi)^2), \quad (4.8.36)$$

and the gauge field is

$$A = \frac{\sqrt{3}c}{8g^2} \tanh^m g\sigma \sin^{\frac{m}{2}-1} \theta \left(\sin \theta \cos \frac{m\phi}{2} d\psi - \sin \frac{m\phi}{2} d\theta \right). \quad (4.8.37)$$

We have verified that these fields obey equations of motion (4.2.2). For $c = 0$ they describe empty AdS_5 . Generically, this metric is singular for $\sigma = 0, +\infty$ and $\theta = 0, \pi$. To check if these are physical singularities note that the Ricci scalar takes the form

$$R = -20g^2 + \frac{c^2 m^2 (\sin \theta \sinh^2 g\sigma)^{m-2}}{4 \cosh^{2m+2} g\sigma}.$$

It does not diverge if $m \geq 2$; otherwise there is a curvature singularity at $\theta = 0 = \pi$ and at $\sigma = 0$. Indeed this seems to be a generic behaviour of the curvature invariants; for instance, the square of the Ricci tensor is

$$R_{\mu\nu} R^{\mu\nu} = 80g^4 - \frac{2g^2 c^2 m^2 (\sin \theta \sinh^2 g\sigma)^{m-2}}{\cosh^{2m+2} g\sigma} + \frac{c^4 m^4 (\sin \theta \sinh^2 g\sigma)^{2m-4}}{8 \cosh^{4m+4} g\sigma}.$$

One typical pathology of this type of solutions is the presence of Closed Timelike Curves. We can show, however, that (4.8.36) is free of Closed Timelike Curves if the parameter c obeys

$$c \leq 2g. \quad (4.8.38)$$

To see this, let us analyse the closed directions of the metric ϕ and ψ . Since $g_{\phi\phi} = \sinh^2 g\sigma/4g^2$, $\partial/\partial\phi$ is always spacelike. Since

$$g_{\psi\psi} = \frac{\sinh^2 g\sigma}{4g^2} \left(1 - \frac{\chi^2}{\sinh^2 g\sigma} \right), \quad \chi^2 \equiv \left(\frac{c}{2g} \right)^2 \tanh^{2m} g\sigma \sin^m \theta \cos^2 \frac{m\phi}{2},$$

$\partial/\partial\psi$ is always spacelike for the non singular solutions ($m \geq 2$) as long as (4.8.38). The fact that two given vector fields are spacelike does not guarantee that a linear combination of them is still spacelike, for non-diagonal metrics. This is, in fact, a subtle way in which Closed Timelike Curves may emerge in spacetime. Examples are discussed in [25, 26, 27, 28]. Thus, we must consider the vector field $k = A\partial_\phi + B\partial_\psi$, which, for appropriately chosen A, B will still have closed orbits. The norm of this vector field can be written

$$|k|^2 = \frac{\sinh^2 g\sigma}{4g^2} \left(A^2 + B^2 \left[1 - \frac{\chi^2}{\sinh^2 g\sigma} \right] + 2AB(\cos\theta - \chi) \right) .$$

We could not find any choice of A, B for which this quantity becomes negative. Thus it seems that for (4.8.38) there are no Closed Timelike Curves (or Closed Null Curves) in the spacetime.

“Static” coordinates, in the sense that these are the static coordinates of empty AdS_5 , are obtained introducing a new angular coordinate ϕ' and a new radial coordinate R given by

$$\phi' = \phi - 2gt , \quad R = \frac{\sinh g\sigma}{g} .$$

Replacing ϕ, σ by ϕ', R in (4.8.36), the solutions become time dependent:

$$ds^2 = ds_{AdS_5}^2 - 2 \left[(1 + g^2 R^2) dt + \frac{gR^2}{2} (d\phi' + \cos\theta d\psi) \right] w' - w'^2 , \quad (4.8.39)$$

where

$$ds_{AdS_5}^2 = -(1 + g^2 R^2) dt^2 + \frac{dR^2}{1 + g^2 R^2} + \frac{R^2}{4} (d\theta^2 + \sin^2\theta d\psi^2 + (d\phi' + \cos\theta d\psi)^2) ,$$

and

$$w' = \frac{c}{4g^2} \left(\frac{g^2 R^2}{1 + g^2 R^2} \right)^m \sin^{\frac{m}{2}-1} \theta \left(\sin\theta \cos \frac{m(\phi' + 2gt)}{2} d\psi - \sin \frac{m(\phi' + 2gt)}{2} d\theta \right) . \quad (4.8.40)$$

The solutions are time dependent in this coordinate chart. Note that $\partial/\partial t$ is an everywhere timelike vector field. Nevertheless, the solution still has, as required by supersymmetry, an everywhere timelike Killing vector field, which is $V = \partial_t - 2g\partial_{\phi'}$, and in this sense is stationary. In the case of black holes it is with respect to V that there is no ergoregion [4, 29]. Thinking of V as the generator of time translations corresponds to working in a co-rotating frame, with respect to which these solutions are stationary. Note also that V becomes null on the conformal boundary of the spacetime. Thus, as for asymptotically AdS_5 black holes the boundary is rotating at the speed of light in the co-rotating frame. However, the conformal boundary is different from AdS_5 , and has metric

$$ds^2 = -dt^2 + \frac{1}{g^2} (d\theta^2 + \sin^2\theta d\psi^2 + (d\phi' + \cos\theta d\psi)^2) - \frac{c}{2g^2} \left[dt + \frac{d\phi' + \cos\theta d\psi}{2g} \right] \sin^{\frac{m}{2}-1} \theta \left(\sin\theta \cos \frac{m(\phi' + 2gt)}{2} d\psi - \sin \frac{m(\phi' + 2gt)}{2} d\theta \right) . \quad (4.8.41)$$

We have checked that this geometry is not conformally flat (Weyl tensor is non-zero). In this sense, the deformations we are considering do not have the same conformal boundary as AdS_5 ; thus they are *not* asymptotically AdS_5 , and these coordinates should not be dubbed “static”.

It would be interesting to know the exact amount of supersymmetry these spacetimes preserve (which is at least 1/4, and cannot be more than 1/2 [30]) and compute the conserved quantities associated to the Killing symmetries.⁴

ϕ dependent deformations of the Gutowski-Reall black hole

We now take,

$$H(x) = A^2(1 - x^2), \quad (4.8.42)$$

with $0 < A^2 < 1$, corresponding to the Gutowski-Reall black hole. We find

$$w = \frac{\sinh^2 g\sigma}{2g} \left(1 + \frac{1 - A^2}{2 \sinh^2 g\sigma} + \frac{(1 - A^2)^2}{6 \sinh^4 g\sigma} \right) (d\phi + \cos \theta \psi) + \frac{\sin \theta \Sigma^\psi}{4g^2} d\psi - \frac{\Sigma^x}{4g^2} d\theta, \quad (4.8.43)$$

where, noting that the periodicity of ϕ is $\Delta\phi = 4\pi/A^2$

$$\begin{aligned} \Sigma^\psi = \frac{1}{A^2} \sum_{n \in \mathbb{Z}/\{0\}} \frac{2}{n} \left[\left(c_n^+ \sin^{\frac{n}{2}} \theta \tanh^{A^{2n}} g\sigma + c_n^- \sin^{-\frac{n}{2}} \theta \tanh^{-A^{2n}} g\sigma \right) \frac{\cos \frac{A^{2n}\phi}{2}}{\sin \theta} \right. \\ \left. - \left(a_n^+ \sin^{\frac{n}{2}} \theta \tanh^{A^{2n}} g\sigma + a_n^- \sin^{-\frac{n}{2}} \theta \tanh^{-A^{2n}} g\sigma \right) \frac{\sin \frac{A^{2n}\phi}{2}}{\sin \theta} \right], \end{aligned} \quad (4.8.44)$$

$$\begin{aligned} \Sigma^x = \frac{1}{A^2} \sum_{n \in \mathbb{Z}/\{0\}} \frac{2}{n} \left[\left(a_n^+ \sin^{\frac{n}{2}} \theta \tanh^{A^{2n}} g\sigma - a_n^- \sin^{-\frac{n}{2}} \theta \tanh^{-A^{2n}} g\sigma \right) \frac{\cos \frac{A^{2n}\phi}{2}}{\sin \theta} \right. \\ \left. + \left(c_n^+ \sin^{\frac{n}{2}} \theta \tanh^{A^{2n}} g\sigma - c_n^- \sin^{-\frac{n}{2}} \theta \tanh^{-A^{2n}} g\sigma \right) \frac{\sin \frac{A^{2n}\phi}{2}}{\sin \theta} \right]. \end{aligned} \quad (4.8.45)$$

Taking

$$c_m^+ = \frac{cA^2}{2},$$

for a given positive m , and all remaining $c_n^\pm = 0 = a_n^\pm$, the full spacetime metric is of the form (4.2.3) with

$$\begin{aligned} w = \frac{\sinh^2 g\sigma}{2g} \left(1 + \frac{1 - A^2}{2 \sinh^2 g\sigma} + \frac{(1 - A^2)^2}{6 \sinh^4 g\sigma} \right) (d\phi + \cos \theta d\psi) \\ + \frac{c \tanh^{A^{2m}} g\sigma \sin^{\frac{m}{2}-1} \theta}{4g^2} \left(\sin \theta \cos \frac{A^{2m}\phi}{2} d\psi - \sin \frac{A^{2m}\phi}{2} d\theta \right), \end{aligned} \quad (4.8.46)$$

$$f^{-1} = 1 + \frac{1 - A^2}{3 \sinh^2 g\sigma}, \quad (4.8.47)$$

and

$$ds_B^2(\mathcal{K}) = d\sigma^2 + \frac{\sinh^2 g\sigma}{4g^2} \left(\frac{d\theta^2}{A^2} + A^2 \sin^2 \theta d\psi^2 + \cosh^2 g\sigma (d\phi + \cos \theta d\psi)^2 \right), \quad (4.8.48)$$

⁴There is an overlap between the solutions studied in this section and AdS_5 deformations found in [21]. However, therein, these solutions were not analysed, and the method presented here allowed us to deform not only AdS_5 but also solutions with different $H(x)$ in a similar fashion. Moreover, the special case with $m = 2$ was studied in [31, 32] and it corresponds to a Gödel type deformation.

while the gauge field is

$$\begin{aligned}
A = & \frac{\sqrt{3}}{2} f dt + \frac{\sqrt{3}}{2} \left(1 + 2 \frac{1 - A^2}{3 \sinh^2 g\sigma} + \frac{(1 - A^2)^2}{2 \sinh^4 g\sigma} + \frac{(1 - A^3)^2}{18 \sinh^6 g\sigma} \right) \frac{\sinh^2 g\sigma}{2g} (d\phi + \cos \theta d\psi) \\
& + \frac{\sqrt{3}c}{8g^2} \left(1 + \frac{1 - A^2}{3 \sinh^2 g\sigma} \right) \tanh^{A^2 m} g\sigma \sin^{\frac{m}{2} - 1} \theta \left(\sin \theta \cos \frac{A^2 m \phi}{2} d\psi - \sin \frac{A^2 m \phi}{2} d\theta \right).
\end{aligned}
\tag{4.8.49}$$

These deformations of the Gutowski-Reall black hole preserve 1/4 of the supersymmetry.⁵ For any positive m the Ricci scalar (and presumably the other curvature invariants) does not diverge at the horizon. In fact, the deformation terms are subleading corrections, at the horizon, both in the metric and in the curvature invariants. The analysis of the asymptotic structure is analogous to the previous section.

A similar analysis for all other solutions of (4.6.19) could now be done, including the most general AdS_5 black holes (4.8.10).

4.9 Conclusions and Discussion

The main goal of this paper was to investigate more general supersymmetric black hole solutions in AdS_5 than the ones known hitherto. With this purpose, we constructed a family of Kähler bases using some assumptions that are compatible with the existence of an event horizon. These assumptions are restrictive and, from the outset, our analysis did not cover possible AdS_5 black rings. Nevertheless the analysis, and the family of Kähler bases that emerged from it, still proved fruitful.

Firstly, the function that characterises the family of bases, obeys a remarkably simple 6th order differential equation. A family of solutions, albeit not the most general one, is a cubic polynomial, which turns out to describe all known AdS_5 supersymmetric black holes. The remaining solutions of the sixth order equation that we found are spaces with non-compact horizons or spaces with singular horizons. This suggests that indeed, the family of solutions found so far describes the most general black holes with spherical topology and two axisymmetries in AdS_5 . More general black holes, with fewer isometries are not excluded and seem compatible with the results in [34]. However, following a similar analysis to the one herein for less symmetric base spaces does not seem as tractable a problem and presents a challenge. In the appendix we make some preliminary analysis in that direction.

Secondly, we found an infinite set of supersymmetric deformations of both AdS_5 space and the black holes living on it. These deformations vanish at the horizon and they change the asymptotic structure of the spacetime. Interestingly, these deformations, are time dependent, when one writes AdS_5 in static coordinates, but there is still an everywhere timelike Killing vector field. Also, they provide an example of supersymmetric AdS_5 solutions, where the five dimensional spacetime has less spatial isometries than the base space. Of course it would be interesting to understand better these solutions and if they have some CFT correspondence. Let us note that a similar set of deformations, albeit more restrictive, was studied for the ungauged theory in [35], where it was shown that any asymptotically flat solution could be embedded in a Gödel type universe. This is the vanishing cosmological constant limit of the $m = 2$ deformation presented herein. All remaining regular deformations vanish in that limit.

⁵As for the empty AdS_5 case the Gödel type deformation ($m = 2$) was previously studied in [33].

There are several directions in which one could extend the work herein. One of the outstanding questions in this field, is the possible existence of AdS_5 black rings. In order to consider black rings, an analysis similar to the one in section 4.5 could, perhaps, be followed, replacing (4.5.2) by something of the type

$$ds_B^2(\mathcal{K}) \simeq ds_2^2(\rho, \theta) + f_{11}(\theta)\rho^2 (d\phi^1)^2 + f_{22}(\theta)R^2 (d\phi^2)^2 + f_{12}(\theta)\rho R d\phi^1 d\phi^2 , \quad (4.9.1)$$

where R is constant. But losing the property that the base of the solution is a Kähler cone in the vicinity of a possible horizon makes the analysis much harder. One other possible generalisation of our study is to seek other $G(\rho)$ that approach ρ^2 in the vicinity of a horizon and become asymptotically Bergmann. We have not been able to find other interesting examples.

Finally, let us mention that the issue of the existence of multi-black hole solutions in AdS_5 remains open. Clearly, a strategy to look for such solutions is to consider a Kähler base that reduces to a conical Kähler manifold at a set of points. However, one expects fewer isometries in such case, making the problem more difficult, since the base is not toric. Still, until a physical argument is given excluding the possibility of having multi-black hole solutions in AdS_5 this seems an interesting open question.

Acknowledgements

We are very grateful to Roberto Emparan, Jan Gutowski and Harvey Reall for discussions and suggestions on drafts of this paper. C.H. would also like to thank J. Lucietti and H.Kunduri for an interesting conversation. P.F would like to thank Centro de Física do Porto for hospitality, during the early stages of this work. C.H. and F.P.C are supported by FCT through the grants SFRH/BPD/5544/2001 and SFRH/BPD/20667/2004. P.F. is supported by a FI fellowship of the DURSI (Generalitat de Catalunya) and by the grants DURSI 2005 SGR 00082, CICYT FPA 2004-04582-C02-02 and EC FP6 program MRTNCT-2004-005104. This work was also supported by Fundação Calouste Gulbenkian through *Programa de Estímulo à Investigação*, by the FCT grants POCTI/FNU/38004/2001 and POCTI/FNU/50161/2003. Centro de Física do Porto is partially funded by FCT through POCTI programme.

4.A Non-toric Kähler cones

Equation (4.6.19) was obtained for toric Kähler cones, admitting a $U(1)^2$ action. Some such cones provide the base (near the horizon) for black holes admitting a $U(1)^2$ spatial isometry. If one would like to search for black objects with a smaller spatial isometry group one could consider cones with less symmetry. So, we consider now the possibility that the 2d base of the Sasakian space is not toric. From the discussion in section 4.5.1 we can see that the Sasakian space still has one isometry, as $\eta = d\phi + \xi$ where ξ is parallel to the 2d base. Thus, the four dimensional cone will only admit a one dimensional isometry group. Let us derive, in this more general case, what is the constraint analogous to (4.6.19).

To study the near-horizon geometry of 5d solutions having non-toric Kähler cones as their bases, let us define these bases by the following set of 1-forms:

$$e^\rho = d\rho , \quad e^\eta = \rho\eta , \quad e^w = \rho\sqrt{H}dw , \quad (4.A.1)$$

where we introduced the function

$$H(w, \bar{w}) \equiv \hat{\mathcal{K}}_{w\bar{w}} . \quad (4.A.2)$$

In this basis the Kähler form of the cone and G^+ read

$$J = -(\mathbf{e}^\rho \wedge \mathbf{e}^\eta + i\mathbf{e}^w \wedge \mathbf{e}^{\bar{w}}) , \quad (4.A.3)$$

and

$$G^+ = -3gf^{-1}(w, \bar{w})(\mathbf{e}^\rho \wedge \mathbf{e}^\eta - i\mathbf{e}^w \wedge \mathbf{e}^{\bar{w}}) . \quad (4.A.4)$$

The most general ansatz for G^- then reads

$$G^- = -LJ - f(T\mathbf{e}^\rho \wedge \mathbf{e}^w + \text{c.c.}) - f(iT\mathbf{e}^\eta \wedge \mathbf{e}^w + \text{c.c.}) . \quad (4.A.5)$$

We find easily that (4.6.5) is still valid. We obtain therefore

$$f^{-1}L(\rho, w, \bar{w}) = \frac{1}{4g}\nabla^2 f^{-1} = \frac{1}{g\rho^4 2H}\partial_w \partial_{\bar{w}} c(w, \bar{w}) . \quad (4.A.6)$$

The complex function T is determined by imposing the integrability condition (4.2.8). For the sake of simplicity, we solve these constraints assuming that $T = T(\rho, w, \bar{w})$. We obtain in this way the following set of equations:

$$i\partial_\rho \rho^2 T - \partial_\phi T - \frac{1}{\rho^3 \sqrt{H}} \partial_w (cl - 3gc^2) = 0 , \quad (4.A.7)$$

$$\partial_w(\sqrt{HT}) - \partial_{\bar{w}}(\sqrt{HT}) - i4H \frac{cl}{\rho^4} = 0 , \quad (4.A.8)$$

$$\partial_w(\sqrt{HT}) + \partial_{\bar{w}}(\sqrt{HT}) = 0 . \quad (4.A.9)$$

The general solution is

$$T = \frac{i}{2\rho^4 \sqrt{H}} \partial_w (cl - 3gc^2) + \frac{1}{\rho^2 \sqrt{H}} T_0(w) , \quad (4.A.10)$$

where $T_0(w)$ is holomorphic. Plugging this back in (4.A.8) we obtain a constraint on the geometry of the base, namely

$$\partial_w \partial_{\bar{w}} \left(cl - 3gc^2 + \frac{2}{g}c \right) = 0 , \quad (4.A.11)$$

where

$$cl = \frac{1}{2gH} \partial_w \partial_{\bar{w}} c , \quad (4.A.12)$$

and

$$c = \frac{1}{3g^2} + \frac{1}{12g^2 H(w, \bar{w})} \partial_w \partial_{\bar{w}} \ln H(w, \bar{w}) . \quad (4.A.13)$$

Equation (4.A.11) is a generalisation of (4.6.19), to which it reduces for toric Kähler cones. It can be easily reduced to a 4th order non-linear partial differential equation which reads

$$cl - 3gc^2 + \frac{2}{g}c = h(w) + \bar{h}(\bar{w}) . \quad (4.A.14)$$

Another way of writing the 6th order equation is

$$\nabla_2^2 \left(\nabla_2^2 R_2 + \frac{1}{2}(R_2)^2 \right) = 0 , \quad (4.A.15)$$

where ∇_2^2 and R_2 are the Laplacian operator and the scalar curvature on the 2d base space; the latter can be expressed as

$$R_2 = -\frac{2}{H} \partial_w \partial_{\bar{w}} \ln H . \quad (4.A.16)$$

Requiring this space to be compact implies that

$$\nabla_2^2 R_2 + \frac{1}{2} (R_2)^2 = \text{const} , \quad (4.A.17)$$

for in this case any harmonic function is constant. The trivial solutions $R_2 = \text{const} > 0$ lead to empty AdS_5 and the black hole of Gutowski and Reall. For general toric cones this equation reduces to $H^2 H'''' = \text{const}$. Note that $R_2 = 0$ is also a solution, showing that (4.A.17) does not necessarily lead to compact spaces.

Bibliography

- [1] J. M. Maldacena, “The large N limit of superconformal field theories and supergravity,” *Adv. Theor. Math. Phys.* **2** (1998) 231 [arXiv:hep-th/9711200].
- [2] E. Witten, “Anti-de Sitter space and holography,” *Adv. Theor. Math. Phys.* **2** (1998) 253 [arXiv:hep-th/9802150].
- [3] S. S. Gubser, I. R. Klebanov and A. M. Polyakov, “Gauge theory correlators from non-critical string theory,” *Phys. Lett. B* **428** (1998) 105 [arXiv:hep-th/9802109].
- [4] J. B. Gutowski and H. S. Reall, “Supersymmetric AdS(5) black holes,” *JHEP* **0402** (2004) 006 [arXiv:hep-th/0401042].
- [5] J. B. Gutowski and H. S. Reall, “General supersymmetric AdS(5) black holes,” *JHEP* **0404** (2004) 048 [arXiv:hep-th/0401129].
- [6] Z. W. Chong, M. Cvetič, H. Lu and C. N. Pope, “Five-dimensional gauged supergravity black holes with independent rotation parameters,” *Phys. Rev. D* **72** (2005) 041901 [arXiv:hep-th/0505112].
- [7] Z. W. Chong, M. Cvetič, H. Lu and C. N. Pope, “General non-extremal rotating black holes in minimal five-dimensional gauged supergravity,” *Phys. Rev. Lett.* **95**, 161301 (2005) [arXiv:hep-th/0506029].
- [8] H. K. Kunduri, J. Lucietti and H. S. Reall, “Supersymmetric multi-charge AdS(5) black holes,” *JHEP* **0604** (2006) 036 [arXiv:hep-th/0601156].
- [9] Z. W. Chong, M. Cvetič, H. Lu and C. N. Pope, “Non-extremal rotating black holes in five-dimensional gauged supergravity,” [arXiv:hep-th/0606213].
- [10] J. Kinney, J. M. Maldacena, S. Minwalla and S. Raju, “An index for 4 dimensional super conformal theories,” [arXiv:hep-th/0510251].
- [11] M. Berkooz, D. Reichmann and J. Simon, “A Fermi surface model for large supersymmetric AdS(5) black holes,” [arXiv:hep-th/0604023].
- [12] P. J. Silva, “Thermodynamics at the BPS bound for black holes in AdS,” [arXiv:hep-th/0607056].
- [13] S. Kim and K. M. Lee, “1/16-BPS black holes and giant gravitons in the AdS(5) x S⁵ space,” [arXiv:hep-th/0607085].

-
- [14] R. Emparan and H. S. Reall, “A rotating black ring in five dimensions,” *Phys. Rev. Lett.* **88**, 101101 (2002) [arXiv:hep-th/0110260].
- [15] H. Elvang, R. Emparan, D. Mateos and H. S. Reall, “Supersymmetric black rings and three-charge supertubes,” *Phys. Rev. D* **71** (2005) 024033 [arXiv:hep-th/0408120].
- [16] I. Bena and N. P. Warner, “One ring to rule them all ... and in the darkness bind them?,” [arXiv:hep-th/0408106].
- [17] J. P. Gauntlett and J. B. Gutowski, “General concentric black rings,” *Phys. Rev. D* **71** (2005) 045002 [arXiv:hep-th/0408122].
- [18] H. Elvang, R. Emparan, D. Mateos and H. S. Reall, “A supersymmetric black ring,” *Phys. Rev. Lett.* **93**, 211302 [arXiv:hep-th/0407065].
- [19] J. C. Breckenridge, R. C. Myers, A. W. Peet and C. Vafa, “D-branes and spinning black holes,” *Phys. Lett. B* **391**, 93 (1997) [arXiv:hep-th/9602065].
- [20] H. S. Reall, “Higher dimensional black holes and supersymmetry,” *Phys. Rev. D* **68** (2003) 024024 [Erratum *Phys. Rev. D* **70** (2004) 089902] [arXiv:hep-th/0211290].
- [21] J. P. Gauntlett and J. B. Gutowski, “All supersymmetric solutions of minimal gauged supergravity in five dimensions,” *Phys. Rev. D* **68** (2003) 105009 [Erratum *Phys. Rev. D* **70** (2004) 089901] [arXiv:hep-th/0304064].
- [22] D. Martelli, J. Sparks and S. T. Yau, “The geometric dual of a-maximisation for toric Sasaki-Einstein manifolds,” [arXiv:hep-th/0503183].
- [23] D. Martelli, J. Sparks and S. T. Yau, “Sasaki-Einstein manifolds and volume minimisation,” [arXiv:hep-th/0603021].
- [24] J. P. Gauntlett, D. Martelli, J. F. Sparks and D. Waldram, “A new infinite class of Sasaki-Einstein manifolds,” *Adv. Theor. Math. Phys.* **8** (2005) 987 [arXiv:hep-th/0403038].
- [25] C. A. R. Herdeiro, “Special properties of five dimensional BPS rotating black holes,” *Nucl. Phys. B* **582** (2000) 363 [arXiv:hep-th/0003063].
- [26] C. A. R. Herdeiro, “Spinning deformations of the D1-D5 system and a geometric resolution of closed timelike curves,” *Nucl. Phys. B* **665** (2000) 189 [arXiv:hep-th/0212002].
- [27] C. A. R. Herdeiro, “Closed causal curves in string theory,” Prepared for 10th Marcel Grossmann Meeting on Recent Developments in Theoretical and Experimental General Relativity, Gravitation and Relativistic Field Theories (MG X MMIII), Rio de Janeiro, Brazil, 20-26 Jul 2003.
- [28] V. E. Hubeny, M. Rangamani and S. F. Ross, “Causal inheritance in plane wave quotients,” *Phys. Rev. D* **69** (2004) 024007 [arXiv:hep-th/0307257].
- [29] S. W. Hawking and H. S. Reall, “Charged and rotating AdS black holes and their CFT duals,” *Phys. Rev. D* **61** (2000) 024014 [arXiv:hep-th/9908109].
- [30] J. Grover, J. B. Gutowski and W. Sabra, “Vanishing Preons in the Fifth Dimension,” [arXiv:hep-th/0608187].

-
- [31] K. Behrndt and M. Pospel, “Chronological structure of a Goedel type universe with negative cosmological constant,” *Phys. Lett. B* **580**, 1 (2004) [arXiv:hep-th/0310090].
- [32] J. P. Gauntlett, J. B. Gutowski and N. V. Suryanarayana, “A deformation of $\text{AdS}_5 \times S^5$,” *Class. Quant. Grav.* **21**, 5021 (2004) [arXiv:hep-th/0406188].
- [33] K. Behrndt and D. Klemm, “Black holes in Goedel-type universes with a cosmological constant,” *Class. Quant. Grav.* **21**, 4107 (2004) [arXiv:hep-th/0401239].
- [34] S. Hollands, A. Ishibashi and R. M. Wald, “A higher dimensional stationary rotating black hole must be axisymmetric,” [arXiv:gr-qc/0605106.]
- [35] T. Ortin, “A note on supersymmetric Goedel black holes, strings and rings of minimal $d = 5$ supergravity,” *Class. Quant. Grav.* **22**, 939 (2005) [arXiv:hep-th/0410252].
- [36] J. B. Gutowski and W. Sabra, “General supersymmetric solutions of five-dimensional supergravity,” *JHEP* **0510**, 039 (2005) [arXiv:hep-th/0505185].

Chapter 5

Black Saturn

Henriette Elvang,^a Pau Figueras^b

^a*Center for Theoretical Physics,
Massachusetts Institute of Technology, Cambridge, MA 02139, USA*

^b*Departament de Física Fonamental
Universitat de Barcelona, Diagonal 647, E-08028, Barcelona, Spain*

elvang@lns.mit.edu, pfigueras@ffn.ub.es

ABSTRACT

Using the inverse scattering method we construct an exact stationary asymptotically flat 4+1-dimensional vacuum solution describing “black saturn”: a spherical black hole surrounded by a black ring. Angular momentum keeps the configuration in equilibrium. Black saturn reveals a number of interesting gravitational phenomena: (1) The balanced solution exhibits 2-fold continuous non-uniqueness for fixed mass and angular momentum; (2) Remarkably, the 4+1d Schwarzschild black hole is not unique, since the black ring and black hole of black saturn can counter-rotate to give zero total angular momentum at infinity, while maintaining balance; (3) The system cleanly demonstrates rotational frame-dragging when a black hole with vanishing Komar angular momentum is rotating as the black ring drags the surrounding spacetime. Possible generalizations include multiple rings of saturn as well as doubly spinning black saturn configurations.

5.1 Introduction

Multi-black hole spacetimes play an interesting role in black hole physics. A central question is how to keep a configuration of multiple black holes in equilibrium. Two Schwarzschild black holes attract each other and cannot be in equilibrium without external forces to hold them in place. The simplest way to achieve a stationary balanced configuration is by adding enough electric charge to each black hole, so that the electromagnetic repulsion exactly cancels the gravitational attraction. In 3+1 dimensions, the resulting solution, and its generalization to multiple black holes, is of course the well-known extremal multi-Reissner Nordstrom black hole solution [1].

For asymptotically flat vacuum solutions, rotation seems to be the only candidate for keeping black holes apart. However, for the 3+1-dimensional axisymmetric double Kerr solution [2], the spin-spin interaction [3] is not sufficiently strong to balance the gravitational attraction of black holes with regular horizons [4, 5, 6, 7]. Hence multi-Kerr black hole spacetimes are not in equilibrium, but suffer from singular struts which provide the pressure to keep the black holes apart [5].

We present here a 4+1-dimensional stationary vacuum solution for which angular momentum does provide sufficient force to keep two black objects apart. The possibility of balanced, regular multi-black hole vacuum spacetimes can be motivated as follows. The five-dimensional vacuum Einstein's equations admit black ring solutions [8] which have horizons of topology $S^2 \times S^1$. Rotation prevents the black ring from collapsing. Very thin black rings are kept in equilibrium by a Newtonian force balance between a string-like tension and a centrifugal force arising from the rotation [9] (see also [10]). With this Newtonian balance in mind, it is natural to ask if rotation provides a sufficiently strong force to also keep a black ring in equilibrium in an "external potential". This could for instance be in the gravitational field of a Myers-Perry black hole [11] at the center of the black ring. Our solution realizes this possibility: a black ring balanced by rotation around a concentric spherical black hole in an asymptotically flat spacetime. We call this balanced configuration *black saturn*.

It should be emphasized that the black hole and the black ring generally have strong gravitational backreactions, so that only for very thin black rings with large S^1 radius does the motivation of a black ring in an external potential apply. On the other hand, the gravitational interactions between the two objects give rise to interesting phenomena, such as frame-dragging, which we examine in detail. We summarize here a selection of physical properties of black saturn:

- *Continuous non-uniqueness*: The total mass M and angular momentum J measured at infinity can be distributed continuously between the two black objects in the balanced saturn configuration. Thus the solution exhibits 2-fold continuous non-uniqueness. An additional discrete non-uniqueness exists in regimes that admit both thin and fat black rings.
- *Counter rotation*: The black ring and the S^3 black hole have independent rotation parameters, and they can be co-rotating as well as counter-rotating while maintaining balance. (We define co- and counter-rotation in terms of the relative sign of the angular velocities.)
- *Non-uniqueness of the 4+1d Schwarzschild black hole*: Strikingly, the black ring and S^3 black hole can be counter-rotating to give zero total ADM angular momentum at infinity. This means that the 4+1-dimensional Schwarzschild-Tangherlini black hole is not the only asymptotically flat black hole solution with $J = 0$ at infinity; in fact the $J = 0$ black saturn configurations are 2-fold continuously non-unique.

The existence of the $J = 0$ black saturn solutions does not contradict the uniqueness theorem [12] that the Schwarzschild black hole is the only static asymptotically flat vacuum black hole solution; the reason is simply that black saturn, while being stationary, is non-static.

We also conclude that the slowly spinning Myers-Perry black hole is not unique; allowing for non-connected horizons one can get around the perturbative results of [13].

- *Rotational frame-dragging*: The gravitational interaction between the black ring and the S^3 black hole manifests itself in form of rotational frame-dragging. This is most cleanly illustrated when the intrinsic angular momentum (measured by the Komar integral) of the S^3 black hole is set to zero, $J_{\text{Komar}}^{\text{BH}} = 0$. The angular velocity Ω^{BH} , however, is not zero but follows the behavior of the angular velocity Ω^{BR} of the black ring. We interpret this as frame-dragging: the rotating black ring drags the spacetime around with it, and in effect the black hole rotates too, despite having no intrinsic spin, $J_{\text{Komar}}^{\text{BH}} = 0$. It is exciting to have access to rotational frame-dragging in an exact solution.
- *Countering frame-dragging*: Counter-rotation makes it possible to tune the intrinsic rotation $J_{\text{Komar}}^{\text{BH}}$ of the S^3 black hole, so that it “cancels” the effect of dragging caused by the surrounding black ring. This gives a solution for which the angular velocity of the black hole vanishes: $\Omega^{\text{BH}} = 0$ while $J_{\text{Komar}}^{\text{BH}} \neq 0$.

We have found no black saturn configurations ($J = 0$ or J nonzero) for which the total horizon area of the S^3 black hole and black ring exceeds the area $a_{\text{H}}^{\text{Schw}}$ of the static 4+1-dimensional Schwarzschild black hole of the same ADM mass,¹ however there are saturn configurations with total area arbitrarily close to $a_{\text{H}}^{\text{Schw}}$ for any value of J . The resulting phase diagram of 4+1-dimensional black holes is discussed in more detail in [14], where black saturn thermodynamics is also studied.

It is worth noting that for 4+1-dimensional asymptotically flat black hole spacetimes the continuous non-uniqueness will go much further than the 2-fold continuous non-uniqueness of the simple black saturn system presented here. An obvious generalization of our solutions includes multiple rings of saturn. As argued above, the total mass and angular momentum can be distributed continuously between the n black objects in such a spacetime, subject to balance conditions, and the result is $2(n - 1)$ -fold continuous non-uniqueness. Including the second angular momentum gives doubly spinning multiple black saturns with $3(n - 1)$ -fold continuous non-uniqueness, also for the $J_1 = J_2 = 0$ configurations. If, as anticipated, the total area is bounded by $a_{\text{H}}^{\text{Schw}}$ for given total mass, each component of an n -black hole system will necessarily have smaller area as n increases.

Supersymmetric black hole solutions with one or more concentric balanced black rings around a rotating S^3 black hole were constructed by Gauntlett and Gutowski [15]. Being supersymmetric, the solutions are extremally charged and saturate the BPS bound of 4+1-dimensional supergravity with $U(1)$ vector multiplets. For the supersymmetric solutions, it is not possible to observe dragging effects or counter-rotation, as we do for our non-supersymmetric vacuum solutions, because the supersymmetric solutions have vanishing angular velocities. The first order nature of the supersymmetry conditions [16, 17] makes the construction of multi-black hole solutions a fairly straightforward superposition of harmonic functions. For non-supersymmetric black holes we do not have this luxury, and instead we have to solve the full second order Einstein’s equations.

The black saturn solution is found using the inverse scattering method. This solution generating method was first adapted to Einstein’s equations by Belinsky and Zakharov [18, 19], and has been used extensively to generate four-dimensional vacuum solutions (see for instance [20] and references therein). Recently, the inverse scattering method, and closely related solution generating techniques, have been applied to generate five-dimensional rotating black

¹This observation leads to the general expectation that for fixed mass the entropy of the d -dimensional Schwarzschild black hole serves as an upper bound on the total entropy in any stationary d -dimensional asymptotically flat balanced black hole vacuum spacetime.

hole vacuum solutions. The Myers-Perry black hole with two independent rotation parameters was constructed by a smart implementation of the inverse scattering method by Pomeransky [21]. Also, the unbalanced black ring with rotation on the S^2 was constructed [22, 23]; this solution was constructed independently in [24] without use of solution generating techniques. The original balanced S^1 rotating black ring [8] has also been constructed by these methods [25, 26]. Most recently, Pomeransky and Sen'kov have succeeded in constructing a doubly-spinning black ring solution [27] using the inverse scattering method (numerical results were also obtained recently [28]).

We briefly review relevant aspects of the inverse scattering method in section 5.2, where we also provide details of the construction of the black saturn solution. Section 5.3 contains an analysis of the solution, including computations of the physical parameters and the balance condition. The physics of the black saturn system is studied in section 5.4. Open questions are discussed in section 5.5.

5.2 Construction of the solution

We review in section 5.2.1 the inverse scattering method with focus on the Belinsky-Zakharov (BZ) n -soliton transformations [18, 19] (a detailed review can be found in the book [20]). In section 5.2.2 we discuss the seed solution and generate the black saturn solution by soliton transformations. The final result for the metric is presented in section 5.2.3.

5.2.1 The inverse scattering method

The inverse scattering method can be used as a solution generating method for stationary axisymmetric spacetimes. These are D -dimensional spacetimes with $D - 2$ commuting Killing vector fields, one of which is time. The method allows construction of new solutions from known ones by means of purely algebraic manipulations.

We write the D -dimensional stationary axisymmetric spacetime as

$$ds^2 = G_{ab} dx^a dx^b + e^{2\nu} (d\rho^2 + dz^2) , \quad (5.2.1)$$

where $a, b = 1, \dots, D - 2$ and all components of the metric are functions of ρ and z only: $G_{ab} = G_{ab}(\rho, z)$ and $\nu = \nu(\rho, z)$. Without loss of generality the coordinates can be chosen such that

$$\det G = -\rho^2 . \quad (5.2.2)$$

Then Einstein's equations separate into two groups, one for the $(D - 2) \times (D - 2)$ matrix G ,

$$\partial_\rho U + \partial_z V = 0 , \quad (5.2.3)$$

where

$$U = \rho (\partial_\rho G) G^{-1} , \quad V = \rho (\partial_z G) G^{-1} , \quad (5.2.4)$$

and the other for the metric factor $e^{2\nu}$,

$$\partial_\rho \nu = \frac{1}{2} \left[-\frac{1}{\rho} + \frac{1}{4\rho} \text{Tr}(U^2 - V^2) \right] , \quad \partial_z \nu = \frac{1}{4\rho} \text{Tr}(UV) . \quad (5.2.5)$$

The equations (5.2.5) for ν satisfy the integrability condition $\partial_\rho \partial_z \nu = \partial_z \partial_\rho \nu$ as a consequence of (5.2.3). Hence, once a solution $G_{ij}(\rho, z)$ to (5.2.3) is found, one can determine $\nu(\rho, z)$ by direct integration.

The matrix equations (5.2.2) and (5.2.3) form a completely integrable system, meaning that one can find a set of spectral equations (a ‘‘Lax pair’’ or ‘‘L-A pair’’) whose compatibility conditions are exactly (5.2.2) and (5.2.3). The spectral equations for (5.2.2) and (5.2.3) are

$$D_1 \Psi = \frac{\rho V - \lambda U}{\lambda^2 + \rho^2} \Psi, \quad D_2 \Psi = \frac{\rho U + \lambda V}{\lambda^2 + \rho^2} \Psi, \quad (5.2.6)$$

with commuting differential operators D_1 and D_2 given by

$$D_1 = \partial_z - \frac{2\lambda^2}{\lambda^2 + \rho^2} \partial_\lambda, \quad D_2 = \partial_\rho + \frac{2\lambda\rho}{\lambda^2 + \rho^2} \partial_\lambda, \quad (5.2.7)$$

The complex spectral parameter λ is independent of ρ and z , and the generating function $\Psi(\lambda, \rho, z)$ is a $(D-2) \times (D-2)$ matrix such that $\Psi(0, \rho, z) = G(\rho, z)$.

The linearity of (5.2.6) allows algebraic construction of new solutions from known solutions based on the ‘‘dressing method’’. Given a known ‘‘seed’’ solution G_0 , one constructs the corresponding matrices U_0 and V_0 in (5.2.4), and determines a generating matrix ψ_0 which solves (5.2.6) with U_0 and V_0 . Then one seeks a new solution of the form

$$\Psi = \chi \Psi_0, \quad (5.2.8)$$

where $\chi = \chi(\lambda, \rho, z)$ is the dressing matrix. Inserting (5.2.8) into (5.2.6) now gives a set of equations for χ . The matrix χ is further constrained by requiring that the new metric $G = \Psi(\lambda = 0, \rho, z)$ is real and symmetric.

We are here interested in so-called ‘‘ n -soliton’’ dressing matrices, which are characterized by having n simple poles in the complex λ -plane, and we further restrict to cases where the poles are located on the real axis; this determines the location of the poles to be [18, 19, 20]

$$\tilde{\mu}_k = \pm \sqrt{\rho^2 + (z - a_k)^2} - (z - a_k), \quad (5.2.9)$$

where a_k are n real constants. We refer to the ‘‘+’’ pole as a soliton and denote it by μ_k , while the ‘‘-’’ pole is an anti-soliton denoted by $\bar{\mu}_k$. Note $\mu_k \bar{\mu}_k = -\rho^2$.

In addition to the n real constants a_k , an n -soliton transformation is determined by n arbitrary constant real $(D-2)$ -component vectors $m_0^{(k)}$, which we shall refer to as the BZ vectors. The components of these vectors will be called BZ parameters. In our applications, the BZ vectors control the addition of angular momentum to a static seed solution.

Given a seed solution G_0 , the n -soliton transformation yields a new solution G with components

$$G_{ab} = (G_0)_{ab} - \sum_{k,l=1}^n \frac{(G_0)_{ac} m_c^{(k)} (\Gamma^{-1})_{kl} m_d^{(l)} (G_0)_{db}}{\tilde{\mu}_k \tilde{\mu}_l}. \quad (5.2.10)$$

(Repeated spacetime indices $a, b, c, d = 1, \dots, D-2$ are summed.) The components of the vectors $m^{(k)}$ are

$$m_a^{(k)} = m_{0b}^{(k)} [\Psi_0^{-1}(\tilde{\mu}_k, \rho, z)]_{ba}, \quad (5.2.11)$$

where Ψ_0 is the generating matrix which solves (5.2.6) with U_0 and V_0 determined by G_0 as in (5.2.4), and $m_{0b}^{(k)}$ are the BZ parameters.

The symmetric matrix Γ is defined as

$$\Gamma_{kl} = \frac{m_a^{(k)} (G_0)_{ab} m_b^{(l)}}{\rho^2 + \tilde{\mu}_k \tilde{\mu}_l}, \quad (5.2.12)$$

and the inverse Γ^{-1} of Γ appears in (5.2.10).

The new matrix G of (5.2.10) does not obey (5.2.2); instead, an n -soliton transformation gives

$$\det G = (-1)^n \rho^{2n} \left(\prod_{k=1}^n \tilde{\mu}_k^{-2} \right) \det G_0, \quad (5.2.13)$$

with $\det G_0 = -\rho^2$. One can deal with this problem and obtain a physical solution $G^{(\text{ph})}$ such that $\det G^{(\text{ph})} = -\rho^2$, by multiplying G by a suitable factor of ρ and $\tilde{\mu}_k$'s. In four spacetime dimensions, this method of uniform renormalization works well and allows one to construct for instance (multi)Kerr-NUT solutions from just flat Minkowski space. In higher dimensions, however, uniform renormalization typically leads to nakedly singular solutions.

One way around this problem is to restrict the soliton transformation to a 2×2 block of the seed solution and perform uniform renormalization on this block. This has been applied to reproduce black ring solutions with a single angular momentum [23, 26]. The drawback of this method is clearly that it can only produce solutions with rotation in at most a single plane. This would be sufficient for our purposes here, but we prefer to present the solution generating method in a more general setting so as to facilitate generalization of our black saturn solution to include angular momentum in two independent planes. We therefore follow the strategy of [21] which is applicable in any spacetime dimension and does not suffer from the above-mentioned limitations.

The idea is to note that the factor multiplying $\det G_0$ in (5.2.13) is independent of the BZ vectors $m_0^{(k)}$. Start with a diagonal seed solution $(G_0, e^{2\nu_0})$ and remove first solitons with trivial BZ parameters (so as to not introduce any off-diagonal components in the matrix G). Then add back the *same* solitons but now with general BZ parameters. The resulting solution G satisfies $\det G = -\rho^2$ by construction. Moreover, the metric factor $e^{2\nu}$ of the full solution can easily be obtained from the seed G_0 as [21]

$$e^{2\nu} = e^{2\nu_0} \frac{\det \Gamma_{kl}}{\det \Gamma_{kl}^{(0)}}, \quad (5.2.14)$$

where $\Gamma^{(0)}$ and Γ are constructed as in (5.2.12) using G_0 and G , respectively.

We now turn from the general discussion to the construction of the black saturn solution.

5.2.2 Seed and soliton transformation for black saturn

For the analysis of axisymmetric solutions we make use of the results of [29, 30]. We refer to these papers for general discussions of higher-dimensional Weyl solutions and the analysis of the corresponding rod configurations.

The rod configuration for the seed of black saturn is shown in figure 5.1. The thick solid black lines correspond to rod sources of uniform density $+1/2$, whereas the dashed line segment corresponds to a rod source of uniform negative density $-1/2$. The rods in the t direction correspond to black hole horizons. Note that for $a_1 = a_5$ the negative rod is eliminated and the solution describes a static black ring around an S^3 black hole. This is an unbalanced

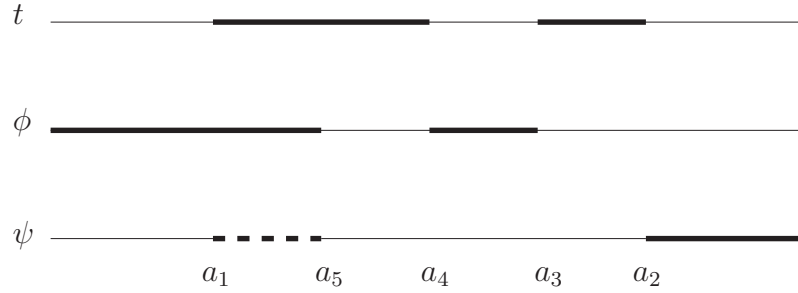


Figure 5.1: Sources for the seed metric G_0 . The solid rods have positive density and the dashed rod has negative density. The rods are located at the z -axis with $\rho = 0$ and add up to an infinite rod with uniform density such that $\det G_0 = -\rho^2$. The labeling of the rod endpoints is a little untraditional, but is simply motivated by the fact that we are going to use the inverse scattering method to add solitons at $z = a_1, a_2$ and a_3 .

configuration with a conically singular membrane keeping the black ring and the S^3 black hole apart. The negative density rod is included in order to facilitate adding angular momentum to the black ring.

Using the techniques of [29] we construct the full 4+1-dimensional vacuum solution corresponding to the rod configuration in figure 5.1. We find

$$G_0 = \text{diag} \left\{ -\frac{\mu_1 \mu_3}{\mu_2 \mu_4}, \frac{\rho^2 \mu_4}{\mu_5 \mu_3}, \frac{\mu_5 \mu_2}{\mu_1} \right\}, \quad \det G_0 = -\rho^2. \quad (5.2.15)$$

The first term in G_0 corresponds to the tt -component, the second to the $\phi\phi$ -component and the third to the $\psi\psi$ -component. The μ_i are ‘‘solitons’’ as introduced in (5.2.9), i.e.

$$\mu_i = \sqrt{\rho^2 + (z - a_i)^2} - (z - a_i), \quad (5.2.16)$$

where the a_i are the rod endpoints in figure 5.1. The metric factor $e^{2\nu}$ of the seed can be written as

$$e^{2\nu} = k^2 \frac{\mu_2 \mu_5 (\rho^2 + \mu_1 \mu_2)^2 (\rho^2 + \mu_1 \mu_4) (\rho^2 + \mu_1 \mu_5) (\rho^2 + \mu_2 \mu_3) (\rho^2 + \mu_3 \mu_4)^2 (\rho^2 + \mu_4 \mu_5)}{\mu_1 (\rho^2 + \mu_3 \mu_5) (\rho^2 + \mu_1 \mu_3) (\rho^2 + \mu_2 \mu_4) (\rho^2 + \mu_2 \mu_5) \prod_{i=1}^5 (\rho^2 + \mu_i^2)}. \quad (5.2.17)$$

The integration constant k will be fixed in section 5.3.3 for the full black saturn solution.

We assume the ordering

$$a_1 \leq a_5 \leq a_4 \leq a_3 \leq a_2 \quad (5.2.18)$$

of the rod endpoints.²

The solution (5.2.15) and (5.2.17) with the ordering (5.2.18) is singular and not in itself of physical interest. However, with a 1-soliton transformation we add an anti-soliton which mixes the t and ψ directions in such a way that the negative density rod moves to the t -direction and cancels the segment $[a_1, a_5]$ of the positive density rod. It turns out that this leaves a naked singularity at $z = a_1$, but choosing the BZ vector appropriately completely eliminates that

²If instead we had chosen the different ordering $a_5 \leq a_1 \leq a_4 \leq a_3 \leq a_2$, then there would have been no negative density rod, and the solution (5.2.15) and (5.2.17) would describe two S^3 black holes and two conical singularities, one for each of the two finite rods in the angular directions. We will not use this ordering, but always take the rod endpoints to satisfy (5.2.18).

singularity (see section 5.3.2). Taking $a_2 = a_3$ in the seed solution, this 1-soliton transformation gives the S^1 rotating black ring of [8]. We show this explicitly in appendix 5.A.2.

Keeping $a_3 < a_2$, the above sketched 1-soliton transformation gives a rotating black ring around an S^3 black hole. This configuration can be balanced and we study its physical properties in detail in section 5.4.3. Including two more soliton transformations allow us to give the S^3 black hole independent rotation in two planes. The steps of generating the black saturn solution by a 3-soliton transformations are as follows:

1. Perform the following three 1-soliton transformations on the seed solution (5.2.15):

- Remove an anti-soliton at $z = a_1$ with trivial BZ vector $(1,0,0)$; this is equivalent to dividing $(G_0)_{tt}$ by $-\rho^2/\bar{\mu}_1^2 = -\mu_1^2/\rho^2$.
- Remove a soliton at $z = a_2$ with trivial BZ vector $(1,0,0)$; this is equivalent to dividing $(G_0)_{tt}$ by $(-\rho^2/\mu_2^2)$.
- Remove an anti-soliton at $z = a_3$ with trivial BZ vector $(1,0,0)$; this is equivalent to dividing $(G_0)_{tt}$ by $-\rho^2/\bar{\mu}_3^2 = -\mu_3^2/\rho^2$.

The result is the metric matrix

$$G'_0 = \text{diag} \left\{ \frac{\rho^2 \mu_2}{\mu_1 \mu_3 \mu_4}, \frac{\rho^2 \mu_4}{\mu_3 \mu_5}, \frac{\mu_2 \mu_5}{\mu_1} \right\}. \quad (5.2.19)$$

2. Rescale G'_0 by a factor of $\frac{\mu_1 \mu_3}{\rho^2 \mu_2}$ to find

$$\tilde{G}_0 = \frac{\mu_1 \mu_3}{\rho^2 \mu_2} G'_0 = \text{diag} \left\{ \frac{1}{\mu_4}, \frac{\mu_1 \mu_4}{\mu_2 \mu_5}, -\frac{\mu_3}{\bar{\mu}_5} \right\}, \quad (5.2.20)$$

where $\bar{\mu}_5 = -\rho^2/\mu_5$. This will be the seed for the next soliton transformation.

3. The generating matrix

$$\tilde{\Psi}_0(\lambda, \rho, z) = \text{diag} \left\{ \frac{1}{(\mu_4 - \lambda)}, \frac{(\mu_1 - \lambda)(\mu_4 - \lambda)}{(\mu_2 - \lambda)(\mu_5 - \lambda)}, -\frac{(\mu_3 - \lambda)}{(\bar{\mu}_5 - \lambda)} \right\} \quad (5.2.21)$$

solves (5.2.6) with \tilde{G}_0 . Note $\tilde{\Psi}(0, \rho, z) = \tilde{G}_0$.

4. Perform now a 3-soliton transformation with \tilde{G}_0 as seed:

- Add an anti-soliton at $z = a_1$ (pole at $\lambda = \bar{\mu}_1$) with BZ vector $m_0^{(1)} = (1, 0, c_1)$,
- Add a soliton at $z = a_2$ (pole at $\lambda = \mu_2$) with BZ vector $m_0^{(2)} = (1, 0, c_2)$, and
- Add an anti-soliton at $z = a_3$ (pole at $\lambda = \bar{\mu}_3$) with BZ vector $m_0^{(3)} = (1, b_3, 0)$.

Denote the resulting metric \tilde{G} . The constants c_1 , c_2 , and b_3 are the BZ parameters of the transformation.

5. Rescale \tilde{G} to find

$$G = \frac{\rho^2 \mu_2}{\mu_1 \mu_3} \tilde{G}. \quad (5.2.22)$$

This is needed to undo the rescaling of step 2, so that $\det G = -\rho^2$.

6. Construct $e^{2\nu}$ using (5.2.14). Note that Γ was found in the process of constructing G and that $\Gamma_0 = \Gamma|_{c_1=c_2=b_3=0}$. The result $(G, e^{2\nu})$ is the solution we want.

Some comments are in order. First, the rescaling in step 2 is simply a choice of convenience that yields a simple form for the generating matrix $\tilde{\Psi}_0$. Secondly, with $c_1 = c_2 = b_3 = 0$, the effect of the 3-soliton transformation in step 4 is simply to undo the transformation of step 1. Since (5.2.13) is independent of the BZ parameters c_1 , c_2 and b_3 , we are guaranteed to have $\det G = \det G_0 = -\rho^2$, after step 5 has undone the rescaling of step 2. Finally, in step 4 we could have added the (anti-)solitons with general BZ vectors $m_0^{(k)} = (a^{(k)}, b^{(k)}, c^{(k)})$ for $k = 1, 2, 3$. However, $b^{(k)} \neq 0$, $k = 1, 2$, or $c^{(3)} \neq 0$ lead to irremovable singularities and we therefore set $b^{(1)} = b^{(2)} = c^{(3)} = 0$. Finally, the solution is invariant under rescalings of the BZ vectors, $m_0^{(k)} \rightarrow \sigma_k m_0^{(k)}$ (no sum on k) for any nonzero σ_k , and we use the scaling freedom to set $a^{(k)} = 1$ without loss of generality.

In this paper we focus entirely on the black saturn solution with angular momentum only in a single plane, so we set $b_3 = 0$ in the following. The more general solution with $b_3 \neq 0$ remains to be analyzed.

2-soliton transformation

With $b_3 = 0$ the transformation described above is essentially a 2-soliton transformation. In fact, the saturn solution with $b_3 = 0$ can be produced by a 2-soliton transformation in much the same way as above. The resulting metric takes a slightly different form, but can be shown, using the explicit form of the μ_i 's in (5.2.16), to be identical to the metric resulting from the 3-soliton transformation after a constant rescaling of the BZ parameters c_1 and c_2 .

5.2.3 Saturn solution

The black saturn solution constructed by the above 3-soliton transformation with $b_3 = 0$ can be written³

$$ds^2 = -\frac{H_y}{H_x} \left[dt + \left(\frac{\omega_\psi}{H_y} + q \right) d\psi \right]^2 + H_x \left\{ k^2 P (d\rho^2 + dz^2) + \frac{G_y}{H_y} d\psi^2 + \frac{G_x}{H_x} d\phi^2 \right\}. \quad (5.2.23)$$

For convenience we have chosen to write $e^{2\nu} = k^2 H_x P$. Here k is the integration constant for the metric factor $e^{2\nu_0}$ given in (5.2.17), and $G_{x,y}$, $H_{x,y}$, and P are functions of ρ and z which will be given below. The constant q is included in order to ensure asymptotic flatness (we determine the value of q in the analysis of section 5.3.3).

With $b_3 = 0$, our soliton transformations leave the $\phi\phi$ -part of the metric invariant, so from the static seed (5.2.15) we have

$$G_x = (G_0)_{\phi\phi} = \frac{\rho^2 \mu_4}{\mu_3 \mu_5}. \quad (5.2.24)$$

The metric (5.2.23) involves the functions

$$P = (\mu_3 \mu_4 + \rho^2)^2 (\mu_1 \mu_5 + \rho^2) (\mu_4 \mu_5 + \rho^2), \quad (5.2.25)$$

³After performing the BZ transformation, we shift t as $t \rightarrow t - q\psi$ in order to ensure asymptotic flatness. At this point ψ is not assumed to be periodic so the shift does not effect the global structure of the solution. The periodicities of ψ and ϕ will be fixed in section 5.3. We have also reversed the sense of rotation by taking $\psi \rightarrow -\psi$.

and

$$H_x = F^{-1} \left[M_0 + c_1^2 M_1 + c_2^2 M_2 + c_1 c_2 M_3 + c_1^2 c_2^2 M_4 \right], \quad (5.2.26)$$

$$H_y = F^{-1} \frac{\mu_3}{\mu_4} \left[M_0 \frac{\mu_1}{\mu_2} - c_1^2 M_1 \frac{\rho^2}{\mu_1 \mu_2} - c_2^2 M_2 \frac{\mu_1 \mu_2}{\rho^2} + c_1 c_2 M_3 + c_1^2 c_2^2 M_4 \frac{\mu_2}{\mu_1} \right], \quad (5.2.27)$$

where

$$M_0 = \mu_2 \mu_5^2 (\mu_1 - \mu_3)^2 (\mu_2 - \mu_4)^2 (\rho^2 + \mu_1 \mu_2)^2 (\rho^2 + \mu_1 \mu_4)^2 (\rho^2 + \mu_2 \mu_3)^2, \quad (5.2.28)$$

$$M_1 = \mu_1^2 \mu_2 \mu_3 \mu_4 \mu_5 \rho^2 (\mu_1 - \mu_2)^2 (\mu_2 - \mu_4)^2 (\mu_1 - \mu_5)^2 (\rho^2 + \mu_2 \mu_3)^2, \quad (5.2.29)$$

$$M_2 = \mu_2 \mu_3 \mu_4 \mu_5 \rho^2 (\mu_1 - \mu_2)^2 (\mu_1 - \mu_3)^2 (\rho^2 + \mu_1 \mu_4)^2 (\rho^2 + \mu_2 \mu_5)^2, \quad (5.2.30)$$

$$M_3 = 2\mu_1 \mu_2 \mu_3 \mu_4 \mu_5 (\mu_1 - \mu_3) (\mu_1 - \mu_5) (\mu_2 - \mu_4) (\rho^2 + \mu_1^2) (\rho^2 + \mu_2^2) \\ \times (\rho^2 + \mu_1 \mu_4) (\rho^2 + \mu_2 \mu_3) (\rho^2 + \mu_2 \mu_5), \quad (5.2.31)$$

$$M_4 = \mu_1^2 \mu_2 \mu_3^2 \mu_4^2 (\mu_1 - \mu_5)^2 (\rho^2 + \mu_1 \mu_2)^2 (\rho^2 + \mu_2 \mu_5)^2, \quad (5.2.32)$$

and

$$F = \mu_1 \mu_5 (\mu_1 - \mu_3)^2 (\mu_2 - \mu_4)^2 (\rho^2 + \mu_1 \mu_3) (\rho^2 + \mu_2 \mu_3) (\rho^2 + \mu_1 \mu_4) \\ \times (\rho^2 + \mu_2 \mu_4) (\rho^2 + \mu_2 \mu_5) (\rho^2 + \mu_3 \mu_5) \prod_{i=1}^5 (\rho^2 + \mu_i^2). \quad (5.2.33)$$

Finally we have

$$G_y = \frac{\mu_3 \mu_5}{\mu_4}, \quad (5.2.34)$$

and the off-diagonal part of the metric is given by

$$\omega_\psi = 2 \frac{c_1 R_1 \sqrt{M_0 M_1} - c_2 R_2 \sqrt{M_0 M_2} + c_1^2 c_2 R_2 \sqrt{M_1 M_4} - c_1 c_2^2 R_1 \sqrt{M_2 M_4}}{F \sqrt{G_x}}. \quad (5.2.35)$$

Here $R_i = \sqrt{\rho^2 + (z - a_i)^2}$.

Setting $c_1 = c_2 = 0$ gives $\omega_\psi = 0$ and $G_y H_x / H_y = \mu_2 \mu_5 / \mu_1 = (G_0)_{\psi\psi}$. The full solution can be seen to simply reduce to the seed solution (5.2.15) and (5.2.17) in this limit.

Taking $c_1 = 0$ and then setting $a_1 = a_5 = a_4$ we obtain the singly spinning Myers-Perry black hole, which was constructed similarly in [21]. For details, see appendix 5.A.1. Taking instead $c_2 = 0$ and then setting $a_2 = a_3$ we obtain the S^1 spinning black ring of [8]. Appendix 5.A.2 presents the explicit coordinate transformation from Weyl coordinates (ρ, z) to ring coordinates (x, y) . The black ring was obtained in [25] and [26] with a different transformation which involved two solitons and started with a different seed metric. The 1-soliton transformation used here appears to be simpler.⁴

It is useful to note that the only effect of changing the signs of both BZ parameters c_1 and c_2 , taking $(c_1, c_2) \rightarrow (-c_1, -c_2)$, is a change of sense of the overall direction of rotation, i.e. the only effect is $G_{t\psi} \rightarrow -G_{t\psi}$.

⁴We thank Roberto Emparan for sharing with us the idea of obtaining the S^1 -spinning black ring by a 1-soliton transformation.

The metric (5.2.23) is sufficiently complicated that it is difficult to check algebraically that the Einstein vacuum equations are solved. We have resorted to numerical methods in order to check the vanishing of all components of the Ricci tensor.

Next we present an analysis of the main properties of the black saturn solution.

5.3 Analysis

We introduce a convenient parameterization of the solution, and then analyze the rod structure. The BZ parameter c_1 will be fixed in order to eliminate the singularity left-over from the negative density rod of the seed solution. Next it is shown that the solution is asymptotically flat. Regularity is analyzed and the balance condition obtained by elimination of a conical singularity. We analyze the horizon structure, and compute a number of physical quantities for the solution: the ADM mass and angular momentum, as well as angular velocities, temperatures and horizon areas of the two black holes. We compute the Komar integrals for mass and angular momentum and obtain a Smarr relation. We study various limits of the solution, and we comment on the analysis of closed timelike curves (of which we find none).

5.3.1 Parameterization

The seed solution (5.2.15)-(5.2.17) contains five dimensionfull parameters, namely the rod endpoints a_i , $i = 1, \dots, 5$. Since the whole rod configuration can be shifted along the z -axis without changing the solution, the description in terms of the a_i 's is redundant; in addition to the ordering (5.2.18) and the directions of the rods as given in figure 5.1 we only need the lengths of the rods. It is useful to also take out the overall scale of the solution so that the seed solution is described in terms of three dimensionless parameters and an overall scale.

We choose the overall scale L to be⁵

$$L^2 = a_2 - a_1, \quad (5.3.1)$$

and we introduce three dimensionless parameters κ_i as

$$\kappa_i = \frac{a_{i+2} - a_1}{L^2}, \quad \text{for } i = 1, 2, 3. \quad (5.3.2)$$

As a consequence of the ordering (5.2.18), the κ_i 's satisfy

$$0 \leq \kappa_3 \leq \kappa_2 < \kappa_1 \leq 1. \quad (5.3.3)$$

(We exclude $\kappa_2 = \kappa_1$ for the balanced solution for reasons which will be apparent in section 5.3.4.) We shift and scale the z coordinate accordingly: set

$$z = L^2 \bar{z} + a_1. \quad (5.3.4)$$

Then \bar{z} is dimensionless. As we shall see in the following, the black ring horizon is located at $\rho = 0$ for $\bar{z} \in [\kappa_3, \kappa_2]$, and the S^3 black hole horizon at $\rho = 0$ for $\bar{z} \in [\kappa_1, 1]$.

The new parameterization effectively corresponds to taking

$$a_1 \rightarrow 0, \quad a_5 \rightarrow \kappa_3, \quad a_4 \rightarrow \kappa_2, \quad a_3 \rightarrow \kappa_1, \quad a_2 \rightarrow 1, \quad (5.3.5)$$

⁵The coordinates ρ and z , and hence the rod endpoints a_i , have dimensions (length)².

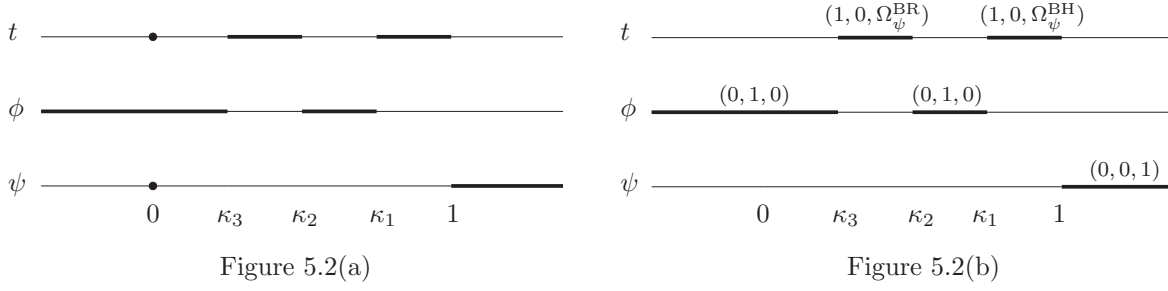


Figure 5.2: Rod structure of the black saturn solution. Note that the rods are placed on the \bar{z} -axis, see section 5.3.2 for the definition of \bar{z} . The dots in figure 5.2(a) denote singularities at $\bar{z} = 0$, which are removed by the fixing c_1 according to (5.3.7) (figure 5.2(b)). This choice makes the $\rho = 0$ metric smooth across $\bar{z} = 0$. Figure 5.2(b) also shows the directions of the rods.

while carefully keeping track of the scale L .

The soliton transformations introduce the two dimensionfull BZ parameters, c_1 and c_2 . It is convenient to redefine the BZ parameter c_2 by introducing the dimensionless parameter \bar{c}_2 as

$$\bar{c}_2 = \frac{c_2}{c_1(1 - \kappa_2)}. \quad (5.3.6)$$

With this parameterization many expressions for the physical parameters simplify.

5.3.2 Rod structure

The rod structure at $\rho = 0$ is illustrated in figure 5.2. Harmark [30] introduces the “direction” of a given rod as the zero eigenvalue eigenvector of the metric matrix G at $\rho = 0$. The direction of each rod is indicated in figure 5.2(b). To summarize:

- The semi-infinite rod $\bar{z} \in] - \infty, \kappa_3]$ and the finite rod $[\kappa_2, \kappa_1]$ have directions $(0, 1, 0)$, i.e. they are sources for the $\phi\phi$ -part of the metric.
- The semi-infinite rod $[1, \infty[$ has direction $(0, 0, 1)$, i.e. it is sourcing the $\psi\psi$ -part of the metric.
- The finite rod $[\kappa_3, \kappa_2]$ corresponds to the location of the black ring horizon. It has direction $(1, 0, \Omega_\psi^{\text{BR}})$. The finite rod $[\kappa_1, 1]$ corresponds to the location of the S^3 black hole horizon. It has direction $(1, 0, \Omega_\psi^{\text{BH}})$. The angular velocities Ω_ψ^{BR} and Ω_ψ^{BH} will be given in section 5.3.5.

Note that the negative density rod of the seed solution figure 5.1 is no longer present. The soliton transformation which added the anti-soliton at $z = a_1$ has made the $+1/2$ and $-1/2$ density rods in the t and ψ direction cancel. However, the cancellation of the rods left a singularity at $z = a_1$, i.e. $\bar{z} = 0$. This shows up as a $(z - a_1)^{-1} \sim \bar{z}^{-1}$ divergence in G_{tt} and $G_{\psi\psi}$, as indicated by dots in figure 5.2(a). Luckily, the singularities are removed completely by setting

$$|c_1| = L \sqrt{\frac{2\kappa_1\kappa_2}{\kappa_3}}. \quad (5.3.7)$$

With c_1 fixed according to (5.3.7), the metric at $\rho = 0$ is completely smooth across $\bar{z} = 0$. This means that we have successfully removed the negative density rod at $\bar{z} \in [0, \kappa_3]$ ($z \in [a_1, a_5]$), and there is no longer any significance to the point $\bar{z} = 0$ ($z = a_1$) in the metric, as illustrated in figure 5.2(b).

The condition (5.3.7) will be imposed throughout the rest of the paper. Since $(c_1, c_2) \rightarrow (-c_1, -c_2)$ just changes the overall direction of rotation, we choose $c_1 > 0$ without loss of generality.

5.3.3 Asymptotics

We introduce asymptotic coordinates (r, θ)

$$\rho = \frac{1}{2}r^2 \sin 2\theta, \quad z = \frac{1}{2}r^2 \cos 2\theta, \quad (5.3.8)$$

such that

$$d\rho^2 + dz^2 = r^2 (dr^2 + r^2 d\theta^2). \quad (5.3.9)$$

The asymptotic limit is $r^2 = 2\sqrt{\rho^2 + z^2} \rightarrow \infty$. Requiring that $G_{t\psi} \rightarrow 0$ when $r \rightarrow \infty$ determines the constant q in the metric (5.2.23) to be

$$q = L \sqrt{\frac{2\kappa_1\kappa_2}{\kappa_3}} \frac{\bar{c}_2}{1 + \kappa_2 \bar{c}_2}. \quad (5.3.10)$$

We have used the definition (5.3.6) of \bar{c}_2 and imposed (5.3.7) for c_1 .

To leading order, the asymptotic metric is

$$e^{2\nu} = k^2 \left[1 + \kappa_2 \bar{c}_2 \right]^2 \frac{1}{r^2} + \dots, \quad (5.3.11)$$

which motivates us to choose the constant k to be

$$k = \left| 1 + \kappa_2 \bar{c}_2 \right|^{-1}. \quad (5.3.12)$$

We shall assume⁶ that $\bar{c}_2 \neq -\kappa_2^{-1}$. The asymptotic metric then takes the form

$$ds^2 = -dt^2 + dr^2 + r^2 d\theta^2 + r^2 \sin^2 \theta d\psi^2 + r^2 \cos^2 \theta d\phi^2. \quad (5.3.13)$$

Below we show that the angles ψ and ϕ have periodicities

$$\Delta\psi = \Delta\phi = 2\pi, \quad (5.3.14)$$

so that the solution indeed is asymptotically flat.

⁶The solution with $\bar{c}_2 = -\kappa_2^{-1}$ is nakedly singular. See sections 5.3.4 and 5.4.6 for further comments.

5.3.4 Regularity and balance

In order to avoid a conical singularity at the location of a rod, the period $\Delta\eta$ of a spacelike coordinate $\eta(=\psi, \phi)$ must be fixed as

$$\Delta\eta = 2\pi \lim_{\rho \rightarrow 0} \sqrt{\frac{\rho^2 e^{2\nu}}{g_{\eta\eta}}} . \quad (5.3.15)$$

Requiring regularity on the rod $\bar{z} \in [1, \infty]$ fixes the period of ψ to be $\Delta\psi = 2\pi$, and regularity on the rod $\bar{z} \in [-\infty, \kappa_3]$ determines $\Delta\phi = 2\pi$. We have used (5.3.7) and (5.3.12).⁷ According to the discussion in the previous section this ensures asymptotic flatness of the solution.

Next we consider regularity as $\rho \rightarrow 0$ for the finite rod $\bar{z} \in [\kappa_2, \kappa_1]$. Eq. (5.3.15) gives

$$\Delta\phi = 2\pi \frac{\kappa_1 - \kappa_2}{|1 + \kappa_2 \bar{c}_2| \sqrt{\kappa_1(1 - \kappa_2)(1 - \kappa_3)(\kappa_1 - \kappa_3)}} . \quad (5.3.16)$$

When no constraints other than (5.3.7) are imposed, the metric has a conical singular membrane in the plane of the ring, extending from the inner S^1 radius of the black ring to the horizon of the S^3 black hole.

We can avoid this conical singularity and balance the solution by requiring the right hand side of (5.3.16) to be equal to 2π . Solving for \bar{c}_2 this gives us the balancing, or equilibrium, condition for black saturn, i.e.

$$\bar{c}_2 = \frac{1}{\kappa_2} \left[\epsilon \frac{\kappa_1 - \kappa_2}{\sqrt{\kappa_1(1 - \kappa_2)(1 - \kappa_3)(\kappa_1 - \kappa_3)}} - 1 \right] , \quad \text{with} \quad \begin{cases} \epsilon = +1 & \text{when } \bar{c}_2 > -\kappa_2^{-1} \\ \epsilon = -1 & \text{when } \bar{c}_2 < -\kappa_2^{-1} \end{cases} . \quad (5.3.17)$$

The solution with $\bar{c}_2 = -\kappa_2^{-1}$ is nakedly singular. Thus the choice of sign ϵ divides the balanced black saturn solutions into two separate sectors. The limit of removing the S^3 black hole to leave just the balanced black ring requires setting $\bar{c}_2 = 0$ and according to (5.3.17) this is only possible for $\epsilon = +1$. We are going to study the $\epsilon = +1$ solutions in detail in section 5.4, but will also discuss some properties of the $\epsilon = -1$ solutions (see sections 5.3.7 and 5.4.6).

5.3.5 Horizons

The rod analysis of section 5.3.2 showed that the two horizon rods had directions $(1, 0, \Omega_\psi^i)$, $i = \text{BR, BH}$, for the black ring and the S^3 black hole. Equivalently, the Killing vectors $\xi = \partial_t + \Omega_\psi^i \partial_\psi$ are null on the respective horizons. The angular velocities Ω_ψ^i are

$$\Omega_\psi^{\text{BH}} = \frac{1}{L} [1 + \kappa_2 \bar{c}_2] \sqrt{\frac{\kappa_2 \kappa_3}{2\kappa_1}} \frac{\kappa_3(1 - \kappa_1) - \kappa_1(1 - \kappa_2)(1 - \kappa_3)\bar{c}_2}{\kappa_3(1 - \kappa_1) + \kappa_1 \kappa_2(1 - \kappa_2)(1 - \kappa_3)\bar{c}_2^2} , \quad (5.3.18)$$

$$\Omega_\psi^{\text{BR}} = \frac{1}{L} [1 + \kappa_2 \bar{c}_2] \sqrt{\frac{\kappa_1 \kappa_3}{2\kappa_2}} \frac{\kappa_3 - \kappa_2(1 - \kappa_3)\bar{c}_2}{\kappa_3 - \kappa_3(\kappa_1 - \kappa_2)\bar{c}_2 + \kappa_1 \kappa_2(1 - \kappa_3)\bar{c}_2^2} . \quad (5.3.19)$$

The black ring and the S^3 black hole generally have different angular velocities.

⁷If we had not imposed the condition (5.3.7), which removes the singularity at $\bar{z} = 0$, then (5.3.15) would have given $\Delta\phi = \frac{\pi}{L} \sqrt{\frac{2\kappa_3}{\kappa_1 \kappa_2}} c_1$ for $\bar{z} \in [0, \kappa_3]$. Requiring $\Delta\phi = 2\pi$ is precisely the condition (5.3.7).

Myers-Perry black hole horizon geometry

One black hole horizon is located at $\rho = 0$ for $\kappa_1 \leq \bar{z} \leq 1$ and the metric on a spatial cross-section of the horizon can be written

$$ds_{\text{BH}}^2 = \frac{2L^2(\bar{z} - \kappa_1)(\bar{z} - \kappa_3)}{(\bar{z} - \kappa_2)} d\phi^2 + L^2 s_{\text{BH}}^2 g(\bar{z})(1 - \bar{z}) d\psi^2 + \frac{L^2(\bar{z} - \kappa_2) d\bar{z}^2}{(1 - \bar{z})(\bar{z} - \kappa_1)(\bar{z} - \kappa_3)g(\bar{z})}, \quad (5.3.20)$$

where the constant s_{BH} is

$$s_{\text{BH}} = \frac{\kappa_3(1 - \kappa_1) + \kappa_1\kappa_2(1 - \kappa_2)(1 - \kappa_3)\bar{c}_2^2}{\kappa_3\sqrt{(1 - \kappa_1)(1 - \kappa_2)(1 - \kappa_3)} [1 + \kappa_2\bar{c}_2]^2}, \quad (5.3.21)$$

and the function $g(\bar{z})$ is

$$\begin{aligned} g(\bar{z}) &= 2\kappa_1\kappa_3(1 - \kappa_1)(1 - \kappa_2)(1 - \kappa_3)(\bar{z} - \kappa_2) \\ &\times [1 + \kappa_2\bar{c}_2]^2 \left[(1 - \kappa_1)^2\kappa_3 \left[\kappa_1(\bar{z} - \kappa_2) - \kappa_3 \left(\kappa_1 - \kappa_2(1 - \bar{z})^2 - \kappa_1\kappa_2(2 - \bar{z}) \right) \right] \right. \\ &\quad + 2\kappa_1\kappa_2\kappa_3(1 - \kappa_1)(1 - \kappa_2)(1 - \kappa_3)(1 - \bar{z})(\bar{z} - \kappa_1)\bar{c}_2 \\ &\quad \left. + \kappa_1^2\kappa_2(1 - \kappa_2)^2(1 - \kappa_3)^2\bar{z}(\bar{z} - \kappa_1)\bar{c}_2^2 \right]^{-1}. \end{aligned} \quad (5.3.22)$$

Note that $s_{\text{BH}} \geq 0$. One can check that $g(\bar{z})$ is positive for $\kappa_1 \leq \bar{z} \leq 1$, so for $s_{\text{BH}} > 0$, the horizon is topologically an S^3 . Metrically the S^3 is distorted by rotation, as is the case for a Myers-Perry black hole, and here the horizon is further deformed by the presence of the black ring.

Black ring horizon geometry

The black ring horizon is located at $\rho = 0$ for $\kappa_3 \leq \bar{z} \leq \kappa_2$. The metric of a spatial cross section of the horizon can be written

$$ds_{\text{BR}}^2 = \frac{2L^2(\kappa_2 - \bar{z})(\bar{z} - \kappa_3)}{(\kappa_1 - \bar{z})} d\phi^2 + L^2 s_{\text{BR}}^2 f(\bar{z})(\kappa_1 - \bar{z}) d\psi^2 + \frac{L^2 d\bar{z}^2}{(\kappa_2 - \bar{z})(\bar{z} - \kappa_3)f(\bar{z})}, \quad (5.3.23)$$

where the constant s_{BR} is

$$s_{\text{BR}} = \sqrt{\frac{\kappa_2 - \kappa_3}{\kappa_1(\kappa_1 - \kappa_3)(1 - \kappa_3)} \frac{(\kappa_3 - \kappa_3(\kappa_1 - \kappa_2)\bar{c}_2 + \kappa_1\kappa_2(1 - \kappa_3)\bar{c}_2^2)}{\kappa_3 [1 + \kappa_2\bar{c}_2]^2}}, \quad (5.3.24)$$

and the function $f(\bar{z})$ is

$$\begin{aligned} f(\bar{z}) &= 2\kappa_1\kappa_3(\kappa_1 - \kappa_3)(1 - \kappa_3)(1 - \bar{z}) \\ &\times [1 + \kappa_2\bar{c}_2]^2 (\kappa_2 - \kappa_3)^{-1} \left[\kappa_3 \left[\kappa_2(\kappa_1 - \bar{z}) + \kappa_3 \left(\kappa_2(1 - \kappa_1(2 - \bar{z})) - \kappa_1(1 - \bar{z})^2 \right) \right] \right. \\ &\quad + 2\kappa_1\kappa_2\kappa_3(1 - \kappa_3)(1 - \bar{z})(\kappa_2 - \bar{z})\bar{c}_2 \\ &\quad \left. + \kappa_1\kappa_2^2(1 - \kappa_3)^2\bar{z}(\kappa_2 - \bar{z})\bar{c}_2^2 \right]^{-1}. \end{aligned} \quad (5.3.25)$$

It follows from (5.3.3) that $s_{\text{BR}} \geq 0$, and it can be checked that $f(\bar{z})$ is positive for $\kappa_3 \leq \bar{z} \leq \kappa_2$. The coordinate ψ parametrizes a circle whose radius depends on \bar{z} . The coordinates (\bar{z}, ϕ) parameterize a deformed two-sphere. The topology of the horizon is therefore $S^1 \times S^2$. As is the case for the black ring [8, 9], the metric of the horizon is not a direct product of the $S^1 \times S^2$ (contrary to the supersymmetric case [31, 33, 32, 15]). For black saturn the black ring horizon is further distorted by the presence of the S^3 black hole.

Horizon areas

It is straightforward to compute the horizon areas. We find

$$\mathcal{A}_{\text{BH}} = 4L^3\pi^2 \sqrt{\frac{2(1-\kappa_1)^3}{(1-\kappa_2)(1-\kappa_3)}} \frac{1 + \frac{\kappa_1\kappa_2(1-\kappa_2)(1-\kappa_3)}{\kappa_3(1-\kappa_1)} \bar{c}_2^{-2}}{(1 + \kappa_2 \bar{c}_2)^2}, \quad (5.3.26)$$

$$\mathcal{A}_{\text{BR}} = 4L^3\pi^2 \sqrt{\frac{2\kappa_2(\kappa_2 - \kappa_3)^3}{\kappa_1(\kappa_1 - \kappa_3)(1 - \kappa_3)}} \frac{1 - (\kappa_1 - \kappa_2)\bar{c}_2 + \frac{\kappa_1\kappa_2(1-\kappa_3)}{\kappa_3} \bar{c}_2^{-2}}{(1 + \kappa_2 \bar{c}_2)^2}. \quad (5.3.27)$$

Note that for all real \bar{c}_2 and $0 < \kappa_3 < \kappa_2 < \kappa_1 < 1$, the expressions for the horizon areas are real and positive, hence well-defined. In particular, there are no signs of closed timelike curves.

Temperatures

We compute the temperatures using [30] and find

$$T_{\text{H}}^{\text{BH}} = \frac{1}{2L\pi} \sqrt{\frac{(1-\kappa_2)(1-\kappa_3)}{2(1-\kappa_1)}} \frac{(1 + \kappa_2 \bar{c}_2)^2}{1 + \frac{\kappa_1\kappa_2(1-\kappa_2)(1-\kappa_3)}{\kappa_3(1-\kappa_1)} \bar{c}_2^{-2}}, \quad (5.3.28)$$

$$T_{\text{H}}^{\text{BR}} = \frac{1}{2L\pi} \sqrt{\frac{\kappa_1(1-\kappa_3)(\kappa_1 - \kappa_3)}{2\kappa_2(\kappa_2 - \kappa_3)}} \frac{(1 + \kappa_2 \bar{c}_2)^2}{1 - (\kappa_1 - \kappa_2)\bar{c}_2 + \frac{\kappa_1\kappa_2(1-\kappa_3)}{\kappa_3} \bar{c}_2^{-2}}. \quad (5.3.29)$$

The ordering (5.3.3) ensures that the temperatures are non-negative.

The expressions for the temperatures are complimentary to those for the horizon areas (5.3.26)-(5.3.27): with the entropy being one quarter times the horizon area, $S = \mathcal{A}/(4G)$, we have two very simple expressions:

$$T_{\text{H}}^{\text{BH}} S^{\text{BH}} = \frac{\pi}{2G} L^2(1 - \kappa_1), \quad T_{\text{H}}^{\text{BR}} S^{\text{BR}} = \frac{\pi}{2G} L^2(\kappa_2 - \kappa_3). \quad (5.3.30)$$

The former vanishes in the limit $\kappa_1 \rightarrow 1$ which gives an extremal rotating S^3 black hole. The latter vanishes when $\kappa_2 = \kappa_3$, which we interpret as the limit where the black ring becomes singular, as the $j = 1$ limit of the fat black rings.

5.3.6 ADM mass and angular momentum

The solution is asymptotically flat and it is straightforward to compute the ADM mass M and angular momentum J using the asymptotic coordinates introduced in section 5.3.3. We find

$$M = \frac{3\pi L^2}{4G} \frac{\kappa_3(1 - \kappa_1 + \kappa_2) - 2\kappa_2\kappa_3(\kappa_1 - \kappa_2)\bar{c}_2 + \kappa_2[\kappa_1 - \kappa_2\kappa_3(1 + \kappa_1 - \kappa_2)]\bar{c}_2^{-2}}{\kappa_3[1 + \kappa_2\bar{c}_2]^2}, \quad (5.3.31)$$

and

$$\begin{aligned}
J = \frac{\pi L^3}{G} \frac{1}{\kappa_3 [1 + \kappa_2 \bar{c}_2]^3} \sqrt{\frac{\kappa_2}{2\kappa_1 \kappa_3}} & \left[\kappa_3^2 - \bar{c}_2 \kappa_3 \left[(\kappa_1 - \kappa_2)(1 - \kappa_1 + \kappa_3) + \kappa_2(1 - \kappa_3) \right] \right. \\
& + \bar{c}_2^2 \kappa_2 \kappa_3 \left[(\kappa_1 - \kappa_2)(\kappa_1 - \kappa_3) + \kappa_1(1 + \kappa_1 - \kappa_2 - \kappa_3) \right] \\
& \left. - \bar{c}_2^3 \kappa_1 \kappa_2 \left[\kappa_1 - \kappa_2 \kappa_3 (2 + \kappa_1 - \kappa_2 - \kappa_3) \right] \right]. \quad (5.3.32)
\end{aligned}$$

It is worth noting that for any $\bar{c}_2 \in \mathbb{R}$ the ADM mass (5.3.31) is positive as a simple consequence of the ordering (5.3.3).

5.3.7 Komar integrals

Komar integrals evaluated on the horizon of each black hole allow us to compute a measure of the mass and angular momentum of the two objects of the saturn system.

Komar masses

In five spacetime dimensions, the Komar mass is given by

$$M_{\text{Komar}} = \frac{3}{32\pi G} \int_S *d\xi, \quad (5.3.33)$$

where ξ is the dual 1-form associated to the asymptotic time translation Killing field ∂_t and S is the boundary of any spacelike hypersurface. Eq. (5.3.33) measures the mass contained in S , so the mass of each black hole in a multi-black hole spacetime is computed by taking S to be at the horizon H_i . Instead, if we take S to be the S^3 at infinity, then (5.3.33) gives the total mass of the system, which coincides with the ADM mass. In terms of the metric components we have

$$M_{\text{Komar}}^i = \frac{3}{32\pi G} \int_{H_i} dz d\phi d\psi \frac{1}{\sqrt{-\det g}} g_{zz} g_{\phi\phi} \left[-g_{\psi\psi} \partial_\rho g_{tt} + g_{t\psi} \partial_\rho g_{t\psi} \right], \quad (5.3.34)$$

which for the saturn solution gives

$$M_{\text{Komar}}^{\text{BH}} = \frac{3\pi L^2}{4G} \frac{\kappa_3(1 - \kappa_1) + \kappa_1 \kappa_2(1 - \kappa_2)(1 - \kappa_3) \bar{c}_2^2}{\kappa_3(1 + \bar{c}_2 \kappa_2)}, \quad (5.3.35)$$

$$M_{\text{Komar}}^{\text{BR}} = \frac{3\pi L^2}{4G} \frac{\kappa_2 [1 - (1 - \kappa_2) \bar{c}_2] [\kappa_3 - \kappa_3(\kappa_1 - \kappa_2) \bar{c}_2 + \kappa_1 \kappa_2(1 - \kappa_3) \bar{c}_2^2]}{\kappa_3(1 + \bar{c}_2 \kappa_2)^2}. \quad (5.3.36)$$

Note that (5.3.35)-(5.3.36) give

$$M_{\text{ADM}} = M_{\text{Komar}}^{\text{BR}} + M_{\text{Komar}}^{\text{BH}}, \quad (5.3.37)$$

so the Komar masses add up to the ADM mass (5.3.31), even in the presence of the conical singularity. We discuss the sign of the Komar masses at the end of this subsection.

Komar angular momenta

The angular momentum Komar integral is given by

$$J_{\text{Komar}} = \frac{1}{16\pi G} \int_S *d\zeta, \quad (5.3.38)$$

where ζ is the 1-form dual to the Killing field ∂_ψ , and S is the boundary of any spacelike hypersurface. Now (5.3.38) measures the angular momentum contained within S , and therefore, if we choose S to be the horizons H_i , we can compute the ‘‘intrinsic’’ angular momentum of each black object. We have

$$J_{\text{Komar}}^i = \frac{1}{16\pi G} \int_{H_i} dz d\phi d\psi \frac{1}{\sqrt{-\det g}} g_{zz} g_{\phi\phi} \left[-g_{\psi\psi} \partial_\rho g_{t\psi} + g_{t\psi} \partial_\rho g_{\psi\psi} \right], \quad (5.3.39)$$

which gives

$$J_{\text{Komar}}^{\text{BH}} = -\frac{\pi L^3}{G} \sqrt{\frac{\kappa_1 \kappa_2}{2\kappa_3}} \frac{\bar{c}_2 \left[\kappa_3(1 - \kappa_1) + \kappa_1 \kappa_2(1 - \kappa_2)(1 - \kappa_3) \bar{c}_2^2 \right]}{\kappa_3(1 + \bar{c}_2 \kappa_2)^2}, \quad (5.3.40)$$

$$J_{\text{Komar}}^{\text{BR}} = \frac{\pi L^3}{G} \sqrt{\frac{\kappa_2}{2\kappa_1 \kappa_3}} \times \frac{\left[\kappa_3 - \kappa_2(\kappa_1 - \kappa_3) \bar{c}_2 + \kappa_1 \kappa_2(1 - \kappa_2) \bar{c}_2^2 \right] \left[\kappa_3 - \kappa_3(\kappa_1 - \kappa_2) \bar{c}_2 + \kappa_1 \kappa_2(1 - \kappa_3) \bar{c}_2^2 \right]}{\kappa_3(1 + \bar{c}_2 \kappa_2)^3}. \quad (5.3.41)$$

The Komar angular momenta add to up to J_{ADM} given in (5.3.32),

$$J_{\text{ADM}} = J_{\text{Komar}}^{\text{BR}} + J_{\text{Komar}}^{\text{BH}}, \quad (5.3.42)$$

even without imposing the balance condition (5.3.17).

We shall refer to the Komar angular momentum as the ‘‘intrinsic’’ angular momentum of the black hole. Note that for $\bar{c}_2 = 0$, the S^3 black hole carries no intrinsic spin $J_{\text{Komar}}^{\text{BH}} = 0$. This was expected since the soliton transformation with $c_2 = 0$ did not add spin to the S^3 black hole directly.

Smarr relations

Black rings [8] and Myers-Perry black holes [11] satisfy the same Smarr formula

$$\frac{2}{3} M = T_{\text{H}} S + J \Omega. \quad (5.3.43)$$

Using the expressions of the Komar masses (5.3.35)-(5.3.36) and the Komar angular momenta (5.3.40)-(5.3.41) we find that both the black ring and the black hole separately obey this Smarr relation:

$$\frac{2}{3} M_{\text{Komar}}^{\text{BR}} = T_{\text{H}}^{\text{BR}} S^{\text{BR}} + \Omega_{\psi}^{\text{BR}} J_{\text{Komar}}^{\text{BR}}, \quad \frac{2}{3} M_{\text{Komar}}^{\text{BH}} = T_{\text{H}}^{\text{BH}} S^{\text{BH}} + \Omega_{\psi}^{\text{BH}} J_{\text{Komar}}^{\text{BH}}. \quad (5.3.44)$$

These Smarr relations are mathematical identities which relates the physical quantities measured at the horizon, and they can be derived quite generally for multi-black hole vacuum spacetimes [14]. The relations (5.3.44) hold without imposing the balance condition (5.3.17).

Sign of Komar masses

We have already noted that the total ADM mass (5.3.31) is always positive. Positivity of $M_{\text{Komar}}^{\text{BH}}$ in (5.3.35) requires that $\bar{c}_2 > -\kappa_2^{-1}$, and this selects the $\epsilon = +1$ case of the balance condition in section 5.3.4. Furthermore, imposing the balance condition (5.3.17) with $\epsilon = +1$ implies that \bar{c}_2 takes values $-\kappa_2^{-1} < \bar{c}_2 < (1 - \kappa_2)^{-1}$, and thus both $M_{\text{Komar}}^{\text{BH}}$ in (5.3.35) and $M_{\text{Komar}}^{\text{BR}}$ in (5.3.36) are positive.

On the other hand, imposing the balance condition (5.3.17) with $\epsilon = -1$ means that $\bar{c}_2 < -\kappa_2^{-1}$, and — as can be seen from (5.3.35)-(5.3.36) — this gives $M_{\text{Komar}}^{\text{BH}} < 0$ while $M_{\text{Komar}}^{\text{BR}} > 0$.

One might take as a criterium for establishing the physical relevance of a multi-black hole system that each of the components in the system has positive mass. Clearly, at large separations the Komar mass of each object should agree with the positive ADM mass of the object, but that does not imply that the Komar masses in tightly bound gravitational systems need to be positive.⁸ How, physically, can a solution with negative Komar mass occur?

It follows from the Smarr relation (5.3.44) that the Komar mass can be negative provided that the angular velocity Ω and Komar angular momentum J_{Komar} have opposite signs *and* that ΩJ_{Komar} is sufficiently large and negative to overwhelm the positive $T_{\text{H}}S$ -term. In black saturn, the physical mechanism behind opposite signs of Ω^{BH} and $J_{\text{Komar}}^{\text{BH}}$ is rotational frame-dragging: the rotating black ring drags the S^3 black hole so that its horizon is spinning in the opposite direction of its “intrinsic” angular momentum. We examine this effect in detail in section 5.4.3. In that section we focus on solutions with $\bar{c}_2 = 0$, hence $\epsilon = +1$, and these have $J_{\text{Komar}}^{\text{BH}} = 0$; however, that analysis also serves to illustrate the physics which lies behind having $\Omega^{\text{BH}} J_{\text{Komar}}^{\text{BH}} < 0$.

In conclusion, the solutions with $M_{\text{Komar}}^{\text{BH}} > 0$ ($\epsilon = +1$) and $M_{\text{Komar}}^{\text{BH}} < 0$ ($\epsilon = -1$) appear to be equally valid. We shall primarily focus on the $M_{\text{Komar}}^{\text{BH}} > 0$ solutions when we study the physics of black saturn in section 5.4, but we comment briefly on the $M_{\text{Komar}}^{\text{BH}} < 0$ solutions in section 5.4.6.

Finally, let us remark that single black hole spacetimes with counter-rotation (in the sense of $\Omega J < 0$) and negative Komar mass, but positive ADM mass, have been constructed numerically as solutions of five-dimensional Einstein-Maxwell theory with a Chern-Simons term [34]. In that case, part of the energy and angular momentum is carried by the electromagnetic fields making counter-rotation and negative Komar mass possible.

5.3.8 Closed timelike curves

One might expect the plane of the ring to be a natural place for closed timelike curves (CTCs) to appear, and we have focused our analysis on this region. For the case $\bar{c}_2 = 0$, we find analytically that $G_{\psi\psi} > 0$ for $\rho = 0$ and $z < \kappa_3$ (the plane outside the ring) and $\kappa_2 < z < \kappa_1$ (the plane between the ring and the black hole). So for $\bar{c}_2 = 0$ there are no CTCs in the plane of the ring (cf. [35]).

When $\bar{c}_2 \neq 0$ the metric components are sufficiently complicated that we resort to numerical checks. We have performed such checks for examples where the S^3 black hole and the black ring are counter-rotating as well as co-rotating. Among other examples we have checked the counter-rotating cases with $J = 0$; no CTCs were found.

⁸We thank Roberto Emparan for discussions about this point, and also Harvey Reall for helpful comments.

CTCs tend to appear when solutions are over-spinning, at least that is the case for supersymmetric black holes [36, 31, 32, 33, 15]. Hence we have checked in detail cases where the black hole and the ring are co-rotating and fast spinning. One such example is studied in section 5.4.4. For this 1-parameter family of solutions the S^3 black hole angular velocity covers a large range of co- and counter-rotation; we have checked numerically for CTCs in the plane of the ring and found none.

While we have found no signs of the appearance of closed timelike curves in our analysis, we emphasize that our numerical checks are not exhaustive. Rewriting the solution in ring coordinates (x, y) will probably be helpful for checking for CTCs.

5.3.9 Limits

Black saturn combines a singly spinning Myers-Perry spherical black hole with a black ring in a balanced configuration, and it is possible to obtain either of these solutions as limits of the balanced black saturn solution with $\epsilon = +1$. We describe here the appropriate limits, while details are relegated to the appendix.

Myers-Perry black hole limit

In the general solution, one can remove the black ring by first setting the BZ parameter $c_1 = 0$, thus eliminating the black ring spin, and then removing the black ring rod by taking $\kappa_2 = \kappa_3 = 0$. For the physical solution, where the singularity at $\bar{z} = 0$ has been removed, c_1 is fixed by (5.3.7) and we have to take the limit $\kappa_2, \kappa_3 \rightarrow 0$, in such a way that c_1 remains finite. This can be accomplished by first taking $\kappa_2 \rightarrow \kappa_3$ and then $\kappa_3 \rightarrow 0$. We provide details of this limit in appendix 5.A.1.

Black ring limit

The black ring [8] is obtained by simply removing the S^3 black hole from the saturn configuration. This is done by first setting the angular momentum of the black hole to zero by taking $\bar{c}_2 = 0$, and then setting $\kappa_1 = 1$, which removes the S^3 black hole. We show in appendix 5.A.2 that the remaining solution is exactly the black ring of [8] by rewriting the solution explicitly in ring coordinates x, y . The balance condition (5.3.17) becomes the familiar equilibrium condition for a single black ring.

No merger limit

It would be interesting if one could use the black saturn system to study a controlled merger of the S^3 black hole and the black ring. Unfortunately, this is not possible. Based on the rod configuration given in figure 5.2(b), the merger should correspond to merging the two horizon rods, $[\kappa_3, \kappa_2]$ of the black ring and $[\kappa_1, 1]$ of the S^3 black hole. Thus the merger would correspond to taking $\kappa_1 \rightarrow \kappa_2$. Imposing the balance condition (5.3.17), $\kappa_1 \rightarrow \kappa_2$ implies $\bar{c}_2 \rightarrow -\kappa_2^{-1}$. The solution with $\bar{c}_2 = -\kappa_2^{-1}$ is nakedly singular, and hence the suggested merger limit is singular. As a side remark, we point out that the singular nature of the merger limit is in fact very similar to why two balanced Kaluza-Klein black holes held apart by a static bubble-of-nothing cannot be merged by taking a similar limit [37].

5.4 Physics of black saturn

We examine a selection of interesting physical properties of black saturn. In section 5.4.1 we establish that black saturn has 2-fold continuous non-uniqueness. Section 5.4.2 reviews basic properties of the Myers-Perry black hole and the black ring; properties which will be helpful for understanding the physics of black saturn.

It is useful to clarify notions of rotation and intrinsic spin:

- A black hole is rotating when its angular velocity Ω^i is nonzero.
- Co(counter)-rotation means Ω^{BH} and Ω^{BR} have the same (opposite) sign.
- We use the term *intrinsic* angular momentum to refer to the angular momentum J_{Komar} measured by the Komar integral evaluated at the horizon of the black hole.

The two black objects in black saturn interact gravitationally, and one effect is frame-dragging. This is cleanly illustrated for the case where the S^3 black hole has vanishing intrinsic angular momentum, $J_{\text{Komar}}^{\text{BH}} = 0$, but is nonetheless rotating, $\Omega^{\text{BH}} \neq 0$. We found in section 5.3.7 that $J_{\text{Komar}}^{\text{BH}} = 0$ for $\bar{c}_2 = 0$, so in section 5.4.3 we study the $\bar{c}_2 = 0$ subfamily of black saturn configurations.

The general black saturn configurations with $\bar{c}_2 \neq 0$ are studied in sections 5.4.4 and 5.4.5. For $\bar{c}_2 \neq 0$ the S^3 black hole and the black ring have independent rotation parameters, and this makes it possible to have counter-rotating solutions and configurations with vanishing total angular momentum, $J = 0$. Having $\bar{c}_2 \neq 0$ is also necessary for realizing the full 2-fold continuous non-uniqueness.

Note that we are imposing the balance condition (5.3.4) with $\epsilon = +1$ throughout this section, with the exception of subsection 5.4.6.

5.4.1 Parameter counting and non-uniqueness

We begin by counting the parameters in the saturn solution. The full solution has six parameters: $\kappa_{1,2,3}$, satisfying $0 \leq \kappa_3 \leq \kappa_2 < \kappa_1 \leq 1$, one scale L , and the two BZ parameters c_1 and c_2 . The parameter c_1 is fixed according to (5.3.7) in order to avoid a naked singularity at $\bar{z} = 0$. We conveniently rescaled c_2 to introduce the dimensionless parameter $\bar{c}_2 \propto c_2$ in (5.3.6). So the unbalanced solution has four dimensionless parameters, $\kappa_{1,2,3}$ and \bar{c}_2 , and the scale L . The balance condition (5.3.17) imposes a constraint between \bar{c}_2 and $\kappa_{1,2,3}$, and in conclusion, the balanced black saturn solution has three dimensionless parameters and one scale L .

Fixing the ADM mass M of the full system fixes the scale L , and leaves three dimensionless parameters. Fixing further the only other conserved asymptotic quantity, namely the angular momentum J , leaves two free dimensionless parameters. Thus black saturn has 2-fold continuous non-uniqueness. We examine the non-uniqueness in greater detail in the following sections.

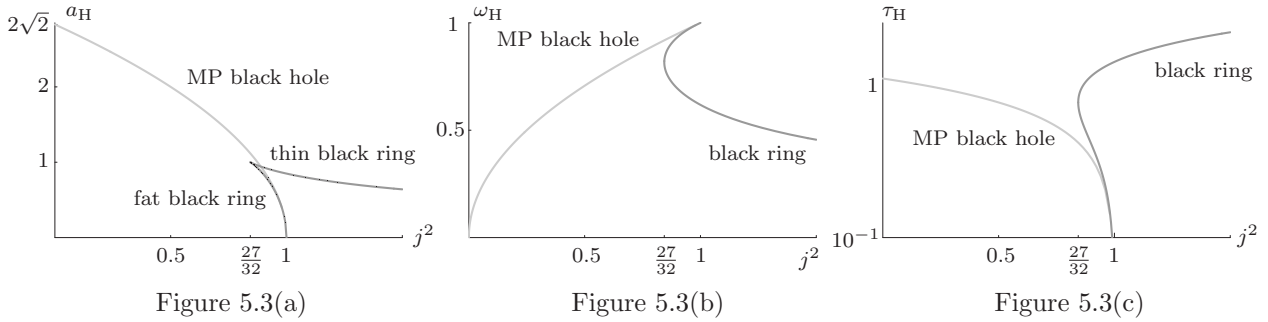


Figure 5.3: Behavior of the reduced physical parameters for the Myers-Perry black hole (light gray) and the black ring (dark gray). Note that we are using a logarithmic scale for the temperature.

Fixed mass reduced parameters

We introduce the fixed mass reduced parameters

$$\begin{aligned}
 j^2 &= \frac{27\pi}{32G} \frac{J^2}{M^3}, & a_{\text{H}}^i &= \frac{3}{16} \sqrt{\frac{3}{\pi}} \frac{\mathcal{A}_i}{(GM)^{3/2}}, \\
 \omega_i &= \sqrt{\frac{8}{3\pi}} \Omega_{\psi}^i (GM)^{1/2}, & \tau_i &= \sqrt{\frac{32\pi}{3}} T_{\text{H}}^i (GM)^{1/2},
 \end{aligned}
 \tag{5.4.1}$$

which allow us to compare physical properties of configurations with the same ADM mass M . The script i labels the quantity corresponding to the black ring ($i = \text{BR}$) or the S^3 black hole ($i = \text{BH}$). We will also use the total horizon area,

$$a_{\text{H}}^{\text{total}} = a_{\text{H}}^{\text{BR}} + a_{\text{H}}^{\text{BH}},
 \tag{5.4.2}$$

in order to study the “phase diagram” (total entropy vs. j^2) of the black saturn. Occasionally we simply use a_{H} for $a_{\text{H}}^{\text{total}}$.

The reduced temperature and angular velocity are normalized such that $\tau_{\text{BH}} = 1$ for the five-dimensional Schwarzschild black hole ($j = 0$), and $\omega_{\text{BH}} = 1$ for the maximally rotating (singular) Myers-Perry black hole ($j = 1$).⁹

5.4.2 Myers-Perry black hole and black rings

In preparation for studying the physical properties of black saturn, we review the basic properties of the Myers-Perry black hole [11] and the black ring [8] with a single angular momentum. Figure 5.3 shows for fixed mass the behaviors of the area, angular velocity and temperature of the Myers-Perry black hole and the black ring as the reduced angular momentum j is varied.

For the Myers-Perry black hole the reduced angular velocity grows linearly with the reduced angular momentum — in fact our normalization is such that $\omega_{\text{MP}} = j_{\text{MP}}$. (In order to better represent the near- $j = 1$ behavior we choose here to plot the physical properties vs. j^2 rather than j , as it was done in [9].) Increasing j , the area a_{H}^{MP} decreases and the black hole gets colder (τ_{MP} decreases). As $j \rightarrow 1$, the S^3 horizon flattens out as a pancake in the plane of rotation, and at $j = 1$ the solution becomes nakedly singular.

⁹Our normalizations of τ_i and ω_i differ from the conventions used in [9].

Black rings come in two types: thin and fat black rings. The distinction is based on the “phase diagram” showing a_{H}^{BR} vs. j^2 (see figure 5.3(a)): thin rings are those on the upper branch, while the fat rings are those on the lower branch. As $j \rightarrow 1$, the S^2 of fat rings flatten out in the plane of rotation, and the inner S^1 radius gets smaller while the outer S^1 radius grows (the shape of black rings was studied in detail in [9]). As j increases, the fat rings spin faster and become colder, much like the fast spinning Myers-Perry black hole. As $j \rightarrow 1$, the fat rings approach the same naked ring singularity of the $j = 1$ Myers-Perry solution.

A thin black ring has a nearly round S^2 , and the S^1 radius is larger than the S^2 radius. As j increases, thin black rings get hotter as the S^2 gets smaller (and the ring thinner), and the angular velocity decreases. We shall see that many “phases” of black saturn also have versions of the “thin” and the “fat” black ring branches.

5.4.3 Configurations with $J_{\text{Komar}}^{\text{BH}} = 0$

Throughout this section we study the subfamily of black saturn with $\bar{c}_2 = 0$. It was shown in section 5.3.7 that for $\bar{c}_2 = 0$ the intrinsic angular momentum of the S^3 black hole vanishes, $J_{\text{Komar}}^{\text{BH}} = 0$.

When $\bar{c}_2 = 0$ it is simple to solve the balance condition (5.3.17) for κ_3 : there are two solutions, but only one of them satisfies the constraints $0 < \kappa_3(\kappa_1, \kappa_2) < \kappa_2 < \kappa_1 < 1$. In order to illustrate the physics of the solution, we choose to further fix a physical quantity, so that we are left with a 1-parameter family of solutions. The extra physical parameter to be fixed will be either the reduced area of the black ring a_{H}^{BR} (section 5.4.3) or the S^3 black hole a_{H}^{BH} (section 5.4.3). Alternatively, we fix in section 5.4.3 the Komar mass of the black hole and test the gravitational interaction between the S^3 black hole and the black ring.

Fixed area black ring

As shown in figure 5.3(a), the reduced area a_{H}^{BR} of a single black ring takes values $0 < a_{\text{H}}^{\text{BR}} \leq 1$. We can therefore fix the reduced black ring area at any value between 0 and 1 and then “grow” the S^3 black hole at the center of the black ring. The result is illustrated for representative values of a_{H}^{BR} in figure 5.4.

For any value $0 < a_{\text{H}}^{\text{BR}} \leq 1$, there exist both a fat and a thin black ring, and the S^3 black hole can be grown from either. This is illustrated most clearly in figure 5.4(b), where we have fixed $a_{\text{H}}^{\text{BR}} = 0.8$ and plotted $a_{\text{H}}^{\text{total}}$ vs. j^2 . The standard Myers-Perry black hole “phase” is shown in light gray, the black ring “phase” in darker gray. The black saturn configuration with fixed $a_{\text{H}}^{\text{BR}} = 0.8$ (black curve) starts at the thin and fat black ring branches at $a_{\text{H}} = 0.8$. Since $J_{\text{Komar}}^{\text{BH}} = 0$, the S^3 black hole contributes no angular momentum, and hence j decreases as long as the black hole grows, i.e. until reaching the cusp of the curve in figure 5.4(b).

Figure 5.4(a) shows similarly the growth of an S^3 black hole at the center of the ring, but now with a_{H}^{BR} fixed at smaller values, $a_{\text{H}}^{\text{BR}} = 0.1$ (dotted) and 0.05 (solid). The plot shows the saturn “phases” grow from the standard fat black ring branch; they meet the thin black ring branch at very large values of j not shown in figure 5.4(a). For such small fixed areas of the black ring, the S^3 black hole is allowed to grow very large, and these saturn “phases” dominate the standard black ring branch entropically.

Figures 5.4(c) and 5.4(d) show that the S^3 black hole is rotating, i.e. it has non-zero angular velocity ω_{BH} . That the S^3 black hole rotates despite carrying no intrinsic angular momentum ($J_{\text{Komar}}^{\text{BH}} = 0$) is naturally interpreted as gravitational frame-dragging: the rotating black ring

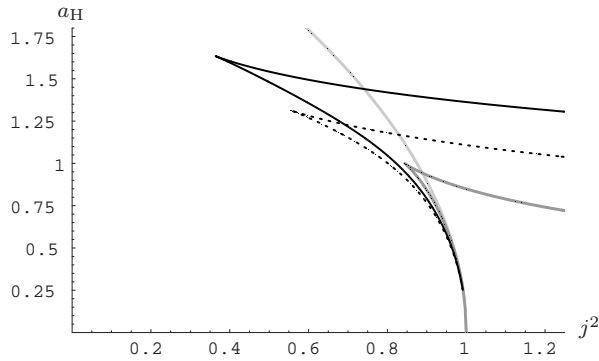


Figure 5.4(a): Total a_H for $a_H^{BR} = 0.05$ (solid) and $a_H^{BR} = 0.1$ (dotted).

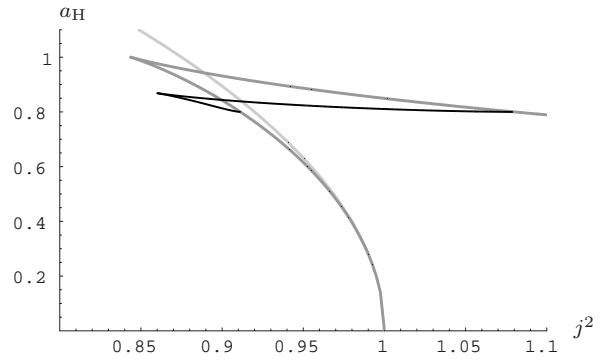


Figure 5.4(b): Total a_H for $a_H^{BR} = 0.8$.

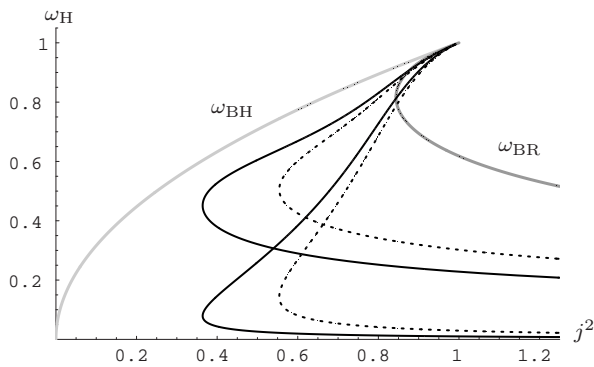


Figure 5.4(c): ω_{BR} (upper curve) and ω_{BH} (lower curve) for $a_H^{BR} = 0.05$ (solid) and $a_H^{BR} = 0.1$ (dotted).

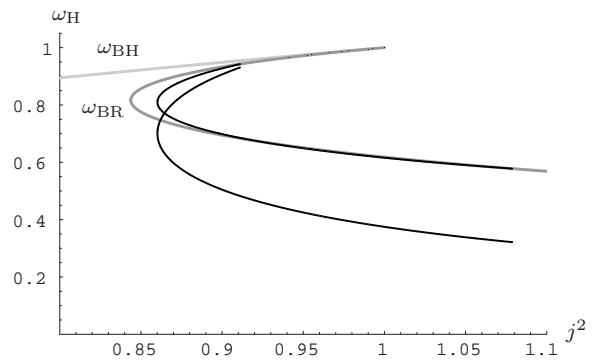


Figure 5.4(d): ω_{BR} (upper curve) and ω_{BH} (lower curve) for $a_H^{BR} = 0.8$.

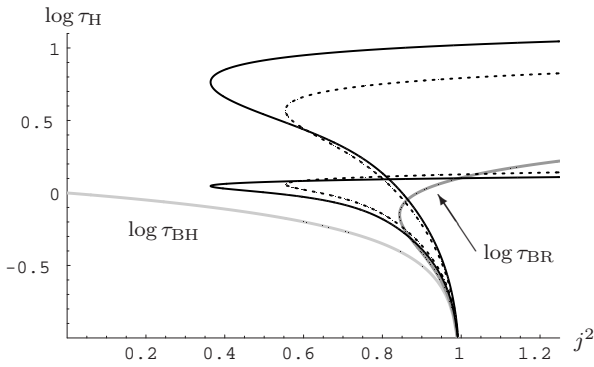


Figure 5.4(e): τ_{BR} (lower curve) and τ_{BH} (upper curve) for $a_H^{BR} = 0.05$ (solid) and $a_H^{BR} = 0.1$ (dotted).

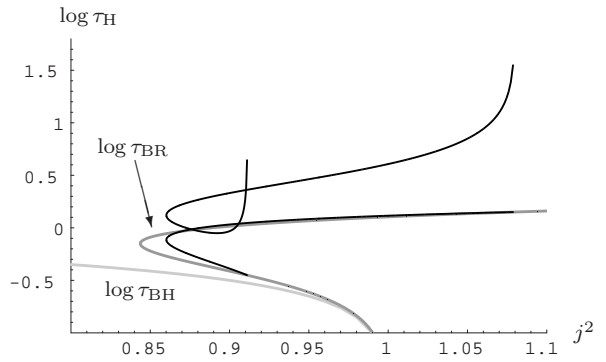


Figure 5.4(f): τ_{BR} (lower curve) and τ_{BH} (upper curve) for $a_H^{BR} = 0.8$.

Figure 5.4: For fixed total mass and some representative values of the a_H^{BR} , the various reduced quantities are plotted vs. j^2 . The gray curves correspond to the Myers-Perry black hole (light gray) and the black ring (darker gray) respectively.

drags the spacetime surrounding it and that causes the S^3 horizon to rotate. This interpretation is supported by the fact that the angular velocity ω_{BH} follows, and is always smaller than, ω_{BR} .

To gain a better understanding of the physics of the black saturn, we first focus on the cases of small values of the fixed black ring area. The relevant plots are figure 5.4(a) ($a_{\text{H}}^{\text{total}}$ vs. j^2), figure 5.4(c) (angular velocities vs. j^2), and figure 5.4(e) (temperatures¹⁰ vs. j^2) for fixed $a_{\text{H}}^{\text{BR}} = 0.1$ (dotted) and 0.05 (solid). For these values of the black ring area, the thin black ring is very thin, has large S^1 radius and is rotating slowly (ω_{BR} is small). A small S^3 black hole at the center of such a thin black ring will hardly feel the surrounding ring. Indeed, for large j , the S^3 black hole has very small angular velocity ω_{BH} (figure 5.4(c)), and it has large temperature τ_{BH} (figure 5.4(e)) which decreases as the black hole grows. Thus the black hole behaves much like a small-mass Schwarzschild black hole, and we expect its horizon to be nearly round as long as it has small area.

Instead of growing the S^3 black hole from the thin black ring branch, consider starting with the fat black ring with $a_{\text{H}}^{\text{BR}} = 0.05$ or 0.1. The fat black ring has j near 1, the horizon is flattened out and it rotates fast. The S^3 black hole growing from this configuration will naturally be highly affected by the surrounding black ring. Consequently, the dragging-effect is much stronger, and indeed figure 5.4(c) shows that the S^3 black hole is rotating fast. Its temperature is very small (figure 5.4(e)), so it behaves much like the highly spinning small area Myers-Perry black hole near $j = 1$. Thus we expect the S^3 black hole to flatten out in the plane of the ring in this regime of black saturn.

Figures 5.4(b), 5.4(d), and 5.4(f) show the equivalent plots for the black ring area fixed at a larger value $a_{\text{H}}^{\text{BR}} = 0.8$. In this case, the distinction between growing the black hole from the thin or fat black ring branches is less pronounced. The S^3 black hole is always dragged along to that the angular velocity is far from zero, but even as the black ring becomes fat, the S^3 black hole never spins so fast that it enters the regime of the near- $j = 1$ Myers-Perry black hole as the area goes to zero. This effect can be seen from the temperature τ_{BH} which increases as $a_{\text{H}}^{\text{BH}} \rightarrow 0$ — compare figures 5.4(e) and 5.4(f).

Increasing the fixed value of the black ring area, a_{H}^{BR} , the corresponding black saturn “phase” becomes smaller and smaller, and for fixed $a_{\text{H}}^{\text{BR}} = 1$ we find no saturn solutions. This is because growing the S^3 black hole with $J_{\text{Komar}}^{\text{BH}} = 0$ decreases the total angular momentum j , and for the black ring with $j = \sqrt{27/32}$ and $a_{\text{H}}^{\text{BR}} = 1$, there are no black ring solutions with less angular momentum.

Finally, let us note that it is possible to fix the black ring area to be zero, $a_{\text{H}}^{\text{BR}} = 0$. The $a_{\text{H}}^{\text{BR}} = 0$ saturn configuration describes a nakedly singular ring rotating around the S^3 black hole, which is also rotating as it is being dragged along by the ring singularity. The reduced area of the S^3 black hole vs. j^2 for this configuration is shown as a dotted curve in figure 5.5.

Fixed area black hole

We keep $\bar{c}_2 = 0$ as before, so that $J_{\text{Komar}}^{\text{BH}} = 0$, but instead of keeping the black ring area a_{H}^{BR} fixed as in the previous subsection we now fix the S^3 black hole area a_{H}^{BH} . Thus we “grow” a black ring around the S^3 black hole area of fixed area. A balanced black ring cannot exist for arbitrarily small angular momentum while keeping the configuration in equilibrium, so the black ring grows from a nakedly singular ring around the Myers-Perry black hole; this is nothing

¹⁰Note that we plot temperatures on a logarithmic scale in order to better capture the structure of all phases in one plot.

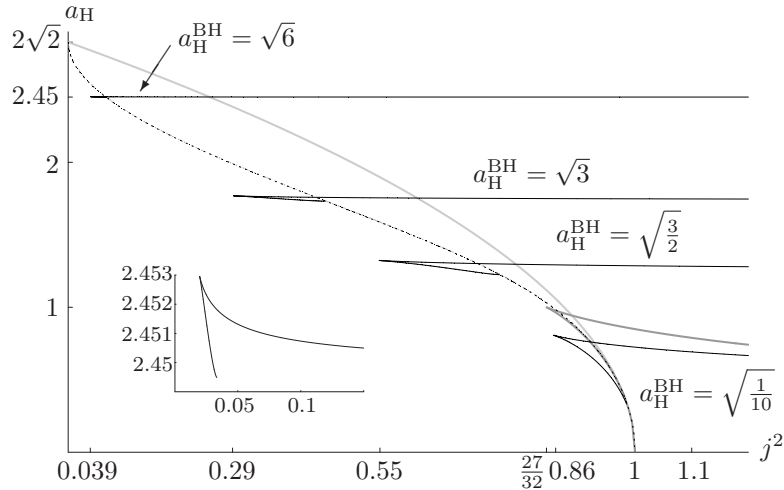


Figure 5.5: Plots of a_H vs. j^2 for different representative values of $(a_H^{\text{BH}})^2 = 6, 3, \frac{3}{2}, \frac{1}{10}$ (black solid curves). The dotted curve corresponds to a Myers-Perry black hole surrounded by a nakedly singular ring. Again, the gray curves correspond to the Myers-Perry hole (gray) and the black ring (darker gray). The smaller plot zooms in on the small j part of the $a_H^{\text{BH}} = \sqrt{6}$ curve.

but the $a_H^{\text{BR}} = 0$ configuration discussed at the end of the previous section, and shown as the dotted curve in figure 5.5.

Figure 5.5 shows black saturn phases with fixed black hole area for representative values of a_H^{BH} . For each value of a_H^{BH} , the corresponding curve has a fat and a thin black ring phase. Note that the thin ring branches extend to large values of j .

The large- j tails of the constant a_H^{BH} curves show that balanced saturn configurations can have very large entropies. It can be argued [14] that for any fixed value of $0 < a_H^{\text{BH}} < 2\sqrt{2}$, the tails extend to arbitrarily large j . This in turn means that for any j there exist black saturn configurations with total area a_H^{total} arbitrarily close to $2\sqrt{2}$. We refer to [14] for further details.

When the S^3 black hole area is close to zero, the black saturn curves approach the phase of the single black ring. Since the black hole itself does not carry any intrinsic spin, we can set its area to zero, $a_H^{\text{BH}} = 0$, and then black saturn simply reduces to the black ring solution.

It is worth noting that for large values of a_H^{BH} , the black saturn curves also extend to small values of j . For $\bar{c}_2 = 0$, the saturn phases never reach $j = 0$. This is expected because $j = 0$ requires that the black hole and the black ring are counter-rotating and that is never the case for the $\bar{c}_2 = 0$.

Saturn frame-dragging

Above we have seen that in the presence of the rotating black ring of black saturn, an S^3 black hole with no intrinsic spin ($J_{\text{Komar}}^{\text{BH}} = 0$) can be rotating ($\omega_{\text{BH}} \neq 0$). We have interpreted this as a consequence of gravitational frame-dragging. We test this interpretation by studying the geometry of the black saturn configuration (still keeping $\bar{c}_2 = 0$). If indeed we are seeing frame-dragging, then the effect should be very small when the black ring is thin and very far from the S^3 black hole, and increase as the black ring and the black hole come closer. We keep $m_{\text{BH}} = M_{\text{Komar}}^{\text{BH}}/M$ fixed and let the distance between the black hole and black ring vary.

To characterize the configuration, we first introduce the reduced inner and outer S^1 (horizon)

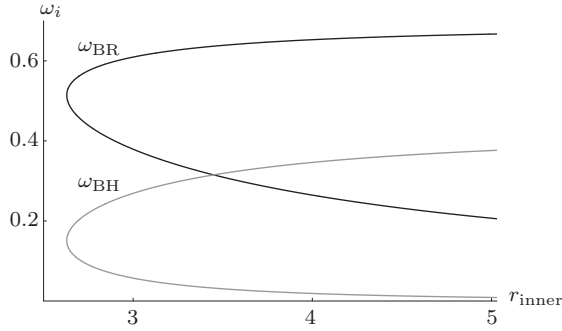


Figure 5.6(a)

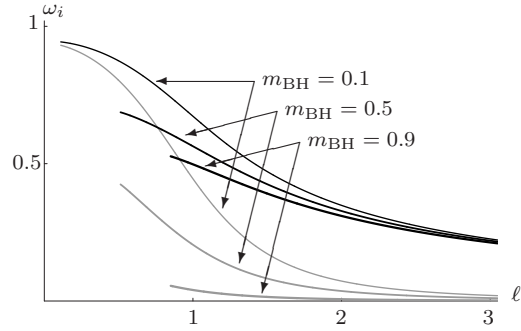


Figure 5.6(b)

Figure 5.6: Test of frame-dragging: Figure 5.6(a) shows angular velocities ω_i vs. the inner radius of the black ring r_{inner} for fixed Komar mass $m_{\text{BH}} = M_{\text{Komar}}^{\text{BH}}/M = 0.5$. Figure 5.6(b) shows the angular velocities ω_i vs. the proper distance ℓ between the black hole and the black ring for three different mass distributions: $m_{\text{BH}} = M_{\text{Komar}}^{\text{BH}}/M = 0.1, 0.5, \text{ and } 0.9$.

radii of the black ring

$$r_{\text{inner}} = (GM)^{-1/2} \sqrt{G_{\psi\psi}} \Big|_{\rho=0, \bar{z}=\kappa_2}, \quad r_{\text{outer}} = (GM)^{-1/2} \sqrt{G_{\psi\psi}} \Big|_{\rho=0, \bar{z}=\kappa_3}. \quad (5.4.3)$$

It is shown in [9] that for a single black ring of fixed mass, the inner radius r_{inner} decreases monotonically when going from the thin black ring (i.e. large- j) regime to the fat black ring branch, and that $r_{\text{inner}} \rightarrow 0$ when $j \rightarrow 1$ for the fat black rings. However, when a black hole is present at the center of the ring, as in black saturn, there is a lower bound on the inner radius of the black ring.¹¹

Figure 5.6(a) shows the angular velocities of the S^3 black hole and the black ring plotted vs. r_{inner} for fixed Komar mass $m_{\text{BH}} = 0.5$. The lower branch of the ω_{BR} curve (black) corresponds to the slowly rotating “thin” black ring. For large radius, the S^3 black hole is not affected much and ω_{BH} is correspondingly small (gray curve). As r_{inner} decreases the black ring spins faster and so does the S^3 black hole. Clearly there is a lower bound for r_{inner} , but surprisingly, the ring starts growing after reaching this minimum. It turns out that on the “upper” branch of the ω_{BR} curve, the inner and outer S^1 radii approach each other, so that the ring again becomes thin. But contrary to the standard thin black rings, the angular velocity increases as the ring grows. Eventually, as the black ring becomes thinner, the area a_{H}^{BR} goes to zero leaving just a nakedly singular black ring around a Myers-Perry black hole (dotted curve in figure 5.5).

As shown in figure 5.6(a), the S^3 black hole angular velocity, ω_{BH} , follows that of the black ring. In particular, ω_{BH} continues to grow even if the inner radius of the black ring is growing. This may at first seem to contradict that the rotation of the S^3 black hole is caused by frame-dragging, since it would seem that the S^3 black hole should slow down as the black ring becomes thinner and its S^1 radius grows. However, since the S^3 black hole is itself rotating, it flattens out in the plane of rotation. To study this effect we compute the proper distance between the S^3 black hole and the black ring (for fixed mass):

$$\ell = (GM)^{-1/2} \int_{\kappa_2}^{\kappa_1} d\bar{z} \sqrt{G_{\bar{z}\bar{z}}}. \quad (5.4.4)$$

¹¹As pointed out in section 5.3.9, there is no smooth merger limit for the balanced black saturn system.

As expected, the proper distance ℓ increases as the inner radius of the black ring increases along the lower branch in figure 5.6(a). But even as the inner radius r_{inner} of the black ring increases (upper branch), the proper distance ℓ continues to decrease. This confirms that the black hole, as it is spinning faster, flattens out into the plane of rotation. Figure 5.6(b) shows the angular velocities as functions of the proper distance ℓ , for three different mass distributions $m_{\text{BH}} = 0.1, 0.5, \text{ and } 0.9$. The angular velocity of the black ring increases as the proper distance ℓ decreases. And $\omega_{\text{BH}} \rightarrow 0$ when ℓ becomes large. This is precisely the behavior one would expect from frame-dragging.

Moreover, figure 5.6(b) shows that the effect of dragging depends on the relative masses of the black ring and the S^3 black hole: the effect of a thin small-mass black ring on a large-mass black hole is weak ($m_{\text{BH}} = 0.9$), but the effect of a thick massive black ring on a small-mass black hole is strong ($m_{\text{BH}} = 0.1$).

The above analysis gives strong evidence that we are indeed observing rotational frame-dragging.

5.4.4 Black hole with intrinsic spin

We now take $\bar{c}_2 \neq 0$ and study the more general saturn configurations. When $\bar{c}_2 \neq 0$, the S^3 black hole and the black ring have independent rotation parameters, in particular we can have $J_{\text{Komar}}^{\text{BH}} \neq 0$. As a result, the two black objects can be co- or counter-rotating. We illustrate the physics in two examples.

Counter-rotation and $\Omega_{\text{BH}}=0$

In the previous section, the S^3 black hole had no intrinsic rotation, $J_{\text{Komar}}^{\text{BH}} = 0$, and it was rotating only because it was dragged along by the black ring. With $\bar{c}_2 \neq 0$ the S^3 black hole has its own intrinsic angular momentum $J_{\text{Komar}}^{\text{BH}} \neq 0$, and it is possible to let the S^3 black hole counter-rotate in such a way that the intrinsic angular momentum cancels the effect of the dragging, so that the S^3 horizon becomes non-rotating, $\omega_{\text{BH}} = 0$.

As an example of this effect, figure 5.7 shows a curve of black saturn solution with $\omega_{\text{BH}} = 0$ fixed. In addition we have also fixed $a_{\text{H}}^{\text{BR}} = 0.8$. This $\omega_{\text{BH}} = 0$ curve starts at the thin black ring branch with $a_{\text{H}} = 0.8$ and the black hole grows ‘‘Schwarzschild style’’ (zero angular velocity, high temperature which decreases as the black hole grows). As the black ring becomes fatter, the black hole is affected more and more by the ring, and at some point its intrinsic counter-rotation can no longer resist the dragging of the black ring; at this point the $\omega_{\text{BH}} = 0$ curve ends.

The possibility of making the S^3 horizon non-rotating by turning on ‘‘intrinsic’’ angular momentum is reminiscent of the situation for the 4+1d supersymmetric S^3 black hole. This black hole also has a non-rotating horizon, $\Omega = 0$, and it can be shown [38] that this requires angular momentum to be stored in the Maxwell fields inside the horizon. Similar configurations were also discussed in [34]. Of course, for black saturn there are no Maxwell fields to carry the angular momentum, but the picture of having contributions to the rotation from ‘‘inside’’ the horizon to make $\omega_{\text{BH}} = 0$ is common for the two systems.

Reaching $j = 0$

One might have expected the only solution with $j = 0$ to be the Schwarzschild black hole. However, taking into account solutions with more than one component of the horizon, counter-

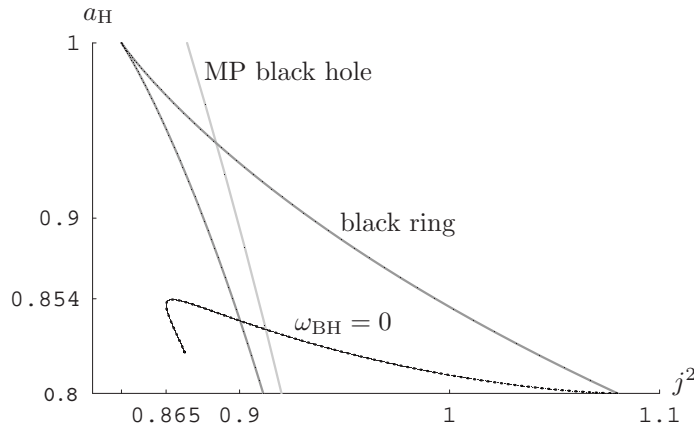


Figure 5.7: Black saturn with a non-spinning black hole. The plot shows $a_{\text{H}}^{\text{total}}$ vs. j^2 for fixed $a_{\text{H}}^{\text{BR}} = 0.8$ and $\omega_{\text{BH}} = 0$ (dotted curve). For reference, the dark gray curve is the black ring while the lighter gray curve is the Myers-Perry black hole.

rotation can give $j = 0$. For black saturn this is possible while maintaining balance.

Figure 5.8 shows a saturn configuration with $a_{\text{H}}^{\text{BR}} = 0.01$ and $\omega_{\text{BR}} = 0.3$ in the phase diagram $a_{\text{H}}^{\text{total}}$ vs. j^2 . To reach $j = 0$ requires that the black ring has small area, but otherwise there is nothing special about the values chosen for a_{H}^{BR} and ω_{BR} ; they just illustrate the physics well. For large values j , the black ring and the S^3 black hole are co-rotating, as can be seen from the j vs. ω_{BH} plot in figure 5.8. As the angular velocity of the black hole decreases, the total angular momentum j decreases and the area of the S^3 black hole grows. The area reaches a maximum close to where the black hole angular velocity vanishes. As the S^3 black hole counter-rotates, $\omega_{\text{BH}} < 0$, the area decreases. Eventually, the counter-rotation is such that the total angular momentum at infinity vanishes, $j = 0$. The black hole can be even more counter-rotating and then j becomes negative. Note from the j vs. ω_{BH} plot in figure 5.8 that when the black holes are co-rotating j is almost linear in the angular momentum, just as it is for a Myers-Perry black hole, and the range covered $-1 \lesssim \omega_{\text{BH}} \lesssim 1$, is nearly the same.

It is clear from figure 5.8 that the 4+1d Schwarzschild black hole and the slowly spinning Myers-Perry black holes are not unique. We show in section 5.4.5 that there is a 2-fold continuous family of black saturn solutions with $j = 0$.

5.4.5 Non-uniqueness

In the previous sections we have examined a number of examples which — among other phenomena — all illustrated non-uniqueness in the phase diagram a_{H} vs. j^2 . It is clear from these examples that black saturn covers large regions of the phase diagram. We now explore how large.

Non-uniqueness in the phase diagram

To study the region of the phase diagram covered by black saturn, we choose random sets of points $(\kappa_1, \kappa_2, \kappa_3)$ satisfying the ordering (5.3.3) and plot the corresponding point $(j, a_{\text{H}}^{\text{total}})$ in

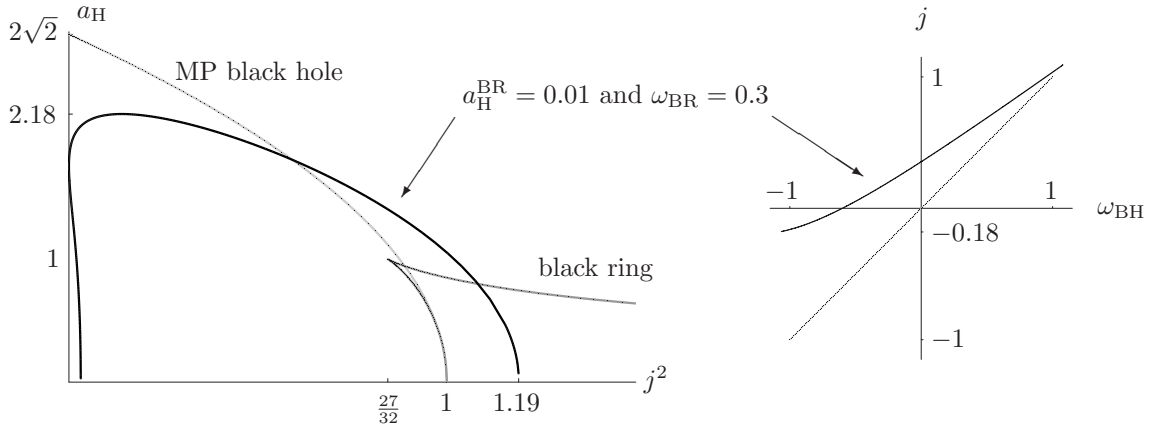


Figure 5.8: Left: Plot of a_H vs. j^2 for fixed $a_H^{\text{BR}} = 0.01$ and $\omega_{\text{BR}} = 0.3$ (black curve). Included are also the “phases” of a single Myers-Perry black hole (gray) and the black ring (darker gray). Right: j is plotted vs. the black hole for black saturn with $a_H^{\text{BR}} = 0.01$ and $\omega_{\text{BR}} = 0.3$ and for comparison with the corresponding curve for a single Myers-Perry black hole (light gray). The saturn configuration reaches $j = 0$ and extends to negative j .

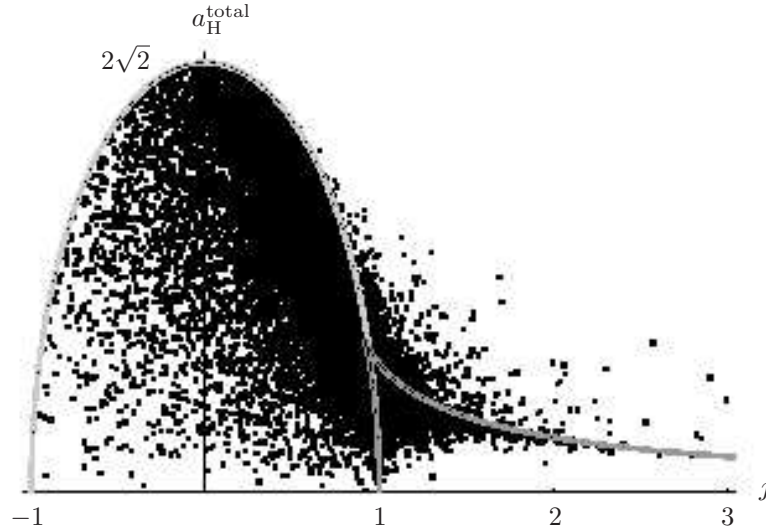


Figure 5.9: Non-uniqueness in the phase diagram: The plot shows the distribution of black saturn for 100.000 randomly chosen black saturn configurations.

the phase diagram.¹² Figure 5.9 shows the distribution of 100.000 such points.

We first note that we find no points with $j < -1$, thus black saturn takes values of $j \geq -1$. The asymmetry between positive and negative j is just a choice of rotation direction, which can be reversed by simply taking $\psi \rightarrow -\psi$ in the black saturn metric.¹³

Next the total area a_H^{total} is always less than the area of the static Schwarzschild black hole, which has $a_H^{\text{Schw}} = 2\sqrt{2}$. We believe that there are black saturn configurations with a_H^{total}

¹²The BZ parameter \bar{c}_2 is fixed in terms of $(\kappa_1, \kappa_2, \kappa_3)$ by the balance condition (5.3.17) with $\epsilon = +1$.

¹³It may also be noted that while ω_{BH} takes both positive and negative values, we find that ω_{BR} is always positive. The bound $\omega_{\text{BR}} > 0$ is intuitively a consequence of the fact that the black ring needs to rotate in order to keep the system balanced.

arbitrarily close to $a_{\text{H}}^{\text{Schw}}$. In fact for the dataset shown, we have

$$\min(a_{\text{H}}^{\text{Schw}} - a_{\text{H}}^{\text{total}}) = 9.5 \cdot 10^{-4}. \quad (5.4.5)$$

The distribution¹⁴ of black saturn configurations in the phase diagram figure 5.9 indicates that the region bounded by the Myers-Perry phase (shown in light gray for both positive and negative j) is fully covered by black saturn solutions. But there are also points outside this region: for j greater than ~ 0.5 , there are black saturn solutions with total area greater than the Myers-Perry black hole and the black ring.

By tuning the distribution, it can be shown [14] that the whole open strip

$$0 < a_{\text{H}}^{\text{total}} < 2\sqrt{2} = a_{\text{H}}^{\text{Schw}}, \quad j \geq 0, \quad (5.4.6)$$

is covered with black saturn configurations. For any $j \geq 0$ the high-entropy configurations are black saturn with an almost static S^3 black hole (accounting for the high entropy) surrounded by a large thin black ring (carrying the angular momentum). This type of configuration allow us to have black saturns with total area arbitrarily close to the bound set by the static Schwarzschild black hole. Details of this and the structure of the phase diagram are presented in [14].

Balanced saturn with zero angular momentum $j=0$

The phase diagram figure 5.9 strongly indicates that the $j = 0$ black saturn configurations are non-unique. We confirm the non-uniqueness in this section by studying the ranges of area, angular velocity and temperature covered by the balanced $j = 0$ saturn solutions.

Figure 5.10 shows the regions of the $(\omega_i, a_{\text{H}}^i)$ plane covered by the black ring and the S^3 black hole in saturn configurations with $j = 0$. Since $\omega_{\text{BH}} < 0$ and $\omega_{\text{BR}} > 0$, the two objects are clearly counter-rotating. Note that the black ring area a_{H}^{BR} has been multiplied by a factor of 50 in order for the plot be visible in the same plot as the S^3 black hole. The total area $a_{\text{H}}^{\text{total}}$ never exceeds that of the 4+1d Schwarzschild black hole.

The points in figure 5.10 are colored according to the temperature τ_i of the corresponding black hole/ring: Light gray means hot and black means cold. The scales used for the black hole and the black ring temperatures are different, as shown in figure 5.10. The S^3 black hole temperature varies roughly between 0 and 3 (roughly like the Myers-Perry black hole which varies between 0 and 1), while the black ring is much hotter with temperature varying between 13 and $\sim 10^3$. This, and the very small area of the black ring, signals that these are very thin, large radius black rings.

We further note that there is discrete non-uniqueness in the black ring sector of $j = 0$ black saturn. This can be seen by the “skirt” hanging over the righthand-part of the black ring area vs. ω_{BR} “bell”. The rings here have lower temperatures than the other rings with the same parameters, and it is therefore natural to interpret this “skirt” as a fat ring branch.

The points $(\omega_{\text{BH}}, a_{\text{H}}^{\text{BH}})$ lie in the wedge shown in figure 5.10. For each point in this S^3 black hole wedge there is one (or two, in case of additional discrete non-uniqueness) corresponding point(s) in the black ring “bell”. But it is not clear which S^3 black hole goes together with which black ring(s). That is illustrated better in figure 5.11, which shows two plots of ω_{BR} vs. ω_{BH} . The first is colored according to the area of the black hole a_{H}^{BH} , while the second is colored according to the area of the black ring a_{H}^{BR} . Light gray means large area, black small area. As shown, different scales are used in the two plots.

¹⁴The density in the distribution is caused by the discrete non-uniqueness in regions where both thin and fat black rings exist, but can also be affected by the particular distribution of points $(\kappa_1, \kappa_2, \kappa_3)$.

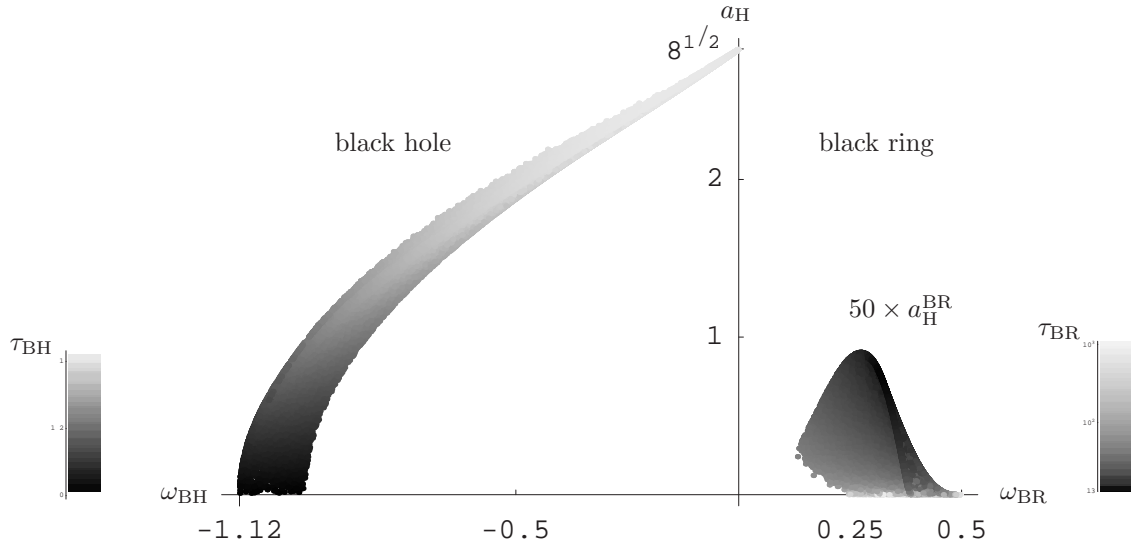


Figure 5.10: Non-uniqueness with $j = 0$: The plot shows the areas of the black hole (left) and black ring (right) vs. their respective angular velocities. Note that in order to fit the black hole and black ring areas on the same plot we have multiplied the black area by a factor of 50. The black holes are clearly counter-rotating. The points in the plots are colored according to the temperature. The black ring is always much hotter than the black hole, so different color scales are used for the black hole and the black ring.

In both figure 5.10 and figure 5.11 certain edges of the plots are rugged, and there are small white uncovered regions. This is simply due to the finite number of points generated for each plot, since some regions are covered less than others (this was also visible in figure 5.9).

Fixed j plots

We displayed in the previous section the regions of parameter space (ω_i, a_H^i) covered by saturn configurations with $j = 0$. Likewise we can explore non-uniqueness for saturn configurations with j fixed at other values. Figure 5.12 shows (ω_i, a_H^i) plots for representative values of fixed j .

When $j > \sqrt{27/32} \sim 0.92$, the S^3 black hole angular velocity ω_{BH} and area a_{H}^{BH} vary over a large range of values. This is shown in figures 5.12(a)-(d). As j becomes smaller than $j = \sqrt{27/32}$, which is the minimum value of j for the single black ring, the black ring of saturn has very small area and the range of the S^3 black hole parameters are more constrained, see figures 5.12(e)-(f). When the black ring and S^3 black hole are counter-rotating so that j is negative, the S^3 black hole parameters differ only little from the parameters of the Myers-Perry black hole, and the black ring is very thin and contributes little to the total area.

5.4.6 Solutions with $\epsilon = -1$

Up to this point we have examined the physics of black saturn solutions for which the condition for balance (5.3.4) was imposed with the choice of sign $\epsilon = +1$, and hence $\bar{c}_2 > -\kappa_2^{-1}$. Here we briefly discuss the balanced saturn solutions with $\epsilon = -1$ for which $\bar{c}_2 < -\kappa_2^{-1}$.

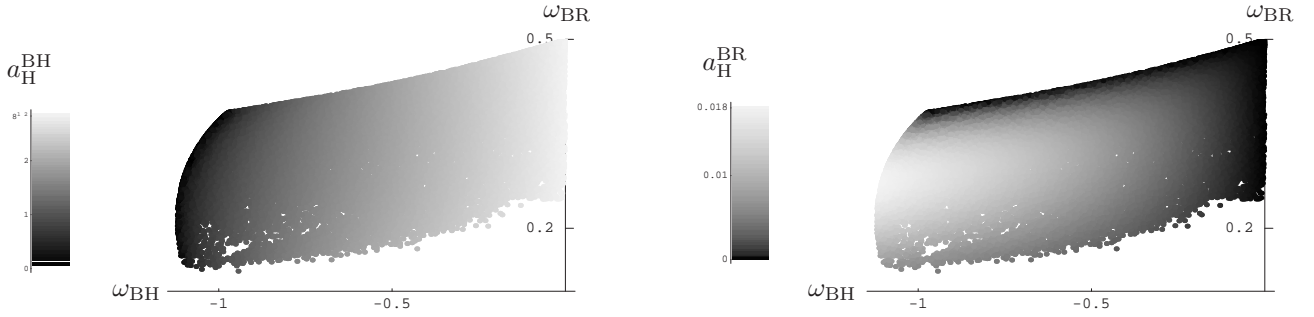


Figure 5.11: Non-uniqueness with $j = 0$: The two plots show the regions covered in “angular velocity space” when the angular momentum is fixed to zero, $j = 0$. Clearly the ring and the black hole are counter-rotating. On the left plot, the color shows the area of the black hole, while on the right plot it is the area of the black ring. Note again the scales are different and the black ring area is much smaller than that of the black hole.

As pointed out at the end of section 5.3.7, the solutions with $\bar{c}_2 > -\kappa_2^{-1}$ have positive Komar masses, while for $\bar{c}_2 < -\kappa_2^{-1}$, the Komar mass of the S^3 black hole is negative. We interpret this as an effect of extreme rotational frame-dragging, which makes $\Omega^{\text{BH}} J_{\text{Komar}}^{\text{BH}}$ so negative that the Smarr relation (5.3.44) renders the Komar mass negative.

In the limit $\bar{c}_2 \rightarrow -\kappa_2^{-1}$, several of the dimensionful physical parameters diverge. However, the dimensionless fixed-mass reduced quantities remain finite. In particular, the dimensionless proper distance ℓ , defined in (5.4.4), between the black ring and the S^3 goes to zero when $\bar{c}_2 \rightarrow -\kappa_2^{-1}$. So this is a singular merger limit which ends in the nakedly singular $\bar{c}_2 = -\kappa_2^{-1}$ solution.

The balanced saturn solutions with $\bar{c}_2 < -\kappa_2^{-1}$ occupy only a small region of the phase diagram $(j, a_{\text{H}}^{\text{total}})$. They have $j \simeq -1$ and total area $0 < a_{\text{H}}^{\text{total}} \lesssim 1$. We interpret these solutions as tightly bound gravitational systems; they probably deserve a closer study than the one provided here.

5.5 Discussion

We have presented and analyzed a new exact solution to 4+1-dimensional vacuum Einstein equations describing Black Saturn: a Myers-Perry black hole surrounded by a black ring which is balanced by rotation in the plane of the ring. The system exhibits a number of interesting properties, such as non-uniqueness and frame-dragging, which were summarized in the Introduction.

Most surprising is probably the result that the 4+1-dimensional Schwarzschild black hole and slowly spinning Myers-Perry black holes are not unique. Black saturn shows that once multiple black hole horizons are considered (and staticity not assumed for the $J = 0$ configurations) black holes in 4+1-dimensions have large degeneracies. This and the structure of the phase diagram for 4+1-dimensional black holes can be found in [14].

We expect both black objects in black saturn to have ergoregions whenever their angular velocities are non-zero. This is always the case for the black ring, whose ergosurface is expected to have topology $S^1 \times S^2$ [8]. The S^3 black hole can be tuned to have zero angular velocity, and it is natural to expect that the solution, despite having non-vanishing intrinsic angular momentum, has no ergoregion. Generally, however, we expect an ergoregion bounded by an

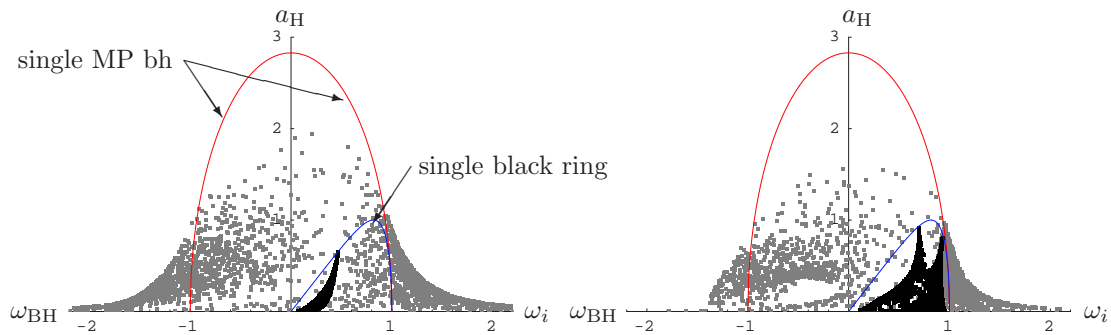
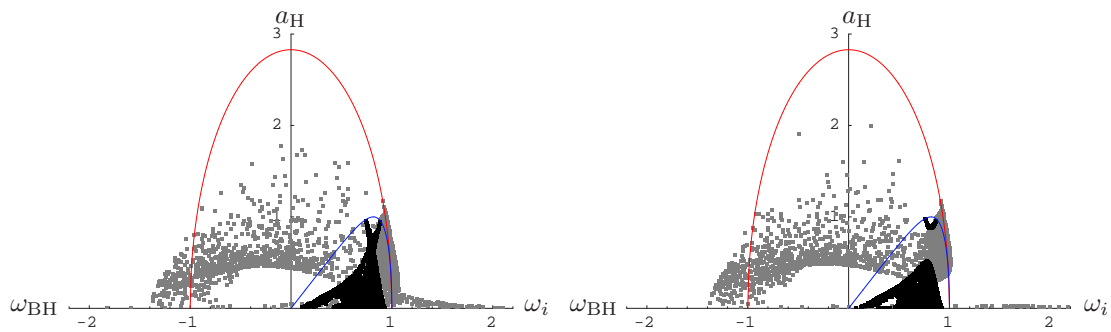
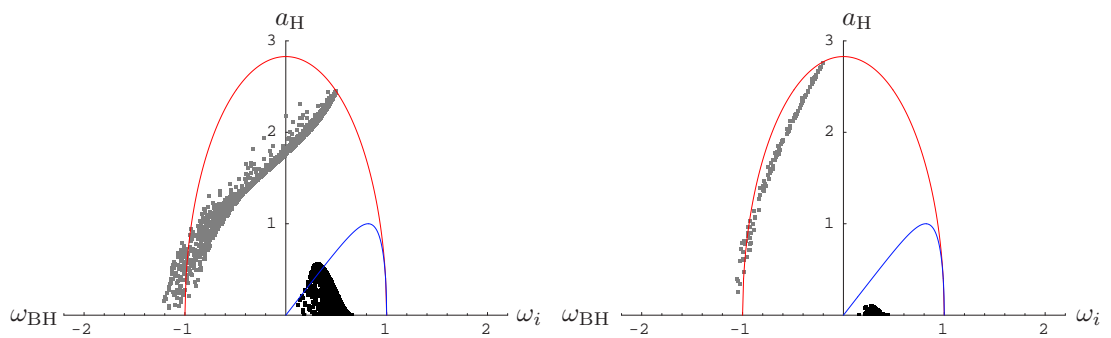
Figure 5.12(a): $j = 1.2$.Figure 5.12(b): $j = 0.95$.Figure 5.12(c): $j = 0.93$.Figure 5.12(d): $j = 0.925$.Figure 5.12(e): $j = 0.5$. The a_{BR} is multiplied by a factor of 10.Figure 5.12(f): $j = 0.2$. The a_{BR} is multiplied by a factor of 10.

Figure 5.12: For fixed total mass and some representative values of j^2 , the area of the black hole (gray dots) and the area of the black ring (black dots) are plotted against their respective angular velocities. The superimposed curves correspond to the area of a single Myers-Perry black hole against its angular velocity (upper curve), and similarly for the black ring. For these curves, the angular momentum j is of course not fixed. Note that for the black hole we included both the positive and negative ω_{BH} .

S^3 ergosurface. The metric in Weyl axisymmetric coordinates (ρ, z) is sufficiently complicated that we have not extracted useful equations for the ergoregions. We hope this will be addressed in future work, and note that it may be useful to first examine the $\rho = 0$ metric in order to examine the intersections of the ergosurfaces with the plane of the ring.

It would be desirable to transform the black saturn metric to a simpler coordinate system. The supersymmetric concentric black hole - black ring solutions of [15] can be written in ring coordinates (x, y) and it would presumably simplify our solution considerably to write it in such coordinates. We have presented in appendix 5.A.2 the coordinate transformation from Weyl axisymmetric coordinates (ρ, z) to ring coordinates (x, y) for the simpler limit of the black ring without the S^3 black hole. We leave it to future work to convert the full black saturn solution to ring coordinates. We expect that ring coordinates will make it easier to study the ergoregions.

Focusing on the plane of the ring, we have numerically checked examples of co- and counter-rotating configurations, and found no closed timelike curves (CTCs). While we see no signs of CTCs — the horizon areas and temperatures are positive and well-defined in the full range of parameters — this should be analyzed in greater detail than done in this paper. Writing the solution in ring coordinates (x, y) will likely facilitate such an analysis.

The 1st law of thermodynamics for black saturn is studied in [14]. (We refer to refs. [39] and [40] for other works on black ring thermodynamics.) Black saturn is an example of an equilibrium system of two black objects which generally have different temperatures and different angular velocities. This is therefore only a classical equilibrium. It is shown in [14] that imposing thermodynamic equilibrium, in the sense of the two objects having equal temperatures and equal angular velocities, reduces the continuous family of saturns to a one-parameter family of equilibrium solutions with only discrete non-uniqueness. The phase diagram of equilibrium solutions is presented in [14].

The saturn system may well be classically unstable. The black ring of black saturn likely suffers from the same instabilities as the single black ring [8]. Using the Poincaré (or “turning-point”) method, it was argued in [41] that (at least) one mode of instability would appear at the cusp of the black ring curve in the area vs. angular momentum phase diagram. At the cusp, where the thin and fat black ring branches meet, the black ring has minimum angular momentum and maximum entropy (for given mass). Studying the potential for the radial balance of a black ring, evidence was found [9] that a thin black ring would be stable under small radial perturbations while a fat black ring would be unstable. The radial instability of fat black rings appear exactly at the cusp, and so this mode is a physical concretization of the mode predicted by the turning-point method [41].¹⁵

Under radial perturbations, the analysis of [9] indicated that fat black rings either collapse to S^3 black hole (if perturbed inward) or possibly expand to become a thin black ring (if perturbed outwards). The latter may not happen in a dynamical process if thin black rings suffer from other classical instabilities, such as the Gregory-Laflamme instability [42], not captured by the turning-point method. Showing that Gregory-Laflamme modes always fit on (thin) black rings, refs. [10, 9] argued that thin black rings very likely suffer from Gregory-Laflamme instabilities. Likewise, we expect thin black rings of the black saturn system to be unstable to Gregory-Laflamme instabilities.

While some stability properties of black saturn can be expected to be inherited from the individual components, the Myers-Perry black hole and the single black ring, there can also be

¹⁵Due to the continuous non-uniqueness, the implementation of the turning-point method for black saturn does not seem possible. Following [9] one can try to compute the radial potential for the black ring in black saturn, but here one also has to choose to fix some non-conserved quantities in order to carry out the analysis.

new instabilities for the black saturn system, for instance, perturbation of the center-of-mass of the S^3 black hole away from the center of the ring.

We constructed the black saturn solution using the inverse scattering method [18, 19, 20]. The seed solution and the soliton transformations invite a number of interesting generalizations of black saturn:

- *Multiple rings of saturn:* It is straightforward to generalize the seed solution to include more rod sources that will correspond to black ring horizons. One can also add negative density rods to facilitate the addition of angular momentum for each black ring using (anti)soliton transformations like we did in section 5.2.2. Provided all singularities can be removed as done here, and the system balanced, the generated solution will describe “the multiple rings of black saturn”. One interesting property of multiple ring solutions is the high degree of continuous non-uniqueness as we discussed in the Introduction.
- *Doubly spinning black saturn:* The 3-soliton transformation in section 5.2.2 adds a second angular momentum for the S^3 black hole when $b_3 \neq 0$. An analysis of this solution is required to check that all possible singularities can be eliminated. Then it will be interesting to study the physics of this doubly spinning saturn system. We expect that the second “intrinsic” spin J_ϕ^{Komar} will only be non-vanishing for the S^3 black hole, but that the black ring will also have non-vanishing angular velocity on the S^2 . This would be interpreted as rotational dragging of the S^3 black hole on the black ring.

The 3-soliton construction of section 5.2.2 does not give the most general doubly spinning black saturn configuration, because the black ring would not carry independent angular momentum on the S^2 . The more general black saturn configuration should be possible to obtain with the methods recently used to construct the doubly spinning black ring [27].

Doubly spinning black rings likely suffer from superradiant instabilities [43]. It would be interesting to see if such an instability is present also when the black ring is only being dragged on the S^2 by the S^3 black hole.

- *Dipole black saturn:* Black rings can carry non-conserved “dipole charges” [44]. Adding dipole charge(s) to the black ring will give a dipole black saturn solution. The techniques [45] for adding dipole charge by combining two or more vacuum solutions should apply here.
- *Charged black saturn:* Vacuum solutions can be charged up to carry conserved charges — and for black rings also dipole charges. Lifting the solutions to ten dimensions and using boosts and dualities it is easy to charge up Myers-Perry black holes and black rings to carry, say D1- and D5-charges. The same transformations give a D1-D5-charged black saturn configuration (although not the most general such solution). For black rings there is a technical difficulty in adding the third charge, momentum P , as detailed in [46]. This can be overcome by starting with a dipole black ring, and in this way a class of non-supersymmetric three-charge black rings have been obtained [47].

Likewise, a D1-D5-P black saturn solution can be obtained from dipole black saturn, and this would lead to (a subclass of) non-supersymmetric generalizations of the supersymmetric concentric black ring solutions [15]. It would be interesting if techniques can be developed to add independent charges to multi-component black hole systems.

As discussed in the Introduction, one motivation for the existence of black saturn is to think of a thin black ring balanced in the external potential of the S^3 black hole. We have of course seen clear evidence of the gravitational interactions between the black ring and the S^3 black hole, for instance the rotational dragging (see section 5.4.3). So considering the black hole as providing an external potential should only be seen as a motivation for the case where the black ring is very thin with large S^1 radius so that the interactions between the objects is negligible. Following the method of [9] one can take the system off-shell and study the equilibrium of forces on a very thin black ring around a small black hole. Presumably this would give a Newtonian balance between a string-like tension of the ring and the angular velocity in the background gravitational potential of the S^3 black hole.

The balanced black saturn solution presented here has two separate sectors. These arise from two different ways of imposing the balance condition, as described in section 5.3. We have focused almost entirely on the sector where the Komar masses of both the black ring and the S^3 black hole are non-negative. However, the other sector — for which the S^3 black hole Komar mass is negative — may also contain interesting physics. We interpret the possibility of negative Komar mass as a consequence of extreme rotational dragging experienced by the S^3 black hole when its Komar angular momentum cannot counter the dragging by the black ring. It would be interesting to understand this strongly interacting system better.

The 3+1 dimensions double-Kerr solution can be constructed with methods similar to the ones used in this paper. While it is not possible for two Kerr-black holes to be balanced by spin-spin interactions alone, one could ask if it is for two Myers-Perry black holes in 4+1 dimensions. The static solution describing two (or more) Myers-Perry black holes held apart by conical singular membranes is easy to construct using the methods of [29]; this family of solutions was studied in [48]. Angular momentum can be added by soliton transformations similar to the ones used here. It is not clear if the resulting solution can be made free of singularities and, even if so, if the black holes can be held apart by the spin-spin interactions.

Little is known about what types of black holes are admitted by the Einstein equations in six and higher-dimensions. The main focus has been on spacetimes with a single connected black hole horizon, but black saturn has shown that interesting physics arises in higher-dimensional multi-black hole systems. It will be interesting to see what exotic multi-black hole solutions higher-dimensional gravity has to offer.

Acknowledgements

We are grateful to Gary Horowitz, Harvey Reall, Enric Verdaguer and especially Roberto Emparan for discussions of the inverse scattering method and saturn physics. We thank Chethan Krishnan for pointing out that a clarification was needed for comparison of the results of the 2- and 3-soliton transformations.

PF would like to thank the Theoretical Physics group at Imperial College London for hospitality and also the Center for Theoretical Physics at MIT for warm hospitality while part of this work was done. HE thanks the Aspen Center for Physics for a fruitful stay during the summer 2006. HE also thanks the Theoretical Physics group at Uppsala University and the Niels Bohr Institute for hospitality during the final stages of this work.

HE was supported by a Pappalardo Fellowship in Physics at MIT and by the US Department of Energy through cooperative research agreement DE-FG0205ER41360. PF was supported by FI and BE fellowships from AGAUR (Generalitat de Catalunya), DURSI 2005 SGR 00082, CICYT FPA 2004-04582-C02-02 and EC FP6 program MRTN-CT-2004-005104.

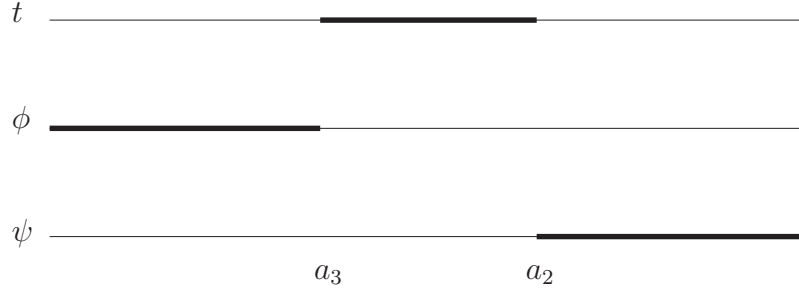


Figure 5.13: Sources for the Myers-Perry black hole. The timelike rod is aligned along $(1, 0, \Omega_{\psi}^{\text{BH}})$.

5.A Limits

In this section we provide details of the Myers-Perry black hole limit and the black ring limit of the black saturn solution.

5.A.1 Myers-Perry black hole

From the rod structure figure 5.2(b) of the full solution, one can see that the Myers-Perry black hole with a single angular momentum is obtained by eliminating the rod corresponding to the black ring. There is however an issue of the order of limits. First one can note that from our general saturn solution, with c_1 and c_2 arbitrary, the following two limits result in the same solution:

$$\text{Limit 1 : } a_1 \rightarrow a_5, \quad \text{then } a_5 \rightarrow a_4, . \quad (5.A.1)$$

$$\text{Limit 2 : } a_5 \rightarrow a_4, \quad \text{then } a_1 \rightarrow a_4, . \quad (5.A.2)$$

As long as c_1 and c_2 are kept fixed (i.e. the regularity condition (5.3.7) is *not* imposed), these two limits are equivalent and give the metric

$$\begin{aligned} G_{tt} &= -\frac{\mu_3 [-c_2^2 \mu_2^2 \mu_3 + (\rho^2 + \mu_2 \mu_3)^2]}{\mu_2 [c_2^2 \mu_3 \rho^2 + (\rho^2 + \mu_2 \mu_3)^2]}, & G_{t\psi} &= -\frac{c_2 \mu_3 (\rho^2 + \mu_2^2)(\rho^2 + \mu_3^2)}{\mu_2 [c_2^2 \mu_3 \rho^2 + (\rho^2 + \mu_2 \mu_3)^2]}, \\ G_{\psi\psi} &= \frac{\mu_2^2 (\rho^2 + \mu_2 \mu_3)^2 - c_2^2 \mu_3 \rho^2}{\mu_2 [c_2^2 \mu_3 \rho^2 + (\rho^2 + \mu_2 \mu_3)^2]}, & G_{\phi\phi} &= \frac{\rho^2}{\mu_3}, \\ e^{2\nu} &= \frac{k^2 \mu_2 [c_2^2 \mu_3 \rho^2 + (\rho^2 + \mu_2 \mu_3)^2]}{(\rho^2 + \mu_2^2)(\rho^2 + \mu_3^2)(\rho^2 + \mu_2 \mu_3)}. \end{aligned} \quad (5.A.3)$$

To bring the metric given above to an asymptotically flat form one has to perform change the coordinates according to $t = t' - c_2 \psi'$ and $\psi = \psi'$. Finally, to show that this solution given in (5.A.3) is indeed the Myers-Perry black hole with a single angular momentum, one can change to prolate spheroidal coordinates as done in [30] and [21].

Now if we are interested in obtaining the Myers-Perry black hole as a limit of the black saturn configuration, we must remove the black ring in a limit where the condition (5.3.7) is imposed on c_1 . Note that in Limit 1 of (5.A.1), $c_1 \rightarrow \infty$. This is the reason we consider Limit 2 in (5.A.1).

In the parametrization introduced in section 5.3.1 Limit 2 is

$$\kappa_3 \rightarrow \kappa_2, \quad \text{then } \kappa_2 \rightarrow 0. \quad (5.A.4)$$

By first taking $\kappa_3 \rightarrow \kappa_2$ we eliminate the divergence in c_1 and then the $\kappa_2 \rightarrow 0$ limit can be taken safely. The resulting metric is (5.A.3).

With \bar{c}_2 fixed by the balanced condition (5.3.17), this limit can only be taken for $\epsilon = +1$, and one finds

$$\bar{c}_2 = 1 - \frac{1}{2\kappa_1} \quad (5.A.5)$$

and all physical parameters are then functions of the dimensionless parameter κ_1 and the scale L , which are related to the standard Myers-Perry black hole parameters r_0 and a through

$$r_0^2 = \frac{L^2}{2\kappa_1}, \quad a = \frac{L(1 - 2\kappa_1)}{\sqrt{2\kappa_1}}. \quad (5.A.6)$$

5.A.2 Black ring limit

The ψ -spinning black ring is obtained by first setting $c_2 = 0$, then taking $a_2 = a_3$. We must continue to impose the condition (5.3.7) for c_1 ; note that this condition is independent of a_2 . We find

$$G_{tt} = -\frac{\mu_1 \left[\mu_5(\rho^2 + \mu_1\mu_3)^2(\rho^2 + \mu_1\mu_4)^2 - c_1^2 \mu_3 \mu_4 (\mu_1 - \mu_5)^2 \rho^4 \right]}{\mu_4 \left[\mu_5(\rho^2 + \mu_1\mu_3)^2(\rho^2 + \mu_1\mu_4)^2 + c_1^2 \mu_1^2 \mu_3 \mu_4 (\mu_1 - \mu_5)^2 \rho^2 \right]}, \quad (5.A.7)$$

$$G_{t\psi} = -\frac{c_1 \mu_3 \mu_5 (\mu_1 - \mu_5) (\rho^2 + \mu_1^2) (\rho^2 + \mu_1 \mu_3) (\rho^2 + \mu_1 \mu_4)}{\left[\mu_5(\rho^2 + \mu_1\mu_3)^2(\rho^2 + \mu_1\mu_4)^2 + c_1^2 \mu_1^2 \mu_3 \mu_4 (\mu_1 - \mu_5)^2 \rho^2 \right]}, \quad (5.A.8)$$

$$G_{\psi\psi} = \frac{\mu_3 \mu_5 \left[\mu_5(\rho^2 + \mu_1\mu_3)^2(\rho^2 + \mu_1\mu_4)^2 - c_1^2 \mu_1^4 \mu_3 \mu_4 (\mu_1 - \mu_5)^2 \right]}{\mu_1 \left[\mu_5(\rho^2 + \mu_1\mu_3)^2(\rho^2 + \mu_1\mu_4)^2 + c_1^2 \mu_1^2 \mu_3 \mu_4 (\mu_1 - \mu_5)^2 \rho^2 \right]}, \quad (5.A.9)$$

$$e^{2\nu} = k^2 \frac{\mu_3(\rho^2 + \mu_1\mu_5)(\rho^2 + \mu_3\mu_4)(\rho^2 + \mu_4\mu_5)}{4\mu_1(\rho^2 + \mu_1\mu_3)(\rho^2 + \mu_1\mu_4)(\rho^2 + \mu_3\mu_5)^2 \prod_{i \neq 2} (\rho^2 + \mu_i^2)} \times \left[\mu_5(\rho^2 + \mu_1\mu_3)^2(\rho^2 + \mu_1\mu_4)^2 + c_1^2 \mu_1^2 \mu_3 \mu_4 (\mu_1 - \mu_5)^2 \rho^2 \right]. \quad (5.A.10)$$

Note that for $c_1 = 0$ we obtain the metric for the static black ring. The corresponding rod structure is depicted in figure 5.14.

To verify that this solution really describes the ψ -ring, we rewrite the metric in ring coordinates (x, y) , i.e.

$$ds^2 = -\frac{F(y)}{F(x)} \left(dt + C_\lambda R \frac{1+y}{F(y)} d\psi \right)^2 + \frac{R^2}{(x-y)^2} F(x) \left[-\frac{G(y)}{F(y)} d\psi^2 - \frac{dy^2}{G(y)} + \frac{dx^2}{G(x)} + \frac{G(x)}{F(x)} d\phi^2 \right], \quad (5.A.11)$$

where

$$G(\xi) = (1 - \xi^2)(1 + \nu\xi), \quad F(\xi) = (1 + \lambda\xi), \quad C_\lambda = \sqrt{\lambda(\lambda - \nu) \frac{1 + \lambda}{1 - \lambda}}. \quad (5.A.12)$$

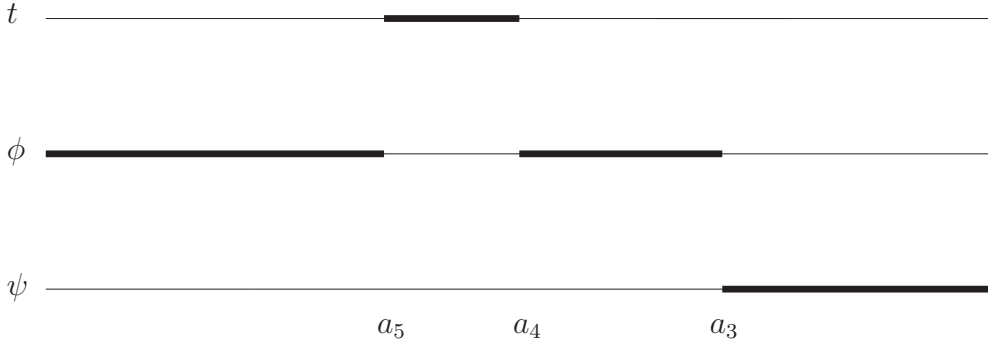


Figure 5.14: Sources for the black ring. The timelike rod has direction $(1, 0, \Omega_\psi^{\text{BR}})$.

The coordinate transformation from Weyl coordinates (ρ, z) to ring coordinates (x, y) is

$$\rho = \frac{R^2 \sqrt{-G(x)G(y)}}{(x-y)^2}, \quad z = \frac{R^2(1-xy)[2+\nu(x+y)]}{2(x-y)^2}. \quad (5.A.13)$$

Note that

$$d\rho^2 + dz^2 = K(x, y) \left[-\frac{dy^2}{G(y)} + \frac{dx^2}{G(x)} \right], \quad (5.A.14)$$

with

$$K(x, y) = -\frac{R^4}{4(x-y)^3} [x+y+\nu(1+xy)][2+\nu(1+x+y-xy)][2+\nu(-1+x+y+xy)]. \quad (5.A.15)$$

The rod endpoints are related to the parameters ν and λ as

$$a_1 = R^2\alpha, \quad a_5 = -\frac{R^2}{2}\nu, \quad a_4 = \frac{R^2}{2}\nu, \quad a_3 = \frac{R^2}{2}. \quad (5.A.16)$$

Here $\alpha < -\nu/2$ is a constant which will be determined below. With this choice, $\rho^2 + (z - a_i)^2$ is a perfect square for $i = 3, 4, 5$ (but not for $i = 1$ for choice of $\alpha < -\nu/2$) so we have simple expressions for $\mu_i = R_i - (z - a_i) = \sqrt{\rho^2 + (z - a_i)^2} - (z - a_i)$:

$$\mu_5 = -\frac{R^2(1-x)(1+y)(1+\nu y)}{(x-y)^2}, \quad (5.A.17)$$

$$\mu_4 = -\frac{R^2(1-x)(1+y)(1+\nu x)}{(x-y)^2}, \quad (5.A.18)$$

$$\mu_3 = -\frac{R^2(1-y^2)(1+\nu x)}{(x-y)^2}. \quad (5.A.19)$$

The expression for μ_1 , however, involves an explicit squareroot, $R_1 = \sqrt{\rho^2 + (z - a_1)^2}$. We write $\mu_1 = R_1 - (z - a_1)$, but keep R_1 unevaluated. Then collect powers of R_1 and simplify the expressions for each metric component when only even powers of R_1 are replaced by their expression in terms of x, y . Then we end up in general for each metric component with expressions of the form

$$g_{\mu\nu} \sim \frac{p_0 + p_1 R_1}{q_0 + q_1 R_1}, \quad (5.A.20)$$

where $p_{0,1}$ and $q_{0,1}$ are functions of x, y . Now it turns out, as can explicitly be verified, that for all cases, $p_0/q_0 = p_1/q_1$ so that $g_{\mu\nu} = p_0/q_0$. Thus we have eliminated the squareroot R_1 from the expressions, and indeed p_0/q_0 is a simple function of x, y . For example, we find

$$G_{tt} = -\frac{2 - 2\alpha(1+y) - \nu(1-y)}{2 - 2\alpha(1+x) - \nu(1-x)}. \quad (5.A.21)$$

We bring G_{tt} to the standard form given in (5.A.11) by choosing

$$\alpha = \frac{\nu(1+\lambda) - 2\lambda}{2(1-\lambda)}. \quad (5.A.22)$$

The condition that $\alpha \leq -\nu/2$ is then simply that $\nu \leq \lambda$, while $-\infty < \alpha$ gives $\lambda < 1$. We have therefore recovered the bound

$$0 < \nu \leq \lambda < 1 \quad (5.A.23)$$

on the black ring parameters λ and ν .

With this choice (5.A.22) for α we have

$$e^{2\nu} = \frac{k^2(1-\nu)^2}{1-\lambda} \frac{R^2}{(x-y)^2} \frac{F(x)}{K(x,y)}, \quad (5.A.24)$$

so that choosing the integration constant k as

$$k^2 = \frac{(1-\lambda)}{(1-\nu)^2} \quad (5.A.25)$$

we recover the x, y -part of the metric (5.A.11). With these choices for α (the position of the “fake” rod endpoint) and k , the full metric (5.A.7) becomes (5.A.11).

Note that in the black ring limit with $\bar{c}_2 = 0$, the periods (5.3.15) are $\Delta\psi = \Delta\phi = 2\pi k$, which with k given above agrees precisely with the result for the black ring [44]. Likewise all physical parameters of the neutral black ring are reproduced from this limit of the black saturn solution.

Bibliography

- [1] S. D. Majumdar, “A class of exact solutions of Einstein’s field equations,” *Phys. Rev.* **72**, 390 (1947).
A. Papapetrou, “A Static Solution Of The Equations Of The Gravitational Field For An Arbitrary Charge Distribution,” *Proc. Roy. Irish Acad. (Sect. A)* **51**, 191 (1947).
J. B. Hartle and S. W. Hawking, “Solutions of the Einstein-Maxwell equations with many black holes,” *Commun. Math. Phys.* **26**, 87 (1972).
- [2] D. Kramer and G. Neugebauer, “The superposition of two Kerr solutions,” *Phys. Lett. A.* **75** 4 (1980) 259-261
- [3] R. Wald, “Gravitational spin interaction,” *Phys. Rev. D* **6**, 406 (1972).
- [4] C. Hoenselaers, “Remarks on the Double-Kerr Solution,” *Progr. Theor. Phys.* **72** No. 4 (1984) 761
- [5] W. Dietz and C. Hoenselaers, “Two Mass Solutions of Einstein’s Vacuum Equations: The Double Kerr Solution,” *Ann. Phys. (USA)* **165** (1985) 319-383
- [6] V. S. Manko and E. Ruiz, “Exact solution of the double-Kerr equilibrium problem,” *Class. Quant. Grav.* **18**, L11-L15 (2001)
- [7] H. Stephani, D. Kramer, M. MacCallum, C. Hoenselaers and E. Herlt, “Exact solutions of Einstein’s field equations,” Cambridge University Press (Cambridge, 2003)
- [8] R. Emparan and H. S. Reall, “A rotating black ring in five dimensions,” *Phys. Rev. Lett.* **88** (2002) 101101 [arXiv:hep-th/0110260].
See also the review: R. Emparan and H. S. Reall, “Black rings,” *Class. Quant. Grav.* **23**, R169 (2006) [arXiv:hep-th/0608012].
- [9] H. Elvang, R. Emparan and A. Virmani, “Dynamics and stability of black rings,” *JHEP* **0612**, 074 (2006) [arXiv:hep-th/0608076].
- [10] J. L. Hovdebo and R. C. Myers, “Black rings, boosted strings and Gregory-Laflamme,” *Phys. Rev. D* **73**, 084013 (2006) [arXiv:hep-th/0601079].
- [11] R. C. Myers and M. J. Perry, “Black Holes In Higher Dimensional Space-Times,” *Annals Phys.* **172**, 304 (1986).

- [12] G. W. Gibbons, D. Ida and T. Shiromizu, “Uniqueness and non-uniqueness of static vacuum black holes in higher dimensions,” *Prog. Theor. Phys. Suppl.* **148**, 284 (2003) [arXiv:gr-qc/0203004];
S. Hwang, *Geometriae Dedicata* **71**, 5 (1998)
- [13] H. Kodama, “Perturbative uniqueness of black holes near the static limit in arbitrary dimensions,” *Prog. Theor. Phys.* **112**, 249 (2004) [arXiv:hep-th/0403239].
- [14] H. Elvang, R. Emparan and P. Figueras, “Phases of five-dimensional black holes,” arXiv:hep-th/0702111.
- [15] J. P. Gauntlett and J. B. Gutowski, “Concentric black rings,” *Phys. Rev. D* **71**, 025013 (2005) [arXiv:hep-th/0408010].
J. P. Gauntlett and J. B. Gutowski, “General concentric black rings,” *Phys. Rev. D* **71**, 045002 (2005) [arXiv:hep-th/0408122].
- [16] J. P. Gauntlett, J. B. Gutowski, C. M. Hull, S. Pakis and H. S. Reall, “All supersymmetric solutions of minimal supergravity in five dimensions,” *Class. Quant. Grav.* **20**, 4587 (2003) [arXiv:hep-th/0209114].
- [17] J. B. Gutowski, D. Martelli and H. S. Reall, “All supersymmetric solutions of minimal supergravity in six dimensions,” *Class. Quant. Grav.* **20**, 5049 (2003) [arXiv:hep-th/0306235].
- [18] V. A. Belinsky and V. E. Zakharov, “Integration Of The Einstein Equations By The Inverse Scattering Problem Technique And The Calculation Of The Exact Soliton Solutions,” *Sov. Phys. JETP* **48** (1978) 985 [*Zh. Eksp. Teor. Fiz.* **75** (1978) 1953].
- [19] V. A. Belinsky and V. E. Sakharov, “Stationary Gravitational Solitons With Axial Symmetry,” *Sov. Phys. JETP* **50** (1979) 1 [*Zh. Eksp. Teor. Fiz.* **77** (1979) 3].
- [20] V. Belinski and E. Verdaguer, “Gravitational solitons,” Cambridge, UK: Univ. Pr. (2001) 258 p.
- [21] A. A. Pomeransky, “Complete integrability of higher-dimensional Einstein equations with additional symmetry, and rotating black holes,” *Phys. Rev. D* **73** (2006) 044004 [arXiv:hep-th/0507250].
- [22] T. Mishima and H. Iguchi, “New axisymmetric stationary solutions of five-dimensional vacuum Einstein equations with asymptotic flatness,” *Phys. Rev. D* **73**, 044030 (2006) [arXiv:hep-th/0504018].
- [23] S. Tomizawa, Y. Morisawa and Y. Yasui, “Vacuum solutions of five dimensional Einstein equations generated by inverse scattering method,” *Phys. Rev. D* **73** (2006) 064009 [arXiv:hep-th/0512252].
- [24] P. Figueras, “A black ring with a rotating 2-sphere,” *JHEP* **0507**, 039 (2005) [arXiv:hep-th/0505244].
- [25] H. Iguchi and T. Mishima, “Solitonic generation of five-dimensional black ring solution,” *Phys. Rev. D* **73**, 121501 (2006) [arXiv:hep-th/0604050].

- [26] S. Tomizawa and M. Nozawa, “Vacuum solutions of five-dimensional Einstein equations generated by inverse scattering method. II: Production of black ring solution,” *Phys. Rev. D* **73** (2006) 124034 [arXiv:hep-th/0604067].
- [27] A. A. Pomeransky and R. A. Sen’kov, “Black ring with two angular momenta,” arXiv:hep-th/0612005.
- [28] H. Kudoh, “Doubly spinning black rings,” *Phys. Rev. D* **75**, 064006 (2007) [arXiv:gr-qc/0611136].
- [29] R. Emparan and H. S. Reall, “Generalized Weyl solutions,” *Phys. Rev. D* **65** (2002) 084025 [arXiv:hep-th/0110258].
- [30] T. Harmark, “Stationary and axisymmetric solutions of higher-dimensional general relativity,” *Phys. Rev. D* **70** (2004) 124002 [arXiv:hep-th/0408141].
- [31] H. Elvang, R. Emparan, D. Mateos and H. S. Reall, “A supersymmetric black ring,” *Phys. Rev. Lett.* **93** (2004) 211302 [arXiv:hep-th/0407065].
- [32] I. Bena and N. P. Warner, “One ring to rule them all ... and in the darkness bind them?,” *Adv. Theor. Math. Phys.* **9** (2005) 667 [arXiv:hep-th/0408106].
- [33] H. Elvang, R. Emparan, D. Mateos and H. S. Reall, “Supersymmetric black rings and three-charge supertubes,” *Phys. Rev. D* **71** (2005) 024033 [arXiv:hep-th/0408120].
- [34] J. Kunz and F. Navarro-Lerida, “Non-uniqueness, counterrotation, and negative horizon mass of Einstein-Maxwell-Chern-Simons black holes,” *Mod. Phys. Lett. A* **21**, 2621 (2006) [arXiv:hep-th/0610075].
- [35] M. Cvetič, G. W. Gibbons, H. Lu and C. N. Pope, “Rotating black holes in gauged supergravities: Thermodynamics, supersymmetric limits, topological solitons and time machines,” arXiv:hep-th/0504080.
- [36] J. C. Breckenridge, R. C. Myers, A. W. Peet and C. Vafa, “D-branes and spinning black holes,” *Phys. Lett. B* **391** (1997) 93 [arXiv:hep-th/9602065].
- [37] H. Elvang and G. T. Horowitz, “When black holes meet Kaluza-Klein bubbles,” *Phys. Rev. D* **67**, 044015 (2003) [arXiv:hep-th/0210303].
- [38] J. P. Gauntlett, R. C. Myers and P. K. Townsend, “Black holes of $D = 5$ supergravity,” *Class. Quant. Grav.* **16**, 1 (1999) [arXiv:hep-th/9810204].
- [39] K. Copsey and G. T. Horowitz, “The role of dipole charges in black hole thermodynamics,” *Phys. Rev. D* **73**, 024015 (2006) [arXiv:hep-th/0505278].
- [40] D. Astefanesei and E. Radu, “Quasilocal formalism and black ring thermodynamics,” *Phys. Rev. D* **73**, 044014 (2006) [arXiv:hep-th/0509144].
- [41] G. Arcioni and E. Lozano-Tellechea, “Stability and critical phenomena of black holes and black rings,” *Phys. Rev. D* **72**, 104021 (2005) [arXiv:hep-th/0412118].
- G. Arcioni and E. Lozano-Tellechea, “Stability and thermodynamics of black rings,” arXiv:hep-th/0502121.

- [42] R. Gregory and R. Laflamme, “Black strings and p-branes are unstable,” *Phys. Rev. Lett.* **70**, 2837 (1993) [arXiv:hep-th/9301052];
R. Gregory and R. Laflamme, “The Instability of charged black strings and p-branes,” *Nucl. Phys. B* **428**, 399 (1994) [arXiv:hep-th/9404071].
For a recent review, see: T. Harmark, V. Niarchos and N. A. Obers, “Instabilities of black strings and branes,” arXiv:hep-th/0701022.
- [43] O. J. C. Dias, “Superradiant instability of large radius doubly spinning black rings,” *Phys. Rev. D* **73**, 124035 (2006) [arXiv:hep-th/0602064].
- [44] R. Emparan, “Rotating circular strings, and infinite non-uniqueness of black rings,” *JHEP* **0403**, 064 (2004) [arXiv:hep-th/0402149].
- [45] S. S. Yazadjiev, “Completely integrable sector in 5D Einstein-Maxwell gravity and derivation of the dipole black ring solutions,” *Phys. Rev. D* **73**, 104007 (2006) [arXiv:hep-th/0602116].
S. S. Yazadjiev, “Solution generating in 5D Einstein-Maxwell-dilaton gravity and derivation of dipole black ring solutions,” *JHEP* **0607**, 036 (2006) [arXiv:hep-th/0604140].
S. S. Yazadjiev, “Rotating dyonic dipole black rings: Exact solutions and thermodynamics,” arXiv:hep-th/0607101.
- [46] H. Elvang and R. Emparan, “Black rings, supertubes, and a stringy resolution of black hole non-uniqueness,” *JHEP* **0311**, 035 (2003) [arXiv:hep-th/0310008].
- [47] H. Elvang, R. Emparan and P. Figueras, “Non-supersymmetric black rings as thermally excited supertubes,” *JHEP* **0502**, 031 (2005) [arXiv:hep-th/0412130].
- [48] H. S. Tan and E. Teo, “Multi-black hole solutions in five dimensions,” *Phys. Rev. D* **68**, 044021 (2003) [arXiv:hep-th/0306044].

Chapter 6

Phases of Five-Dimensional Black Holes

Henriette Elvang,^a Roberto Emparan,^{b,c} Pau Figueras^c

^a *Center for Theoretical Physics,
Massachusetts Institute of Technology, Cambridge MA 02139, USA*

^b *Institució Catalana de Recerca i Estudis Avançats (ICREA)*

^c *Departament de Física Fonamental,
Universitat de Barcelona, Diagonal 647, E-08028 Barcelona, Spain*

elvang@lns.mit.edu, emparan@ub.edu,
pfigueras@fn.ub.es

ABSTRACT

We argue that the configurations that approach maximal entropy in five-dimensional asymptotically flat vacuum gravity, for fixed mass and angular momentum, are ‘black Saturns’ with a central, close to static, black hole and a very thin black ring around it. For any value of the angular momentum, the upper bound on the entropy is equal to the entropy of a static black hole of the same total mass. For fixed mass, spin and area there are families of multi-ring solutions with an arbitrarily large number of continuous parameters, so the total phase space is infinite-dimensional. Somewhat surprisingly, the phases of highest entropy are not in thermal equilibrium. Imposing thermodynamical equilibrium drastically reduces the phase space to a finite, small number of different phases.

6.1 Introduction

In this paper we study the phases of black holes in five-dimensional gravity¹ with total mass M and angular momentum J , *i.e.*, phases in the microcanonical ensemble. A question of particular interest is which configuration maximizes the entropy for given M and J .

¹More precisely: stationary vacuum solutions, $R_{\mu\nu} = 0$, which are asymptotically flat and regular on and outside the black hole horizons.

In five dimensions, in addition to the Myers-Perry (MP) black holes with horizon topology S^3 [1], there exist black rings with topology $S^1 \times S^2$, which imply discrete non-uniqueness in a range of parameters [2]. But black rings turn out to introduce a much larger degeneracy through multi-black hole configurations. To understand these, recall that the S^1 -radius of a black ring can be made arbitrarily large, for a given mass, by thinning the ring. So, given a sufficiently thin and long ring, we can imagine putting a MP black hole at its center. This increases slightly the centripetal pull on the ring, but the effect can be counterbalanced by increasing its rotation. These configurations, dubbed *black Saturns* have been explicitly constructed and analyzed recently in [3]. The black ring can actually encircle the central black hole quite closely, giving rise to effects such as rotational dragging, but here we are more interested in situations where the interactions between the ring and the central black hole are small. In principle the construction method used in [3] allows to systematically add an arbitrary number of rings, but the complication grows enormously with each new ring. Solutions with two black rings (without any central MP black hole) have been constructed in [4].

A scatter-plot sampling of the parameter space of the exact solutions in [3] showed regions of the phase diagram where black Saturns are the entropically dominating solutions. We will argue here that this happens throughout the entire phase diagram: for any values of $M > 0$, $J > 0$, *the phase with highest entropy is a black Saturn*. Naively, one might have thought that a configuration with multiple black holes should increase its entropy by merging them all into a single black hole. That this need not be so for a black Saturn follows from two simple observations:

1. Among all single black objects of a given mass M , the one with maximal entropy is the static ($J = 0$) spherical black hole.
2. A black ring of fixed mass can carry arbitrarily large spin J by making its S^1 -radius large enough (and its S^2 -radius small enough). Conversely, there is always a thin black ring of arbitrarily small mass with any prescribed value of J .

So we may say that static spherical black holes are the most efficient black objects (since they use up a minimal mass) for carrying entropy, and black rings are the most efficient ones for carrying spin. So, given any values of $M > 0$ and $J > 0$, the total entropy will be maximized by putting virtually all the mass in a central static black hole, and having an extremely long, thin and light black ring, carrying all the angular momentum. The total entropy of this black Saturn configuration approaches asymptotically, in the limit of infinitely thin ring, the entropy of a static black hole with the same total mass. We shall argue that in fact for any given value of the total angular momentum, there exist black Saturns spanning the entire range of areas

$$0 < \mathcal{A} < \mathcal{A}_{\max} = \frac{32}{3} \sqrt{\frac{2\pi}{3}} (GM)^{3/2}. \quad (6.1.1)$$

Here \mathcal{A}_{\max} is the area of the static black hole.

We can also infer another remarkable feature of the five-dimensional black hole phase space. Black Saturns with a single black ring exhibit two-fold continuous non-uniqueness [3]: besides the total M and J , two other continuous parameters — say, the mass of the black ring and its dimensionless ‘thickness’ parameter — are needed in order to fully specify the solution. Adding n more rings introduces $2n$ more continuous parameters. Moreover, a ring can have an effect as small as desired on the total black Saturn. So for generic values of M , J and $\mathcal{A} \in (0, \mathcal{A}_{\max})$

there are black Saturns with an arbitrarily large number of rings, and therefore characterized by an arbitrarily large number of continuous parameters.

The phase space thus shows a striking infinite intricacy. However, most of these solutions, in particular the ones that maximize the total area, are not in thermal equilibrium: the temperatures and angular velocities need not be the same on disconnected components of the horizon. We find that imposing thermodynamic equilibrium drastically reduces the phase space to a finite number of families (perhaps only three), each specified by a function $M(J, \mathcal{A})$.

6.2 Phasing in Saturn

We begin by recalling the known single-black-object phases (*i.e.*, with connected horizons), namely, MP black holes and black rings. We only consider solutions with angular momentum in a single rotation plane. In order to eliminate awkward factors from the formulas, we will work with rescaled spins and areas²

$$\tilde{J} \equiv \sqrt{\frac{27\pi}{32G}} J, \quad \tilde{\mathcal{A}} \equiv \sqrt{\frac{27}{256\pi G^3}} \mathcal{A}. \quad (6.2.1)$$

The MP black hole phase with mass M_h and angular momentum J_h is characterized by the area

$$\tilde{\mathcal{A}}_h = 2\sqrt{2\left(M_h^3 - \tilde{J}_h^2\right)}, \quad (6.2.2)$$

and the black rings with mass M_r , in parametric form, by area and angular momentum

$$\tilde{\mathcal{A}}_r = 2\sqrt{M_r^3\nu(1-\nu)}, \quad \tilde{J}_r^2 = M_r^3\frac{(1+\nu)^3}{8\nu}. \quad (6.2.3)$$

To characterize their sizes, we introduce the circumferential radius of the MP black hole in the rotation plane

$$R_h = 2\sqrt{\frac{G}{3\pi}}\sqrt{\frac{2M_h}{1 - \tilde{J}_h^2/M_h^3}} \quad (6.2.4)$$

and the S^1 -radius of the inner rim of the ring,

$$R_1 = 2\sqrt{\frac{G}{3\pi}}\sqrt{M_r\frac{1-\nu}{\nu}}. \quad (6.2.5)$$

The dimensionless parameter $\nu \in (0, 1)$ is a ‘thickness’ parameter for the black ring.³ If we fix M_r , then as $\nu \rightarrow 0$ the angular momentum and R_1 both go to infinity, and the area approaches zero: this is the limit of an infinitely thin ring of infinite radius. In the opposite limit, as $\nu \rightarrow 1$ we find a naked singularity with zero area. The same singular solution is found in the extremal limit of MP black holes, $\tilde{J}_h^2 \rightarrow M_h^3$. The phase diagram with these solutions is shown in figure 6.1. For every value of \tilde{J} , there is at least one black object, and for $\sqrt{27/32} < \tilde{J} < 1$ there are three of them.

²For solutions with a single black object of unit mass these coincide with the reduced spin and area, j and a_H , introduced in [5].

³For more precision and details see [6].

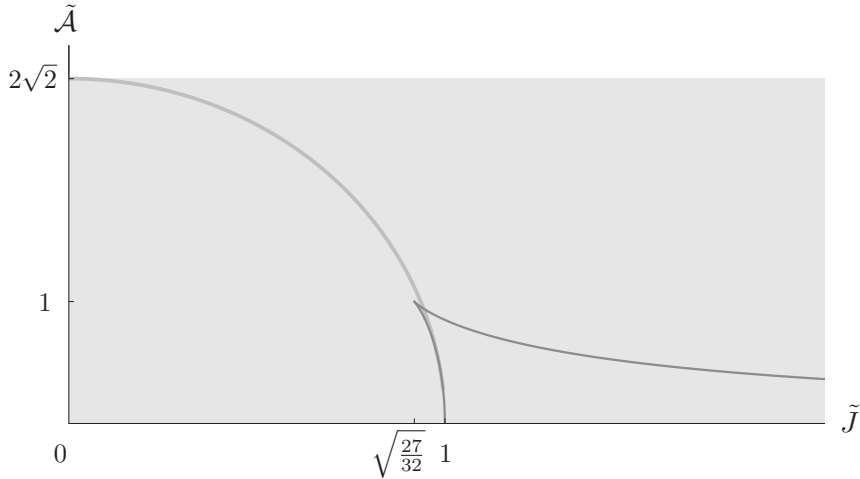


Figure 6.1: Phases of five-dimensional black holes including black Saturns. We fix total mass $M = 1$ and plot total area vs. spin. The solid curves correspond to single MP black holes and black rings. The semi-infinite shaded strip, spanning $0 \leq \tilde{J} < \infty$, $0 < \tilde{\mathcal{A}} < 2\sqrt{2}$, is covered by black Saturns. Each point in the strip actually corresponds to a one-parameter family of Saturn solutions. The top end $\tilde{\mathcal{A}} = 2\sqrt{2}$ with $\tilde{J} \neq 0$ is reached only asymptotically for black Saturns with infinitely long rings. Solutions at the bottom $\tilde{\mathcal{A}} = 0$ are naked singularities. For a fixed value of \tilde{J} we can move from the top of the strip to the bottom by varying the spin of the central black hole \tilde{J}_h from 0 to 1. For fixed area we can move horizontally by having $\tilde{J}_h < 0$ and varying the spin of the ring between $|\tilde{J}_h|$ and ∞ .

Generically, adding spin for fixed mass reduces the area, as also happens for the four-dimensional Kerr solution. So for a given value of M , the maximal entropy is attained by the static black hole,

$$\tilde{\mathcal{A}}_{\max} = (2M)^{3/2}. \quad (6.2.6)$$

In principle any solution that is regular on and outside the horizon, even if it consists of disconnected horizons, is an allowed phase. So now we consider multi-black hole configurations. In classical General Relativity we are free to fix a scale, which we will take to be the total mass M . So, fixing

$$M = 1 \quad (6.2.7)$$

we want to know which solutions exist for a given total J , and what their total entropy is. In particular, we want to find the configurations with maximal entropy.

The simplest black Saturns consist of a central MP black hole and a single black ring. The actual solutions are rather complicated due to the gravitational interactions between both objects, but if $R_1 \gg R_h$ these effects become negligible. If M_h is not much smaller than M_r , this requires a very thin ring, *i.e.*, small ν .⁴ Observe in particular that the dragging effect that the black ring has on the central black hole can be made arbitrarily small, no matter how large \tilde{J}_r , by making the ring thin and long enough. This becomes clear by recalling that black rings resemble boosted black strings, whose dragging falls off asymptotically in the transverse radial direction r like $\sim R_2/r$, where R_2 is the radius of the S^2 of the string. So the effect near the center of the ring is at most $\sim R_2/R_1 \simeq \nu$.

In this approximation, then, we can model a black Saturn as a simple superposition of an MP black hole and a black ring. Take

$$\tilde{\mathcal{A}} = \tilde{\mathcal{A}}_h + \tilde{\mathcal{A}}_r, \quad M = 1 = M_h + M_r, \quad \tilde{J} = \tilde{J}_h + \tilde{J}_r. \quad (6.2.8)$$

⁴Thicker rings with a tiny black hole at the center are of little interest to us here, since they give phases with entropy very close to that of single black rings.

Comparing the plots of black Saturn phases produced using these expressions with those from the exact solutions in [3] confirms that the approximation is good when the rings are thin and long.

Having fixed the scale, configurations in this model have three free parameters, just like in the actual black Saturn solutions. So for fixed $(M, \tilde{J}) = (1, \tilde{J})$, there is a two-parameter family of solutions. Let us take \tilde{J}_h and ν as these two parameters, and ask which values of them give maximal entropy. As discussed in the introduction, we expect to achieve this by putting all the spin on a thin, large ring, of very small mass. Graphical examination of the function $\mathcal{A}(\tilde{J}_h, \nu; \tilde{J})$ for different values of \tilde{J} shows indeed that the maximum area is achieved with $\tilde{J}_h = 0$ and $\nu \rightarrow 0$. So let us set $\tilde{J}_h = 0$, and consider small values of ν . Then

$$\tilde{\mathcal{A}}|_{\tilde{J}_h=0} = 2\sqrt{2} - 6\sqrt{2} \tilde{J}^{2/3} \nu^{1/3} + O(\nu^{2/3}). \quad (6.2.9)$$

We indeed find that the maximal area (6.2.6) is reached from below as $\nu \rightarrow 0$ for *any* value of \tilde{J} .

What is then the region of the plane $(\tilde{J}, \tilde{\mathcal{A}})$ covered when we include the Saturn phases? We now argue that it is the semi-infinite strip

$$\begin{aligned} 0 < \tilde{\mathcal{A}} < \tilde{\mathcal{A}}_{\max} = 2\sqrt{2}, \\ 0 \leq \tilde{J} < \infty, \end{aligned} \quad (6.2.10)$$

plus the point $(\tilde{J}, \tilde{\mathcal{A}}) = (0, 2\sqrt{2})$ for the static black hole (of course the symmetric region with $\tilde{J} < 0$ is covered by reversing the spins):

- We have seen that the upper boundary of the strip ($\tilde{J} > 0, \tilde{\mathcal{A}} = 2\sqrt{2}$) is approached asymptotically as the ring grows infinitely long and infinitesimally thin.
- The lower boundary ($\tilde{J} \geq 0, \tilde{\mathcal{A}} = 0$) corresponds to naked singularities. One way to reach these is to make the central black hole approach the extremal singular solution $\tilde{J}_h^2 \rightarrow M_h^3$, and adjusting the spin of the ring towards $\tilde{J} - M_h^{3/2}$ while sending $M_r \rightarrow 0$ and $\nu \rightarrow 0$. Even if in this limit $R_h \rightarrow \infty$, it is easy to see that, for any finite values of the parameters, we can satisfy $R_1 \gg R_h$ so our approximations hold. Thus there are regular Saturn solutions arbitrarily close to the lower boundary.
- The solutions at the left boundary, with $(\tilde{J} = 0, 0 < \tilde{\mathcal{A}} \leq 2\sqrt{2})$ correspond to black Saturns where the central black hole and the black ring are counterrotating. Such configurations were studied in detail in [3]. To cover the entire range $0 < \tilde{\mathcal{A}} \leq 2\sqrt{2}$ we can simply have a central black hole rotating to get the required area, and a thin black ring counterrotating so that the angular momenta of the ring and the hole cancel. It is possible to achieve $\tilde{J} = 0$ also with fatter rings.
- We can easily see that there is at least one black Saturn for any point within these boundaries. Again, the idea is to have a central black hole, in general spinning, accounting for the area $\tilde{\mathcal{A}}$, and an extremely thin and long ring carrying the required angular momentum to make up for the total \tilde{J} .

So we can argue, by considering only black Saturns with thin rings, that all of the strip (6.2.10) is covered. It is also easy to see why the scatter-plots in [3] found it hard to sample the whole strip: the solutions with the highest entropies are strongly localized in a small region of

the parameter space. Focusing and increasing the size of the sample shows a clear tendency to cover the whole strip, and in particular that entropies higher than those of rotating MP black holes can occur for all $J \neq 0$.

In general there will be not just one black Saturn for every point $(\tilde{J}, \tilde{\mathcal{A}})$ in the strip, but rather a one-parameter family of them. These are guaranteed to exist by continuity, starting from the configuration with an infinitely thin ring described above, and continuously increasing ν while adequately adjusting \tilde{J}_h to keep \tilde{J} and $\tilde{\mathcal{A}}$ fixed. This gives black Saturns with fatter black rings, although at each point in the strip in general there will be restrictions on the upper value for ν , and on the range of \tilde{J}_h .

When we discuss the configurations with maximal entropy, we should note that our approximation based on (6.2.8) actually tends to underestimate slightly the entropy of a black Saturn with a very thin ring. Roughly, the reason is that the interaction between the central black hole and the black ring is attractive, and so it decreases the system's energy. Here we are fixing the total energy, which means that the attraction leaves more rest-energy to be stored in the black hole, giving a larger entropy than in the simple approximation (6.2.8). We have confirmed this effect with the exact solutions in [3]. It is also possible to argue, by modeling the interaction in Newtonian terms, that this does not allow to overshoot and reach areas larger than $2\sqrt{2}$: for small ν , the resulting increase in the area is at least $O(\nu^{2/3})$ and hence smaller than the leading correction in (6.2.9). Other competing effects, like dragging, are even more subdominant. So our conclusion that there do exist black Saturns with area approaching arbitrarily close to a maximum (6.2.6) seems robust and holds even after including interactions.

6.3 Multiple rings and further parameters

Using the same methods we can discuss solutions with multiple black rings. Begin with two concentric black rings, and no central black hole. The exact solutions have been built in [4]. When one of the rings is much longer than the other we can use an approximation analogous to (6.2.8) and simply superimpose two black rings. Arguments of the kind above suggest that the maximal area will be that of a minimally spinning ring (with $\nu = 1/2$), *i.e.*, $\tilde{\mathcal{A}} = 1$. In this case, a strip of unit height, extending to all $\tilde{J} \geq 0$, will be covered by these solutions. So some double-ring configurations will have higher entropy than single rings with the same mass and spin, with the maximal entropy achieved when the innermost ring has $\nu \approx 1/2$ and the outer ring is very thin and light.

Black Saturns with multiple rings are clearly possible too, and when the rings are thin and sparsely spaced we can model them by adding more terms to (6.2.8). For solutions with many rings the cumulative dragging effect may become stronger, but we can always have solutions with thinner and thinner rings where this is negligible. Each class of solutions with fixed number n of rings, and therefore with $2n$ continuous parameters, covers the entire strip (6.2.10).

But there is even more. So far we have restricted ourselves to solutions that rotate in a single plane. It is however possible to have both the MP black hole and the black rings rotate in the plane orthogonal to the ring plane. Black rings with two independent rotation parameters have been constructed recently [7]. For fixed mass the S^2 -spin J_2 is bounded above, for reasons similar to the bound on Kerr black holes. Furthermore, it can be seen that $|J_2| < |J_1|$. But another consequence of having $J_2 \neq 0$ is that J_1 is also bounded above, and the extremal solutions that saturate this bound, for fixed mass, have non-zero area. In other words, given $J_1, J_2 \neq 0$ there is a limit on how small the mass and how large the S^1 radius of the black ring

can be. But even if this second rotation puts an upper limit on the S^1 -radius of a black ring, it is clear that in general it adds yet another set of continuous parameters to the phase diagram with fixed $(M, J_1 = J, J_2 = 0)$ that we have been studying. The second spin of the central black hole, if not too large, can be cancelled against the corresponding S^2 -spin of a black ring. So with each black ring in the black Saturn we get one more continuous parameter.

Still, multi-ring black Saturns may not exhaust the class of asymptotically flat 5D vacuum black holes. Solutions that include bubbles in combination with black holes [8, 9] may play a role. It has also been speculated that black holes with only one axial symmetry might exist [10]. All of these, if they do exist, will add further dimensions to the phase space, but we find it unlikely that they can allow for larger total area than (6.2.6).

It is clear that the general phase space for solutions with non-zero values of the two spins will, for the same reasons, be infinite-dimensional. It will be interesting to analyze its overall features.

6.4 First law of multi-black hole mechanics

Consider a general stationary black Saturn (or any multi-black hole solution) made of N black objects labelled by $i = 1 \dots, N$. Each connected component of the horizon H_i is generated by a Killing vector

$$k_{(i)} = \xi + \Omega_i \zeta, \quad (6.4.1)$$

where ξ and ζ are the canonically normalized Killing vectors that generate time translations and rotations near infinity, and Ω_i is the angular velocity on H_i . Following standard procedure [11] we can write the ADM mass as a Komar integral on a sphere at infinity,

$$M = -\frac{3}{32\pi G} \int_{S_\infty} \epsilon_{abcde} \nabla^d \xi^e. \quad (6.4.2)$$

Since we are in vacuum, Stokes' theorem allows us to write this as

$$M = -\frac{3}{32\pi G} \sum_i \int_{H_i} \epsilon_{abcde} \nabla^d \xi^e. \quad (6.4.3)$$

Using (6.4.1), a standard calculation leads to the Smarr relation

$$M = \frac{3}{2} \sum_i \left(\frac{\kappa_i}{8\pi G} \mathcal{A}_i + \Omega_i J_i \right), \quad (6.4.4)$$

where \mathcal{A}_i and κ_i are the area and surface gravity on H_i , and

$$J_i = \frac{1}{16\pi G} \int_{H_i} \epsilon_{abcde} \nabla^d \zeta^e \quad (6.4.5)$$

is the (Komar) angular momentum of the i -th black object. Ref. [3] checked that (6.4.4) holds for the explicit solutions in [3]. We could define 'Komar masses' for each black object

$$M_i = -\frac{3}{32\pi G} \int_{H_i} \epsilon_{abcde} \nabla^d \xi^e = \frac{3}{2} \left(\frac{\kappa_i}{8\pi G} \mathcal{A}_i + \Omega_i J_i \right), \quad (6.4.6)$$

but note that the latter equalities are actually mathematical identities on each horizon, so they should not be thought of as 'true' Smarr relations.

In a similar manner, a straightforward extension of [11] yields the first law of multi-black hole mechanics⁵

$$\delta M = \sum_i \left(\frac{\kappa_i}{8\pi G} \delta \mathcal{A}_i + \Omega_i \delta J_i \right). \quad (6.4.7)$$

The phase space of black Saturn configurations with up to N black objects is $2N$ -dimensional. One may use the (\mathcal{A}_i, J_i) as variables in it, or perhaps better, the total \mathcal{A} and J , and (\mathcal{A}_i, J_i) , $i = 2, \dots, N$. Fig. 6.1 is in fact a projection of the phase diagram onto the plane (\mathcal{A}, J) . It must be noted that, as is apparent already when $N = 1$, the (\mathcal{A}_i, J_i) variables do not necessarily specify a unique phase, as there may be discrete degeneracies.

6.5 Thermodynamical equilibrium

Black Saturns are valid stationary solutions, regular on and outside the horizons. But there is a glaring problem if they are to be considered as thermodynamical phases: the separate black components have in general different temperatures. Solutions with equal temperatures on all horizons are possible, but in the configurations that maximize the entropy the thin black ring has a temperature that is inversely proportional to its S^2 -radius and hence diverges in the limit of zero thickness. So we find that the system can increase its entropy by creating a large temperature gradient within itself! In other words, it looks like the highest entropy state is not in thermal equilibrium, which seems at odds with basic thermodynamical principles.

A similar problem arises with the horizon angular velocity Ω , which is the intensive ‘potential’ for the angular momentum and therefore would be expected to be homogeneous in a situation of mechanical rotational equilibrium. For a very thin and light black ring $\Omega \sim 1/R_1$ is very small, so in the black Saturns with near-maximal area it is possible to arrange for $\Omega_h = \Omega_r$. Nevertheless, generic stationary black Saturns have a variety of different Ω_i .

In order to understand better these discrepancies, recall that black hole thermodynamics (as opposed to black hole mechanics) really makes sense only when Hawking radiation is included. In the presence of radiation, a generic black Saturn cannot be in thermal equilibrium, even in the microcanonical ensemble. Even if T is homogeneous, the radiation cannot be in mechanical equilibrium between two black objects with different values of Ω . In fact the radiation will couple the different black objects and drive the system towards thermodynamical equilibrium. In the absence of this radiation each black object acts, to some extent, as a separate thermodynamical system of its own. (A further issue comes from the fact that black Saturns within wide parameter ranges are expected to be classically dynamically unstable. We will discuss further this point in the final section.)

If we consider a black Saturn with a single ring, then requiring equal temperatures and angular velocities for the central black hole and the black ring imposes two conditions on the parameters. This removes entirely the continuous non-uniqueness, leaving at most discrete degeneracies. Black Saturns in thermodynamical equilibrium thus form a curve in the plane $(\tilde{J}, \tilde{\mathcal{A}})$. This curve, generated from the exact solutions in [3], is shown in fig. 6.2.

The qualitative properties of the curve are easy to understand. Consider a black Saturn with a thin (though not necessarily very thin) black ring. In order for the temperature of the central black hole and the black ring to be the same, the black hole radius must be roughly the same as the ring’s S^2 radius [6]. Then, the longer the ring, the larger the fraction of the

⁵A first law and a Smarr relation of this kind were found to hold in [9] for explicit solutions with multiple static black holes in Kaluza-Klein cylinders.

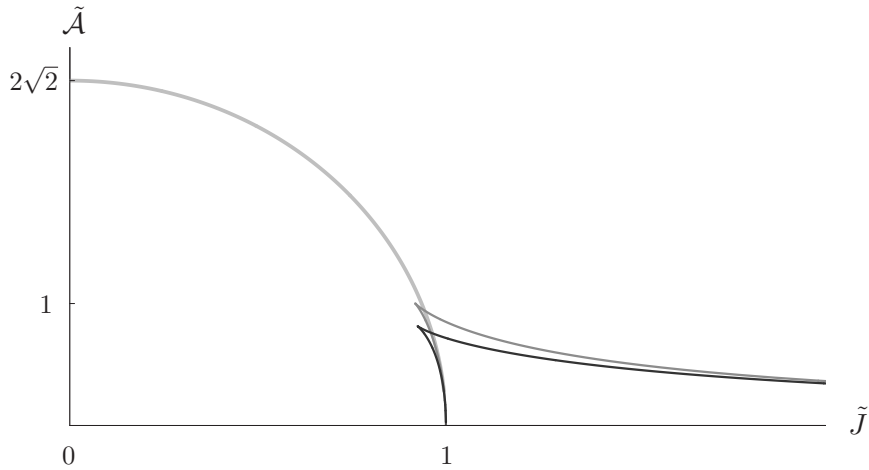


Figure 6.2: Phases in thermodynamical equilibrium. Besides the gray curves for MP black holes and black rings, we have the solid black curve of single-ring black Saturns for which the central black hole and the black ring have equal temperature and equal angular velocity. There is only one black Saturn (and not a continuous family of them) for each point in this curve. The minimum \tilde{J} along the curve is ≈ 0.9245 , slightly above $\sqrt{27/32}$, and the maximum total area is $\tilde{\mathcal{A}} \approx 0.81$. Note that black Saturns are never entropically dominant among the phases in thermodynamical equilibrium. In the text we argue that it is unlikely that multi-ring black Saturns exist as states in thermodynamical equilibrium. Barring more exotic possibilities, this diagram may then contain all thermodynamical equilibrium states of 5D black holes.

total mass it carries. In particular, as $\tilde{J} \rightarrow \infty$ most of the mass is in the ring, so the black Saturn curve asymptotes to that of a single black ring. As the black ring gets thicker a larger fraction of the mass goes into the central black hole, and the total entropy is only a fraction of the entropy of a single ring. When the black ring is fat, the two black objects get distorted and flattened along the rotation plane, approaching the singular zero-area limit at $\tilde{J} = 1$, common to black rings and MP black holes. Although not shown in the figure, along the equilibrium curve the angular velocity is smaller and the temperature higher than those of a single ring of the same \tilde{J} . The reason is that in a black Saturn the angular momentum is distributed over more objects (hence Ω is lower) that are thinner (hence hotter) than in the single black ring.

It looks much more difficult to impose equality of all temperatures and all angular velocities on solutions with two or more black rings (whether with a central MP black hole or not). The reason is that fixing T and Ω determines *uniquely* a black ring [6]. So once we have one ring, if we try to put in another one with the same T and Ω , we are actually trying to put in *the same ring*. There may be a slim chance that, due to non-linearities, a di-ring with two very close-by rings of the same T and Ω exist. This can be settled by examining the exact solutions in [4]. But clearly this is a strongly constrained possibility, and it seems highly unlikely that an arbitrary number of black rings in thermodynamical equilibrium can be piled on top of each other.

So the condition of thermodynamical equilibrium not only removes all continuous non-uniqueness, but it also reduces to a handful the families of possible black objects: MP black holes, black rings, single-ring black Saturns — and this may be all. Barring the possibility of multi-ring black Saturns, and of the conjectural solutions mentioned at the end of section 6.3, all the black hole phases in thermodynamical equilibrium would be present in figure 6.2. Up to a few degeneracies, these phases are specified by functions $M(J, \mathcal{A})$. So the phase space in thermodynamic equilibrium is two-dimensional, and shows only discrete non-uniqueness.

Finally, note that when the second angular momentum is turned on, the phase space of thermodynamic equilibrium becomes three-dimensional, with energy function $M(J_1, J_2, \mathcal{A})$. It seems likely that this phase space consists only of extensions of the families of solutions considered above.

6.6 Discussion

For upon immediately directing my telescope at Saturn, I found that things there had quite a different appearance from that which they had previously been thought by most men to have.

Christiaan Huygens, Systema Saturnium (1659)

The phase structure we have uncovered has certainly quite a different appearance from that which it had previously been thought to have.

An infinite-dimensional phase space, due to configurations with an arbitrarily large number of black holes, is also known to occur in the context of black holes localized in Kaluza-Klein cylinders, or ‘caged’ black holes [12]. However, configurations with multiple caged black holes are all expected to increase their entropy by merging into a single black hole. What is most remarkable about black Saturns is not so much that they are possible, but that they maximize the entropy. The essential idea behind this maximization consists of transferring all the spin of the black hole (which tends to reduce the entropy) into orbital angular momentum carried by a very light object at large radius. In general this can be achieved through non-stationary configurations with, say, faraway gravitational waves, or small black holes, carrying the angular momentum, plus a central black hole close to maximal area. This possibility was in fact considered in [13], but black Saturns realize it solely in terms of stationary solutions.

Black Saturns with very thin and long rings are loosely bound configurations, with negligible binding energy. But more importantly, they are expected to be dynamically unstable. Very thin black rings are likely to suffer from Gregory-Laflamme instabilities [14, 2, 15, 6, 16]. If, as a result, the black ring fragments into smaller MP-like black holes, these will fly apart. This final configuration is reminiscent of those considered in [13] for the decay of ultra-spinning MP black holes in $D \geq 6$. There, the possibility of increasing the area through fragmentation was one of several telltale signs of a classical ultraspinning instability. We have found that five-dimensional rotating MP black holes and black rings might similarly increase their entropy through fragmentation into a black Saturn (which may then fragment further). Could this signal a classical instability of *all* five-dimensional black holes with $J \neq 0$?

Before jumping to this conclusion, it is important to bear in mind that the existence of a configuration with higher total area is merely suggestive of a possible dynamical instability. In addition, there must exist some plausible classical dynamical evolution that drives the initial configuration towards another one close enough to the putative final state (through a curvature singularity, if fragmentation is to occur). In this respect, it seems difficult for an MP black hole, or a black ring, to dynamically evolve into a black Saturn of near-maximal area, which has a black ring of *much larger* extent on the rotation plane than the initial black hole. But it could possibly evolve towards a black Saturn of roughly the same size as the initial black hole, if the final area were higher. This remains to be investigated.

While it may seem striking that the configuration of maximal entropy is classically unstable (except at $J = 0$: the static black hole is stable [17]), it should be recalled that it is not

in thermal equilibrium, so usual thermodynamic reasoning does not really apply here. When Hawking radiation is taken into account, the very thin black ring of black Saturn (or, if it fragments, the very small black holes flying away) will evaporate much faster than the central black hole that carries most of the mass. An important problem is to find the dynamically stable configurations with maximal entropy among those that are in stable thermodynamical equilibrium with Hawking radiation in the microcanonical ensemble. It seems possible that this consists of an MP black hole surrounded by spinning radiation. However, the thermodynamics of other ensembles is likely to be quite different [6]. Another question to bear in mind is that black Saturns with maximal area require infinite volume. In a finite volume with fixed energy, maximal area may not always be attained by a black Saturn. This will be the case when the volume is large compared to, say, the Schwarzschild radius for that energy. But if the box could barely fit a single MP black hole, or a single black ring, then it might not fit a black Saturn of larger area. All these issues must be sorted out depending on the specific application of these ideas one is considering.

Dynamically stable black Saturns having only M and J as conserved charges are likely to exist at least in Einstein-Maxwell theories. If the black ring in the configuration carries a dipole charge [5] it can saturate an extremal (not BPS) bound, in which case the Gregory-Laflamme instability is expected to disappear. Thin dipole black rings have also been argued to be radially stable [6]. So dipole black Saturns can presumably be made classically stable. Supersymmetric multi-ring black Saturns, also expected stable, have been described in [18]. It has been observed that in some cases they can have larger entropy than a single black hole with the same conserved charges. Semi-qualitative arguments similar to the ones in this paper might help understand this effect.

Thin black rings have been argued to exist in any $D \geq 5$, achieving equilibrium in essentially the same manner as in $D = 5$ [15, 6]. So black Saturns should exist, too, in any $D \geq 5$ and in particular the ones that maximize the entropy should share the same features that we have described in this paper. A semi-infinite strip in the (\tilde{J}, \tilde{A}) plane will then be covered by an infinite number of families of solutions, but only a few of them are expected to be in thermal equilibrium.

Finally, our discussion of the phase space has been wholly classical. In quantum gravity the continuous parameters will become discrete. Furthermore, there will be a lower, Planck-length bound on the size of the S^2 of thin black rings in a black Saturn. This will limit the thinness of the ring and force the entropy of a black Saturn to be finitely below the maximal value.

Acknowledgements

We thank Gary Horowitz for comments on the first version of this paper. HE was supported by a Pappalardo Fellowship in Physics at MIT and by the US Department of Energy through cooperative research agreement DE-FG0205ER41360. RE and PF were supported in part by DURSI 2005 SGR 00082, CICYT FPA 2004-04582-C02-02 and EC FP6 program MRTN-CT-2004-005104. PF was also supported by an FI scholarship from Generalitat de Catalunya.

Bibliography

- [1] R. C. Myers and M. J. Perry, “Black Holes In Higher Dimensional Space-Times,” *Annals Phys.* **172**, 304 (1986).
- [2] R. Emparan and H. S. Reall, “A rotating black ring in five dimensions,” *Phys. Rev. Lett.* **88** (2002) 101101 [arXiv:hep-th/0110260]; for a review, see “Black rings,” *Class. Quant. Grav.* **23** (2006) R169 [arXiv:hep-th/0608012].
- [3] H. Elvang and P. Figueras, “Black Saturn,” arXiv:hep-th/0701035.
- [4] H. Iguchi and T. Mishima, “Black di-ring and infinite nonuniqueness,” arXiv:hep-th/0701043.
- [5] R. Emparan, “Rotating circular strings, and infinite non-uniqueness of black rings,” *JHEP* **0403** (2004) 064 [arXiv:hep-th/0402149].
- [6] H. Elvang, R. Emparan and A. Virmani, “Dynamics and stability of black rings,” *JHEP* **0612** (2006) 074 [arXiv:hep-th/0608076].
- [7] A. A. Pomeransky and R. A. Sen’kov, “Black ring with two angular momenta,” arXiv:hep-th/0612005.
- [8] R. Emparan and H. S. Reall, “Generalized Weyl solutions,” *Phys. Rev. D* **65** (2002) 084025 [arXiv:hep-th/0110258].
- [9] H. Elvang, T. Harmark and N. A. Obers, “Sequences of bubbles and holes: New phases of Kaluza-Klein black holes,” *JHEP* **0501** (2005) 003 [arXiv:hep-th/0407050].
- [10] H. S. Reall, “Higher dimensional black holes and supersymmetry,” *Phys. Rev. D* **68** (2003) 024024 [Erratum-ibid. *D* **70** (2004) 089902] [arXiv:hep-th/0211290].
- [11] J. M. Bardeen, B. Carter and S. W. Hawking, “The Four laws of black hole mechanics,” *Commun. Math. Phys.* **31** (1973) 161.
- [12] For reviews, see: B. Kol, “The phase transition between caged black holes and black strings: A review,” *Phys. Rept.* **422** (2006) 119 [arXiv:hep-th/0411240]; T. Harmark and N. A. Obers, “Phases of Kaluza-Klein black holes: A brief review,” arXiv:hep-th/0503020.
- [13] R. Emparan and R. C. Myers, “Instability of ultra-spinning black holes,” *JHEP* **0309** (2003) 025 [arXiv:hep-th/0308056].
- [14] R. Gregory and R. Laflamme, “Black strings and p-branes are unstable,” *Phys. Rev. Lett.* **70**, 2837 (1993) [arXiv:hep-th/9301052].

-
- [15] J. L. Hovdebo and R. C. Myers, “Black rings, boosted strings and Gregory-Laflamme,” *Phys. Rev. D* **73**, 084013 (2006) [arXiv:hep-th/0601079].
- [16] For a review on instabilities of higher-dimensional black objects, see T. Harmark, V. Niarchos and N. A. Obers, “Instabilities of black strings and branes,” arXiv:hep-th/0701022.
- [17] A. Ishibashi and H. Kodama, “Stability of higher-dimensional Schwarzschild black holes,” *Prog. Theor. Phys.* **110** (2003) 901 [arXiv:hep-th/0305185].
- [18] J. P. Gauntlett and J. B. Gutowski, “Concentric black rings,” *Phys. Rev. D* **71**, 025013 (2005) [arXiv:hep-th/0408010]; “General concentric black rings,” *Phys. Rev. D* **71** (2005) 045002 [arXiv:hep-th/0408122].

Chapter 7

Global geometry of the supersymmetric AdS_3/CFT_2 correspondence in M-theory

Pau Figueras,^a Oisín A. P. Mac Conamhna,^b Eoin Ó Colgáin^b

^a*Departament de Física Fonamental
Universitat de Barcelona,
Diagonal 647, E-08028 Barcelona, Spain*

^b*Blackett Laboratory, Imperial College
London, SW7 2AZ, U.K;
The Institute for Mathematical Sciences,
Imperial College, London SW7 2PG, UK.*

pfigueras@ffn.ub.es, o.macconamhna@imperial.ac.uk,
eoin.ocolgain@imperial.ac.uk

ABSTRACT

We study the global geometry of a general class of spacetimes of relevance to the supersymmetric AdS_3/CFT_2 correspondence in eleven-dimensional supergravity. Specifically, we study spacetimes admitting a globally-defined $\mathbb{R}^{1,1}$ frame, a globally-defined frame bundle with structure group contained in $Spin(7)$, and an AdS_3 event horizon or conformal boundary. We show how the global frame bundle may be canonically realised by globally-defined null sections of the spin bundle, which we use to truncate eleven-dimensional supergravity to a gravitational theory of a frame with structure group $Spin(7)$, $SU(4)$ or $Sp(2)$. By imposing an AdS_3 boundary condition on the truncated supergravity equations, we define the geometry of all AdS_3 horizons or boundaries which can be obtained from solutions of these truncations. In the most generic case we study, we reproduce the most general conditions for an AdS_3 manifold in M-theory to admit a Killing spinor. As a consistency check on our definitions of AdS geometries we verify that they are satisfied by known gauged supergravity AdS_3 solutions. We discuss future applications of our results.

7.1 Introduction

The formulation of the AdS/CFT correspondence [1] has stimulated intense and ongoing interest in the geometry of Anti-de Sitter manifolds, and their quantum field theoretic description, in string and M-theory. By now there exists an extensive list of explicit supersymmetric *AdS* solutions of the field equations of ten- and eleven-dimensional supergravity, and an extensive range of solution generating techniques - for example, by taking the near-horizon limit of an elementary or wrapped brane configuration [2]-[6], or by applying the gravity dual of a marginal field theory deformation to a known solution [7], [8]. More generally, there are many known Minkowski solutions which asymptote to *AdS*, either at a horizon or a conformal boundary. The elementary brane solutions describe interpolations from a conical special holonomy manifold at a spacelike infinity to an internal *AdS* spacelike infinity associated to an event horizon; and there are many known globally Minkowski and asymptotically *AdS* solutions admitting an interpretation as the dual of an RG flow to a superconformal fixed point, for example [11]-[13]. More generally still, there are Minkowski solutions without an *AdS* region which may be interpreted as dual to confining gauge theories, such as the warped deformed conifold [14].

Our primary goal in this paper is to define the general global features of the geometry of supersymmetric spacetimes in eleven dimensions which are globally or locally *AdS*₃. The globally *AdS*₃ spacetimes arise as the horizon manifolds of branes, or the fixed point manifolds of RG flows; the locally *AdS*₃ spacetimes can be interpreted as the full brane or RG flow solutions. Our approach is a direct continuation of that of [9], [10]. For our basic set-up, we require the global existence of a warped $\mathbb{R}^{1,1}$ frame, with a global reduction of the frame bundle on the transverse space; the metric is given by

$$ds^2 = 2e^+ \otimes e^- + ds^2(\mathcal{M}_8) + e^9 \otimes e^9, \quad (7.1.1)$$

where we impose that $e^+ = L^{-1}dx^+$, $e^- = dx^-$, and $L < \infty$ globally; that L , the metric on \mathcal{M}_8 , and the basis one-form e^9 are everywhere independent of the coordinates x^\pm ; and that $e^9 \neq 0$ is everywhere non-vanishing. We demand that the flux respects the Minkowski isometries; in other words, that it is given by

$$F = e^{+-} \wedge H + G, \quad (7.1.2)$$

with H and G independent of the Minkowski coordinates, globally. Our final assumption is that \mathcal{M}_8 admits a globally-defined G -structure. We will study globally defined *Spin*(7), *SU*(4) and *Sp*(2) structures on \mathcal{M}_8 . The existence of a globally defined *Spin*(7) structure on \mathcal{M}_8 is equivalent to the existence of a no-where vanishing *Spin*(7) invariant Cayley four-form ϕ on \mathcal{M}_8 . For *SU*(4), the globally-defined forms are the almost complex structure J and the (4,0) form Ω . For *Sp*(2), the existence of the global structure is equivalent to the existence of a triplet of everywhere non-zero almost complex structures J^A , $A = 1, 2, 3$.

Our assumption of the existence of a global frame bundle is a stronger one than the more traditional assumption of the existence of a generic section of the spin bundle - a globally non-vanishing Killing spinor. All sorts of complications can potentially occur in the global behaviour of generic sections of the spin bundle - timelike spinors becoming null, spinors becoming parallel, and so forth - that seriously restrict their usefulness as a global tool. Part of our motivation for assuming the existence of a frame bundle is that it provides significant global control over the geometry, and these issues do not arise. Heuristically, a second motivation is that the workings of AdS/CFT appear to be reflected in the very special global properties of the relevant

supergravity solutions, and we believe that all known AdS , brane or RG flow supergravity solutions satisfy this assumption. A third, more concrete motivation for this assumption is that it has played an important rôle in the recent beautiful work on $\mathcal{N} = 1$ superconformal field theories in four dimensions and interpolations from Calabi-Yau cones to $AdS_5 \times Y^{p,q}$ manifolds in IIB [15]-[21]. The metric and flux for these supergravity solutions are given by

$$\begin{aligned} ds^2 &= \left[1 + \frac{1}{R^4}\right]^{-1/2} ds^2(\mathbb{R}^{1,3}) + \left[1 + \frac{1}{R^4}\right]^{1/2} [dR^2 + R^2 ds^2(\mathcal{M}_5)], \\ F &= (1 + \star)\text{Vol}_{\mathbb{R}^{1,4}} \wedge d \left[1 + \frac{1}{R^4}\right]^{-1}, \end{aligned} \quad (7.1.3)$$

where $ds^2(\mathcal{M}_5)$ is a Sasaki-Einstein metric on $Y^{p,q}$. As $R \rightarrow \infty$, the metric asymptotes to a singular Calabi-Yau cone:

$$ds^2 \rightarrow ds^2(\mathbb{R}^{1,3}) + dR^2 + R^2 ds^2(\mathcal{M}_5). \quad (7.1.4)$$

A global geometry of this form would be singular at $R = 0$. However, in the interpolating solution, this singularity is excised, and removed to infinity. The apex of the cone is thereby rendered non-compact, and opens up into an internal, asymptotically AdS_5 region, at infinite proper distance. The Penrose diagram, in the $t - R$ plane, for the maximal analytic extension of this manifold [22] is shown in Figure 1. An important global assumption in identifying the geometric dual of a-maximisation [21] is that the Calabi-Yau singularity is Gorenstein. This means that the incomplete special holonomy manifold obtained upon excising the singularity is globally Calabi-Yau; it admits an everywhere non-vanishing complex structure and holomorphic three-form. An equivalent statement of this assumption is that the interpolating solution (where the singularity is indeed excised, and removed to infinity) admits a global reduction of the frame bundle to a principal $SU(3)$ sub-bundle, on an incomplete region of spacetime bounded by the special holonomy asymptotics and the AdS horizon - a causal diamond of the Penrose diagram. Analytic extension of the frame bundle across an event horizon appears to be facilitated by the doubling of supersymmetry on the AdS horizon manifold. However we do not explore the issue of analytic extension across a horizon any further here, and we henceforth restrict attention to regions of spacetime bounded by asymptopia and AdS horizons, admitting a global reduction of the frame bundle. This restriction to a causal diamond of a Penrose diagram is in any event in keeping with more general ideas about holography, and also plays an important rôle in the quantum gravity of de Sitter space [23], [24].

We will now begin to explore what information about the geometry of (7.1.1), (7.1.2) we can extract, from eleven-dimensional supergravity, given our global assumptions. Eleven dimensional supergravity is not designed to manipulate frame bundles directly - the Killing spinor equation is instead an equation for sections of the spin bundle. In demanding the existence of a globally defined frame bundle, we have not assumed any a priori realisation of the frame bundle by sections of the spin bundle. Therefore, in order to use eleven-dimensional supergravity, we must find a way of associating globally defined sections of the spin bundle to a globally-defined frame bundle. By this we mean finding the Killing spinors whose bilinears produce the structure forms. Clearly, they should be singlets of the structure group. They may be selected in a natural way, by using the Clifford action of the structure forms on the eleven dimensional spin bundle. This Clifford action is defined for an n -form A on \mathcal{M}_8 by

$$A \cdot \eta = \frac{1}{n!} A_{i_1 \dots i_n} \Gamma^{i_1 \dots i_n} \eta, \quad (7.1.5)$$

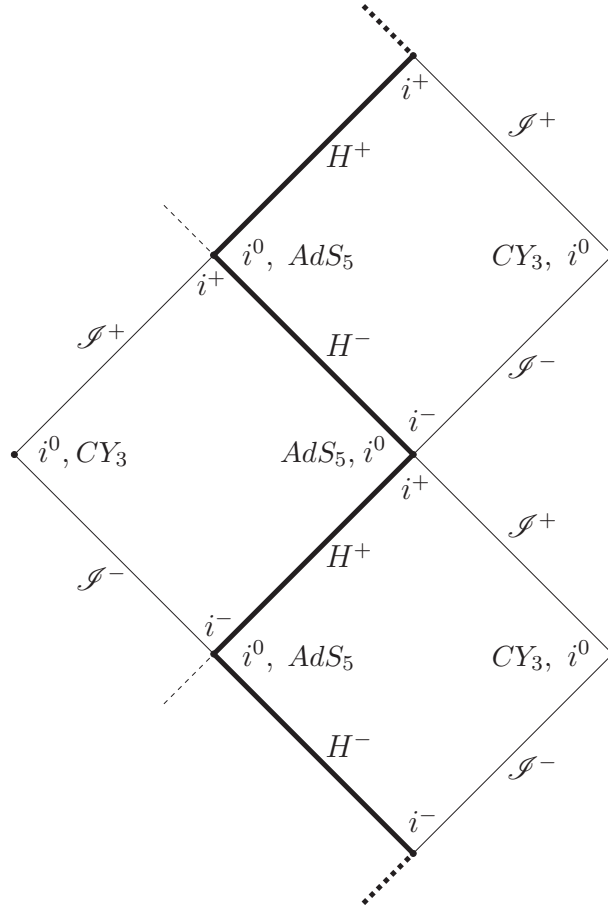


Figure 7.1: Penrose diagram for the maximal analytic extension of an interpolation from a Calabi-Yau cone to AdS_5 in IIB.

where η is a Majorana spinor in eleven dimensions and the Γ^i are eleven-dimensional gamma-matrices, with $i = 1, \dots, 8$. Taking the example of $Spin(7)$, the Clifford action $\phi \cdot \eta$ decomposes an arbitrary spinor η into modules of the structure group of ϕ ; each module is an eigenmodule of the Clifford action of the structure form, with a different eigenvalue. What distinguishes the singlets, in general, is that they are the modules of highest norm eigenvalue. Thus, normalising appropriately, we may obtain the singlets of the structure group $Spin(7)$ as solutions of

$$\frac{1}{14}\phi \cdot \eta = -\eta. \quad (7.1.6)$$

Any globally-defined Killing spinors which give a realisation of the globally defined $Spin(7)$ structure must lie in the two-dimensional solution space of (7.1.6). We will impose one further condition on all Killing spinors throughout this paper: we demand that all Killing spinors have a definite $\mathbb{R}^{1,1}$ chirality; in other words, that they are eigenspinors of Γ^{+-} . Combining this restriction with (7.1.6), we get the global definition of the Killing spinors realising a $Spin(7)$ structure:

$$\Gamma^{+-}\frac{1}{14}\phi \cdot \eta = \pm\eta. \quad (7.1.7)$$

On a special holonomy manifold, in less geometrical language, this would be called the kappa-symmetry projection for a probe M5 brane wrapped on a Cayley four-cycle.

For our global $Spin(7)$ structure, there are two distinct Killing spinor realisations; one where only one solution of (7.1.7) exists globally, and one where both solutions exist globally. When given a wrapped-brane interpretation, the first case can be associated to interpolating solutions involving deformations of the normal bundle of a Cayley four-cycle of a $Spin(7)$ manifold. The second case is associated to interpolations from a $Spin(7)$ cone to an AdS_4 horizon (foliated by AdS_3 leaves). For $SU(4)$ and $Sp(2)$, finding the spinorial realisations of the global frame bundle is very similar, and is discussed in detail in section 7.3.

Having found the spinorial realisation of the frame bundle, we may truncate eleven-dimensional supergravity, globally, to a gravitational theory in eleven dimensions for a frame bundle which is not $Spin(1,10)$, but rather $Spin(7)$, in the generic case we consider. One may re-interpret the BPS conditions for the globally-defined Killing spinor(s) realising the $Spin(7)$ -structure - together with such components of the field equations and Bianchi identity as are not implied by their existence - as being instead the truncation of the field equations of eleven-dimensional supergravity to a frame bundle with structure group $Spin(7)$; in effect, a classical theory of $Spin(7)$ gravity in eleven dimensions.

Let us illustrate this truncation for the most generic case we consider in this paper; a global $Spin(7)$ structure realised by a single solution of (7.1.7). We will refer to this as a Cayley structure, a Cayley frame bundle, or simply Cayley geometry, henceforth. All other cases we study may be regarded as particular cases of this one, with more restrictive global conditions. The BPS conditions with our frame and a single globally defined Killing solution of (7.1.7) may easily be obtained from the results of [25]. The conditions on the intrinsic torsion of the globally-defined $Spin(7)$ -structure are

$$e^9 \wedge \left[-L^3 e^9 \lrcorner d(L^{-3} e^9) + \frac{1}{2} \phi \lrcorner d\phi \right] = 0, \quad (7.1.8)$$

$$(e^9 \wedge + \star_9)[e^9 \lrcorner d(L^{-1} \phi)] = 0. \quad (7.1.9)$$

Here \star_9 denotes the Hodge dual on the space transverse to the Minkowski factor. The operation \lrcorner is defined, for an n -form A and an m -form B , $m > n$, by

$$A \lrcorner B_{\mu_{n+1} \dots \mu_m} = \frac{1}{n!} A^{\mu_1 \dots \mu_n} B_{\mu_1 \dots \mu_n \mu_{n+1} \dots \mu_m}. \quad (7.1.10)$$

Then the flux is given by

$$F = d(e^{+-9}) - \star d(e^{+-} \wedge \phi) - \frac{L^{10/7}}{2} e^9 \lrcorner d(L^{-10/7} \phi) + \frac{1}{4} \phi \diamond [e^9 \lrcorner (e^9 \wedge de^9)] + F^{27}. \quad (7.1.11)$$

We have defined the operation \diamond for an n -form A and a two-form B on \mathcal{M}_8 according to

$$A \diamond B = n A_{[i_1 \dots i_{n-1}} \overset{i_m}{B_{i_n] i_m}. \quad (7.1.12)$$

Observe that $\phi \diamond$ is a map $\phi \diamond : \Lambda^2(\mathcal{M}_8) \rightarrow \Lambda_7^4(\mathcal{M}_8)$. The F^{27} term in the flux is a four-form on \mathcal{M}_8 in the **27** of $Spin(7)$ which is unfixed by the truncation. Thus, the general equations for the truncation of eleven dimensional supergravity to Cayley geometry are the torsion conditions (7.1.8) and (7.1.9), coupled to the Bianchi identity

$$dF = 0 \quad (7.1.13)$$

and, as it turns out (all other field equation components being implied), the $+ - 9$ component of the four-form field equation¹

$$\star \left(d \star F + \frac{1}{2} F \wedge F \right) = 0. \quad (7.1.14)$$

Having obtained the truncated supergravity equations, we must also specify the boundary conditions of interest to us. We will impose the existence of an AdS_3 region, which we view as being associated either to a horizon or a conformal boundary of a globally Minkowski solution. It will be very interesting to explore more sophisticated boundary conditions in the future. Because of the global structure, topological considerations will be important in doing this. Generically, one would expect a solution with an AdS_3 region to go to some flux geometry at other asymptopia. But one could easily imagine imposing more specialised boundary conditions, such as the existence of more than one AdS region - as relevant for the dual of an RG flow between fixed points. From a mathematical point of view, perhaps the most interesting additional boundary condition would be asymptotic fall-off of the flux. This is because far from a gravitating source, the spacelike asymptotics necessarily, and automatically, have $Spin(7)$ holonomy; they must be Ricci-flat by Einstein, and special holonomy by the frame bundle. Solutions of the truncated supergravity equations with these boundary conditions describe interpolations from special holonomy spacelike asymptopia to AdS horizons. Because of the global structure, the AdS horizon geometry of an interpolating solution will be intimately related to that of the asymptotic special holonomy manifold. We will return to a discussion of these boundary conditions in the conclusions.

In this paper, we will impose the most general AdS_3 boundary condition on the supergravity truncations we study, leaving additional specialisations for the future. As we shall explain in detail, we do this by inserting the most general locally AdS_3 frame into the globally-defined $\mathbb{R}^{1,1}$ frame, and converting the equations for the globally-defined Minkowski structure into a set of equations for the locally-defined AdS_3 structure. For the generic case of Cayley geometry, the local AdS structure is G_2 , with associative three-form Φ and co-associative four-form Υ . We shall see that locally, the metric may always be cast in the form

$$ds^2 = \frac{1}{\lambda m^2} \left[ds^2(AdS_3) + \frac{\lambda^3}{4 \sin^2 \theta} d\rho \otimes d\rho \right] + ds^2(\mathcal{N}_7), \quad (7.1.15)$$

where the G_2 structure is defined on \mathcal{N}_7 , and λ , θ and the frame on \mathcal{N}_7 are independent of the AdS_3 coordinates. The restrictions on the intrinsic torsion of the locally defined G_2 structure may be expressed as

$$\hat{\rho} \wedge d(\lambda^{-1} \Upsilon) = 0, \quad (7.1.16)$$

$$\lambda^{5/2} d(\lambda^{-5/2} \sin \theta \text{Vol}_7) = -4m\lambda^{1/2} \cos \theta \hat{\rho} \wedge \text{Vol}_7, \quad (7.1.17)$$

$$d\Phi \wedge \Phi = \frac{4m\lambda^{1/2}}{\sin \theta} (4 - \sin^2 \theta) \text{Vol}_7 - 2 \cos \theta \star_8 d \log \left(\frac{\lambda^{3/2} \cos \theta}{\sin^2 \theta} \right); \quad (7.1.18)$$

¹This equation can of course receive quantum corrections, as can the Killing spinor and Einstein equations, but we will ignore them.

the flux is given by

$$F = \frac{1}{m^2} \text{Vol}_{AdS_3} \wedge d[\rho - \lambda^{-3/2} \cos \theta] + \frac{\lambda^{3/2}}{\sin^2 \theta} (\cos \theta + \star_8) \left(d[\lambda^{-3/2} \sin \theta \Phi] - 4m\lambda^{-1} \Upsilon \right) + 2m\lambda^{1/2} \Phi \wedge \hat{\rho}, \quad (7.1.19)$$

and the definitions of \star_8 and the basis one-form $\hat{\rho}$ hopefully are obvious². In [26], Martelli and Sparks gave a classification of all minimally supersymmetric AdS_3 spacetimes in M-theory; the conditions we have obtained on the local G_2 structure of an AdS_3 region in Cayley geometry are identical to theirs³. We regard these conditions as being valid locally on the horizon or conformal boundary of a globally Minkowski solution, or globally for a globally AdS solution of Cayley geometry⁴.

As we have said, we study truncations of eleven-dimensional supergravity to several different frame bundles, with different spinorial realisations. For a $Spin(7)$ bundle, we study spinorial realisations by either one or two globally defined Killing spinors. We refer to the resulting truncations of eleven-dimensional supergravity as Cayley or $Spin(7)$ geometry, respectively. The AdS_3 conditions we derive from Cayley geometry define the geometry of all M-theory duals of $N = (1, 0)$ two-dimensional CFTs. The AdS_3 conditions we derive from $Spin(7)$ geometry reproduce the $AdS_4 \times \text{Weak } G_2$ Freund-Rubin solutions, with the AdS_4 foliated by AdS_3 leaves. For an $SU(4)$ frame bundle we study three distinct spinorial realisations. The first, with the maximal number (four) of globally-defined Killing spinors, produces a truncation we refer to as $SU(4)$ geometry. The AdS_3 conditions we derive from $SU(4)$ geometry produce the Freund-Rubin $AdS_4 \times SE_7$ solutions. The other two spinorial realisations of an $SU(4)$ frame bundle we study have two globally defined Killing spinors. We refer to the associated truncations as Kähler-4 and Special Lagrangian-4 (SLAG) geometry. Given a wrapped brane interpretation, one would say that a solution of these truncations described an M5-brane wrapped on, respectively, a Kähler or SLAG four-cycle of a Calabi-Yau four-fold, with a membrane extended in the directions transverse to the Calabi-Yau and intersecting the fivebrane in a string. We believe that the AdS_3 conditions we derive from SLAG geometry define all M-theory duals of $N = (1, 1)$ CFTs; and similarly that the AdS_3 conditions we derive from Kähler-4 geometry (together with the AdS_3 conditions of [9] from co-associative geometry with a global Minkowski G_2 frame bundle) define all M-theory duals of $N = (2, 0)$ CFTs. For an $Sp(2)$ frame bundle, we again study three distinct spinorial realisations. The first, with the maximal number (six) of globally-defined Killing spinors, produces a truncation we call $Sp(2)$ geometry. Again, the AdS_3 conditions we derive from $Sp(2)$ geometry just give the appropriate Freund-Rubin solutions, this time the direct product of AdS_4 with a Tri-Sasaki-Einstein manifold. The other two spinorial realisations of an $Sp(2)$ frame bundle we study have three globally defined Killing spinors. We refer to the associated truncations of eleven dimensional supergravity as Quaternionic Kähler (QK) and Complex Lagrangian (CLAG) geometry. We believe that the AdS_3 conditions we derive from these truncations define all M-theory duals of $N = (3, 0)$ and $N = (2, 1)$ CFTs respectively.

The remainder of this paper is organised as follows. For the convenience of the reader who is not interested in their derivation, in section 7.2 we summarise our main technical results: the truncation of eleven-dimensional supergravity to Cayley, Kähler-4, SLAG, QK or CLAG

²The orientations for the various Hodge stars will be specified when they next appear.

³Up to a minor discrepancy in (3.14) of [26] which we have corrected.

⁴A subtlety in the global validity of these conditions for globally AdS manifolds is discussed in section 7.5.

geometry, together with the associated conditions for an AdS_3 region. These equations are the result of involved calculations. As a consistency check, we have verified that explicit Kähler-4 and SLAG AdS_3 solutions, known from gauged supergravity, satisfy our definitions of AdS geometry in the appropriate truncations, by explicitly elucidating their structure. Since our results for Kähler-4 and SLAG geometry are derived directly from Cayley geometry, and our results for CLAG and QK in turn are derived from those for Kähler-4 and SLAG, this serves as a rigid overall consistency check. The remainder of the paper (with the exception of the conclusions) is concerned with the derivation of the results of section 7.2. In section 7.3, we discuss the globally-defined G-structures and spinorial realisations thereof which are of interest to us. In section 7.4, we explain in more detail how to obtain the supergravity truncation in each case. Section 7.5 is concerned with the derivation of the local conditions for an AdS_3 region in each truncation. Section 7.6 discusses the verification of the globalised AdS torsion conditions for known solutions. Section 7.7 concludes with some more observations, speculations and suggestions for future directions.

7.2 Summary of results

In this section, we will summarise our technical results for Cayley, Kähler-4, SLAG, QK and CLAG geometry. In each case, we will give the globally defined spinorial realisation of the frame bundle, the associated truncation of eleven-dimensional supergravity, and a definition of the geometry of an arbitrary AdS_3 region in the truncation. For the Kähler-4 and SLAG geometries, as an overall consistency check, we present a known exact solution of the AdS equations, with its structure made manifest, that we have verified satisfies our AdS conditions.

We take positive orientation in eleven dimensions to be defined by

$$\text{Vol}_{11} = e^- \wedge e^+ \wedge \frac{1}{14} \phi \wedge \phi \wedge e^9. \quad (7.2.1)$$

In every case, the globally-defined Minkowski frame is given by (7.1.1) of the introduction; positive orientation for \star_9 , the Hodge dual on the space transverse to the Minkowski factor, is defined by

$$\text{Vol}_9 = \frac{1}{14} \phi \wedge \phi \wedge e^9. \quad (7.2.2)$$

In every case, the truncation of eleven-dimensional supergravity to the global frame bundle consists of the quoted torsion conditions for the globally-defined Minkowski structure coupled to the Bianchi identity and the $+ - 9$ component of the four-form field equation. The AdS_3 geometries automatically solve the four-form field equation, and for them it is in every case sufficient to impose the Bianchi identity in addition to the torsion conditions to ensure that they are solutions of eleven dimensional supergravity. For the AdS geometries, the warp factor, the frame on the transverse space, and the flux, are independent of the AdS coordinates. We define the basis one-form $\hat{\rho}$ in the local AdS frame in every case according to

$$\hat{\rho} = \frac{\lambda}{2m \sin \theta} d\rho. \quad (7.2.3)$$

The electric flux for the $\mathbb{R}^{1,1}$ geometries, in every case, takes the form

$$F_{\text{elec}} = d(e^{+-9}), \quad (7.2.4)$$

while for the AdS geometries, in every case, it takes the form

$$F_{\text{elec}} = \frac{1}{m^2} \text{Vol}_{AdS_3} \wedge d[\rho - \lambda^{-3/2} \cos \theta]. \quad (7.2.5)$$

Now we will state our results.

7.2.1 Cayley geometry

In this case, \mathcal{M}_8 admits a globally-defined $Spin(7)$ structure which is realised by a single Killing solution of

$$\Gamma^{+-} \frac{1}{14} \phi \cdot \eta = -\eta. \quad (7.2.6)$$

Global truncation The truncation of eleven-dimensional supergravity to this geometry is defined by

$$e^9 \wedge \left[-L^3 e^9 \lrcorner d(L^{-3} e^9) + \frac{1}{2} \phi \lrcorner d\phi \right] = 0, \quad (7.2.7)$$

$$(e^9 \wedge + \star_9)[e^9 \lrcorner d(L^{-1} \phi)] = 0, \quad (7.2.8)$$

$$F = d(e^{+-9}) - \star d(e^{+-} \wedge \phi) - \frac{L^{10/7}}{2} e^9 \lrcorner d(L^{-10/7} \phi) + \frac{1}{4} \phi \diamond [e^9 \lrcorner (e^9 \wedge de^9)] + F^{27}. \quad (7.2.9)$$

AdS geometry The geometry of an AdS_3 region in this truncation is as follows. Locally the metric may be cast in the form

$$ds^2 = \frac{1}{\lambda m^2} \left[ds^2(AdS_3) + \frac{\lambda^3}{4 \sin^2 \theta} d\rho \otimes d\rho \right] + ds^2(\mathcal{N}_7), \quad (7.2.10)$$

where \mathcal{N}_7 admits a G_2 structure, with associative three-form Φ and co-associative four-form Υ . The torsion conditions are

$$\hat{\rho} \wedge d(\lambda^{-1} \Upsilon) = 0, \quad (7.2.11)$$

$$\lambda^{5/2} d(\lambda^{-5/2} \sin \theta \text{Vol}_7) = -4m\lambda^{1/2} \cos \theta \hat{\rho} \wedge \text{Vol}_7, \quad (7.2.12)$$

$$d\Phi \wedge \Phi = \frac{4m\lambda^{1/2}}{\sin \theta} (4 - \sin^2 \theta) \text{Vol}_7 - 2 \cos \theta \star_8 d \log \left(\frac{\lambda^{3/2} \cos \theta}{\sin^2 \theta} \right); \quad (7.2.13)$$

and the magnetic flux is given by

$$F_{\text{mag}} = \frac{\lambda^{3/2}}{\sin^2 \theta} (\cos \theta + \star_8) \left(d[\lambda^{-3/2} \sin \theta \Phi] - 4m\lambda^{-1} \Upsilon \right) + 2m\lambda^{1/2} \Phi \wedge \hat{\rho}. \quad (7.2.14)$$

Positive orientation on the space transverse to the AdS factor is defined by $\frac{1}{7} \Phi \wedge \Upsilon \wedge \hat{\rho}$.

7.2.2 Kähler-4 geometry

In this case, \mathcal{M}_8 admits a globally-defined $SU(4)$ structure. The structure is realised by two globally defined null Killing spinors, which are solutions of

$$\frac{1}{12}\Gamma^{+-}(J \wedge J) \cdot \eta = -\eta. \quad (7.2.15)$$

Global truncation The truncation of eleven-dimensional supergravity to this geometry is defined by the torsion conditions for the global $SU(4)$ structure

$$\begin{aligned} J \lrcorner de^9 &= 0, \\ d(L^{-1}\text{Re}\Omega) &= 0, \\ e^9 \wedge [J \lrcorner dJ - L e^9 \lrcorner d(L^{-1}e^9)] &= 0, \end{aligned} \quad (7.2.16)$$

and the four-form

$$\begin{aligned} F &= d(e^{+-9}) + \frac{1}{2} \star d(e^{+-} \wedge J \wedge J) + \frac{1}{4} L^2 e^9 \lrcorner d(L^{-2} J \wedge J) \\ &\quad - \frac{1}{4} (J \wedge J) \diamond [e^9 \lrcorner (e^9 \wedge de^9)] + F^{\mathbf{20}}. \end{aligned} \quad (7.2.17)$$

Here $F^{\mathbf{20}}$ is a four-form on \mathcal{M}_8 in the $\mathbf{20}$ of $SU(4)$ (a primitive (2,2) form) which is not fixed by the truncation.

AdS geometry The local metric for an AdS_3 region in this geometry is

$$ds^2 = \frac{1}{\lambda m^2} \left[ds^2(AdS_3) + \frac{\lambda^3}{4 \sin^2 \theta} d\rho \otimes d\rho \right] + e^7 \otimes e^7 + ds^2(\mathcal{N}_6), \quad (7.2.18)$$

where \mathcal{N}_6 admits an $SU(3)$ structure. Using J and Ω to denote the structure forms of this local $SU(3)$ structure (hopefully without risk of confusion with the structure forms of the global $SU(4)$ structure), the local AdS_3 torsion conditions are

$$\hat{\rho} \wedge d(\lambda^{-1} J \wedge J) = 0, \quad (7.2.19)$$

$$d(\lambda^{-3/2} \sin \theta \text{Im}\Omega) = 2m\lambda^{-1}(e^7 \wedge \text{Re}\Omega - \cos \theta \hat{\rho} \wedge \text{Im}\Omega), \quad (7.2.20)$$

$$J \lrcorner de^7 = \frac{2m\lambda^{1/2}}{\sin \theta} (2 - \sin^2 \theta) - \cos \theta \hat{\rho} \lrcorner d \log \left(\frac{\lambda^{3/2} \cos \theta}{\sin^2 \theta} \right). \quad (7.2.21)$$

The magnetic flux is

$$F_{\text{mag}} = \frac{\lambda^{3/2}}{\sin^2 \theta} (\cos \theta + \star_8) (d[\lambda^{-3/2} \sin \theta J \wedge e^7] - 2m\lambda^{-1} J \wedge J) + 2m\lambda^{1/2} J \wedge e^7 \wedge \hat{\rho}. \quad (7.2.22)$$

Positive orientation on the space tranverse to the AdS factor is defined by $\frac{1}{6} J \wedge J \wedge J \wedge e^7 \wedge \hat{\rho}$.

Exact solution We have verified that the following is an exact solution of the AdS torsion conditions and Bianchi identity in this truncation. Topologically, the space transverse to the AdS factor is an S^4 bundle over a negatively curved Kähler-Einstein manifold. This solution was first constructed in gauged supergravity, as the near-horizon limit of an M5 brane wrapped on a Kähler four-cycle in a Calabi-Yau four-fold, in [4]. The metric is given by

$$ds^2 = \frac{1}{\lambda m^2} \left[ds^2(AdS_3) + \frac{3}{4} ds^2(KE_4) + (1 - \lambda^3 f^2) DY^a \otimes DY^a + \frac{\lambda^3}{4(1 - \lambda^3 f^2)} d\rho \otimes d\rho \right], \quad (7.2.23)$$

where

$$\lambda^3 = \frac{3}{4(1 + \rho^2/12)}, \quad f^2 = \frac{4}{9}\rho^2. \quad (7.2.24)$$

The Y^a , $a = 1, \dots, 4$ are constrained coordinates on an S^3 , $Y^a Y^a = 1$. We define K^A , $A = 1, 2, 3$, $K^A K^B = -\delta^{AB} - \epsilon^{ABC} K^C$, to be a triplet of self-dual two-forms on KE_4 , and we choose K^3 to label the Kähler form. We define

$$DY^a = dY^a - \frac{1}{4} K^{3cd} \omega_{cd} K^{3a}{}_b Y^b, \quad (7.2.25)$$

where ω_{ab} are the spin connection one-forms of KE_4 . Finally $ds^2(KE_4)$ is normalised such that the Ricci form is given by $\mathcal{R} = -K^3$. Defining the functions

$$g = \frac{\sqrt{3}}{2\lambda^{1/2}m}, \quad h = \frac{\sqrt{1 - \lambda^3 f^2}}{\lambda^{1/2}m}, \quad (7.2.26)$$

the $SU(3)$ structure forms are given by

$$\begin{aligned} e^7 &= h K_{ab}^3 Y^a DY^b, \\ J &= g^2 K^3 + h^2 \frac{1}{2} K_{ab}^3 DY^a \wedge DY^b, \\ \text{Re}\Omega &= -g^2 h [K^2 \wedge K_{ab}^1 Y^a DY^b + K^1 \wedge K_{ab}^2 Y^a DY^b], \\ \text{Im}\Omega &= -g^2 h [K^2 \wedge K_{ab}^2 Y^a DY^b - K^1 \wedge K_{ab}^1 Y^a DY^b]. \end{aligned} \quad (7.2.27)$$

In [5], [6], many infinite families of AdS_3 solutions, generalising this one, were constructed. All these families will satisfy our AdS equations for Kähler geometry.

7.2.3 Special Lagrangian geometry

Again in this case \mathcal{M}_8 admits a globally defined $SU(4)$ structure. It is realised by two globally defined null Killing solutions of

$$\begin{aligned} \Gamma^{+-} \eta &= \pm \eta, \\ \frac{1}{8} \Gamma^{+-} \text{Re}\Omega \cdot \eta &= -\eta. \end{aligned} \quad (7.2.28)$$

Global truncation In this case, the torsion conditions for the global $SU(4)$ structure are

$$\begin{aligned} d(L^{-1/2}J) &= 0, \\ \text{Im}\Omega \wedge d\text{Re}\Omega &= 0, \\ e^9 \wedge [\text{Re}\Omega \lrcorner d\text{Re}\Omega - 2L^{3/2}e^9 \lrcorner d(L^{-3/2}e^9)] &= 0. \end{aligned} \quad (7.2.29)$$

The flux is given by

$$\begin{aligned} F &= d(e^{+-9}) + \star d(e^{+-} \wedge \text{Re}\Omega) + \frac{1}{2}L^{7/4}e^9 \lrcorner d(L^{-7/4}\text{Re}\Omega) \\ &\quad - \frac{1}{2}\text{Re}\Omega \diamond [e^9 \lrcorner (e^9 \wedge de^9)] + F^{20}. \end{aligned} \quad (7.2.30)$$

AdS geometry The local AdS_3 frame and orientation are as for Kähler-4 geometry, and again \mathcal{N}_6 admits an $SU(3)$ structure. The AdS torsion conditions, for the local $SU(3)$ structure forms J, Ω , are

$$e^7 \wedge \hat{\rho} \wedge d\left(\frac{\text{Re}\Omega}{\sin\theta}\right) = 0, \quad (7.2.31)$$

$$d(\lambda^{-1} \sin\theta e^7) = m\lambda^{-1/2}(J + \cos\theta e^7 \wedge \hat{\rho}), \quad (7.2.32)$$

$$\text{Im}\Omega \wedge d\text{Im}\Omega = \frac{m\lambda^{1/2}}{\sin\theta}(6 + 4\cos^2\theta)\text{Vol}_6 \wedge e^7 - 2\cos\theta \star_8 d\log\left(\frac{\lambda^{3/2}\cos\theta}{\sin^2\theta}\right). \quad (7.2.33)$$

The magnetic flux is given by

$$F_{\text{mag}} = -\frac{\lambda^{3/2}}{\sin^2\theta}(\cos\theta + \star_8)(d[\lambda^{-3/2}\sin\theta\text{Im}\Omega] + 4m\lambda^{-1}\text{Re}\Omega \wedge e^7) - 2m\lambda^{1/2}\text{Im}\Omega \wedge \hat{\rho}. \quad (7.2.34)$$

Exact solution We have verified that the following is an exact solution of the AdS torsion conditions and Bianchi identity in this truncation. Topologically, the eight-manifold transverse to the AdS factor is an S^4 bundle over \mathcal{H}^4 . Again this solution was first constructed (in seven-dimensional gauged supergravity) in [4], as the near-horizon limit of an M5 brane wrapped on a SLAG four-cycle of a Calabi-Yau four-fold. The metric is given by

$$\begin{aligned} ds^2 &= \frac{1}{\lambda m^2} \left[ds^2(AdS_3) + \frac{2}{3} ds^2(\mathcal{H}^4) + (1 - \lambda^3 f^2) DY^a \otimes DY^a \right. \\ &\quad \left. + \frac{\lambda^3}{4(1 - \lambda^3 f^2)} d\rho \otimes d\rho \right], \end{aligned} \quad (7.2.35)$$

where

$$\lambda^3 = \frac{2}{3(1 + \rho^2/8)}, \quad f^2 = \frac{9}{16}\rho^2; \quad (7.2.36)$$

the Y^a , $a = 1, \dots, 4$ are constrained coordinates on an S^3 , $Y^a Y^a = 1$, and we define

$$DY^a = dY^a + \omega^a{}_b Y^b, \quad (7.2.37)$$

where ω_{ab} are the spin connection one-forms of \mathcal{H}^4 . Finally $ds^2(\mathcal{H}^4)$ is normalised such that the curvature two-form is given by $R_{ab} = -\frac{1}{3}e^a \wedge e^b$. Defining the functions

$$g = \sqrt{\frac{2}{3}} \frac{1}{\lambda^{1/2}m}, \quad h = \frac{\sqrt{1 - \lambda^3 f^2}}{\lambda^{1/2}m}, \quad (7.2.38)$$

and with $ds^2(\mathcal{H}^4) = \delta_{ab}e^a \otimes e^b$, the $SU(3)$ structure forms are given by

$$\begin{aligned} e^7 &= -gY^a e^a, \\ J &= ghe^a \wedge DY^a, \\ \text{Re}\Omega &= g^3 \frac{1}{3!} \epsilon^{abcd} Y^a e^b \wedge e^c \wedge e^d - gh^2 \frac{1}{2} \epsilon^{abcd} Y^a DY^b \wedge DY^c \wedge e^d, \\ \text{Im}\Omega &= g^2 h \frac{1}{2} \epsilon^{abcd} Y^a DY^b \wedge e^c \wedge e^d - h^3 \frac{1}{3!} \epsilon^{abcd} Y^a DY^b \wedge DY^c \wedge DY^d. \end{aligned} \quad (7.2.39)$$

7.2.4 Quaternionic Kähler geometry

In this case \mathcal{M}_8 admits a globally defined $Sp(2)$ structure. Defining the form Ξ_1 in terms of the three almost complex structures according to

$$\Xi_1 = \frac{1}{2} J^A \wedge J^A, \quad (7.2.40)$$

the $Sp(2)$ structure is realised by three globally defined null Killing solutions of

$$\frac{1}{10} \Gamma^{+-} \Xi_1 \cdot \eta = -\eta. \quad (7.2.41)$$

Global truncation The torsion conditions of the global truncation are

$$\begin{aligned} J^A \lrcorner de^9 &= 0, \\ d(L^{-1} \text{Re}\Omega^A) &= 0, \\ e^9 \wedge [J^A \lrcorner dJ^A - L e^9 \lrcorner d(L^{-1} e^9)] &= 0, \end{aligned} \quad (7.2.42)$$

where there is no sum on A in the third equation. Here Ω^A are the $(4,0)$ forms associated to the almost complex structures J^A . More details of their definition are given in the next section. The flux is

$$\begin{aligned} F &= d(e^{+-9}) + \frac{1}{3} \star d(e^{+-} \wedge \Xi_1) + \frac{1}{6} L^{14/5} e^9 \lrcorner d(L^{-14/5} \Xi_1) \\ &\quad - \frac{1}{4} \Xi_1 \diamond [e^9 \lrcorner (e^9 \wedge de^9)] + F^{14}, \end{aligned} \quad (7.2.43)$$

where F^{14} is a four-form on \mathcal{M}_8 in the **14** of $Sp(2)$ which is unfixed by the truncation.

AdS geometry The local metric for an AdS_3 region in this geometry is

$$ds^2 = \frac{1}{\lambda m^2} ds^2(AdS_3) + e^A \otimes e^A + \hat{\rho} \otimes \hat{\rho} + ds^2(\mathcal{N}_4), \quad (7.2.44)$$

where \mathcal{N}_4 admits a local $SU(2)$ structure, specified by a triplet of self-dual $SU(2)$ forms K^A . The local AdS_3 torsion conditions are

$$\hat{\rho} \wedge d \left[\lambda^{-1} \left(\text{Vol}_4 + \frac{1}{6} \epsilon^{ABC} K^A \wedge e^{BC} \right) \right] = 0, \quad (7.2.45)$$

$$\begin{aligned} \frac{1}{3} \left(K^A + \frac{1}{2} \epsilon^{ABC} e^{BC} \right) \lrcorner de^A &= \frac{2m\lambda^{1/2}}{\sin \theta} (2 - \sin^2 \theta) \\ &- \cos \theta \hat{\rho} \lrcorner d \log \left(\frac{\lambda^{3/2} \cos \theta}{\sin^2 \theta} \right), \end{aligned} \quad (7.2.46)$$

$$\begin{aligned} d[\lambda^{-3/2} \sin \theta (K^2 \wedge e^2 - K^1 \wedge e^1)] &= 2m\lambda^{-1} [K^2 \wedge e^{31} - K^1 \wedge e^{23}] \\ &+ 2m\lambda^{-1} \cos \theta [K^2 \wedge e^2 - K^1 \wedge e^1] \wedge \hat{\rho}, \end{aligned} \quad (7.2.47)$$

together with permutations of the last equation. The magnetic flux is given by

$$\begin{aligned} F_{\text{mag}} &= - \frac{\lambda^{3/2}}{\sin^2 \theta} (\cos \theta + \star_8) \left[d \left(\lambda^{-3/2} \sin \theta \left[\frac{1}{3} K^A \wedge e^A + e^{123} \right] \right) \right. \\ &\quad \left. - 4m\lambda^{-1} \left(\text{Vol}_4 + \frac{1}{6} \epsilon^{ABC} K^A \wedge e^{BC} \right) \right] - 2m\lambda^{1/2} \left[\frac{1}{3} K^A \wedge e^A + e^{123} \right] \wedge \hat{\rho}. \end{aligned} \quad (7.2.48)$$

Positive orientation on the space transverse to the AdS factor is defined by $\frac{1}{6} K^A \wedge K^A \wedge e^{123} \wedge \hat{\rho}$.

7.2.5 Complex Lagrangian geometry

In this case, \mathcal{M}_8 again admits a global $Sp(2)$ structure. Defining

$$\Xi_2 = \frac{1}{2} (J^1 \wedge J^1 - \text{Re}\Omega^2 + \text{Re}\Omega^3), \quad (7.2.49)$$

it is realised by three globally defined null Killing solutions of

$$\Gamma^{+-} \eta = \pm \eta, \quad (7.2.50)$$

$$\frac{1}{10} \Gamma^{+-} \Xi_2 \cdot \eta = -\eta. \quad (7.2.51)$$

Global truncation In this case, effecting the global truncation is technically more difficult. We have performed it under the assumption that $e^9 \wedge de^9 = 0$. Then the torsion conditions are given by

$$\begin{aligned} d(L^{-1/2} J^2) = d(L^{-1/2} J^3) &= 0, \\ e^9 \wedge [J^1 \lrcorner dJ^1 - L e^9 \lrcorner d(L^{-1} e^9)] &= 0. \end{aligned} \quad (7.2.52)$$

The flux is

$$F = d(e^{+-9}) + \frac{1}{2} \star d(e^{+-} \wedge \Xi_2) + \frac{1}{4} L^{11/5} e^9 \lrcorner d(L^{-11/5} \Xi_2) + F^{14}. \quad (7.2.53)$$

AdS geometry The local frame, structure and orientation for an AdS_3 region in this geometry are identical to those in Quaternionic Kähler geometry. We have derived the AdS_3 torsion conditions by decomposing those in SLAG and Kähler-4 geometry (exactly how we do this is discussed in section 7.5) rather than from the equations for the global truncation of the previous paragraph. This means that our AdS equations are independent of the assumption $e^9 \wedge de^9 = 0$ that we made for the global Minkowski frame above. The torsion conditions we find are

$$\hat{\rho} \wedge d[\lambda^{-1}(\text{Vol}_4 + K^3 \wedge e^{12})] = 0, \quad (7.2.54)$$

$$(K^3 + e^{12}) \lrcorner de^3 = \frac{2m\lambda^{1/2}}{\sin \theta} (2 - \sin^2 \theta) - \cos \theta \hat{\rho} \lrcorner d \log \left(\frac{\lambda^{3/2} \cos \theta}{\sin^2 \theta} \right), \quad (7.2.55)$$

$$d(\lambda^{-1} \sin \theta e^1) = m\lambda^{-1/2} (K^1 + e^{23} + \cos \theta e^1 \wedge \hat{\rho}), \quad (7.2.56)$$

$$d(\lambda^{-1} \sin \theta e^2) = m\lambda^{-1/2} (K^2 + e^{31} + \cos \theta e^2 \wedge \hat{\rho}). \quad (7.2.57)$$

The magnetic flux is

$$\begin{aligned} F_{\text{mag}} &= \frac{\lambda^{3/2}}{\sin^2 \theta} (\cos \theta + \star_8) [d(\lambda^{-3/2} \sin \theta [K^3 \wedge e^3 + e^{123}]) - 4m\lambda^{-1} (\text{Vol}_4 + K^3 \wedge e^{12})] \\ &+ 2m\lambda^{1/2} [K^3 \wedge e^3 + e^{123}] \wedge \hat{\rho}. \end{aligned} \quad (7.2.58)$$

7.3 Spinorial realisation of the frame bundles

In this section, we will discuss the spinorial realisations of the globally defined frame bundles we study. A global reduction of the frame bundle to a sub-bundle is by definition equivalent to the existence of a globally-defined G-structure. The existence of a globally defined G-structure, for our purposes, is equivalent to the existence of a set of globally-defined forms, invariant under the action of the structure group G. We will use the action of the structure forms on the spin bundle to define the spinorial realisation of the G-structure. When the flux vanishes asymptotically, the structure forms asymptote to the calibrations of the asymptotic special holonomy manifold.

To start, we will specify the $Spin(1, 10)$ structure we use for eleven dimensional supergravity. We use all the supergravity and spinorial conventions of [25], which are employed consistently throughout [25], [27]-[32], the papers we will use in the next section for truncating supergravity to the frame bundles of this section. We work in the null frame of the introduction,

$$ds^2 = 2e^+ \otimes e^- + ds^2(\mathcal{M}_8) + e^9 \otimes e^9. \quad (7.3.1)$$

We recall that we impose, globally, that $e^+ = L^{-1}dx^+$, $e^- = dx^-$, $L < \infty$, $e^9 \neq 0$; and that L and the frame on the space transverse to the Minkowski factor are independent of the coordinates x^\pm . The orientations we use are defined in section 7.2.

7.3.1 $Spin(7)$ and associated local AdS_3 structures

A global $Spin(7)$ structure in eleven dimensions is defined by the no-where vanishing one-forms e^\pm , e^9 , and the no-where vanishing Cayley four-form ϕ . We choose the components of ϕ to be

$$\begin{aligned} -\phi &= e^{1234} + e^{1256} + e^{1278} + e^{3456} + e^{3478} + e^{5678} + e^{1357} \\ &+ e^{2468} - e^{1368} - e^{1458} - e^{1467} - e^{2358} - e^{2367} - e^{2457}. \end{aligned} \quad (7.3.2)$$

On a special holonomy manifold, ϕ calibrates Cayley four-cycles. The embedding of our $Spin(7)$ structure group in $Spin(1, 10)$ (which is entirely at our discretion) is defined by this choice of ϕ , together with the globally-defined forms e^\pm, e^9 .

The most general geometry we study is Cayley geometry, where the $Spin(7)$ structure is realised by a single globally defined null Killing spinor. This may be chosen to satisfy the projection

$$\frac{1}{14}\Gamma^{+-}\phi \cdot \epsilon = -\epsilon. \quad (7.3.3)$$

With our choice of the components of ϕ , this projection is equivalent to

$$\Gamma^{1234}\epsilon = \Gamma^{3456}\epsilon = \Gamma^{5678}\epsilon = \Gamma^{1357}\epsilon = -\Gamma^{+-}\epsilon = -\epsilon. \quad (7.3.4)$$

We will reserve the notation ϵ for a globally-defined Killing spinor satisfying this projection in the frame (7.3.1). The statements regarding the eigenvalues of the $Spin(7)$ modules of the spin bundle may be verified by evaluating the Clifford action of ϕ in a specific basis for the spin bundle; a useful choice (which we will have used for all the spinor algebra described in this section) is that constructed in [29]. The spinor ϵ is the spinorial realisation of the frame bundle for the geometric dual of an $N = (1, 0)$ CFT.

Having found the spinorial realisation of the Cayley structure, the structure forms may be obtained as bilinears of the Killing spinor (apart from e^- , which is put in by hand in our frame definition). As discussed in detail in [25], [27], the only non-zero bilinears are the one-, two-, and five-forms, which are

$$\begin{aligned} K &= e^+, \\ \Theta &= e^{+9}, \\ \Sigma &= e^+ \wedge \phi. \end{aligned} \quad (7.3.5)$$

An essential point in our construction is the patching of the G-structures of the global $\mathbb{R}^{1,1}$ and local AdS_3 regions. We will now examine this in detail, by imposing the most general local warped product AdS_3 frame ansatz on our globally-defined frame. Globally, we have

$$ds^2 = L^{-1}ds^2(\mathbb{R}^{1,1}) + ds^2(\mathcal{M}_8) + e^9 \otimes e^9. \quad (7.3.6)$$

Observe, that in Poincaré coordinates, every AdS_3 space is foliated by $\mathbb{R}^{1,1}$ leaves:

$$\frac{1}{m^2}ds^2(AdS_3) = e^{-2mr}ds^2(\mathbb{R}^{1,1}) + dr^2. \quad (7.3.7)$$

Therefore we demand that for a local AdS region, L in (7.3.6) is given by

$$L = e^{2mr}\lambda, \quad (7.3.8)$$

for some function λ which is independent of the AdS coordinates. For a general $\mathbb{R}^{1,1}$ solution with an AdS horizon, this expression for L is local and valid for large positive r . For an AdS_3 conformal boundary, it is valid for large negative r . For a globally AdS solution, it is valid for all r . To get an AdS metric, we must also pick out the AdS radial one-form $\hat{r} = \lambda^{-1/2}dr$ from the space transverse to the $\mathbb{R}^{1,1}$ factor. In an AdS region, this one-form will in general be a linear combination of e^9 , and a one-form lying entirely in \mathcal{M}_8 . Using the transitive action

of $Spin(7)$ on \mathcal{M}_8 (an action which, by definition, leaves the Killing spinor and Cayley form invariant) we may choose the part of \hat{r} lying in \mathcal{M}_8 to lie entirely along the basis one-form e^8 . Then we may write the locally-defined AdS_3 frame as a rotation of the globally-defined $\mathbb{R}^{1,1}$ frame, as

$$\begin{aligned}\hat{r} &= \sin \theta e^8 + \cos \theta e^9, \\ \hat{\rho} &= \cos \theta e^8 - \sin \theta e^9,\end{aligned}\tag{7.3.9}$$

with⁵ $0 < \theta \leq \pi/2$. We demand that $\hat{\rho}$, together with the remaining basis one-forms transverse to the AdS factor, are locally independent of the AdS coordinates. The local metric becomes

$$ds^2 = \frac{1}{\lambda m^2} ds^2(AdS_3) + \hat{\rho} \otimes \hat{\rho} + ds^2(\mathcal{N}_7).\tag{7.3.10}$$

This frame-rotation technique was first employed in [33]. Because we have locally picked out a preferred vector on \mathcal{M}_8 , the eleven-dimensional structure group is reduced, locally, from $Spin(7)$ to a G_2 which acts on \mathcal{N}_7 . This G_2 structure is specified by the local decomposition of the globally-defined ϕ , into an associative three-form Φ and a co-associative four-form Υ according to

$$-\phi = \Upsilon + \Phi \wedge e^8,\tag{7.3.11}$$

so that

$$\begin{aligned}\Phi &= e^{127} + e^{347} + e^{567} + e^{246} - e^{136} - e^{145} - e^{235}, \\ \Upsilon &= e^{1234} + e^{1256} + e^{3456} + e^{1357} - e^{1467} - e^{2367} - e^{2457}.\end{aligned}\tag{7.3.12}$$

Having defined the most general global Minkowski and associated local AdS structures of interest to us, we now describe how they may be further reduced, by imposing the existence of even more exceptional global structures. The first exceptional case we consider is where both spinorial singlets of the global $Spin(7)$ structure are Killing. They are defined by the projection

$$\frac{1}{14} \phi \cdot \eta = -\eta.\tag{7.3.13}$$

The local decomposition of the Cayley four-form under G_2 in an AdS_3 patch will be exactly as above; however, the local supersymmetry in the AdS_3 patch will double, so now there will be four locally-defined $Spin(7)$ structures, whose common subgroup is the locally-defined G_2 . The second linearly independent globally defined Killing spinor realising the maximal $Spin(7)$ structure is proportional to the basis spinor [29]

$$\Gamma^- \epsilon.\tag{7.3.14}$$

Now we will look at the spinorial realisations of frame bundles with a reduced structure group.

7.3.2 $SU(4)$ and associated local AdS_3 structures

In this subsection we will define the spinorial realisations of an $SU(4)$ frame bundle of interest to us. What we call $SU(4)$ geometry is when all four spinorial singlets of the structure group of

⁵Obviously, $\theta = 0$ is a special case; it will be discussed separately in section 7.5.

the frame bundle are Killing and globally defined. The other spinorial realisations we consider - defining what we call Kähler-4 and SLAG geometry - are when two of the singlets of the structure group are Killing and globally defined. Again, the Killing spinors may be naturally selected by the action of the structure forms on the spin bundle. With asymptotically vanishing flux, the interpolating solutions of Kähler-4 and SLAG geometry will involve deformations of the normal bundles of respectively Kähler-4 and SLAG-4 cycles of the special holonomy manifolds to which they asymptote.

In the globally defined frame (7.3.1), we demand that \mathcal{M}_8 admits an everywhere non-zero almost complex structure two-form J and a (4,0) form Ω . We may always take the $SU(4)$ structure group to be embedded in $Spin(1, 10)$ such that their components are given by

$$J = e^{12} + e^{34} + e^{56} + e^{78}, \quad (7.3.15)$$

$$\Omega = (e^1 + ie^2)(e^3 + ie^4)(e^5 + ie^6)(e^7 + ie^8). \quad (7.3.16)$$

$SU(4)$ geometry The $SU(4)$ singlets are defined globally by the action of the structure forms on the spin bundle; they are the four solutions of

$$\Gamma^{+-}\eta = \pm\eta, \quad (7.3.17)$$

$$\frac{1}{12}(J \wedge J) \cdot \eta = -\eta, \quad (7.3.18)$$

or equivalently

$$\Gamma^{+-}\eta = \pm\eta, \quad (7.3.19)$$

$$\frac{1}{8}\text{Re}\Omega \cdot \eta = \pm\eta. \quad (7.3.20)$$

A third equivalent form of these conditions is

$$\Gamma^{1234}\eta = \Gamma^{3456}\eta = \Gamma^{5678}\eta = \pm\Gamma^{+-}\eta = -\eta. \quad (7.3.21)$$

$SU(4)$ geometry is defined by requiring that all four solutions of these projections are Killing. Explicitly, the Killing solutions of these equations are proportional to

$$\epsilon, \Gamma^-\epsilon, \frac{1}{4}J \cdot \epsilon, \frac{1}{4}\Gamma^-J \cdot \epsilon. \quad (7.3.22)$$

This maximal realisation of an $SU(4)$ structure is relevant for interpolations from Calabi-Yau cones to Sasaki-Einstein manifolds.

Kähler-4 geometry The spinorial realisation of a Kähler-4 structure is given by two globally defined Killing spinors which satisfy the projection

$$\frac{1}{12}\Gamma^{+-}(J \wedge J) \cdot \eta = -\eta. \quad (7.3.23)$$

This is equivalent to the maximal $SU(4)$ projections supplemented by $\Gamma^{+-}\eta = \eta$. The basis spinors of (7.3.22) which survive this projection are

$$\epsilon, \frac{1}{4}J \cdot \epsilon. \quad (7.3.24)$$

Both of these spinors have positive chirality under Γ^{+-} . The bilinears associated to these basis spinors are

$$\begin{aligned} K &= e^+, \\ \Theta &= e^{+9}, \\ \Sigma_{\pm} &= e^+ \wedge \phi_{\pm}, \end{aligned} \tag{7.3.25}$$

where

$$\phi_{\pm} = - \left(\frac{1}{2} J \wedge J \pm \text{Re}\Omega \right), \tag{7.3.26}$$

with ϕ_+ coming from ϵ and ϕ_- from $\frac{1}{4}J \cdot \epsilon$. This is the spinorial realisation of the $SU(4)$ frame bundle of relevance for the geometric duals of $N = (2, 0)$ conformal field theories.

SLAG geometry The spinorial realisation of the $SU(4)$ frame bundle defining SLAG geometry is specified by two globally defined Killing spinors, which satisfy the projections

$$\begin{aligned} \Gamma^{+-}\eta &= \pm\eta, \\ \frac{1}{8}\Gamma^{+-}\text{Re}\Omega \cdot \eta &= -\eta. \end{aligned} \tag{7.3.27}$$

This is equivalent to the maximal $SU(4)$ projections, supplemented by

$$\Gamma^{+-1357}\eta = -\eta. \tag{7.3.28}$$

The pair of basis spinors surviving this projection are

$$\epsilon, \frac{1}{4}\Gamma^- J \cdot \epsilon. \tag{7.3.29}$$

The bilinears associated to the basis spinor $\frac{1}{4}\Gamma^- J \cdot \epsilon$ are

$$\begin{aligned} K &= -e^-, \\ \Theta &= e^{-9}, \\ \Sigma &= e^- \wedge \left(\frac{1}{2} J \wedge J - \text{Re}\Omega \right). \end{aligned} \tag{7.3.30}$$

Observe that these Killing spinors have opposite $\mathbb{R}^{1,1}$ chirality, so this is the spinorial realisation of the $SU(4)$ frame bundle of relevance for the geometric duals of $N = (1, 1)$ CFTs.

Local AdS_3 structures Now we will give the local AdS_3 structures which arise from each spinorial realisation of the globally-defined $SU(4)$ structures. In this case, picking out a local AdS_3 radial direction with a component on \mathcal{M}_8 reduces the structure group, locally, to $SU(3)$. The metric is given by

$$ds^2 = \frac{1}{\lambda m^2} ds^2(AdS_3) + e^7 \otimes e^7 + \hat{\rho} \otimes \hat{\rho} + ds^2(\mathcal{N}_6), \tag{7.3.31}$$

where the locally defined \mathcal{N}_6 admits the local $SU(3)$ structure. For each of $Spin(7)$ structures which collectively define a Kähler-4 structure, $-\phi_{\pm} = \Upsilon_{\pm} + \Phi_{\pm} \wedge e^8$, we find that the associated local $AdS_3 G_2$ structures are

$$\begin{aligned}\Phi_{\pm} &= J_{SU(3)} \wedge e^7 \mp \text{Im}\Omega_{SU(3)}, \\ \Upsilon_{\pm} &= \frac{1}{2} J_{SU(3)} \wedge J_{SU(3)} \pm \text{Re}\Omega_{SU(3)} \wedge e^7.\end{aligned}\tag{7.3.32}$$

We see how the two local G_2 structures in turn define a local $SU(3)$ structure. For the globally-defined SLAG structures, the G_2 structures of a local AdS_3 patch are

$$\begin{aligned}\Phi_{\pm} &= \pm J_{SU(3)} \wedge e^7 - \text{Im}\Omega_{SU(3)}, \\ \Upsilon_{\pm} &= \pm \frac{1}{2} J_{SU(3)} \wedge J_{SU(3)} + \text{Re}\Omega_{SU(3)} \wedge e^7,\end{aligned}\tag{7.3.33}$$

and collectively they define a different embedding of the local $SU(3)$ in the local G_2 . In both cases

$$\begin{aligned}J_{SU(3)} &= e^{12} + e^{34} + e^{56}, \\ \Omega_{SU(3)} &= (e^1 + ie^2)(e^3 + ie^4)(e^5 + ie^6).\end{aligned}\tag{7.3.34}$$

The local AdS_3 structure for $SU(4)$ geometry is obvious.

7.3.3 $Sp(2)$ and associated local AdS_3 Structures

Finally we will discuss the spinorial realisations of an $Sp(2)$ frame bundle of interest to us. The discussion closely follows that of the $SU(4)$ case.

We obtain a globally defined $Sp(2)$ structure by demanding that \mathcal{M}_8 admits a triplet of everywhere non-zero almost complex structures J^A , $A = 1, 2, 3$. These obey the algebra

$$J^A J^B = -\delta^{AB} + \epsilon^{ABC} J^C.\tag{7.3.35}$$

We can always choose a basis such that the components of the three almost complex are given by

$$J^1 = e^{12} + e^{34} + e^{56} + e^{78},\tag{7.3.36a}$$

$$J^2 = -e^{13} + e^{24} - e^{57} + e^{68},\tag{7.3.36b}$$

$$J^3 = e^{14} + e^{23} + e^{67} + e^{58}.\tag{7.3.36c}$$

Note that $J^1 = J$, with J given in (7.3.15). Each almost complex structure has a corresponding $(4, 0)$ form given by

$$\begin{aligned}\Omega^1 &= \frac{1}{2} J^2 \wedge J^2 - \frac{1}{2} J^3 \wedge J^3 + i J^2 \wedge J^3, \\ \Omega^2 &= \frac{1}{2} J^3 \wedge J^3 - \frac{1}{2} J^1 \wedge J^1 + i J^3 \wedge J^1, \\ \Omega^3 &= \frac{1}{2} J^1 \wedge J^1 - \frac{1}{2} J^2 \wedge J^2 + i J^1 \wedge J^2.\end{aligned}\tag{7.3.37}$$

$Sp(2)$ geometry What we call $Sp(2)$ geometry is defined by the existence of six Killing singlets of the structure group of the global $Sp(2)$ frame bundle, which satisfy the projections

$$\begin{aligned}\Gamma^{+-}\eta &= \pm\eta, \\ \frac{1}{10}\Xi_1 \cdot \eta &= -\eta,\end{aligned}\tag{7.3.38}$$

or equivalently

$$\begin{aligned}\Gamma^{+-}\eta &= \pm\eta, \\ \frac{1}{10}\Xi_2 \cdot \eta &= \pm\eta\end{aligned}\tag{7.3.39}$$

The Killing solutions of these projections are proportional to the basis spinors

$$\epsilon, \frac{1}{4}J^1 \cdot \epsilon, \frac{1}{4}J^2 \cdot \epsilon, \Gamma^-\epsilon, \frac{1}{4}\Gamma^-J^1 \cdot \epsilon, \frac{1}{4}\Gamma^-J^2 \cdot \epsilon.\tag{7.3.40}$$

This realisation of an $Sp(2)$ frame bundle is of relevance for interpolations from Hyperkähler cones to Tri-Sasaki-Einstein manifolds.

QK geometry QK geometry is defined by the existence of three Killing spinorial realisations of the frame bundle which satisfy the projection

$$\frac{1}{10}\Gamma^{+-}\Xi_1 \cdot \eta = -\eta.\tag{7.3.41}$$

This projects out half of the Killing spinors of the maximal structure; the Killing solutions of this projection are proportional to the basis spinors

$$\epsilon, \frac{1}{4}J^1 \cdot \epsilon, \frac{1}{4}J^2 \cdot \epsilon.\tag{7.3.42}$$

The bilinears associated to these basis spinors are

$$\begin{aligned}K^A &= e^+, \\ \Theta^A &= e^{+9}, \\ \Sigma^A &= e^+ \wedge \phi^A,\end{aligned}\tag{7.3.43}$$

where

$$\phi^A = -\frac{1}{2}J^A \wedge J^A - \text{Re}\Omega^A,\tag{7.3.44}$$

with no sum on A . This is the spinorial realisation of an $Sp(2)$ frame bundle of relevance to the geometric duals of $N = (3, 0)$ CFTs. On a special holonomy manifold, the supersymmetric cycle calibrated by Ξ_1 is Kähler-4 with respect to all three complex structures.

CLAG geometry CLAG geometry is defined by the existence of three Killing spinors which satisfy the projections

$$\begin{aligned}\Gamma^{+-}\eta &= \pm\eta, \\ \frac{1}{10}\Gamma^{+-}\Xi_2 \cdot \eta &= -\eta.\end{aligned}\tag{7.3.45}$$

Again, this projects out half of the Killing spinors of the maximal structure; the subspace defined by this projection is spanned by the basis spinors

$$\epsilon, \frac{1}{4}J^1 \cdot \epsilon, \frac{1}{4}\Gamma^- J^2 \cdot \epsilon.\tag{7.3.46}$$

The bilinears associated to the first two of these basis spinors are the same as in (7.3.43) with $A = 1, 3$; the bilinears associated to $\frac{1}{4}\Gamma^- J^2 \cdot \epsilon$ are

$$\begin{aligned}K &= -e^-, \\ \Theta &= e^{-9}, \\ \Sigma &= e^- \wedge \left(\frac{1}{2}J^3 \wedge J^3 - \text{Re}\Omega^3\right).\end{aligned}\tag{7.3.47}$$

This is the spinorial realisation of the frame bundle of relevance to the geometric duals of $N = (2, 1)$ CFTs. On a special holonomy manifold, the supersymmetric cycles calibrated by Ξ_2 are Kähler-4 with respect to J^1 , and SLAG with respect to $-\text{Re}\Omega^2$ and $\text{Re}\Omega^3$.

Local AdS_3 structures In this case, picking out a local AdS_3 radial direction with a component on \mathcal{M}_8 reduces the structure group near an AdS horizon to $SU(2)$. The local metric is given by

$$ds^2 = \frac{1}{\lambda m^2} ds^2(AdS_3) + e^5 \otimes e^5 + e^6 \otimes e^6 + e^7 \otimes e^7 + \hat{\rho} \otimes \hat{\rho} + ds^2(\mathcal{N}_4),\tag{7.3.48}$$

where the locally-defined \mathcal{N}_4 admits a local $SU(2)$ structure. For each of the three $Spin(7)$ structures which are collectively equivalent to a QK structure, $-\phi^A = \Upsilon^A + \Phi^A \wedge e^8$, we find the associated local AdS_3 structures

$$\begin{aligned}\Phi^1 &= e^{567} + K^3 \wedge e^7 + K^2 \wedge e^6 - K^1 \wedge e^5, \\ \Upsilon^1 &= \text{Vol}_{\mathcal{N}_4} + K^3 \wedge e^{56} - K^2 \wedge e^{57} - K^1 \wedge e^{67},\end{aligned}\tag{7.3.49}$$

$$\begin{aligned}\Phi^2 &= e^{567} - K^3 \wedge e^7 + K^2 \wedge e^6 + K^1 \wedge e^5, \\ \Upsilon^2 &= \text{Vol}_{\mathcal{N}_4} - K^3 \wedge e^{56} - K^2 \wedge e^{57} + K^1 \wedge e^{67},\end{aligned}\tag{7.3.50}$$

$$\begin{aligned}\Phi^3 &= e^{567} + K^3 \wedge e^7 - K^2 \wedge e^6 + K^1 \wedge e^5, \\ \Upsilon^3 &= \text{Vol}_{\mathcal{N}_4} + K^3 \wedge e^{56} + K^2 \wedge e^{57} + K^1 \wedge e^{67},\end{aligned}\tag{7.3.51}$$

where the K^A are the self-dual $SU(2)$ invariant two-forms on \mathcal{N}_4 , given by

$$\begin{aligned}K^1 &= e^{14} + e^{23}, \\ K^2 &= -e^{13} + e^{24}, \\ K^3 &= e^{12} + e^{34}.\end{aligned}\tag{7.3.52}$$

They satisfy the algebra $K^A K^B = -\delta^{AB} - \epsilon^{ABC} K^C$. For CLAG geometry, two of the local G_2 structures $\{\Phi^1, \Upsilon^1\}$, $\{\Phi^3, \Upsilon^3\}$, have exactly the same form as for QK geometry, while the third structure is now given by

$$\begin{aligned}\Phi^2 &= -e^{567} + K^1 \wedge e^7 - K^2 \wedge e^6 - K^3 \wedge e^5, \\ \Upsilon^2 &= -\text{Vol}_{\mathcal{N}_4} + K^1 \wedge e^{56} + K^2 \wedge e^{57} - K^3 \wedge e^{67}.\end{aligned}\tag{7.3.53}$$

7.4 Truncating eleven-dimensional supergravity

In this section, we will truncate eleven dimensional supergravity to the global frame bundles of interest to us. The different ways in which we do this are parameterised by the different spinorial realisations of the frame bundles we defined in the previous section. The papers [25], [27]-[32] essentially provide a machine for doing this. The input is the global Minkowski frame, and in each case, the most general Killing spinors satisfying the appropriate global projection conditions. The output (with human intervention) is the most general BPS conditions in each case. These, coupled to the Bianchi identity and outstanding component of the field equations, define the truncation of eleven dimensional supergravity to the frame bundles.

Since they are qualitatively similar to one another (and qualitatively different to the other cases), and have also already received much attention, we will first briefly discuss the maximal structures, before moving on to the remaining cases.

7.4.1 $Spin(7)$, $SU(4)$ and $Sp(2)$ geometry

The BPS conditions for the maximal structures may be obtained by a trivial restriction and globalisation of the local conditions of [30] (for $Spin(7)$) and [31] (for $SU(4)$ and $Sp(2)$) to our global $\mathbb{R}^{1,1}$ frame. To state them, it is convenient to make some frame redefinitions (for this subsection only) so let us define $L = H^{2/3}$, $e^9 = H^{-1/3}\hat{e}^9$, and conformally rescale the frame on \mathcal{M}_8 so that the metric becomes

$$ds^2 = H^{-2/3}[ds^2(\mathbb{R}^{1,1}) + \hat{e}^9 \otimes \hat{e}^9] + H^{1/3}d\tilde{s}^2(\mathcal{M}_8).\tag{7.4.1}$$

The Killing spinors for $Spin(7)$ geometry are given by

$$\epsilon, \quad H^{-1/3}\Gamma^-\epsilon.\tag{7.4.2}$$

The torsion conditions in this case may be succinctly summarised by saying that \hat{e}^9 is Killing, $d\hat{e}^9$ is a two-form on \mathcal{M}_8 in the **21** of $Spin(7)$, and $d\tilde{s}^2(\mathcal{M}_8)$ is globally a metric of $Spin(7)$ holonomy. The flux is given by

$$F = d(e^{+-9}) + F^{27},\tag{7.4.3}$$

where F^{27} is a four-form on \mathcal{M}_8 in the **27** of $Spin(7)$. The Bianchi identity and field equation reduce to

$$dF^{27} = 0,\tag{7.4.4}$$

$$\tilde{\nabla}^2 H = -d\hat{e}^9 \lrcorner d\hat{e}^9 - \frac{1}{2}F^{27} \lrcorner F^{27},\tag{7.4.5}$$

where in the second equation all operations are defined in the conformally rescaled metric. For $SU(4)$ geometry, $d\tilde{s}^2(\mathcal{M}_8)$ is globally restricted further to a metric of $SU(4)$ holonomy, $d\hat{e}^9$ to

the **15**, and F_{mag} to the **20**. For $Sp(2)$ geometry, $d\tilde{s}^2(\mathcal{M}_8)$ has global $Sp(2)$ holonomy, $d\hat{e}^9$ belongs to the **10**, and F_{mag} to the **14**. The most general AdS_3 horizons in these truncations are the Freund-Rubin solutions, the direct products $AdS_4 \times \mathcal{M}_7$. In $Spin(7)$ geometry, \mathcal{M}_7 has weak G_2 holonomy; for $SU(4)$ geometry, \mathcal{M}_7 is Sasaki-Einstein; and for $Sp(2)$ geometry, it is Tri-Sasaki-Einstein. These geometries were discussed in detail in [34]. We have nothing else to say about maximal structures, and will henceforth focus on the remaining cases, where the global frame bundles are realised by half the number of Killing spinors as the maximal structures.

7.4.2 Cayley geometry

Cayley geometry is given by a globally defined $Spin(7)$ frame bundle realised by a single globally defined global null Killing spinor. In [25], the most general local BPS conditions implied by the existence of a single locally defined null Killing spinor were derived. We may thus obtain the truncation of eleven dimensional supergravity to Cayley geometry simply by restricting the conditions of [25] to a Minkowski frame and globalising them. The single null Killing spinor is ϵ , and the torsion conditions and flux are as given in the introduction.

7.4.3 Kähler-4, SLAG, QK and CLAG geometry

Now we move to the remaining cases, where the derivation of the torsion conditions is considerably more involved. We have used a combination of techniques. The Kähler-4 and QK torsion conditions may be extracted, with considerable effort, by restricting and globalising the appropriate local classifications of [31]. We derive the SLAG and CLAG conditions from scratch, using the machinery of [32]. In the Kähler-4 case, the general solution for the Killing spinors, given our frame, is

$$\epsilon; \quad \frac{1}{4}J \cdot \epsilon. \quad (7.4.6)$$

The Killing spinors have constant components in this spinorial basis. The same is true of the QK Killing spinors; in general they are

$$\epsilon; \quad \frac{1}{4}J^1 \cdot \epsilon; \quad \frac{1}{4}J^2 \cdot \epsilon. \quad (7.4.7)$$

For SLAG geometry, the general solution for the Killing spinors is

$$\epsilon; \quad L^{-1/2} \frac{1}{4} \Gamma^- J \cdot \epsilon. \quad (7.4.8)$$

Finally for CLAG, the Killing spinors are

$$\epsilon; \quad \frac{1}{4}J^1 \cdot \epsilon; \quad L^{-1/2} \frac{1}{4} \Gamma^- J^2 \cdot \epsilon. \quad (7.4.9)$$

In all cases, a useful consistency check on our torsion conditions and expressions for the flux is provided by the generalised calibration conditions of [27]:

$$\begin{aligned} dK &= \frac{2}{3} \Theta \lrcorner F + \frac{1}{3} \Sigma \lrcorner \star F, \\ d\Theta &= K \lrcorner F, \\ d\Sigma &= K \lrcorner \star F - \Theta \wedge F. \end{aligned} \quad (7.4.10)$$

These are conditions on the exterior derivatives of the bilinears of the Killing spinors, in eleven dimensions. For any of the Killing spinors we look at, with a flux of the form of (7.1.2), these are equivalent to

$$\begin{aligned} H &= Ld(L^{-1}e^9), \\ d \log L &= \frac{2}{3}Le^9 \lrcorner d(L^{-1}e^9) + \frac{1}{3}\phi \lrcorner \star_9 G, \\ Ld(L^{-1}\phi) &= -\star_9 G + e^9 \wedge G. \end{aligned} \tag{7.4.11}$$

The particular choice of ϕ depends on the particular choice of Killing spinor, and is as given in the previous section. A module of the flux which is in fact fixed by supersymmetry drops out of these equations, so they are not sufficient conditions for supersymmetry in general. However, for the modules which they contain, they provide us with a useful consistency check. The results we obtain are as stated in section two. The details of the calculations are uninteresting, how to do them is explained in [31], [32], and so we have suppressed them.

7.5 The AdS_3 geometries

In this section, we will explain in more detail how we derive the conditions on the geometry of AdS boundary regions of solutions of Cayley, Kähler-4, SLAG, QK and CLAG geometry. By boundary, we mean either event horizon or conformal boundary. For Cayley geometry, we derive the conditions by inserting the local AdS_3 frame of 3.1 into the torsion conditions for the global truncation, and also by demanding that the flux at an AdS boundary respects the AdS isometries. This requirement on the flux means that it takes the form

$$F = \text{Vol}_{AdS_3} \wedge g + F_{\text{mag}}, \tag{7.5.1}$$

with

$$\partial_a g = \partial_a F_{\text{mag}} = \hat{e}^a \lrcorner F_{\text{mag}} = 0, \tag{7.5.2}$$

where \hat{e}^a are the AdS basis one-forms. As explained in section three, the global structure group is reduced locally at an AdS boundary. We define the AdS geometry by the conditions on the intrinsic torsion of the locally defined structure, together with the flux, in each case.

An interesting question is that of the global structure of a manifold with global AdS_3 isometry. Recall the frame rotation of 3.1:

$$\begin{aligned} \hat{r} &= \sin \theta e^8 + \cos \theta e^9, \\ \hat{\rho} &= \cos \theta e^8 - \sin \theta e^9, \end{aligned} \tag{7.5.3}$$

with $\hat{r} = \lambda^{-1/2} dr$ and $L = e^{2mr} \lambda$. In the generic case of a Cayley bundle, provided that $\theta \neq 0$ globally, this frame rotation reduces the global $Spin(7)$ structure associated to the $\mathbb{R}^{1,1}$ isometry to a global G_2 structure associated to the AdS_3 isometry. Thus for a manifold with global AdS_3 isometries, the G_2 structure will only fail to be globally defined if there exist points where $\theta = 0$. It may be readily verified that the torsion conditions and flux for a Cayley bundle imply that $\theta = 0$ in an open neighbourhood is inconsistent with AdS_3 isometry of the neighbourhood - an AdS_3 frame and flux with $\hat{r} = e^9$ does not solve the supergravity equations for a Cayley frame bundle. A much more subtle issue - which we have not attempted to resolve - is what happens

at isolated points of a global AdS manifold where $\theta = 0$, and what the existence of such points implies for the geometry or topology.

In the remainder of this section, we will first discuss how, by imposing AdS_3 isometry on the electric flux (which is universally given by $F_{\text{elec}} = d(e^{+-9})$ in all cases we study) one may introduce local coordinates for the local AdS frame. We will then show how the general necessary and sufficient minimally supersymmetric AdS_3 conditions of Martelli and Sparks may be derived by imposing an AdS_3 boundary condition on an arbitrary solution of Cayley geometry. Finally we will derive the AdS boundary geometry of a solution with a Kähler-4, SLAG, QK or CLAG bundle.

7.5.1 Coordinates for the AdS frame

Imposing AdS_3 isometries on the electric flux, we demand that

$$Ld(L^{-1}e^9) = \hat{r} \wedge g, \quad (7.5.4)$$

with g independent of r . Then using (7.5.3), we get

$$\begin{aligned} e^{2mr} \partial_r (e^{-2mr} \sin \theta) \lambda^{1/2} \hat{\rho} + \lambda^{3/2} \tilde{d}(\lambda^{-3/2} \cos \theta) &= -g, \\ \tilde{d}(\lambda^{-1} \sin \theta \hat{\rho}) &= 0, \end{aligned} \quad (7.5.5)$$

where \tilde{d} denotes the exterior derivative on the space transverse to the AdS factor. Since g , $\hat{\rho}$ and λ are independent of r , the first of these equations implies that the rotation angle θ is also independent of r . Then the second equation implies that locally there exists a coordinate ρ such that

$$\hat{\rho} = \frac{\lambda}{2m \sin \theta} d\rho. \quad (7.5.6)$$

Therefore in general, we may write the metric near an AdS_3 boundary as

$$ds^2 = \frac{1}{\lambda m^2} \left[ds^2(AdS_3) + \frac{\lambda^3}{4 \sin^2 \theta} d\rho \otimes d\rho \right] + ds^2(\mathcal{N}_7), \quad (7.5.7)$$

where \mathcal{N}_7 is defined by

$$ds^2(\mathcal{M}_8) = ds^2(\mathcal{N}_7) + e^8 \otimes e^8. \quad (7.5.8)$$

There is a special case in which we can do more, and integrate the frame rotation completely. In general, in the Minkowski frame, there exists a coordinate z such that the one-form e^9 is given by

$$e^9 = C(dz + \sigma), \quad (7.5.9)$$

for a function C and a one-form σ on \mathcal{M}_8 which are independent of the Minkowski coordinates. When $\sigma = 0$ (equivalently, when $e^9 \wedge de^9 = 0$) both the Minkowski and associated AdS BPS conditions simplify considerably, and we can integrate the frame rotation.

To see how to do this, we first solve for dz in (7.5.3), and then take the exterior derivative. We get

$$d(\lambda^{-1/2} C^{-1} \cos \theta) \wedge dr - \frac{1}{2m} d(\lambda C^{-1}) \wedge d\rho = 0. \quad (7.5.10)$$

We may immediately deduce that $C = \tilde{C}(r, \rho)\lambda$. Then

$$d(\lambda^{-3/2}\tilde{C}^{-1}\cos\theta) \wedge dr = \frac{1}{2m}\partial_r\tilde{C}^{-1}dr \wedge d\rho \quad (7.5.11)$$

implies that

$$\lambda^{-3/2}\cos\theta = f(\rho), \quad (7.5.12)$$

for some arbitrary function f . Therefore, when $\sigma = 0$ in the Minkowski frame, we may write the metric in the AdS frame as

$$ds^2 = \frac{1}{\lambda m^2} \left[ds^2(AdS_3) + \frac{\lambda^3}{4(1 - \lambda^3 f^2)} d\rho \otimes d\rho \right] + ds^2(\mathcal{N}_7). \quad (7.5.13)$$

The electric flux is then given by

$$g = (1 - \partial_\rho f)\lambda^{3/2}d\rho. \quad (7.5.14)$$

It is instructive to compare this expression with the results of [9], where the supersymmetry conditions for AdS boundaries with global Minkowski frames, frame bundles with structure group contained in G_2 , and purely magnetic fluxes, were derived. For the AdS geometries, an expression for the metric of the form of (7.5.13) was found, in every case with $f = \rho$. In the present context, we see that when $\sigma = 0$, f essentially sources the electric flux, and that as in [9], $f = \rho$ implies that the fluxes are purely magnetic. To conclude this subsection, we record the expression for e^8 in the AdS frame, when $\sigma = 0$ in the Minkowski frame:

$$e^8 = \lambda^{-1/2}\sqrt{1 - \lambda^3 f^2}dr + \frac{\lambda^{5/2}f}{2m\sqrt{1 - \lambda^3 f^2}}d\rho. \quad (7.5.15)$$

7.5.2 AdS boundaries in Cayley geometry

In this subsection, we will derive the minimal AdS_3 BPS conditions quoted in the introduction by imposing an AdS_3 boundary condition on Cayley geometry. First we will derive the AdS torsion conditions, and then the relationship between the flux and the torsion in the AdS limit. We start with the torsion conditions

$$e^9 \wedge \left[-L^3 e^9 \lrcorner d(L^{-3}e^9) + \frac{1}{2}\phi \lrcorner d\phi \right] = 0, \quad (7.5.16)$$

$$(e^9 \wedge + \star_9)[e^9 \lrcorner d(L^{-1}\phi)] = 0. \quad (7.5.17)$$

One of the reasons why we have written the torsion conditions in this coordinate independent form is that it makes it much easier to perform the frame rotation. Now we do this, using

$$\begin{aligned} \phi &= -\Upsilon - \Phi \wedge e^8, \\ e^8 &= \sin\theta\hat{r} + \cos\theta\hat{\rho}, \\ e^9 &= \cos\theta\hat{r} - \sin\theta\hat{\rho}, \end{aligned} \quad (7.5.18)$$

to evaluate (7.5.16) and (7.5.17) in the \hat{r} , $\hat{\rho}$ frame. We have seen that θ must be independent of the AdS radial coordinate, and we demand that the only r dependence in the rotated frame

enters in the warping of the $\mathbb{R}^{1,1}$ factor. We split all exterior derivative as $d = \hat{r} \wedge \partial_{\hat{r}} + \hat{\rho} \wedge \partial_{\hat{\rho}} + d_7$. Separating out the $\hat{r} \wedge \hat{\rho}$ and $\cos \theta \hat{r} - \sin \theta \hat{\rho}$ components, (7.5.16) contains the two independent equations

$$\frac{1}{2} \Upsilon \lrcorner d_7 \Phi + \frac{1}{2} \cos \theta \Upsilon \lrcorner \partial_{\hat{\rho}} \Upsilon + \lambda^{7/2} \partial_{\hat{\rho}} (\lambda^{-7/2} \cos \theta) - 6m\lambda^{1/2} \sin \theta = 0, \quad (7.5.19)$$

$$\Upsilon \lrcorner d_7 \Upsilon - \frac{1}{2} \cos \theta \Phi \lrcorner \partial_{\hat{\rho}} \Upsilon - 3d_7 \log \lambda + \cos^2 \theta d_7 \log \left(\frac{\lambda^{3/2} \cos \theta}{\sin^2 \theta} \right) = 0, \quad (7.5.20)$$

where in deriving the second of these equations we have used the G_2 identities $\Phi \lrcorner d_7 \Phi = -\Upsilon \lrcorner d_7 \Upsilon$, $\Phi \lrcorner (A \wedge \Phi) = -4A$. Applying the same procedure to (7.5.17), we find the single condition

$$\begin{aligned} 0 &= 4m\lambda^{1/2} \cos \theta \Upsilon + \lambda^{3/2} \star_7 \partial_{\hat{\rho}} (\lambda^{-3/2} \sin \theta \Phi) + \lambda \sin \theta \partial_{\hat{\rho}} (\lambda^{-1} \Upsilon) \\ &+ \sin \theta \cos \theta d_7 \log \left(\frac{\lambda^{3/2} \cos \theta}{\sin^2 \theta} \right) \wedge \Phi. \end{aligned} \quad (7.5.21)$$

To proceed, we decompose (7.5.19), (7.5.20) and (7.5.21) into modules of G_2 , to extract out the independent conditions. We will then show that these can be repackaged in the form of [26]. First consider (7.5.21). This is an equation for four-forms of G_2 , and hence a priori contains **1**, **7** and **27** parts. To treat the $\partial_{\hat{\rho}}$ terms, it is useful to introduce

$$Q_{ij} = \delta_{ik} (\partial_{\hat{\rho}} e^k)_j, \quad (7.5.22)$$

where indices run from 1 to 7. Since we have chosen the frame so that Φ and Υ have constant components, we may then write

$$\begin{aligned} (\partial_{\hat{\rho}} \Phi)_{i_1 i_2 i_3} &= 3\Phi_{k[i_1 i_2} Q^k{}_{i_3]}, \\ (\partial_{\hat{\rho}} \Upsilon)_{i_1 i_2 i_3 i_4} &= -4\Upsilon_{k[i_1 i_2 i_3} Q^k{}_{i_4]}. \end{aligned} \quad (7.5.23)$$

Since Q is an a priori arbitrary rank 2 tensor of G_2 , it contains **1**, **7**, **14** and **27** parts, and encodes the intrinsic torsion modules of the eight-dimensional G_2 structure contained in the $\hat{\rho}$ derivatives of Φ and Υ . Acting on these G_2 invariant forms, the **14** part of Q drops out of (7.5.23). We can separate out the remaining parts of Q according to

$$Q_{ij} = \frac{1}{7} \gamma \delta_{ij} + \Phi_{ijk} \beta^k + Q_{ij}^{27}, \quad (7.5.24)$$

where Q_{ij}^{27} is a symmetric traceless tensor. Now we insert this expression for Q_{ij} , together with (7.5.23), into (7.5.21). The Q_{ij}^{27} drops out; this is most easily seen by choosing any particular element of the **27** and verifying that its contribution to (7.5.21) vanishes. The remaining terms are given by

$$\begin{aligned} 0 &= [4m\lambda^{1/2} \cos \theta + \lambda^{5/2} \partial_{\hat{\rho}} (\lambda^{-5/2} \sin \theta) + \sin \theta \gamma] \Upsilon \\ &+ \left[\sin \theta \cos \theta d_7 \log \left(\frac{\lambda^{3/2} \cos \theta}{\sin^2 \theta} \right) - 6 \sin \theta \beta \right] \wedge \Phi, \end{aligned} \quad (7.5.25)$$

where in evaluating the **7** terms we have used the G_2 identities given in the appendix of [35]. Therefore we must have

$$\gamma = -4m\lambda^{1/2} \frac{\cos \theta}{\sin \theta} - \partial_{\hat{\rho}} \log (\lambda^{-5/2} \sin \theta), \quad (7.5.26)$$

$$\beta = \frac{1}{6} \cos \theta d_7 \log \left(\frac{\lambda^{3/2} \cos \theta}{\sin^2 \theta} \right). \quad (7.5.27)$$

This exhausts the content of (7.5.21). Now, using our expression for γ , (7.5.19) gives the singlet part of $d_7\Phi$. We find

$$\Upsilon \lrcorner d_7\Phi = \frac{4m\lambda^{1/2}}{\sin\theta}(4 - \sin^2\theta) - 2\cos\theta\partial_{\hat{\rho}}\log\left(\frac{\lambda^{3/2}\cos\theta}{\sin^2\theta}\right). \quad (7.5.28)$$

Next, using our expression for β in (7.5.20), we obtain

$$\Upsilon \lrcorner d_7\Upsilon = 3d_7\log\lambda. \quad (7.5.29)$$

This exhausts all the torsion conditions. Finally, it may be verified that the four conditions (7.5.26)-(7.5.29) are equivalent to

$$\hat{\rho} \wedge d(\lambda^{-1}\Upsilon)^{\mathbf{7}} = 0, \quad (7.5.30)$$

$$\lambda^{5/2}d(\lambda^{-5/2}\sin\theta\text{Vol}_7) = -4m\lambda^{1/2}\cos\theta\hat{\rho} \wedge \text{Vol}_7, \quad (7.5.31)$$

$$d\Phi \wedge \Phi = \frac{4m\lambda^{1/2}}{\sin\theta}(4 - \sin^2\theta)\text{Vol}_7 - 2\cos\theta \star_8 d\log\left(\frac{\lambda^{3/2}\cos\theta}{\sin^2\theta}\right). \quad (7.5.32)$$

Equation (7.5.30) is equivalent to (7.5.29), (7.5.31) to (7.5.26), and (7.5.32) is equivalent to (7.5.27) and (7.5.28).

Next we must impose the AdS boundary condition on the magnetic flux, which in the Minkowski frame is

$$F_{\text{mag}} = -\star d(e^{+-} \wedge \phi) - \frac{L^{10/7}}{2}e^9 \lrcorner d(L^{-10/7}\phi) + \frac{1}{4}\phi \diamond [e^9 \lrcorner (e^9 \wedge de^9)] + F^{\mathbf{27}}. \quad (7.5.33)$$

We define

$$F^{\mathbf{27}} = G^{\mathbf{27}} + H^{\mathbf{27}} \wedge e^8; \quad (7.5.34)$$

eight-dimensional self-duality of $F^{\mathbf{27}}$ then implies that $G^{\mathbf{27}} = \star_7 H^{\mathbf{27}}$ (recall that the $\mathbf{27}$ of $Spin(7)$ is irreducible under G_2). Now we perform the frame rotation, and impose vanishing of the components of F_{mag} along the AdS radial direction. We find the conditions

$$\hat{\rho} \wedge d(\lambda^{-1}\Upsilon) = 0, \quad (7.5.35)$$

$$\begin{aligned} H^{\mathbf{27}} &= \frac{1}{\sin\theta} \star_7 \lambda \partial_{\hat{\rho}}(\lambda^{-1}\Upsilon) + \star_7 d_7 \left(\frac{\cos\theta}{\sin\theta} \Phi \right) + \frac{10m}{7} \lambda^{1/2} \cos\theta \Phi \\ &+ \frac{1}{2} \lambda^{27/14} \partial_{\hat{\rho}}(\lambda^{-27/14} \sin\theta \Phi) + \frac{1}{4} \sin\theta \cos\theta d_7 \log(\lambda^{-3/2} \cos\theta) \lrcorner \Upsilon. \end{aligned} \quad (7.5.36)$$

The first of these equations implies (7.5.30), and together with (7.5.31) and (7.5.32), comprises the torsion conditions given in the introduction. The left-hand side of (7.5.36) only contains a term in the $\mathbf{27}$ of G_2 , and hence the $\mathbf{1}$ and $\mathbf{7}$ parts of the right-hand side must vanish. It may be verified that they do, using (7.5.30), (7.5.31) and (7.5.32). Using (7.5.36), the magnetic flux

may be expressed as

$$\begin{aligned}
F_{\text{mag}} = & \hat{\rho} \wedge \left[-\frac{\cos \theta}{\sin \theta} \star_7 \lambda \partial_{\hat{\rho}}(\lambda^{-1} \Upsilon) - \cos \theta \star_7 d_7 \left(\frac{\cos \theta}{\sin \theta} \Phi \right) \right. \\
& \left. + 2m\lambda^{1/2} \Phi - \star_7 \lambda^{3/2} d_7(\lambda^{-3/2} \sin \theta \Phi) \right] \\
& + \left[\star_7 H^{2\tau} - \frac{24m}{7} \lambda^{1/2} \cos \theta \Upsilon - \star_7 \lambda^{3/2} \partial_{\hat{\rho}}(\lambda^{-3/2} \sin \theta \Phi) \right. \\
& \left. - \frac{1}{2} \sin \theta \lambda^{10/7} \partial_{\hat{\rho}}(\lambda^{-10/7} \Upsilon) + \frac{1}{4} \sin \theta \cos \theta d_7 \log \left(\frac{\sin^4 \theta}{\lambda^{9/2} \cos \theta} \right) \wedge \Phi \right]. \quad (7.5.37)
\end{aligned}$$

After some manipulation, this expression may be shown to be equivalent to

$$F_{\text{mag}} = \frac{\lambda^{3/2}}{\sin^2 \theta} \left(\cos \theta + \star_8 \right) \left(d[\lambda^{-3/2} \sin \theta \Phi] - 4m\lambda^{-1} \Upsilon \right) + 2m\lambda^{1/2} \Phi \wedge \hat{\rho}, \quad (7.5.38)$$

which is in turn equivalent to

$$\lambda^{3/2} d(\lambda^{-3/2} \sin \theta \Phi) = \star_8 F_{\text{mag}} - \cos \theta F_{\text{mag}} + 2m\lambda^{1/2} (\Upsilon + \cos \theta \Phi \wedge \hat{\rho}). \quad (7.5.39)$$

This exhausts all conditions.

7.5.3 AdS boundaries in Kähler-4 and SLAG geometry

There are two ways in which we can derive the BPS conditions for an AdS boundary in Kähler-4 or SLAG geometry. The first is to impose the frame rotation on the appropriate global truncation of eleven dimensional supergravity, just as for Cayley geometry. The second and technically simpler way is to use the local AdS structures of section 7.3. This is what we have done. An AdS region in Kähler-4 geometry admits a pair of local G_2 structures, which are equivalent to a local $SU(3)$ structure, according to

$$\begin{aligned}
\Phi_{\pm} &= J_{SU(3)} \wedge e^7 \mp \text{Im} \Omega_{SU(3)}, \\
\Upsilon_{\pm} &= \frac{1}{2} J_{SU(3)} \wedge J_{SU(3)} \pm \text{Re} \Omega_{SU(3)} \wedge e^7. \quad (7.5.40)
\end{aligned}$$

Both these G_2 structures must satisfy the local Cayley AdS_3 conditions. Similarly for SLAG geometry, where the local G_2 structures of an AdS region are

$$\begin{aligned}
\Phi_{\pm} &= \pm J_{SU(3)} \wedge e^7 - \text{Im} \Omega_{SU(3)}, \\
\Upsilon_{\pm} &= \pm \frac{1}{2} J_{SU(3)} \wedge J_{SU(3)} + \text{Re} \Omega_{SU(3)} \wedge e^7, \quad (7.5.41)
\end{aligned}$$

In each case, the local AdS metric is

$$ds^2 = \frac{1}{\lambda m^2} \left[ds^2(AdS_3) + \frac{\lambda^3}{4 \sin^2 \theta} d\rho \otimes d\rho \right] + e^7 \otimes e^7 + ds^2(\mathcal{N}_6). \quad (7.5.42)$$

For the remainder of this subsection it is understood that structure forms are of $SU(3)$, and we will suppress their subscripts. This doubling of the structures provides a very convenient way of

arriving at the BPS conditions in each case. For example, the Cayley condition $\hat{\rho} \wedge d(\lambda^{-1}\Upsilon) = 0$ decomposes for both Kähler-4 and SLAG into the pair of equations

$$\begin{aligned}\hat{\rho} \wedge d(\lambda^{-1}J \wedge J) &= 0, \\ \hat{\rho} \wedge d(\lambda^{-1}\text{Re}\Omega \wedge e^7) &= 0.\end{aligned}\tag{7.5.43}$$

Similarly, decomposing (7.5.31) and (7.5.32) leads to identical equations for AdS_3 regions in both Kähler-4 and SLAG geometries. What distinguishes these geometries is the decomposition of the flux. Requiring a magnetic flux of the form (7.5.38) for both the local G_2 structures in Kähler-4 geometry, we find the conditions

$$F_{\text{mag}} = \frac{\lambda^{3/2}}{\sin^2\theta}(\cos\theta + \star_8)(d[\lambda^{-3/2}\sin\theta J \wedge e^7] - 2m\lambda^{-1}J \wedge J) + 2m\lambda^{1/2}J \wedge e^7 \wedge \hat{\rho},\tag{7.5.44}$$

$$0 = -\frac{\lambda^{3/2}}{\sin^2\theta}(\cos\theta + \star_8)(d[\lambda^{-3/2}\sin\theta\text{Im}\Omega] + 4m\lambda^{-1}\text{Re}\Omega \wedge e^7) - 2m\lambda^{1/2}\text{Im}\Omega \wedge \hat{\rho}.\tag{7.5.45}$$

For the local AdS structures in SLAG geometry, we instead get

$$0 = \frac{\lambda^{3/2}}{\sin^2\theta}(\cos\theta + \star_8)(d[\lambda^{-3/2}\sin\theta J \wedge e^7] - 2m\lambda^{-1}J \wedge J) + 2m\lambda^{1/2}J \wedge e^7 \wedge \hat{\rho},\tag{7.5.46}$$

$$F_{\text{mag}} = -\frac{\lambda^{3/2}}{\sin^2\theta}(\cos\theta + \star_8)(d[\lambda^{-3/2}\sin\theta\text{Im}\Omega] + 4m\lambda^{-1}\text{Re}\Omega \wedge e^7) - 2m\lambda^{1/2}\text{Im}\Omega \wedge \hat{\rho}.\tag{7.5.47}$$

It is this formal difference in the decomposition of the flux that endows AdS regions in the two geometries with such different properties.

In each case, not all the equations obtained by performing this decomposition of the Cayley AdS conditions are independent. We have reduced them to a minimal set of necessary and sufficient independent conditions, which are quoted in section 7.2.

7.5.4 AdS boundaries in QK and CLAG geometry

To derive the BPS conditions for an AdS boundary in QK or CLAG geometry, we may either impose the frame rotation on the torsion conditions of section 7.4, or (which is again technically more convenient) we can use the local AdS_3 structures of section 7.3 to further decompose the torsion conditions for an AdS region in Kähler-4 or SLAG geometry. The derivation proceeds in a very similar way to that of the derivation of the geometry of AdS regions in Kähler-4 or SLAG from Cayley, and we have suppressed the details. In QK and CLAG geometry, the local AdS metric is

$$ds^2 = \frac{1}{\lambda m^2} \left[ds^2(AdS_3) + \frac{\lambda^3}{4\sin^2\theta} d\rho \otimes d\rho \right] + e^5 \otimes e^5 + e^6 \otimes e^6 + e^7 \otimes e^7 + ds^2(\mathcal{N}_4).\tag{7.5.48}$$

Relabelling $(e^5, e^6, e^7) \rightarrow (e^1, e^2, e^3)$, from section 7.3, we find that an AdS region in QK or CLAG geometry admits three local $SU(3)$ structures; in terms of the $SU(2)$ forms K^A on \mathcal{N}_4 ,

	p	q	a_1	a_2	$\epsilon^{10\Lambda}$	c_1	c_2
SLAG 4-cycle in CY_4	4	1	$\epsilon^{4\Lambda}$	$\epsilon^{-6\Lambda}$	$\frac{3}{2}$	1	$\frac{3}{2}$
Kähler 4-cycle in CY_4	4	1	$\epsilon^{4\Lambda}$	$\epsilon^{-6\Lambda}$	$\frac{4}{3}$	1	$\frac{4}{3}$

Table 7.6.1: Known solutions of wrapped M5-branes on 4-cycles in a CY_4 .

these are given by

$$e^A = e^7, \tag{7.5.49}$$

$$J^A = K^A + \frac{1}{2}\epsilon^{ABC}e^B \wedge e^C, \tag{7.5.50}$$

$$\text{Re}\Omega^1 = K^3 \wedge e^2 + K^2 \wedge e^3, \tag{7.5.51}$$

$$\text{Im}\Omega^1 = K^3 \wedge e^3 - K^2 \wedge e^2, \tag{7.5.52}$$

together with permutations of the last two equations. In QK geometry, each of these local structures must individually satisfy the conditions for a local $AdS_3 SU(3)$ structure in Kähler-4 geometry. In CLAG geometry, the structure forms e^3, J^3 and Ω^3 must together satisfy the AdS conditions in Kähler-4 geometry, while the $e^A, J^A, \Omega^A, A = 1, 2$, must satisfy the AdS conditions in SLAG geometry. In each case, reducing these conditions to a minimal necessary and sufficient independent set, we get the results quoted in section 7.2.

7.6 Explicit solutions

In this section we show that the known solutions with AdS_3 factors fit nicely in the framework developed in the previous sections. To do so we consider solutions describing the near-horizon limit of M5-branes wrapping SLAG 4-cycles and Kähler 4-cycles in a CY_4 . These were first found in [4] in seven-dimensional gauged supergravity. Throughout this section we will follow the notation and conventions of [9].

For the known solutions, the eleven-dimensional metric can be put into the form

$$m^2 ds^2 = \Delta^{-2/5} \left[\frac{a_1}{u^2} ds^2(\mathbb{R}^{1,5-d}) + a_2 ds^2(\Sigma_d) \right] + \Delta^{4/5} \left[e^{2q\Lambda} u^{2c_1} DX^a DX^a + e^{-2p\Lambda} u^{2c_2} dX^\alpha dX^\alpha \right], \tag{7.6.1}$$

with $a = 1 \dots p$ and $\alpha = 1 \dots q$ and $p + q = 5$. The constants a_1 and a_2 specify the relative size of the AdS factor and the d -cycle Σ_d . For the cases corresponding to M5-branes wrapping 4-cycles, we have $d = 4, p = 4$ and $q = 1$. The relevant values of the remaining constants for the two cases that we will be discussing are summarized in Table 7.6.1. Following [9], we have defined

$$DX^a = dX^a + B^a_b X^b \tag{7.6.2}$$

where B^a_b is determined by the spin connection on Σ_d . Comparing this form of the metric with (7.1.1), we identify

$$L = \frac{\Delta^{2/5} u^2}{a_1}, \quad C = \frac{\Delta^{2/5} u^{c_2}}{a_1}, \tag{7.6.3}$$

where $e^9 = C dz$ for the case at hand. Introducing new coordinates

$$X^a = u^{-c_1} \cos \tau Y^a, \quad X^\alpha = u^{-c_2} \sin \tau Y^\alpha, \quad c_1 = e^{-2q\Lambda} \sqrt{a_1}, \quad c_2 = e^{2p\Lambda} \sqrt{a_2}, \tag{7.6.4}$$

where Y^a and Y^α parametrise an $(p-1)$ -sphere and an $(q-1)$ -sphere respectively, the metric becomes⁶

$$m^2 ds^2 = \Delta^{-2/5} \left\{ \frac{a_1}{u^2} [ds^2(\mathbb{R}^{1,5-d}) + du^2] + a_2 ds^2(\Sigma_d) + e^{2(q-p)\Lambda} d\tau^2 \right\} + \Delta^{4/5} [e^{2q\Lambda} \cos \tau^2 DY^a DY^a + e^{-2p\Lambda} \sin \tau^2 dY^\alpha dY^\alpha] , \quad (7.6.5)$$

From the definition of Δ in [4], we have that

$$(a_1 \lambda)^{-3} = \Delta^{-6/5} = e^{-2q\Lambda} \cos \tau + e^{2p\Lambda} \sin \tau. \quad (7.6.6)$$

Specialising to our cases of interest $p=4$ and $q=1$ from now on, the metric can be put into the generic form (7.5.13) by introducing a new coordinate ρ as follows. Define

$$f(\rho) = a_1 c_2 e^{-p\Lambda} \sin \tau , \quad (7.6.7)$$

where $f(\rho)$ is the same function as in section 7.5.1. Then, the metric becomes

$$ds^2 = \frac{1}{\lambda m^2} \left[ds^2(AdS_3) + \frac{\lambda^3}{4(1-\lambda^3 f^2)} d\rho \otimes d\rho + \frac{a_2}{a_1} ds^2(\Sigma_4) + \frac{1}{c_1^2} (1-\lambda^3 f^2) DY^a \otimes DY^a \right] , \quad (7.6.8)$$

where, in order to get the form (7.5.13), we have set

$$f(\rho) = \frac{c_2}{2} \rho . \quad (7.6.9)$$

From the analysis in section 7.5.1, we conclude that this solution carries electric flux, which is indeed the case for the solutions presented in [4].

To identify the AdS radial coordinate in \mathcal{M}_8 , one defines a one-form [9]

$$\begin{aligned} e^8 &= \frac{\Delta^{2/5} e^{q\Lambda}}{m} \left(c_1 \cos \tau \frac{du}{u} + \sin \tau d\tau \right) \\ &= \lambda^{-1/2} \sqrt{1-\lambda^3 f^2} dr + \frac{\lambda^{5/2} f}{2m \sqrt{1-\lambda^3 f^2}} d\rho , \end{aligned} \quad (7.6.10)$$

with $u = e^{mr}$. This expression matches our previous one in (7.5.15).

Now we are ready to check that the solutions of [4] satisfy our equations. We discuss the SLAG-4 and the Kähler-4 cases separately.

SLAG-4

For the SLAG-4 case, $B_b^a = \bar{\omega}_b^a$, where $\bar{\omega}_b^a$ is the spin connection on Σ_4 , which is just the four-hyperboloid \mathcal{H}^4 of unit curvature. As described in [9], the $SU(4)$ structure is given by

$$J = e^a \wedge f^a , \quad (7.6.11)$$

$$\Omega = \frac{1}{4!} \epsilon^{abcd} (e^a + i f^a)(e^b + i f^b)(e^c + i f^c)(e^d + i f^d) , \quad (7.6.12)$$

⁶This form of the metric corrects some errors in eq. 9.6 of [9].

where $e^a = \Delta^{-1/5} \sqrt{a_2} m^{-1} \bar{e}^a$ and $f^a = \Delta^{2/5} e^{q\Lambda} u^{c_1} m^{-1} DX^a$. Here $\{\bar{e}^a\}$ denote a basis of 1-forms on \mathcal{H}^4 . In the *AdS* limit, the $SU(4)$ structure decomposes under $SU(3)$ in the following way:

$$\begin{aligned} J &= e^a \wedge (\tilde{f}^a - Y^a e^8) \\ &= J_{SU(3)} + e^7 \wedge e^8, \end{aligned} \quad (7.6.13)$$

where

$$e^7 = -Y^a e^a, \quad \text{and} \quad \tilde{f}^a \equiv \frac{\Delta^{2/5} e^{q\Lambda}}{m} \cos \tau DY^a. \quad (7.6.14)$$

Similarly, the holomorphic 4-form Ω decomposes as

$$\Omega = (\text{Re}\Omega_{SU(3)} + i\text{Im}\Omega_{SU(3)}) \wedge (e^7 + ie^8), \quad (7.6.15)$$

from which we find

$$\text{Re}\Omega_{SU(3)} = \frac{1}{3!} \epsilon^{abcd} Y^a e^{bcd} - \frac{1}{2!} \epsilon^{abcd} Y^a \tilde{f}^{bc} \wedge e^d, \quad (7.6.16)$$

$$\text{Im}\Omega_{SU(3)} = -\frac{1}{3!} \epsilon^{abcd} Y^a \tilde{f}^{bcd} + \frac{1}{2!} \epsilon^{abcd} Y^a \tilde{f}^b \wedge e^{cd}. \quad (7.6.17)$$

Using these expressions, it is straightforward to show that the SLAG-4 solution of [4] satisfies (7.2.31)-(7.2.32). Showing that (7.2.33) also holds requires some more work. Consider first the LHS of (7.2.33). One should first note that

$$D^2 Y^a = \frac{1}{2} \bar{R}^a{}_{bcd} Y^b \bar{e}^c \wedge \bar{e}^d, \quad (7.6.18)$$

where $\bar{R}^a{}_{bcd}$ is the Riemann tensor on \mathcal{H}^4 and hence $\bar{R}_{abcd} = 2k\delta_{a[c}\delta_{d]b}$, with $k = -\frac{1}{3}$. Then, we compute

$$\tilde{d}\text{Im}\Omega = \frac{m\Delta^{-2/5}e^{-q\Lambda}}{\cos \tau} \frac{1}{2!} \epsilon^{abcd} \left[\tilde{f}^{ab} e^{cd} + k \frac{\Delta^{6/5} e^{2q\Lambda}}{a_2} \cos^2 \tau Y^a e^b (\tilde{f}^{cd} - e^{cd}) e^7 \right] \quad (7.6.19)$$

with $q = 1$ for SLAG-4 [9]. Taking the wedge product of the expression above with $\text{Im}\Omega$ we obtain

$$\text{Im}\Omega \wedge d\text{Im}\Omega = 6m \left(\frac{\Delta^{-2/5} e^{-q\Lambda}}{\cos \tau} + k \frac{\Delta^{4/5} e^{q\Lambda}}{a_2} \cos \tau \right) \text{Vol}_6 \wedge e^7, \quad (7.6.20)$$

where on a manifold with $SU(3)$ structure, the volume 6-form may be defined by

$$\begin{aligned} \text{Vol}_6 &= \frac{1}{3!} J \wedge J \wedge J \\ &= -(e^{123} \tilde{f}^{123} + e^{124} \tilde{f}^{124} + e^{134} \tilde{f}^{134} + e^{234} \tilde{f}^{234}). \end{aligned} \quad (7.6.21)$$

To put the result above into a more familiar form, we perform the following change of coordinates:

$$\lambda = \frac{\Delta^{2/5}}{a_1}, \quad \sin \tau = \frac{e^{p\Lambda}}{a_1 c_2} f(\rho), \quad \cos \tau = \frac{e^{q\Lambda}}{(a_1 \lambda)^{3/2}} (1 - \lambda^3 f^2)^{1/2}. \quad (7.6.22)$$

Finally, introducing the values of a_1, a_2, c_1, c_2 , for the SLAG-4 solutions of [4], and using that $\cos \theta = \lambda^{3/2} f(\rho)$, (7.6.20) can be cast in the following form:

$$\text{Im}\Omega \wedge d\text{Im}\Omega = \frac{3m\lambda^{1/2}}{\sin \theta} (1 + \cos^2 \theta) \text{Vol}_6 \wedge e^7. \quad (7.6.23)$$

One can then show that this matches the RHS of (7.2.33). Furthermore, we have also checked that the Bianchi identity for the four-form field strength is satisfied. To do this, the following identities are useful:

$$\begin{aligned}
 d[\epsilon^{abcd}Y^aDY^b \wedge DY^c \wedge DY^d] &= -\epsilon^{abcd}Y^a \wedge DY^b \wedge DY^c \wedge e^d \wedge (Y^e e^e), \\
 d[\epsilon^{abcd}Y^aDY^b \wedge e^c \wedge e^d] &= -\left[2\epsilon^{abcd}Y^aDY^b \wedge DY^c \wedge e^d + \frac{1}{3}\epsilon^{abcd}Y^a e^b \wedge e^c \wedge e^d\right] \wedge Y^e e^e, \\
 d[\epsilon^{abcd}Y^a e^b \wedge e^c \wedge e^d] &= -3\epsilon^{abcd}Y^aDY^b \wedge e^c \wedge e^d \wedge (Y^e e^e), \\
 \epsilon^{abcd}DY^a \wedge DY^b \wedge e^c \wedge e^d &= -2\epsilon^{abcd}Y^aDY^b \wedge DY^c \wedge e^d \wedge (Y^e e^e).
 \end{aligned} \tag{7.6.24}$$

Kähler-4

For the Kähler-4 solutions presented in [4], one can take $B^{12} = B^{34}$ with all other components vanishing. Then one has

$$B^{12} + B^{34} = -\frac{1}{2} \bar{\omega}_{ab} K^{3ab}, \tag{7.6.25}$$

where K^3 is defined in (7.3.52). Making the following ansatz for the $SU(4)$ structure,

$$J = e^1 \wedge e^2 + e^3 \wedge e^4 + f^1 \wedge f^2 + f^3 \wedge f^4, \tag{7.6.26}$$

$$\Omega = (e^1 + ie^2)(e^3 + ie^4)(f^1 + if^2)(f^3 + if^4), \tag{7.6.27}$$

we find, in the AdS limit, that the $SU(3)$ structure is given by

$$\begin{aligned}
 e^7 &= K_{ab}^3 Y^a \tilde{f}^b, \\
 J_{SU(3)} &= e^1 \wedge e^2 + e^3 \wedge e^4 + \tilde{f}^1 \wedge \tilde{f}^2 + \tilde{f}^3 \wedge \tilde{f}^4, \\
 \text{Re}\Omega_{SU(3)} &= -K^2 \wedge K_{ab}^1 Y^a \tilde{f}^b - K^1 \wedge K_{ab}^2 Y^a \tilde{f}^b, \\
 \text{Im}\Omega_{SU(3)} &= -K^2 \wedge K_{ab}^2 Y^a \tilde{f}^b + K^1 \wedge K_{ab}^1 Y^a \tilde{f}^b,
 \end{aligned} \tag{7.6.28}$$

where the K^A , $A = 1, 2, 3$, have been defined in (7.3.52). These expressions are just the same as those in eq.(7.2.27). Now it is a straightforward exercise to check that our equations (7.2.19)-(7.2.21) are satisfied and so is the Bianchi identity.

7.7 Conclusions

In this paper, we have formalised a proposal for a universal feature of the global geometry of supergravity solutions of relevance to the supersymmetric AdS_3/CFT_2 correspondence in M-theory. A supergravity solution associated to a CFT - a region of spacetime containing a local AdS region - should admit a globally-defined $\mathbb{R}^{1,1}$ frame, and a global reduction of its frame bundle, to one with structure group contained in $Spin(7)$. From this starting assumption, we have seen how many individual features of AdS/CFT geometry may be assembled into a coherent overall picture. Probe brane kappa-symmetry projections arise from the global definition of the spinorial realisation of the frame bundle. Solutions with asymptotically vanishing flux automatically asymptote to special holonomy manifolds. The existence of a globally-defined frame bundle allows for the global truncation of the field equations of eleven-dimensional supergravity. The general necessary and sufficient conditions for minimally supersymmetric AdS_3 geometry in M-theory may be derived by imposing an AdS_3 boundary condition on the truncation of supergravity to a Cayley frame bundle. The same applies for AdS_2 with an $SU(5)$

frame bundle [10], AdS_4 (with magnetic fluxes) and a G_2 frame bundle; and AdS_5 with an $SU(3)$ frame bundle [9]. The minimal truncations, and associated AdS conditions, may be refined by further reducing the structure group of the frame bundle and/or by demanding additional Killing spinor realisations. Freund-Rubin or gauged supergravity AdS solutions satisfy the general equations for AdS horizons in the appropriate geometries.

One of the original motivations for this work, and that of [9], [10], was to map out the supersymmetric AdS landscape of M-theory. At this point, it is worth summarising what has been achieved. The strategy in each of these papers is first to impose the existence of a global Minkowski frame bundle, realised by Killing spinors of a definite Minkowski chirality, and then to impose a general AdS boundary condition on the global truncation of eleven-dimensional supergravity to the Minkowski frame bundle. Modulo quotients, this approach covers all supersymmetric AdS spacetimes which may be obtained from solutions with globally defined Minkowski frame bundles, and definite chirality Minkowski Killing spinors. For AdS_2 , with the exception of near-horizon limits of M5 branes wrapped on the direct product of a SLAG-3 and a Kähler-2 cycle in a manifold of $SU(3) \times SU(2)$ holonomy, and modulo some technical caveats, the results of [10] are complete. For AdS_3 with less than sixteen supersymmetries, we believe that the combined results of this paper and [9] are complete. We have certainly covered all cases which admit a wrapped brane interpretation, and in full generality. There exist half-BPS AdS_3 solutions of M-theory; we have not performed a general investigation of this interesting case here and we leave it for the future. For AdS_4 with electric fluxes, the Freund-Rubin solutions are exhaustive. For AdS_4 with purely magnetic fluxes, admitting a wrapped brane interpretation and modulo some technical caveats explained therein, the results of [36] and [9] are complete. The existence or otherwise of supersymmetric AdS_4 solutions with dyonic fluxes is an open problem. For AdS_5 spacetimes admitting a wrapped brane interpretation, and again modulo some technical caveats detailed in [9], the results of [33] and [37] are complete. This, then, is the status of the classification; the most interesting cases that have not been covered are half-BPS AdS_3 and dyonic AdS_4 . If there exist any other AdS solutions of M-theory which are not covered by the classification, they will necessarily have very complicated and unusual geometry.

This global framework, and the results of the classification, open the way for many future applications. The most obvious is to use the geometrical insight provided by the AdS torsion conditions to construct new explicit AdS solutions. A more important question is the development of a theory of boundary conditions for solutions of the truncated supergravity equations. With our general AdS_3 boundary condition, we have taken a first step in this direction, but there are many other possibilities to be explored. As we mentioned before, a class of boundary conditions which is particularly interesting mathematically is special holonomy spacelike asymptotics with vanishing fluxes, and spacelike AdS asymptotics associated to event horizons. To our knowledge, the only known solutions of this form are the elementary brane solutions, associated to interpolations from conical special holonomy manifolds to Freund-Rubin AdS horizons. These interpolating solutions are intimately associated to the resolution of singularities of the asymptotic special holonomy manifolds; and in these cases, the AdS/CFT correspondence provides a definition of how the singularities may be resolved quantum gravitationally. This has been made manifest in the work on the $Y^{p,q}$ /quiver gauge theory correspondence in IIB. Open string theory on the Calabi-Yau - with Dirichlet boundary conditions restricting the open strings to the vicinity of the singularity - reduces at low energies to a conformally invariant quiver gauge theory. The AdS/CFT correspondence states that this field theory is dual to the low-energy limit of closed IIB strings on a large-volume $AdS_5 \times Y^{p,q}$ manifold. The field theory

at weak 't Hooft coupling encodes the toric data of the Calabi-Yau singularity. It also encodes, at strong 't Hooft coupling, the Sasaki-Einstein data of the AdS manifold. This means that, at low energies, the physical content of open string theory near a conical Calabi-Yau singularity and closed string theory on a large-volume AdS blow-up of the singularity are contained in the same quantum field theory. Going from weak to strong 't Hooft coupling in the field theory gives a quantum definition of the singularity-resolving geometrical interpolation. It would be very interesting if other interpolating solutions, associated to the resolution of other types of special holonomy singularities, could be constructed. Extending the intuition obtained from conical interpolations, it seems likely that such solutions will be associated to the resolution of singularities of collapsing supersymmetric cycles of the asymptotic special holonomy manifolds. Understanding how to construct such solutions - and how to associate a given AdS near-horizon geometry to a special holonomy infinity, and vice versa - will require a detailed understanding of how to match the boundary data at each spacelike infinity. It will certainly require the use of more sophisticated geometrical techniques than those employed here. A complementary approach to finding explicit interpolating solutions would be to try to establish existence or obstruction theorems. An example of such a result - an obstruction theorem for Sasaki-Einstein metrics - has recently appeared in the context of conical interpolations in IIB [38]. It will be interesting to explore a more general extension of this kind of approach.

Another extension will be to consider more general boundary conditions for solutions of the global supergravity truncations - solutions with an AdS region which asymptote to flux geometries, or solutions with multiple AdS regions. Known solutions are likely to provide useful insights into the general form of boundary conditions one should impose in these cases.

Though we have focussed on its classical, geometrical limit throughout this paper, the AdS/CFT correspondence is of course a quantum phenomenon. We have a much less satisfactory understanding of the quantum aspects of AdS/CFT in M-theory than we do in IIB, and improving this situation is a major outstanding problem. Perhaps the most promising line of attack is to exploit the duality between M-theory and IIB, where things are much better understood. This can work in two directions. By imposing T^2 isometries on the eleven-dimensional supergravity truncations - or their AdS limits - one could obtain the subset of M-theory solutions which can be reduced and T-dualised to IIB. This is how the $Y^{p,q}$ were discovered. Conversely, where a IIB AdS/CFT dual is known, if the geometry admits a lift to M-theory one could do so, in the hope of gaining an understanding of how the known quantum field theory encodes the eleven-dimensional geometrical data. Ultimately it might be possible to extend the intuition thus obtained to M-theory geometries not admitting a IIB reduction, though this will certainly require significant new insights.

7.8 Acknowledgements

We are grateful to Bo Feng, Anastasios Petkou, Daniel Waldram and in particular Jerome Gauntlett for useful discussions. PF was supported by a BE and an FI fellowship from AGAUR (Generalitat de Catalunya), DURSI 2005 SGR 00082, CICYT FPA 2004-04582-C02-02 and EC FP6 program MRTN-CT-2004-005104. OC is supported by EPSRC, and is grateful to the University of Crete for hospitality during the final stages of this work.

Bibliography

- [1] J. M. Maldacena, “The Large N Limit of Superconformal Field Theories and Supergravity”, *Adv.Theor.Math.Phys.* 2 (1998) 231-252; *Int.J.Theor.Phys.* 38 (1999) 1113-1133, hep-th/9711200.
- [2] J. Maldacena and C. Nuñez, “Supergravity description of field theories on curved manifolds and a no go theorem”, *Int.J.Mod.Phys. A*16 (2001) 822-855, hep-th/0007018.
- [3] J. Maldacena and C. Nuñez, “Towards the large N limit of pure N=1 super Yang Mills”, *Phys.Rev.Lett.* 86 (2001) 588-591, hep-th/0008001.
- [4] J. P. Gauntlett, N. Kim and D. Waldram, “M-fivebranes wrapped on supersymmetric cycles”, *Phys. Rev. B* **63** (2001) 126001, hep-th/0012195.
- [5] J. P. Gauntlett, O. A. P. Mac Conamhna, T. Mateos and D. Waldram, “New supersymmetric AdS3 solutions”, *Phys.Rev.* D74 (2006) 106007, hep-th/0608055.
- [6] J. P. Gauntlett, O. A. P. Mac Conamhna, T. Mateos and D. Waldram, “Supersymmetric AdS3 solutions of type IIB supergravity”, *Phys.Rev.Lett* 97 (2006) 171601, hep-th/0606221.
- [7] O. Lunin and J. Maldacena, “Deforming field theories with $U(1) \times U(1)$ global symmetry and their gravity duals”, *JHEP* 0505 (2005) 033, hep-th/0502086.
- [8] J. P. Gauntlett, S. Lee, T. Mateos and D. Waldram, “Marginal Deformations of Field Theories with AdS_4 Duals”, *JHEP* 0508 (2005) 030, hep-th/0505207.
- [9] J. P. Gauntlett, O. A. P. Mac Conamhna, T. Mateos and D. Waldram, “AdS spacetimes from wrapped M5 branes”, *JHEP* 0611 (2006) 053, hep-th/0605146.
- [10] O. A. P. Mac Conamhna and E. Ó Colgáin, “Supersymmetric wrapped membranes, AdS(2) spaces, and bubbling geometries”, hep-th/0612196.
- [11] C. N. Gowdigere and N. P. Warner, “Holographic Coulomb Branch Flows with N=1 Supersymmetry”, *JHEP* 0603 (2006) 049, hep-th/0505019.
- [12] R. Corrado, K. Pilch and N. P. Warner, “An N = 2 Supersymmetric Membrane Flow”, R. Corrado, K. Pilch and N. P. Warner, *Nucl.Phys. B*629 (2002) 74-96, hep-th/0107220.
- [13] D. Z. Freedman, S. S. Gubser, K. Pilch and N. P. Warner, “Renormalization Group Flows from Holography–Supersymmetry and a c-Theorem”, *Adv.Theor.Math.Phys.* 3 (1999) 363-417, hep-th/9904017.

-
- [14] I. R. Klebanov and M. J. Strassler, “Supergravity and a Confining Gauge Theory: Duality Cascades and χ SB-Resolution of Naked Singularities”, JHEP 0008 (2000) 052, hep-th/0007191.
- [15] I. R. Klebanov and E. Witten, “Superconformal Field Theory on Threebranes at a Calabi-Yau Singularity”, Nucl.Phys. B536 (1998) 199-218, hep-th/9807080.
- [16] J. P. Gauntlett, D. Martelli, J. Sparks and D. Waldram, “Sasaki-Einstein Metrics on $S^2 \times S^3$ ”, Adv.Theor.Math.Phys. 8 (2004) 711-734, hep-th/0403002.
- [17] B. Feng, A. Hanany and Y.-H. He, “D-Brane Gauge Theories from Toric Singularities and Toric Duality”, Nucl.Phys. B595 (2001) 165-200, hep-th/0003085.
- [18] D. Martelli and J. Sparks, “Toric Geometry, Sasaki-Einstein Manifolds and a New Infinite Class of AdS/CFT Duals”, Commun.Math.Phys. 262 (2006) 51-89, hep-th/0411238.
- [19] S. Benvenuti, S. Franco, A. Hanany, D. Martelli and J. Sparks, “An Infinite Family of Superconformal Quiver Gauge Theories with Sasaki-Einstein Duals”, JHEP 0506 (2005) 064, hep-th/0411264.
- [20] K. Intriligator and B. Wecht, “The Exact Superconformal R-Symmetry Maximizes a”, Nucl.Phys. B667 (2003) 183-200, hep-th/0304128.
- [21] D. Martelli, J. Sparks and S.-T. Yau, “The Geometric Dual of a-maximisation for Toric Sasaki-Einstein Manifolds”, Commun.Math.Phys. 268 (2006) 39-65, hep-th/0503183.
- [22] M. J. Duff, G. W. Gibbons and P. K. Townsend, “Macroscopic superstrings as interpolating solitons”, Phys.Lett. B332 (1994) 321-328, hep-th/9405124.
- [23] A. Strominger, “The dS/CFT correspondence”, JHEP 0110 (2001) 034, hep-th/0106113.
- [24] N. Goheer, M. Kleban and L. Susskind, “The trouble with de Sitter space”, JHEP 0307 (2003) 056, hep-th/0212209.
- [25] J. P. Gauntlett, J. B. Gutowski and S. Pakis, “The Geometry of D=11 Null Killing Spinors”, JHEP 0312 (2003) 049, hep-th/0311112.
- [26] D. Martelli and J. Sparks, “G-Structures, Fluxes and Calibrations in M-Theory”, Phys.Rev. D68 (2003) 085014, hep-th/0306225.
- [27] J. P. Gauntlett and S. Pakis, “The Geometry of D=11 Killing Spinors”, JHEP 0304 (2003) 039, hep-th/0212008.
- [28] O. A. P. Mac Conamhna, “Refining G-structure classifications”, Phys.Rev. D70 (2004) 105024, hep-th/0408203.
- [29] M. Cariglia and O. A. P. Mac Conamhna, “Null structure groups in eleven dimensions”, Phys.Rev. D73 (2006) 045011, hep-th/0411079.
- [30] M. Cariglia and O. A. P. Mac Conamhna, “Classification of supersymmetric spacetimes in eleven dimensions”, Phys.Rev.Lett. 94 (2005) 161601, hep-th/0412116.

-
- [31] O. A. P. Mac Conamhna, “Eight-manifolds with G-structure in eleven dimensional supergravity”, *Phys.Rev. D72* (2005) 086007, hep-th/0504028.
- [32] O. A. P. Mac Conamhna, “The geometry of extended null supersymmetry in M-theory”, *Phys.Rev. D73* (2006) 045012, hep-th/0505230.
- [33] J. P. Gauntlett, D. Martelli, J. Sparks and D. Waldram, “Supersymmetric AdS5 solutions of M-theory”, *Class.Quant.Grav.* 21 (2004) 4335-4366, hep-th/0402153.
- [34] B. S. Acharya, J. M. Figueroa-O’Farrill, C. M. Hull and B. Spence, “Branes at conical singularities and holography”, *Adv.Theor.Math.Phys.* 2 (1999) 1249-1286, hep-th/9808014.
- [35] A. Bilal, J.-P. Derendinger, K. Sfetsos, “(Weak) G_2 Holonomy from Self-duality, Flux and Supersymmetry”, *Nucl.Phys. B628* (2002) 112-132, hep-th/0111274.
- [36] A. Lukas and P. M. Saffin, “M-theory compactification, fluxes and AdS4”, *Phys.Rev. D71* (2005) 046005, hep-th/0403235.
- [37] H. Lin, O. Lunin and J. Maldacena, “Bubbling AdS space and 1/2 BPS geometries”, *JHEP* 0410 (2004) 025, hep-th/0409174.
- [38] J. P. Gauntlett, D. Martelli, J. Sparks and S.-T. Yau, “Obstructions to the existence of Sasaki-Einstein metrics”, hep-th/0607080.